


# DEVELOPMENT OF ADJUVANTED MULTI-ANTIGEN LIVER-STAGE MALARIA VACCINES

THESIS SUBMITTED FOR THE DEGREE OF
DOCTOR OF PHILOSOPHY

TRINITY TERM 2016

BENEDICT RENÉ HALBROTH
WOLFSON COLLEGE

WORD COUNT: ≈ 34,000 WORDS
(EXCLUDING BIBLIOGRAPHY, APPENDICES, TABLES AND DIAGRAMS)

**DPhil Supervisors**

Prof Adrian V. S. Hill

Dr Alexandra J. Spencer

**College Supervisor**

Prof Paul Leeson

**VacTrain Supervisor**

Prof Tom H. M. Ottenhoff

(LUMC, Leiden, The Netherlands)

The research leading to these results has received funding from the European Union Seventh Framework Programme FP7/2012-2016 under grant agreement n° 316655 (VACTRAIN).

# Development of Adjuvanted Multi-Antigen Liver-Stage Malaria Vaccines

Benedict Halbroth, Wolfson College, University of Oxford
Thesis submitted for the degree of Doctor of Philosophy, Trinity Term 2016

Despite promising progress in malaria vaccine development in recent years, an efficacious subunit vaccine against *P. falciparum* remains to be licensed and deployed. The most advanced candidates in clinical development focus on two pre-erythrocytic antigens (CSP and ME-TRAP), but many more immunogenic antigens have been recently identified. The work described in this thesis aimed to improve on the immunogenicity and efficacy of the leading liver-stage vaccine candidate (ChAd63-MVA ME-TRAP), which is known to confer protection by eliciting high levels of antigen-specific $CD8^+$ T cells. To achieve this, two different strategies were pursued. First, several prime-boost regimens with vectors encoding combinations of two liver-stage antigens were investigated. When mixed, vectors expressing LSA1 and LSAP2 conferred highest levels of protective efficacy in mice and were therefore considered for inclusion in the final second generation viral vectored liver-stage malaria vaccine. Second, the MHC class II invariant chain (Ii) was developed as a molecular adjuvant. Immunogenicity analyses of ChAd63 encoding ME-TRAP fused to several different versions of Ii showed that the transmembrane domain of Ii has the ability to strongly increase antigen-specific $CD8^+$ T-cell responses, even in the absence of the rest of the Ii protein. This finding may lead to the discovery of numerous similar adjuvants (such as the transmembrane domain of the Newcastle disease virus fusion protein). Furthermore, experiments showed that the Ii chain sequence can also be xenogenised without losing adjuvanticity. Both strategies have been combined in numerous novel adjuvanted multi-antigen vaccines, which were ranked for immunogenicity and efficacy in inbred and outbred mice. The viral vectors of the best combination (ChAdOX1-sharkTM/Ii-LSA1-LSAP2 and MVA-tPA-LSA1-LSAP2) are currently being produced to GMP grade and will progress to initial clinical trials in early 2017.

# Acknowledgments

First and foremost, I would like to thank my fantastic supervisors, Dr Alex Spencer and Prof Adrian Hill, for their excellent supervision, guidance, support, and continuous encouragement during the last three years. I could not have asked for better supervision. I am extremely grateful for this invaluable experience, which would not have been possible without you.

I would also like to thank Prof Simon Draper for your help, guidance, support, and contribution to our literature review, as well as Dr Sarah Sebastian for your invaluable support and assistance, especially at the beginning of my project.

Many thanks to the many vital members of the Jenner Institute. Special thanks to Anita Gola, Ahmed Salman, and Marta Ulaszewska, who always offered me their helping hand when needed, as well as Julie Furze, Andrew Worth, and Katie Ewer, who all saved my experiments numerous times by offering their help and expertise. Thanks to Ali Turner and all members of the Vector Core facility as well as Viv Clark, Heather Gray, and all staff at the FGF for the excellent collaboration during my DPhil. Furthermore, thank you to Alex Fyfe and Sumi Biswas for providing mosquitoes throughout my project.

I would especially like to thank all the students and postdocs at the Jenner Institute for your help, support, countless discussions, and all good times. In particular, Anita, Marta, Ahmed, Pawan, Adam, Florian, Carly, Georgie, Matt, Janet, Joe, Dave, Dan, Lynda, Naif, Vincent, Fede, Christos, Andrew, Ed, Paulo, and Craig – you guys are amazing, both scientifically and as friends. Because of you I cannot think of anywhere else I would rather have worked and studied. I wish you all best of all luck for the future!

Many thanks to everyone involved in VacTrain, especially all supervisors and ESR, as well as Prof Bernd van der Zeijst and Dr Wendy van Hemmen for coordinating and managing our training network, and Prof Tom Ottenhoff for being my mentor. Special thanks also to Dr Leander Grode and Dr Bernd Eisele and their team at VPM for welcoming me with open arms during my secondment in their company.

Finally, I would like to thank all my wonderful friends, who have supported me unconditionally throughout my project. In particular, thank you to my mother, Eva Halbroth. Without your support and belief in my abilities, I would not have had the opportunity to pursue my goals. I count myself extremely fortunate to have you!

# Authorship Statement

This thesis has been composed by me and is entirely based on my own work, unless stated otherwise. In summary, the following contributions are acknowledged:

- The Viral Vector Core Facility of the Jenner Institute produced all viral vectors used in this thesis. All DNA plasmids needed for virus production were cloned by me.
- Dr Ahmed Salman provided frozen blood stocks of all transgenic *P. berghei* parasites. The preparation of infectious sporozoites from these blood stocks for challenge experiments was performed by me. *In vivo* imaging for verification of the parasites' ability to infect mouse hepatocytes was performed in collaboration with Dr Ahmed Salman.
- Marta Ulaszewska, Anita Gola, Dr Ahmed Salman, and Dr Alex Spencer helped conducting some of the *in vivo* experiments presented in Chapter E.
- A few of the original DNA plasmids were cloned by other scientists of the Jenner Institute. These contributions are specifically acknowledged in Supplemental Table I-1 (p. 215).

# Table of Contents

**Abstract** ..... **III**

**Acknowledgments** ..... **IV**

**Authorship Statement** ..... **VI**

**Table of Content** ..... **VII**

**Table of Figures** ..... **XI**

**List of Tables** ..... **XIII**

**List of Abbreviations** ..... **XIV**

**Chapter A Introduction** ..... **1**

A1 Malaria ..... 2

A1.1 The Burden of the Malaria Disease ..... 2
A1.2 Life Cycle of Malaria Parasites ..... 3

A1.2.1 Life Cycle of P. falciparum ..... 3
A1.2.2 Life Cycle of P. berghei ..... 5

A2 Immunity to Malaria ..... 7

A2.1 Key Elements of the Immune System ..... 7

A2.1.1 Innate Immunity ..... 7
A2.1.2 Adaptive Immunity ..... 8

A2.2 Natural Immunity to Malaria ..... 11
A2.3 Current Vaccination Strategies Against Malaria ..... 14

A2.3.1 Whole Sporozoite Vaccination (WSV) ..... 14
A2.3.2 Subunit Vaccination ..... 18

A3 Thesis Aims ..... 25

**Chapter B Materials and Methods** ..... **27**

B1 Materials ..... 28

B1.1 Reagents ..... 28
B1.2 Solutions and Buffers ..... 31

B2 Methods ..... 34

B2.1 Molecular Biology ..... 34

B2.1.1 Software ..... 34
B2.1.2 Agarose Gel Electrophoresis ..... 34
B2.1.3 Restriction Endonuclease Digest ..... 34
B2.1.4 DNA Ligation ..... 35
B2.1.5 In-Fusion® Cloning ..... 35

B2.1.6 Polymerase Chain Reaction ... 36
B2.1.7 Site-Directed Mutagenesis ... 37
B2.1.8 Bacterial Transformation ... 38
B2.1.9 DNA Preparation ... 38
B2.1.10 Viral Vector Cloning ... 40
B2.1.11 Summary of Cloned Plasmids ... 41
B2.2 Vaccine Production ... 41
B2.2.1 Adenoviral Vectors ... 41
B2.2.2 Modified Vaccinia Ankara (MVA) Vectors ... 42
B2.2.3 Summary of Viral Vectors ... 42
B2.3 Animals and Animal Handling ... 43
B2.3.1 Ethics and Laboratory Mice ... 43
B2.3.2 Immunisation of Mice ... 43
B2.3.3 Intraperitoneal Injections ... 44
B2.3.4 Blood and Serum Samples ... 44
B2.3.5 Spleen Samples ... 44
B2.3.6 Liver Samples ... 45
B2.3.7 Sporozoite Challenge ... 45
B2.3.8 Thin Blood Smears ... 46
B2.3.9 In Vivo Imaging ... 46
B2.4 Immunology ... 47
B2.4.1 Peptides ... 47
B2.4.2 Intracellular Cytokine Staining (ICS) of PBMC and Splenocytes ... 47
B2.4.3 ELISpot Assay ... 50
B2.4.4 Luminescence Immunoprecipitation Assay (LIPS) ... 50
B2.5 Microscopy and Protein Expression ... 51
B2.5.1 Cell Transfection ... 51
B2.5.2 Fluorescence Microscopy ... 51
B2.5.3 Cell Lysis and Western Blots ... 52
B2.6 Insectary and Parasites ... 53
B2.6.1 Parasite Strains ... 53
B2.6.2 Preparation of Sporozoites ... 54
B2.6.3 Cryopreservation of Blood-Stage Parasites ... 54
B2.7 Data analysis ... 54
B2.7.1 Software ... 54
B2.7.2 Statistical Tests ... 55

**Chapter C Combination of Liver-Stage Antigens ... 56**

C1 Introduction ... 57
C1.1 Liver-Stage Antigens ... 58
C1.1.1 Thrombospondin Related Adhesive Protein (TRAP) ... 58
C1.1.2 Liver-Stage Antigen 1 (LSA1) ... 58
C1.1.3 Liver-Stage Associated Protein 2 (LSAP2) ... 60

C1.1.4 Upregulated in Infectious Sporozoites 3 (UIS3) ... 61
C1.1.5 Falstatin ... 62
C2 Results ... 63
C2.1 Combination of Novel Antigens with TRIP ... 63
C2.1.1 Experimental Setup ... 63
C2.1.2 Immunogenicity of Vaccine Combinations ... 64
C2.1.3 Efficacy of Vaccine Combinations ... 67
C2.1.4 Immunogenicity in Lymph Nodes, Spleen, and Liver ... 69
C2.2 Combination of Novel Liver-Stage Antigens (LSA1 + LSAP2) ... 73
C2.2.1 Efficacy of a Prime-Boost Regimen ... 73
C2.2.2 Immunogenicity and Efficacy after ChAd63 Prime-Only ... 74
C2.2.3 Long-Term Immunogenicity ... 75
C2.3 Assessment of Novel Dual Antigen Expressing Adenoviral Vectors ... 80
C3 Discussion ... 83

**Chapter D Development of a Molecular Adjuvant ... 89**

D1 Introduction ... 90
D1.1 Structure and Isoforms ... 90
D1.2 Invariant Chain HLA class II Interaction ... 92
D1.3 Invariant Chain MHC class I Interaction ... 94
D1.4 Evidence for Ii-Adjuvanticity ... 95
D1.5 Development of Ii for Clinical Usage ... 96
D2 Results ... 97
D2.1 Truncation of Ii ... 97
D2.1.1 Design and Cloning of Truncated Ii-ME-TRAP Constructs ... 97
D2.1.2 Immunogenicity of Truncated Ii-ME-TRAP Fusion Constructs ... 98
D2.2 Understanding the Positive Effect of Ii Truncation on Adjuvanticity ... 101
D2.3 Xenogenisation of Ii ... 105
D3 Discussion ... 109

**Chapter E Development of Adjuvanted Multi-Antigen Liver-Stage Malaria Vaccines ... 113**

E1 Introduction ... 114
E2 Results ... 115
E2.1 Cloning of Clinical Vaccine Candidates ... 115
E2.2 Comparison of Immunogenicity: ChAd63 vs ChAdOX1 ... 117
E2.3 Comparison of Vaccine Candidates in Inbred Mice ... 119
E2.3.1 Analyses of ChAdOX1 vaccines ... 119
E2.3.2 Analyses of MVA vectors ... 126
E2.3.3 Analyses of ChAdOX1-MVA Prime-Boost Regimens ... 128
E2.4 Comparison of Vaccine Candidates in Outbred Mice ... 132

E2.4.1 Analyses of ChAdOX1 vaccines ..... 132
E2.4.2 Analyses of ChAdOX1-MVA Prime-Boost Regimens ..... 133
E3 Discussion ..... 141

**Chapter F Mechanisms of Ii Adjuvantation and a Search for Additional Adjuvants ..... 148**

F1 Introduction ..... 149
F2 Results ..... 150
F2.1 Invariant Chain Fusion Alters Intracellular Antigen Trafficking ..... 150
F2.2 Importance of Ii Trimerisation ..... 152
F2.3 Newcastle Disease Virus Fusion Protein TMD as Molecular Adjuvant ..... 157
F3 Discussion ..... 160

**Chapter G Concluding Remarks ..... 165**

G1 Summary of Findings ..... 166
G2 Future Directions ..... 170
G2.1 Viral Vectors Encoding LSA1-LSAP2 in Clinical Trials ..... 170
G2.2 Sequence Optimisation ..... 170
G2.3 Novel Adjuvants ..... 171
G2.4 Multi-Stage Vaccination Regimens ..... 171
G2.5 Administration Route: Prime-Target Approach ..... 172
G3 Final Remarks ..... 173

**Chapter H References ..... 174**

**Chapter I Appendix ..... 199**

I1 Supplemental Figures ..... 200
I2 Supplemental Tables ..... 215
I3 Peptides ..... 228

# List of Figures


Figure A-1. Life Cycle of *P. falciparum* ..... 5
Figure A-2. Comparison of the liver-stage development in WSV approaches. ..... 15
Figure B-1. Gating Strategy. ..... 49
Figure C-1. Experimental setup to analyse immunogenicity and efficacy of antigen combinations ..... 64
Figure C-2. Post boost T-cell immunogenicity of co-administered liver-stage vaccines. ..... 66
Figure C-3. Assessment of antibody responses in BALB/c mice after co-administration of liver-stage vaccines. ..... 67
Figure C-4. Efficacy of vaccine combinations after sporozoite challenge. ..... 69
Figure C-5. T-cell responses in lymph nodes, spleen, and liver after vaccine co-administration. ..... 71
Figure C-6. Functionality of antigen-specific $CD4^+$ and $CD8^+$ T cells in the liver. ..... 73
Figure C-7. Combination of LSA1 and LSAP2 in a prime-only regimen. ..... 75
Figure C-8. Setup of the long-term immunogenicity experiment. ..... 76
Figure C-9. Post-prime and post-boost immunogenicity. ..... 77
Figure C-10. Long-term immunogenicity and efficacy ..... 80
Figure C-11. Immunogenicity of dual antigen expressing ChAd63 in BALB/c. ..... 82
Figure D-1. Isotypes of the human Ii. ..... 91
Figure D-2. Subdomains of the human Ii. ..... 92
Figure D-3. Processing and presentation of exogenous antigens on MHC class II molecules. ..... 94
Figure D-4. Initial truncation of Ii in Ii-ME-TRAP constructs. ..... 97
Figure D-5. Further truncation of the Ii. ..... 98
Figure D-6. Effect of truncated Ii sequences as adjuvant for ME-TRAP in mice vaccinated with ChAd63 vectors. ..... 100
Figure D-7. Adjuvanticity of homogenic mouse Ii. ..... 102
Figure D-8. Immunogenicity against the Ii adjuvant. ..... 104
Figure D-9. Adjuvanticity of xenogenised Ii. ..... 108
Figure E-1. Immunogenicity of ChAd63 and ChAdOX1. ..... 117
Figure E-2. Immunogenicity of ChAdOX1 vaccine candidates in BALB/c mice. ..... 120
Figure E-3. Immunogenicity of adjuvanted single vs dual antigen expressing vectors. ..... 121
Figure E-4. Immunogenicity in CBA mice. ..... 123
Figure E-5. Immunogenicity and efficacy of LSA1 expressing ChAdOX1 vectors in BALB/c. ..... 124
Figure E-6. Immunogenicity and efficacy of dual antigen expressing ChAdOX1 in BALB/c. ..... 126
Figure E-7. Immunogenicity of novel MVA encoding LSA1 and/or LSAP2. ..... 127
Figure E-8. Immunogenicity and efficacy of a 1-week ChAdOX1-MVA prime-boost regimen in BALB/c. ..... 129
Figure E-9. Immunogenicity and efficacy of a 6-week ChAdOX1-MVA prime-boost regimen in BALB/c. ..... 131

Figure E-10. Immunogenicity of adjuvanted single vs dual antigen expressing vectors. ..... 133
Figure E-11. Immunogenicity of a 1-week ChAdOX1-MVA prime-boost regimen in outbred mice. ..... 134
Figure E-12. Efficacy of a 1-week ChAdOX1-MVA prime-boost regimen in CD1 mice. ..... 135
Figure E-13. Comparison of immunogenicity of ChAdOX1 expressing tPA or sharkTM/Ii as a leader sequence in a 1-week ChAdOX1-MVA prime-boost regimen in outbred mice. ..... 136
Figure E-14. Comparison (immunogenicity and efficacy) of mono and dual antigen expressing vectors in CD1. ..... 138
Figure E-15. Immunogenicity and efficacy of a 6-week ChAdOX1-MVA prime-boost regimen in CD1. ..... 140
Figure F-1. Invariant chain fusion alters the pattern of TRAP expression ..... 152
Figure F-2. Immunogenicity of mutated (Q64A) Ii fused to ME-TRAP. ..... 153
Figure F-3. Western blot of unfused and adjuvanted ME-TRAP constructs. ..... 155
Figure F-4. Western blot of ME-TRAP constructs fused to mutated Ii-TMD ..... 156
Figure F-5. Immunogenicity of humanTM(III59aaa)/Ii-ME-TRAP. ..... 157
Figure F-6. Immunogenicity of NC/TMD-ME-TRAP. ..... 159

Supplemental Figure I-1. In vivo imaging ..... 200
Supplemental Figure I-2. Efficacy of a ChAd63-MVA prime-boost regimen encoding LSA1 and LSAP2. ..... 201
Supplemental Figure I-3. Long-term post-boost immunogenicity ..... 202
Supplemental Figure I-4. Effect of endogenous signal peptide (eSP) removal from TRAP. ..... 203
Supplemental Figure I-5. Immune response to ME-TRAP fused to Ii truncations. ..... 204
Supplemental Figure I-6. Effect of fusion of ME-TRAP to (truncated) Ii in mice vaccinated with ChAd63 vectors. ..... 205
Supplemental Figure I-7. Effect of truncated Ii sequences as adjuvant. ..... 206
Supplemental Figure I-8. Effect of fusion of ME-TRAP to xenogenised Ii in mice vaccinated with ChAd63 vectors. ..... 207
Supplemental Figure I-9. Adjuvanticity of selected xenogenised Ii sequences. ..... 208
Supplemental Figure I-10. MUSCLE alignment of Ii transmembrane domains ..... 209
Supplemental Figure I-11. Immunogenicity of a 6-week prime boost regimen with ChAdOX1 and MVA vectors in BALB/c mice. ..... 210
Supplemental Figure I-12. Functionality of antigen-specific $CD4^+$ and $CD8^+$ T cells post boost. ..... 211
Supplemental Figure I-13. Efficacy of single and dual antigen expressing vectors against sporozoite challenge with *Pb*(*Pf*LSA1). ..... 213
Supplemental Figure I-14. Immunogenicity of a 6-week prime boost regimen with ChAdOX1 and MVA vectors in CD1 mice ..... 214

# List of Tables


Table B-1. Standard restriction endonuclease digest. 34
Table B-2. Standard ligation reaction. 35
Table B-3. In-Fusion® cloning reaction. 36
Table B-4. PCR components. 37
Table B-5. PCR cycling conditions. 37
Table B-6. Ligation protocol for linearised, mutated plasmid DNA. 38
Table B-7. Laboratory Mice. 43
Table B-8. Transgenic parasites used in this thesis 53
Table D-1. Literature documenting Ii adjuvanticity. 95
Table D-2. Homology analysis of Ii sequences. 105
Table E-1. Comparison of Ii transmembrane domains 116
Table E-2. List of ChAdOX1 and MVA vectors. 116

Supplemental Table I-1. Summary of cloned plasmid DNA and bacterial artificial chromosomes. 215
Supplemental Table I-2. Summary of viral vectors. 223
Supplemental Table I-3. Homology Analysis of full-length Ii sequences. 227
Supplemental Table I-4. Peptide sequences of *P. falciparum 3D7* LSA1. 228
Supplemental Table I-5. Peptide sequences of *P. falciparum 3D7* LSAP2. 229
Supplemental Table I-6. Peptide sequences of *P. falciparum 3D7* UIS3. 230
Supplemental Table I-7. Peptide sequences of *P. falciparum* Falstatin 231
Supplemental Table I-8. Peptide sequences of *P. falciparum 3D7* CSP. 232
Supplemental Table I-9. Peptide sequences of *P. falciparum T996* TRAP and *P. falciparum 3D7* TRAP (= TRIP) 233
Supplemental Table I-10. Peptide sequences of the human Ii 235

# List of Abbreviations

| | |
|---|---|
| aa | Amino acid |
| ACK | Ammonium chloride potassium |
| AMA1 | Apical membrane antigen 1 |
| ANOVA | Analysis of variance |
| AP | Alkaline phosphatase |
| APC | Antigen presenting cell |
| BAC | Bacterial artificial chromosome |
| bp | Base pair |
| BSA | Bovine serum albumin |
| CD | Cluster of differentiation |
| CEF | Chick embryo fibroblasts |
| ChAd | Chimpanzee adenovirus |
| CHMI | Controlled human malaria infection |
| CLIP | Class II-associated invariant chain peptide |
| CLR | C-type lectin receptors |
| CMV | Cytomegalovirus |
| CPS | Chemical Prophylaxis Sporozoite Vaccination |
| DC | Dendritic cell |
| $dH_2O$ | Distilled water |
| DNA | Deoxyribonucleic acid |
| D-PBS | Dulbecco's Phosphate Buffered Saline |
| EDTA | Ethylenediaminetetraacetic acid |
| ELISpot | Enzyme-linked immunosorbent assay |
| EMA | European Medicines Agency |
| EPI | Expanded Program on Immunization |
| ER | Endoplasmic reticulum |
| EU | European Union |
| FCS | Fetal calf serum |
| GAP | Genetically Attenuated Parasite |
| GFP | Green fluorescent protein |
| GMP | Good manufacturing practice |
| GSK | GlaxoSmithKline |
| HBsAg | Hepatitis B surface antigen |
| HEPES | 4-(2-hydroxyethyl)-1-piperazineethanesulfonic acid |
| HLA | Human leucocyte antigen |
| ICP | Inhibitor of cysteine proteases |
| IE | CMV immediate-early |
| IFN | Interferon |

| | |
|---|---|
| Ii | Invariant chain |
| IL | Interleukin |
| IM | Intramuscular |
| IP | Intraperitoneal |
| ITV | Infection-Treatment Vaccination |
| IU | Infectious units |
| kb | Kilobase |
| LB | Lysogeny broth |
| LIPS | Luminescence immunoprecipitation assay |
| LSA1 | Liver-stage antigen 1 |
| LSAP2 | Liver-stage associated protein 2 |
| LSEC | Liver sinusoidal endothelial cell |
| LU | Luminescence units |
| MEM | Minimum Essential Medium |
| MHC | Major histocompatibility complex |
| MSP1 | Merozoite surface protein 1 |
| MVA | Modified vaccinia Ankara |
| NEB | New England Biolabs |
| NHP | Non-human primate |
| NK | Natural killer (cell) |
| NLR | NOD-like receptor |
| PABA | Para-aminobenzoic acid |
| PAGE | Polyacrylamide gel electrophoresis |
| PAMP | Pathogen-associated molecular patterns |
| *Pb* | *Plasmodium berghei* |
| PBMC | Peripheral blood mononuclear cell |
| PBS | Phosphate buffered saline |
| PCR | Polymerase chain reaction |
| *Pf* | *Plasmodium falciparum* |
| PFU | Plaque forming units |
| PRR | Pattern-recognition receptors |
| PV | Parasitophorous vacuole |
| PVM | Parasitophorous vacuole membrane |
| RAS | Radiation Attenuated Sporozoite |
| RBC | Red blood cell |
| RESA | Ring-infected erythrocyte surface antigen |
| RFP | Red fluorescent protein |
| Rh5 | Reticulocyte binding protein homolog 5 |
| RLR | RIG-I-like receptors |
| rLuc | Renilla luciferase |
| rpm | Rounds per minute |
| RPMI | Roswell Park Memorial Institute medium |
| RT | Room temperature |

| | |
|---|---|
| SC | Subcutaneous |
| SDS | Sodium dodecyl sulfate |
| SEB | Staphylococcal enterotoxin B |
| SEM | Standard error of the mean |
| SFU | Spot forming units |
| SOC | Super Optimal Broth with Catabolite Repression |
| Spz | Sporozoite |
| Ta | Annealing temperature |
| TAE | Tris-acetate-EDTA |
| $T_{CM}$ | Central memory T cells |
| TCR | T cell receptor |
| $T_{EM}$ | Effector memory T cells |
| TK | Thymidine kinase |
| TLR | Toll-like receptors |
| Tm | Melting temperature |
| TMD | Transmembrane domain |
| TNF | Tumor necrosis factor |
| tPA | Tissue plasminogen activator |
| UIS3 | Up-regulated in infective sporozoites gene 3 |
| VLP | Virus like particles |
| WHO | World Health Organisation |
| WSV | Whole sporozoite vaccination |

# Chapter A

# Introduction

# A1 Malaria

## A1.1 The Burden of the Malaria Disease

Malaria is a mosquito-borne infectious disease caused by parasitic protozoa belonging to the *Plasmodium* genus. Six species of *Plasmodium* infect humans and cause one of the most important and life-threatening diseases worldwide: *P. falciparum* (the deadliest species), *P. vivax*, *P. ovale curtisi*, *P. ovale wallikeri, P. malariae*, *P. knowlesi*. According to the Global Burden of Disease Study, malaria caused about 438,000 deaths in 2015 [1] with children under the age of five in sub-Saharan Africa of highest risk. Furthermore, malaria caused more than 200 million clinical episodes in a population of approximately 3.2 billion people living in regions at risk of infection.

The clinical disease usually appears between 10–15 days after the bite of an infected mosquito and includes symptoms such as fever, fatigue, vomiting, headache, and general malaise, but can aggravate and lead to severe malaria that can manifest in many ways, including yellow skin, seizures, haemoglobinuria, kidney failure, coma, and ultimately death. Typically, malaria causes its symptoms in a cyclic nature with fever reoccurring every two days in *P. vivax* and *P. ovale* infections (tertian fever) or every three days in *P. malariae* infections (quartan fever). However, the cyclic reoccurrence of fever caused by *P. falciparum* is much less pronounced (every 36–48 hours), often appearing as a continuous fever.

Apart from the frightful humanitarian impact of the disease, malaria also causes a massive economic and social burden on endemic countries. Therefore, there is an urgent need for improved strategies to control malaria, such as novel medication (considering the problem of growing antimalarial drug resistance), mosquito control, or the development of a highly effective vaccine. In 2006, the WHO published a Malaria Vaccine Technology Roadmap suggesting a landmark goal to ‘develop and license a first-generation

*P. falciparum* malaria vaccine that has a protective efficacy of more than 50% against severe malaria and death and lasts longer than one year by 2015'. Substantial progress has been made in the following years and the RTS,S vaccine candidate, the first ever malaria vaccine that entered phase III clinical trials, has brought the field to within sight of this goal [2]. The updated 2030 Malaria Vaccine Technology Roadmap calls for a second generation vaccine to achieve 75% efficacy over two years for both *P. falciparum* and *P. vivax*, and for a vaccine that can prevent malaria transmission [3].

## A1.2 Life Cycle of Malaria Parasites

This thesis will focus on the development of a vaccine against *P. falciparum* – the parasite species that currently causes highest levels of morbidity and mortality. However, as *P. falciparum* itself is not capable of infecting small animals, alternative rodent parasites, such as *P. berghei*, *P. yoelii*, *P. chabaudi*, or *P. vinckei* have been established. Even though none of these rodent parasites can perfectly mimic the life cycle of *P. falciparum*, *P. berghei* parasites were used in this thesis to challenge vaccinated mice, as they can be modified to express selected *P. falciparum* antigens [4–10].

In the following, the life cycle of both parasites, *P. falciparum* and *P. berghei*, will be described in detail.

### A1.2.1 Life Cycle of P. falciparum

**Pre-erythrocytic stage.** When an infected female *Anopheles* mosquito takes a blood meal, it injects infectious sporozoites that mainly travel to the liver. Here, sporozoites migrate through Kupffer cells and liver sinusoidal endothelial cells to enter the perisinusoidal space (space of Disse) [11]. The sporozoites then transverse several hepatocytes before progressing their liver-stage development in one hepatocyte [12]. During approximately seven days, sporozoites replicate asexually 10,000–40,000 fold [13]

within a parasitophorous vacuole (PV) and develop to merozoites. Then, merozoites leave hepatocytes in small vesicles (merosomes) and enter the bloodstream [14].

**Erythrocytic stage.** The merozoites that have left the hepatocytes invade red blood cells (RBC), in which they replicate asexually again and transform into ring-stage trophozoites. After developing into mature trophozoites, the parasites develop into erythrocytic schizonts, which rupture and release approximately twenty new merozoites back into the blood stream [15]. These reinfect RBC causing an exponential increase of the parasite burden and the cyclic nature of the erythrocytic stage (36–48 h for *P. falciparum*). All symptoms of the clinical manifestations of the malaria disease are caused by parasites of the erythrocytic stage.

**Sexual stage.** Inside RBC, some of the merozoites differentiate into a sexual stage with male and female gametocytes (microgametocytes and macrogametocytes). These can be ingested by another *Anopheles* mosquito during a blood meal. The microgametes then penetrate macrogametes, which generates zygotes that embed in the mosquito gut [16] and turn into motile ookinetes that invade the midgut wall to form oocysts. Within these oocysts new sporozoites develop, which are released by oocyst rupture. The sporozoites then migrate to the mosquitoes' salivary glands, from where they can be injected into a new human host.

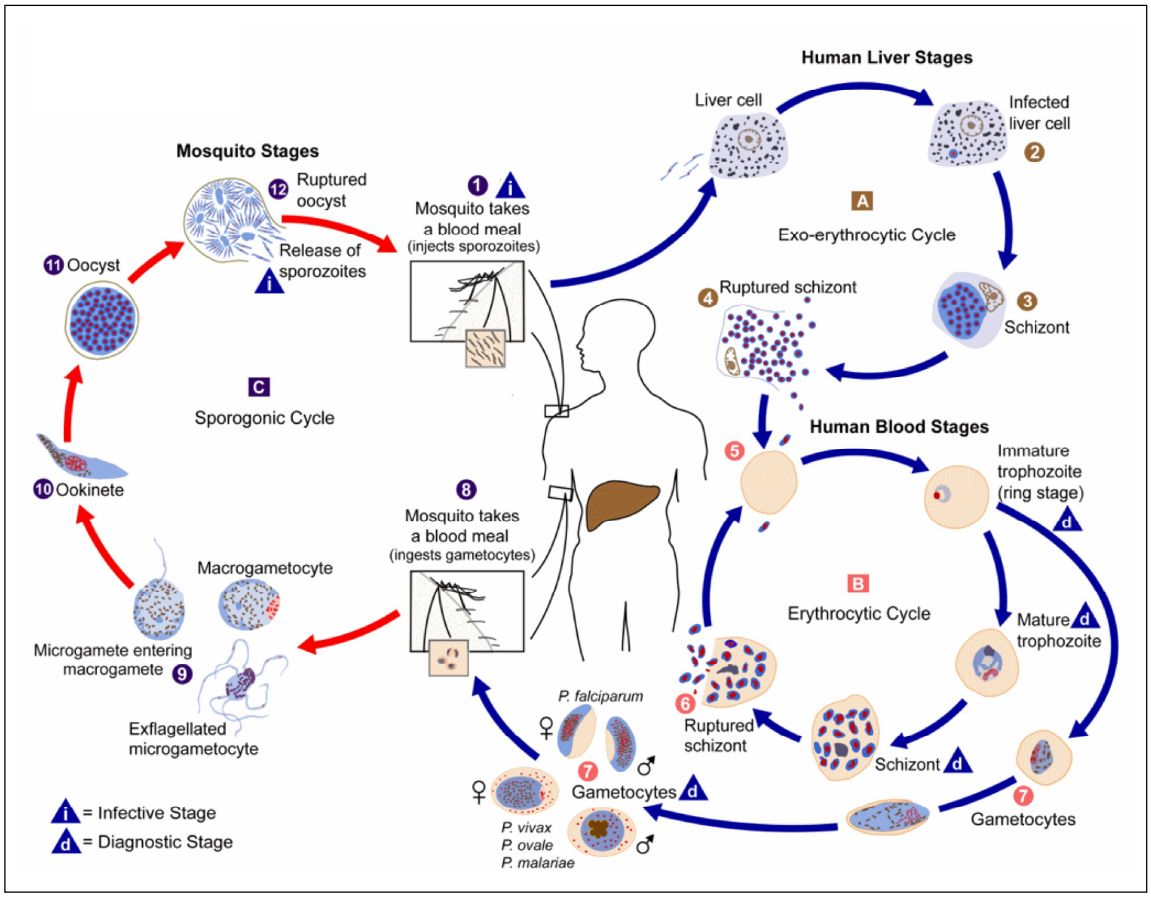



**Figure A-1. Life Cycle of *P. falciparum* adapted from [17].** During a blood meal, a malaria-infected female *Anopheles* mosquito inoculates the human host with sporozoites ❶. Sporozoites infect liver cells ❷ and mature into schizonts ❸, which rupture and release merozoites ❹. After this initial replication in the liver (exo-erythrocytic schizogony A), the parasites undergo asexual multiplication in the erythrocytes (erythrocytic schizogony B). Merozoites infect red blood cells ❺. The ring stage trophozoites mature into schizonts, which rupture releasing merozoites. Some parasites differentiate into sexual erythrocytic stages (gametocytes) ❼. Blood stage parasites are responsible for the clinical manifestations of the disease. The gametocytes, male (microgametocytes) and female (macrogametocytes), are ingested by an *Anopheles* mosquito during a blood meal ❽. The parasites' multiplication in the mosquito is known as the sporogonic cycle C. While in the mosquito's stomach, the microgametes penetrate the macrogametes generating zygotes ❾. The zygotes in turn become motile and elongated (ookinetes) ❿, which invade the midgut wall of the mosquito where they develop into oocysts ⓫. The oocysts grow, rupture, and release sporozoites ⓬, which make their way to the mosquito's salivary glands. Inoculation of the sporozoites ❶ into a new human host perpetuates the malaria life cycle. Adapted from [17].

### A1.2.2 Life Cycle of P. berghei

Murine plasmodial species have a very similar life cycle compared to *P. falciparum*. The only major difference is that the duration of the liver-stage in all murine species is much shorter compared to human species such as *P. falciparum* (48–52 h for *P. berghei*).

Nonetheless, *P. berghei* has been widely used in preclinical malaria research to understand the biology of the parasites and to investigate vaccine candidates in murine models. More recently, new technologies have allowed researchers to specifically modify the genome of plasmodia (such as the addition of luciferase as a transgene [18, 19]) leading to the generation of murine parasites expressing *P. falciparum* antigens, which have been used to understand the function of these transgenic proteins *in vivo* [20] and to investigate *P. falciparum* vaccine candidates in mice [4–10]. This thesis will use several of recently developed mono and double transgenic *P. berghei* parasites to assess novel malaria vaccine candidates based on *P. falciparum* liver-stage antigens.

# A2 Immunity to Malaria

## A2.1 Key Elements of the Immune System

The innate immune system with non-specific defence mechanisms against invading pathogens is complemented by a specific and highly effective adaptive immune system. The latter has two unique capabilities: it has the ability to specifically recognise at least $10^8$ different patterns of foreign particles and it has the ability to remember infections. As efficacy of any vaccine is based on the induction of immunological memory, it is essential that activation of the adaptive immune system is achieved by vaccination. Even though innate and adaptive immunity are described separately below, both parts of the immune system depend on one another and interact in many ways [21–23].

### A2.1.1 Innate Immunity

The innate immune system is more primitive compared to the adaptive immune system. It includes secreted protein components (complement, cytokines, acute phase proteins), as well as phagocytic cells (such as macrophages and granulocytes) and natural killer (NK) cells, which all provide immediate host defence. These cells generally lack immunological memory, although NK cells have recently been described to possess characteristics of adaptive immunity with the ability to acquire memory, similarly to T and B cells [24]. Innate immune cells recognise non-self material that has already been tagged by antibodies of the adaptive immune system, but are also able to recognise highly conserved patterns of pathogens, known as pathogen-associated molecular patterns (PAMP) by so-called pattern-recognition receptors (PRR). Many different PRR are known, such as toll-like receptors (TLR), C-type lectin receptors (CLR) with the mannose receptors and the asialoglycoprotein receptor family, NOD-like receptors (NLR), or RIG-I-like receptors (RLR).

With the activation of PRR, intracellular signalling cascades are initiated that lead to the secretion of chemokines and cytokines as well as phenotypical maturation of professional antigen presenting cells (APC), which is essential for mounting adaptive immune responses [22].

### A2.1.2 Adaptive Immunity

This part of the immune system is also characterised by humoral (antibodies, which are produced by plasma cells) and cellular components (B and T cells), but also by its enormous heterogeneity. The major feature of the adaptive immune system is that each cell has a unique specificity for a peptide or protein sequence which can bind to their cell surface receptor, either a B-cell receptor (BCR) or T-cell receptor (TCR). It is through the rearrangements and splicing of variable regions of their T- or B-cell receptor genes which leads to the diversity, with at least $10^8$ of the approximate $10^{12}$ lymphocytes have different antigen receptors on their cell membranes [21]. Consequently, the adaptive immune system is capable of recognising at least $10^8$ different antigenic determinants, known as epitopes. To make sure that self-antigens are tolerated, a complex process during the development of each immune cell identifies and eliminates self-targeting cells.

To achieve the high level of heterogeneity, T cells have antibody-like receptors on their cell membrane (so-called T-cell receptors), which enable them to recognise epitopes presented on the cell surface of somatic cells via specialised membrane proteins, the major histocompatibility complexes (MHC), also called human leucocyte antigens (HLA) in man. These proteins fulfil two major functions. (1) They have the ability to bind and present fragments of proteins. (2) They are autologous antigens themselves and therefore show the immune system that the presenting cell belongs to its own body. This ensures that foreign cells and infected autologous cells are attacked, but uninfected host cells are tolerated.

T cells are distinguished based on cell surface molecules, which are known as CD4 and CD8 in the cluster of differentiation (CD) nomenclature:

**CD4⁺ T cells.** In general, CD4⁺ T cells do not have cytotoxic or phagocytic activity, but help other immune cells by activating or directing them, therefore often called T helper cells. Class II MHC molecules of APC exclusively interact with CD4⁺ T cells, which subsequently help to trigger an appropriate immune response. T helper cells are also essential in B-cell antibody class switching, in maximising bactericidal activity of phagocytes, and in the activation and growth of CD8⁺ T cells. Many subtypes of CD4⁺ T cells are known, such as Th1, Th2, Th17, or T regulatory cells [25, 26].

**CD8⁺ T cells.** This subtype of T cells are also known as cytotoxic T cells, cytotoxic T lymphocytes (CTL), cytolytic T cells, or killer T cells, as they are capable of inducing death in infected somatic cells or tumour cells by producing several cytotoxins (such as perforin, granulysin, or granzymes) and expressing Fas ligand after recognising their targets on MHC class I molecules [25, 26].

**T cell activation and memory.** Naïve CD4⁺ or CD8⁺ T cells interact with activated dendritic cells (DC) in lymphatic organs where the antigen-specific T-cell response can be triggered. This "priming process" requires at least three steps to succeed. (1) The naïve T cell binds with its TCR as well as its CD4- or CD8-co-receptors to a peptide-loaded MHC complex of an APC. (2) Next, the T cell has to interact with several additional co-stimulatory factors to become activated. Most importantly, the DC´s co-stimulatory B7 molecules (CD80 = B7.1 and CD86 = B7.2) bind CD28, thereby boosting the TCR signal and stimulating following T-cell proliferation. (3) Secreted cytokines influence the differentiation of T cells into their subpopulations [27].

After priming, T cells leave lymphatic organs and migrate to their target tissue, where they can detect their antigens and release effector molecules. CD4⁺ effector T cells are

subdivided into numerous subtypes with different effector functions. Th1 cells secret primarily IFN-γ, interleukin 2 (IL-2), IL-3, lymphotoxin, and granulocyte-macrophage colony-stimulating factor (GM-CSF) to coordinate the immune reaction against intracellular pathogens, but also stimulate B cells to produce IgG antibodies against extracellular microorganisms. Th2 cells secret IL-4, IL-5, IL-6, IL-10, and IL-13, activate naïve B cells, and induce a class change particularly to immunoglobulin E and A (IgE and IgA). Th17 cells are described to support Th1 and Th2 cells, but the detection of their cytokines in high levels (IL-17, IL-21, IL-22, and IL-26) is often associated with autoimmune diseases. Another $CD4^+$ T cell subtype, the so-called T-reg cells, produce IL-10 and TGF-β, thereby supressing T-cell induced immune reactions [27].

$CD8^+$ effector T cells interact with MHC class I molecules, which can be found on all nucleated cells. As described above, several steps are needed to prime $CD8^+$ effector T cells. The TCR interacts with MHC class I molecules of DC, which for instance presents parasitic peptides. Then, the co-stimulatory molecules CD80 and CD86 are essential for clonal expansion. As a result, a direct activation of $CD8^+$ T cells is rare and only occurs if a DC is infected itself and expresses an extraordinary amount of CD80 and CD86. Nonetheless, with the help of $CD4^+$ T cells that are bound to the same target cell, proliferation and differentiation into $CD8^+$ T memory cells is possible. If the primed $CD8^+$ effector T cells recognise their antigen, presented by any nucleated cell on a MHC class I molecule, they secrete vast amounts of cytokines (such as TNF or IFN-γ), kill their target cells via the secretion of perforin and granzyme B, or induce apoptosis of the target cell by binding to the Fas receptor (CD95) with their Fas ligand (CD95L or CD178) [27].

In the absence of the pathogenic antigen, most T cells become apoptotic and only a small fraction further develop into a persistent memory T-cell population. These antigen-experienced T cells are capable of mounting a faster and stronger immune response at their second encounter with their antigen compared to their initial activation. Despite

great heterogeneity of memory T cells, two main subtypes can be characterised by distinct homing and effector function: central memory T cells ($T_{CM}$) and effector memory T cells ($T_{EM}$). Human $T_{CM}$ express CD45R0 as well as CCR7 and CD62L, which mediate extravasation through high endothelial venules and migration to secondary lymphoid organs. They are more sensitive to antigenic stimulation, less dependent on costimulation, and provide more effective stimulatory feedback to DC and B cells compared to naïve T cells. After activation $T_{CM}$ mainly produce IL-2, but then proliferate and differentiate to an effector phenotype producing large amounts of IFN-γ or IL-4. In contrast to $T_{CM}$, $T_{EM}$ express chemokine receptors and adhesion molecules that are required for homing to inflamed tissues and are much faster in executing their effector function by producing IFN-γ, IL-4, and IL-5 within hours of antigenic stimulation ($CD8^+$ $T_{EM}$ also carry large amounts of perforin) [28].

## A2.2 Natural Immunity to Malaria

Immunity to severe malaria disease (or death), can be developed rapidly, potentially after only one infection [29]. However, immunity to malaria infection (of any severity) seems to be very slow and requires multiple infections [30, 31]. In fact, natural immunity might never be complete, as evidence suggests that protected adults in endemic regions still become parasitemic (yet remain asymptomatic) [30, 32]. Despite anti-parasitic immunity, which reduces the parasite burden, the immune response may also involve a regulatory component reducing clinical disease symptoms [33–35].

Interestingly, natural immunity is mainly directed against the erythrocytic stage of the parasite. In comparison, sporozoites and immature liver stages induce little, if any, inflammation [36, 37]. This could be due to the extremely low number of infected hepatocytes or the lack of ligands for innate PRR to recognise the parasite. Evidence in BALB/c mice comparing liver-stage inflammation after infection with viable *P. yoelii* or

radiation-attenuated parasites suggests that PAMP could also be actively sequestered away from PRR. Furthermore, as the liver receives blood directly from the gut, it generally has a relatively immune tolerant environment to minimise inflammation. This does not mean, however, that vaccine efforts should mimic natural immunity and focus on erythrocytic stages – particularly given such immunity is non-sterilising [38].

**Innate immune response to malaria.** Sporozoites have developed multiple strategies to evade the innate immune response. For instance, as only a small number of sporozoites are injected during a mosquito bite and the sporozoites then quickly migrate to the liver [39, 40], there might not be enough antigen and time for the innate immune system to activate. Being in the liver, the parasites have the capability of suppressing Kupffer cell activation, mainly mediated by CSP [36, 41]. Furthermore, liver-stage parasites seem to be able to block pro-inflammatory cytokine production through the production of heme oxygenase-1 [42] and CSP (which interferes indirectly with the NF-κB signalling pathway [38, 43]), and also to inhibit hepatocyte apoptosis, protecting them during liver-stage development. Nonetheless, there is evidence that sporozoites cannot completely avoid recognition by the innate immune system: sporozoites that reach the lymphatic system are taken up by DC [44], and cellular infiltrates can be found surrounding hepatocytes in murine models when injected with infectious, but not heat-killed, sporozoites [42, 45–47]. Activation of the innate immune system also seems to have a protective effect, since innate cell infiltrates are greater in BALB/c mice compared to those in C57BL/6 mice (which are more susceptible to and more difficult to protect against malaria) [48] and the differences in virulence between *P. yoelii* and *P. berghei* correlate with liver infiltrates following infection with those parasites [45].

When parasites reach the blood stage, the innate immune system responds quickly by producing pro-inflammatory cytokines [49, 50] that contribute to protection, but also cause disease symptoms. This response is triggered by many host-parasite interactions,

such as the recognition of glycosylphosphatidylinositol anchors or haemozoin by TLR2, -4, and -9 [51–55].

**Adaptive immune response to malaria.** The liver, as an autonomous priming site for naïve $CD8^+$ T cells, houses numerous cell types capable of presenting antigen on MHC class I or II. Examples are hepatic DC, stellate cells, liver sinusoidal endothelial cells (LSEC), or Kupffer cells [16, 56–58]. Hepatocytes themselves also present antigen, however mostly on MHC class I molecules [56].

However, there is not much evidence supporting an important role for adaptive liver-stage specific cellular immunity following a natural malaria infection. This might be due to the miniscule number of infected hepatocytes or impairment of liver-stage immunity by blood-stage infections [59, 60]. Nonetheless, a few liver-stage antigens have been associated with adaptive T-cell responses, such as the liver-stage antigen 1 (LSA1) [61–64], the thrombospondin-related adhesion protein (TRAP) [65], and the circumsporozoite protein (CSP) [66].

Contrary to natural immunity, the cellular adaptive immune response has been shown to be fundamental to vaccine-induced protection using irradiated sporozoites and liver-stage vaccines. As lymphocytes and hepatocytes are able to interact by projecting extensions through the fenestrations of LSEC [67], cytotoxic T cells (either primed in the liver or lymph nodes/spleen) can screen hepatocytes for their epitopes and kill infected liver cells [67–74, 74]. Liver-resident lymphocytes, which consist of more $CD8^+$ T cells compared to $CD4^+$ T cells (contrary to the ratio in blood [75]), may contribute to protection.

There is also some evidence for T-cell responses against blood-stage antigens [76, 77], such as the merozoite surface protein 1 (MSP1) [78, 79], however, naturally acquired immunity to malaria is mainly based on antibodies against blood-stage parasites. In 1961, Cohen et al. showed that children who received serum from malaria immune adults were

protected against malaria [80] and many other studies have confirmed the protective effect of blood-stage antibodies in natural immunity since then [81–90]. Inhibition of RBC invasion, opsonisation and antibody-dependent cellular inhibition seem to be important mechanisms [91]. However, despite this knowledge, blood-stage vaccines aiming for induction of protective antibody levels have not achieved high levels of efficacy yet. Instead, the most advanced malaria vaccine in clinical development (RTS,S) induces an antibody response against CSP, which can also be a target of neutralising antibodies during natural infection [81, 92].

## A2.3 Current Vaccination Strategies Against Malaria

Considerable progress has been made in malaria vaccine development. Whole-parasite immunisation approaches as well as combinations of pre-erythrocytic subunit vaccines are now reporting high-level efficacy, whilst new approaches to the development of blood-stage and transmission-blocking vaccines are entering clinical assessment. In the following, recent developments in malaria vaccine research will be introduced.

### A2.3.1 Whole Sporozoite Vaccination (WSV)

Many of today´s vaccines contain whole pathogens that are either inactivated or live-attenuated. Consistent with this, whole sporozoite vaccination (WSV) approaches against malaria have also been widely investigated. As heat-killed sporozoites did not protect mice from malaria [93], it became clear that viable, liver-invading parasites would be necessary to induce protective immunity leading to the development of a number of sporozoite attenuation approaches (Figure A-2): Radiation Attenuated Sporozoites (RAS), Genetically Attenuated Parasites (GAP), and Infection-Treatment Vaccination (ITV) / Chemical Prophylaxis Sporozoite Vaccination (CPS).

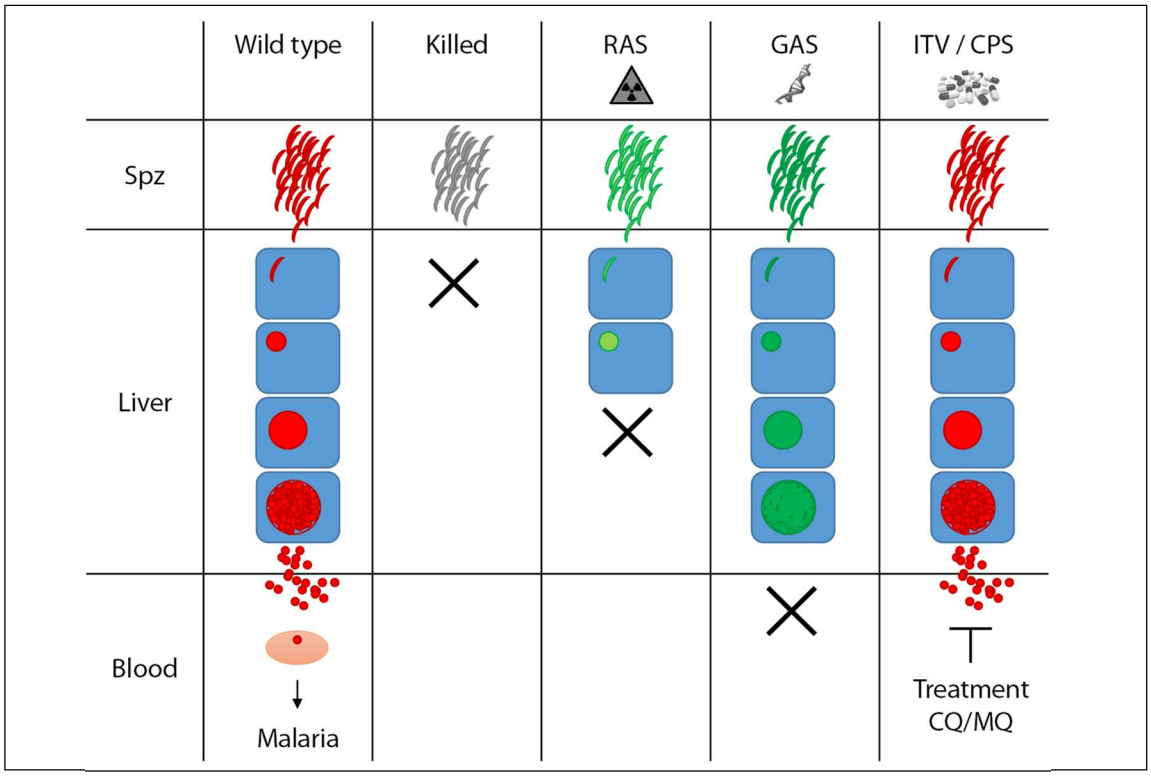



**Figure A-2. Comparison of the liver-stage development in WSV approaches.** Spz, sporozoites; RAS, Radiation Attenuated Sporozoites; GAS, Genetically Attenuated Parasites; ITV, Infection-Treatment Vaccination; CPS, Chemical Prophylaxis Sporozoite Vaccination; CQ, chloroquine, MQ, mefloquine.

#### *A2.3.1.1 Radiation Attenuated Sporozoites (RAS)*

It has been known since the 1960s that delivering radiation-attenuated *P. berghei* sporozoites intravenously (IV) or by mosquito bites can confer sterile protection against infectious sporozoite challenge in mice [94]. Thereafter, it was shown that it is also possible to sterilely protect human volunteers with this strategy [95, 96]. However, more than 1,000 mosquito bites were necessary to achieve protective immunity, which led to the general opinion that WSV was not deployable as a mass vaccination regimen.

In 2002, a biotechnology company (Sanaria Inc.) was founded to develop a way to manufacture: (1) aseptic, radiation-attenuated, purified and cryopreserved *P. falciparum* sporozoites (PfSPZ); under (2) current good manufacturing practice (cGMP) standards in adequate quantities to administer a sporozoite containing vaccine; by (3) a route that can be standardised and clinically achievable [97]. Having overcome many production

obstacles, cryopreserved sporozoites showed promising results in mice and NHP [97, 98]. Seder et al. reported a Phase I/IIa clinical trial in 40 adults to determine safety, immunogenicity, and protective efficacy against controlled human malaria infection (CHMI) of the radiation-attenuated, aseptic, purified, and cryopreserved PfSPZ vaccine given IV [99]. Most strikingly, six of six volunteers who received the highest vaccine dose (five doses of 1.35 x $10^5$ PfSPZ) were sterilely protected against CHMI, confirming that cryopreserved PfSPZ can be highly efficacious if administered IV. Future clinical trials will investigate the duration of protection as well as the efficacy against heterologous parasite strains, and will try to establish correlates of protection [99].

It was a remarkable achievement to prove the ability to produce attenuated cryopreserved PfSPZ under GMP standards in high enough quantities to conduct clinical trials, as well as to demonstrate their protective efficacy in humans. Nonetheless, substantial obstacles still have to be overcome to allow mass deployment. For instance, as IV administration seems to be crucial for protection, the PfSPZ vaccine is currently not suited for deployment in infants or young children, the target population in Africa. Furthermore, as PfSPZ have to be shipped and stored in liquid nitrogen vapour phase, it will be difficult to deliver the vaccine to rural areas. Assuming that the positive trial results of the PfSPZ vaccine can be confirmed and protective immunity lasts for a reasonable duration, it could, however, be considered as a vaccine for use by the military, travellers or for possible local malaria elimination campaigns in small island-based populations [100].

#### *A2.3.1.2 Genetically Attenuated Parasites (GAP)*

Parasites can also be attenuated by knocking out genes that are essential for liver-stage development. This strategy overcomes the problem of fine-tuning the irradiation process of live parasites as part of the GMP process in RAS, with the advantage that the parasite-

based vaccine is also homogenous and genetically defined. Many parasite genes have been identified, which cause an arrest of the parasite development at distinct time points during liver-stage development when knocked out in murine parasites [101–105]. Remarkably, parasites that were engineered to develop into the later liver-stage forms induced superior effector and memory $CD8^+$ T-cell responses and higher levels of protective immunity in inbred and outbred mice compared to RAS that arrest at earlier liver-stages [106]. A first clinical dose-escalation study investigating a *P. falciparum* $p52^-/p36^-$ GAP showed that this parasite, when given in a high dose (exposure to 200 infected mosquitoes), was still able to complete liver-stage development [107, 108]. Consequently, a new *P. falciparum* GAP that is deficient in P52, P36, and SAP1 (named GAP3KO), was developed and intensively tested for complete liver-stage arrest in preclinical models, including an improved humanised mouse model transplanted with human hepatocytes and human erythrocytes [109]. In a recent human phase I trial, all volunteers remained negative for patent parasitaemia and induced significant immune responses. Hence, GAP3KO will proceed to clinical development [110].

#### *A2.3.1.3 Infection-Treatment Vaccination (ITV) / Chemical Prophylaxis Sporozoite Vaccination (CPS)*

Wild type sporozoites can also be used to induce protective immunity when their development is stopped using chemoprophylaxis. After preclinical proof of concept [111], Roestenberg et al. published a first-in-human trial, which showed 100% protection against homologous CHMI delivered by five mosquito bites one month after discontinuation of chloroquine treatment (which was used during the vaccination period to stop the progression of wild type sporozoites to blood stages) [112]. In addition to CPS strategies using chloroquine, strategies with alternative antimalarial drugs are being investigated. Recently, a clinical trial using mefloquine showed comparable efficacy after CPS immunisation and CHMI [113]. Furthermore, antibiotics that prevent the development

of the parasite apicoplast in the liver (such as azithromcycin, clindamycin, and piperaquine) have been investigated in preclinical mouse studies and showed promising results [114, 115].

### A2.3.2 Subunit Vaccination

As described above, developing vaccines based on attenuated parasites involves significant technical and logistical challenges. Subunit vaccine approaches based on commercially available and scalable vaccine platforms could overcome these issues. However, only a small number of historical candidate antigens have been tested extensively with only limited success in clinical trials. As many more antigens are now being identified from the parasite's genome using omic technologies, novel combinations of antigens can be developed for inclusion in subunit vaccines that could offer higher levels of protection. Several combinations of liver-stage antigens will be discussed in this thesis. Similarly important is the development of vaccine delivery platforms capable of inducing strong immune responses required to protect against the parasite. In recent years, significant advances have been made in this regard, offering further hope for the development of a highly effective subunit vaccine [100].

#### *A2.3.2.1 Pre-erythrocytic Subunit Vaccines*

The development of vaccines against the pre-erythrocytic stage of malaria appears most appealing for three main reasons. (1) Parasites would be cleared before the symptomatic blood-stage. (2) Antigenic polymorphism of pre-erythrocytic stages is far more limited, promising possible strain-transcending immunity against heterologous parasites. (3) The small number of parasites is still manageable and possibly more susceptible to effective immunity compared to later parasite stages, which are characterised by a high parasite burden. On the contrary, the escape of just one parasite from pre-erythrocytic immunity

would lead to blood-stage infection and therefore only delay disease onset in non-immunes.

**RTS,S.** The most advanced malaria vaccine is RTS,S, which has recently been assessed in a large scale phase III clinical trial. It was genetically engineered and contains the repeat region (R) and T-cell epitopes (T) of CSP fused to the hepatitis B surface antigen HBsAg (S) that was assembled with further unfused copies of HBsAg (S) in a 1:4 ratio [116] to form virus-like particles (VLP), which proved to be remarkably immunogenic by inducing high levels of antibodies against CSP. A chemical adjuvant, AS01 (monophosphoryl lipid A and the saponin based QS21 in a liposomal formulation), was added to further increase the immune response of the vaccine [117–120]. Even though efficacy only ranged from about 25–50% in infants and children [2, 121–124], the vaccine has now received a positive scientific opinion from the European Medicines Agency (EMA) for use outside the European Union (EU) [125] and will be the first ever efficacious vaccine against a parasite in humans if it is licensed. However, efficacy still has to be improved, perhaps by inclusion of other subunit components against the sporozoite or other life cycle stages of the parasite.

**Liver-stage subunit vaccines.** Analyses of the immune response induced by WSV have repeatedly shown that high frequencies of liver-stage specific $CD8^+$ T cells are associated with sterile protection [126, 127]. RTS,S, however, mostly confers protection by inducing high titres of anti-sporozoite antibodies [128, 129]. The addition of a vaccine component that strongly induces $CD8^+$ T-cell responses against the liver-stage could therefore result in improved vaccine efficacy. As T-cell responses against CSP are directed against highly polymorphic regions [130, 131] and CSP expression during liver-stage development is less durable in comparison to other liver-stage antigens [132], the most advanced liver-stage vaccine candidate is not CSP, but ME-TRAP, which encodes a multiple epitope (ME)

string, consisting of T- and B-cell epitopes from pre-erythrocytic *P. falciparum* antigens [133], fused to the thrombospondin-related adhesive protein (TRAP) [134]. Many vector platforms and heterologous prime-boost regimens have been assessed for their ability to induce high frequencies of ME-TRAP-specific $CD8^+$ T-cells, very much spear-headed by the Jenner Institute, University of Oxford. The first generation vaccines were based on a prime-boost regimen including a DNA vaccine expressing ME-TRAP, followed by a recombinant and replication-deficient poxvirus (Modified Vaccinia Ankara, MVA) expressing the same antigen. It demonstrated increased immunogenicity compared to each vector alone, and partial protection manifesting as significant delay to patent blood-stage parasitaemia after heterologous sporozoite CHMI was achieved [135, 136]. Subsequently, Webster et al. investigated whether the replacement of plasmid DNA with an attenuated recombinant fowlpox virus (FP9) vaccine encoding ME-TRAP [137] is beneficial. This vaccination regimen induced higher frequencies of antigen-specific T-cells in mice and a similar efficacy in human CHMI trials with 2 of 16 volunteers sterilely protected and one of them still protected 6 and 20 months later against sporozoite CHMI re-challenge [138]. However, in a following Phase IIb field trial among 1- to 6-year-old children in Kenya, vaccine immunogenicity was significantly lower (4x lower IFN-γ producing T cells measured in *ex-vivo* ELISpot assays than in UK volunteers) and no protection against febrile malaria was achieved [139, 140]. Consequently, the use of more potent recombinant replication-deficient adenoviral vectors were considered as priming vectors, particularly given that they had shown greatly superior T-cell responses and protective efficacy in mice [141, 142]. As prevalence of neutralising human adenoviruses is common in human populations, a number of recombinant and replication-deficient chimpanzee adenoviral vectors encoding malaria antigens, such as AdC6, AdC7, AdC9/AdC68 or ChAd63 were investigated in a collaboration between the University of Oxford, the University of Pennsylvania and Okairòs Srl (recently acquired by GSK) [143–

145]. Most importantly, a vaccination regimen with recombinant ChAd63 and MVA encoding ME-TRAP had been shown to be highly immunogenic in animal models, including rhesus macaques [146], and progressed to clinical trials. In a recent clinical study, this vaccination regimen induced exceptionally high frequencies of antigen-specific T cells [147] as well as sterile efficacy against heterologous sporozoites in three of fourteen vaccinees and delay to patent parasitaemia in five more [148]. Interestingly, detailed analysis could only associate mono-functional IFN-γ producing $CD8^+$ T cells with protection, consistent with recent data collected from mouse models [145]. Furthermore, the ChAd63-MVA not only induced high T-cell responses, but also increased the number of recognised epitopes compared to previous vaccination regimens. Encouragingly, Ogwang et al. confirmed these promising results in a phase Ib dose escalation study in healthy Kenyan adults [149]. Age de-escalation studies to assess safety, immunogenicity and efficacy of the ChAd63–MVA heterologous prime-boost vaccination regimen encoding ME-TRAP in African children and infants, also co-administered with vaccines of the WHO "Expanded Program on Immunization" (EPI), are now being conducted and the results are awaited (NCT01635647, NCT02083887).

Despite these encouraging developments, ChAd63-MVA and other liver-stage subunit vaccines still do not provide protective sterilising immunity in the majority of vaccinees. Hence, multiple approaches have been explored to increase immunogenicity and efficacy of viral vectored vaccines, however, with mostly limited success. In 2014, Spencer et al. demonstrated that fusion of ME-TRAP to the MHC class II invariant chain (Ii) could consistently enhance $CD8^+$ T-cell responses across various animal species, including rhesus macaques, when expressed from ChAd63 and MVA vectors [150]. Since protective liver-stage immunity has been strongly associated with increased $CD8^+$ T cell responses, progress of this approach into human clinical trials would be of highest interest. However, as concerns were raised that tolerance against the Ii, a self-antigen, could be broken by

inclusion of the antigen in a strong T-cell inducing vaccination regimen, clinical translation of human Ii chain has been delayed. Chapter D of this thesis will discuss ways to minimise this potential risk to allow progression into clinical trials. Furthermore, given that currently explored liver-stage vaccines lack sufficient efficacy to justify mass deployment, there is now general consensus that a truly effective vaccine will have to contain a combination of several parasite antigens. This hypothesis will also be discussed in this thesis (Chapter C).

#### *A2.3.2.2 Blood-Stage Subunit Vaccines*

The development of vaccines against blood-stage parasites has been extremely challenging [151]. A large number of blood-stage candidate vaccines have progressed to phase I/II clinical trials, but none have reported significant efficacy [152, 153]. This could be due to several factors. First, the development and production of vaccine candidates has mainly been focussed on recombinant protein-in-adjuvant formulations, which were historically challenging to produce with the right protein conformation using heterologous expression systems. Equally problematic has been the extensive antigenic polymorphism [154, 155], coupled with the need for exceptionally high antibody concentrations in order to confer protection – even in animal models [153, 156–158]. Most vaccination approaches have been based on the two blood-stage antigens merozoite surface protein 1 (MSP1) and apical membrane antigen 1 (AMA1). In a field trial in Mali, AMA1 administered with the adjuvant AS02 suggested some strain-specific efficacy, but could not provide significant protection against clinical malaria, the primary end point [153]. Similarly, a trial in Papua New Guinea with a vaccine comprising MSP1, MSP2, and ring-infected erythrocyte surface antigen (RESA) achieved only modest efficacy with a mostly allele-specific immune response [159]. More recently, a DNA-AdHu5 (viral vector based on human adenovirus serotype 5) regimen was investigated with vectors expressing CSP and AMA1,

which achieved some sterile immunity in vaccinees (27%) with protection associated with cell-mediated immunity mostly to AMA1 [160]. This supported the hypothesis that cell-mediated immunity can contribute to protection against blood-stage malaria and suggested to explore viral-vectored blood-stage vaccines, following their demonstration as stimulators of strong cellular and humoral immune responses in numerous animal models [161–165]. In the following years, Sheehy et al. reported two phase 1a trials with ChAd63-MVA prime-boost regimens encoding MSP1 [166] or AMA1 [167]. Both vaccines were safe and immunogenic with high levels of IgG [168], memory B cells [169], as well as $CD4^+$ and $CD8^+$ T cells [170]. However, this did not translate into high levels of efficacy in subsequent phase II CHMI trials [171].

More optimism has arisen following the identification of improved target antigens in the merozoite. For instance, a receptor-ligand pair, basigin and reticulocyte binding protein homolog 5 (Rh5), was identified as essential and non-redundant for erythrocyte invasion by blood-stage parasites and highly susceptible to cross-strain neutralising antibodies [38, 172–175]. Evidence of high-level efficacy induced by Rh5 based vaccines was also demonstrated in a NHP model [176] and led the way to first clinical trials (NCT02181088). Time will tell if these next-generation blood-stage vaccines can achieve similar high levels of efficacy in humans. Even if only modest levels of efficacy are induced, a successful multi-stage malaria vaccine will certainly benefit from the inclusion of a blood-stage component.

#### *A2.3.2.3 Transmission-Blocking Subunit Vaccines*

Transmission-blocking vaccines (TBV) induce antibodies in humans against antigens of sexual blood-stage gametocytes or mosquito-stage parasites. Once taken up by the mosquito, these antibodies then inhibit parasite development. Immunised vaccinees therefore do not gain direct and immediate benefit from the vaccination, but instead

protect their community (and themselves indirectly) from becoming infected [100, 177]. Therefore, transmission blocking vaccines have often been described as 'community' vaccines. These vaccines may have the advantage that mosquito-stage antigens are much less polymorphic compared to antigens of the other stages of parasite´s life cycle [37, 178]. On the other hand, they are often not expressed inside the human host and the immune response induced by a TBV would not be boosted by a subsequent natural infection. Multiple booster vaccinations may therefore be needed to confer long-lasting transmission blocking efficacy.

Before 2016, the only TBV antigens having entered clinical vaccine trials have been Pfs25 (labelled according to its size as determined in SDS-PAGE [179]) and its orthologue in *P. vivax* (Pvs25), which are expressed on zygote and ookinete stages of the parasite [100, 180]. First studies showed no or only modest transmission blocking activity [181, 182], but antibody titres correlated with blocking activity in standard membrane-feeding assays, which strongly supports its use for preclinical assessment of novel vaccine candidates. Efforts to improve immunogenicity of Pfs25 by the inclusion of various adjuvants have been made and showed promising results in preclinical studies [183–186], justifying their progression to clinical trials. Furthermore, many other promising vaccine candidates are now being explored (reviewed in [187]), which could be included in a future multi-stage malaria vaccine.

## A3 Thesis Aims

As introduced above, multiple different ways are being pursued to develop an effective mass deployable malaria vaccine and promising results have been achieved recently, which suggest that high-efficacy vaccines are in reach. Subunit vaccines could overcome the technical and logistical challenges of whole sporozoite vaccines, which have already proven to be highly efficacious in US vaccinees. However, to achieve these levels of efficacy, subunit malaria vaccines will most likely have to include multiple target antigens of the parasite.

The goal of this thesis was to contribute to the development of effective malaria vaccines targeting the liver-stage by improving existing vaccination strategies. As liver-stage parasites hide within hepatocytes, a strong $CD8^+$ T-cell response has to be induced to ensure parasite clearance [188]. Significant progress in improving $CD8^+$ T-cell immunogenicity has been made by using viral vectors as a vaccine platform with the clinically most advanced liver-stage malaria vaccine being administered in a heterologous ChAd63-MVA prime-boost regimen and encoding ME-TRAP. Immunogenicity and efficacy of this vaccination strategy could be further improved by the addition of (or the replacement with) novel liver-stage antigens which have recently been shown to be highly protective in animal models [10]. Furthermore, the inclusion of some vector-encoded adjuvants has been previously considered [150], but did not progress into clinical trials, because of safety concerns. Further research is therefore needed to overcome these issues. Both strategies will be addressed in this thesis, in order to generate a novel and improved liver-stage vaccine candidate to be tested in clinical trials. In detail, the major aims of this thesis are:

- To investigate the combination of classic and novel liver-stage antigens in prime-boost vaccination regimens (Chapter C).

- To develop a previously described molecular adjuvant for viral vectors and investigate its mechanism (Chapter D and F).
- To combine findings to generate a novel, and efficacious liver-stage vaccine candidate to progress to clinical trials (Chapter E).

# Chapter B

# Materials and Methods

# B1 Materials

## B1.1 Reagents

| Material | Manufacturer / Supplier | Catalogue Number |
|---|---|---|
| 0.2 µm bottle top filter (Nalgene) | Fisher | TKV-240-015F |
| 0.2 µm syringe filter | Sartorius | 16534 |
| 15 mL centrifuge tubes | Fisher, Inc. | FB55950 |
| 24-well tissue culture plates | Fisher, Inc. | TKV123011R |
| 2 mL syringes | Nu-Care Products | M0185 |
| 2X Phusion Master Mix with HF buffer | Thermo Fisher Scientific | F-351 |
| 2/β-Mercaptoethanol [50 mM] | Gibco (Thermo Fisher Scientific) | 31350-010 |
| 50 mL centrifuge tubes | Greiner | 227261 |
| 5x In-Fusion® HD Enzyme Premix | Clontech | ST0345 |
| 6-well tissue culture plates | Fisher, Inc. | TKT-520-030T |
| 8-well microscope slides | VWR International | 631-0451 |
| 96-well U bottom plates | VWR International | 734-0027 |
| 96-well V bottom plates | Thermo Fisher Scientific | DIS-210-150L |
| Agar | Sigma Aldrich | A6686 |
| Agarose | Sigma Aldrich | A9539 |
| Alexa Fluor® 488 donkey anti-mouse IgG (H+L) | Life Technologies (Thermo Fisher Scientific) | A21202 |
| Ammonium chloride ($NH_4Cl$) [0.15 M] | Sigma Aldrich | A4514 |
| Ampicillin | Sigma Aldrich | A5354 |
| Anti-Mouse CD4 eFluor® 450, Clone GK1.5 | eBioscience | 48-0041-82 |
| Anti-Mouse CD8a PerCP-Cyanine5.5, Clone 53-6.7 | eBioscience | 45-0081-82 |
| Anti-Mouse IFN gamma APC, Clone XMG1.2 | eBioscience | 17-7311-82 |
| Anti-Mouse IL-2 PE, Clone JES6-5H4 | eBioscience | 12-7021-82 |
| Anti-Mouse TNFa Alexa Fluor® 488, Clone MP6-XT22 | eBioscience | 53-7321-82 |
| AP conjugate substrate kit | Bio-Rad Laboratories | 1706432 |
| Aqua fluorescent reactive dye | Life Technologies (Thermo Fisher Scientific) | L34957 |
| BD Perm/Wash™ buffer | Becton Dickinson | 554723 |
| BD Plastipak™ 5 mL | Becton Dickinson | 302187 |
| Benzonase® nuclease | Novagen | 70664-3 |
| Betaine | Sigma Aldrich | 61962 |
| Bovine serum albumin (BSA) | PAA Laboratories | K41-001 |

| Material | Manufacturer / Supplier | Catalogue Number |
|---|---|---|
| Cell strainer (70 µm) | Falcon | 352350 |
| Cluster tubes | Corning | 4401 |
| cOmplete Mini, EDTA free | Roche | 11 836 170 001 |
| Corning conical tubes, 250 mL PP Centrifuge tube, plug seal cap | Thermo Fisher Scientific | CFT-900-021Y |
| Criterion™ XT Precast Gel, 3–8% Tris-Acetate | Bio-Rad Laboratories | 345-0131 |
| DAPI (4',6-diamidino-2-phenylindole) | Sigma Aldrich | 101101353 |
| Dimethyl sulphoxide (DMSO) | Sigma Aldrich | D2650 |
| Disposable counting slides | Immune Systems Ltd | BVS100 |
| DMEM medium | Sigma Aldrich | D6546 |
| Dried skimmed milk powder | Waitrose | N/A |
| Dulbecco's PBS (D-PBS) | Sigma Aldrich | D8537 |
| Endotoxin free water | Sigma Aldrich | W3500 |
| Ethanol | Sigma Aldrich | 32221 |
| Ethylenediaminetetraacetic acid (EDTA) | Sigma Aldrich | E7889 |
| Fetal Calf Serum (FCS) | Sigma Aldrich | F-2442 |
| Formalin solution, neutral buffered, 10% | Sigma-Aldrich | HT5011-1CS |
| Fructose | Sigma Aldrich | F0127 |
| Gateway® LR Clonase® II enzyme mix | Invitrogen (Thermo Fisher Scientific) | 11791-020 |
| GeneRuler 1 kb, DNA Ladder, ready-to-use | Thermo Fisher Scientific | SM0313 |
| Giemsa | Sigma Aldrich | GS1L |
| Glutamine | Sigma Aldrich | G7513 |
| Glycerol | Sigma Aldrich | G5516-1L |
| GolgiPlug | Becton Dickinson | 555028 |
| Heparin | Sigma Aldrich | H3149 |
| HiMark™ Pre-Stained HMW Protein Standard | Invitrogen (Thermo Fisher Scientific) (Thermo Fisher Scientific) | LC5699 |
| Hydrochloric Acid (HCl) [1 M] | Sigma Aldrich | S-7653 |
| Immersion oil | Sigma-Aldrich | 10890 |
| Isoflurane | Oxford University Veterinary Services | N/A |
| Kanamycin | Sigma Aldrich | K0254 |
| Ketaset™ (ketamine) | Oxford University Veterinary Services | N/A |
| Potassium bicarbonate KHCO3 [1 mM] | Sigma Aldrich | P-9144 |
| LB agar tablet | Sigma Aldrich | L7025-500TAB |
| LB broth tablet | Sigma Aldrich | L7275-500TAB |

| Material | Manufacturer / Supplier | Catalogue Number |
|---|---|---|
| L-glutamine [4 mM] | Sigma Aldrich | G-7513 |
| Lipofectamine™ | Invitrogen (Thermo Fisher Scientific) | 11668-019 |
| MAIP ELIspot Plates | Millipore | MAIPS4510 |
| MEM a-modification | Sigma Aldrich | M-4526 |
| Methanol | Sigma Aldrich | 32213 |
| Microcentrifuge tubes | Thermo Fisher Scientific | FB74031 |
| Micro-fine Insulin Syringe with needle 0.5 mL 29 g x 12.7 mm | Nu-Care Products | M4892 |
| Micro-fine Insulin Syringe with needle 1 mL 29 g x 12.7 mm | Nu-care products | M4891 |
| Microlance needle 26 g x 5/8 inch | Nu-care products | M4300 |
| Microscope slides | Thermo Fisher Scientific | MNJ-200-010H |
| Microvette tubes | Sarstedt | CB300K2E |
| MinElute gel extraction kit | QIAgen | 28606 |
| Minimum Essential Medium Eagle (MEM) α-modification | Sigma Aldrich | M4526 |
| Mouse IFN-g ELISPOT kit (ALP) | Mabtech | 3321-2A |
| Mowiol® 20-98 | Sigma-Aldrich | 11773 |
| Mr. Frosty cryocontainer | Thermo Fisher Scientific | CRY-120-010T |
| NEB® 5-alpha Competent E. coli (High Efficiency) | New England Biolabs | C2987 |
| Ammonium chloride NH4Cl [0.15 M] | Sigma Aldrich | A-4514 |
| NuPAGE® MOPS SDS Running Buffer (20X) | Thermo Fisher Scientific | NP0001 |
| NuPAGE™ 4–12% Bis-Tris Midi Gel | Life Technologies (Thermo Fisher Scientific) | WG1403BX10 |
| PCR primers | Sigma Aldrich | N/A |
| Pen/strep [100 U penicillin / 100 mg strep] | Sigma Aldrich | P-0781 |
| Percoll | Sigma Aldrich | P1644 |
| Peroxidase-conjugated AffiniPure Donkey Anti-Mouse IgG (H+L) | Jackson ImmunoResearch | 715-035-150 |
| Phosphate buffered saline (PBS) | Sigma Aldrich | D-8537 |
| Phusion® High-Fidelity DNA Polymerase | New England Biolabs | M0530L |
| Propan-2-ol | Thermo Fisher Scientific | P/7490/17 |
| Proteinase K | Sigma Aldrich | P2308 |
| Pyrimethamine | Sigma Aldrich | P-7771 |
| QIAamp DNA mini kit | Qiagen | 51304 |
| Qiagen MinElute DNA purification kit | Qiagen | 28604 |
| Qiagen plasmid midi kit | Qiagen | 12143 |

| Material | Manufacturer / Supplier | Catalogue Number |
|---|---|---|
| QIAprep spin miniprep kit | Qiagen | 27106 |
| Restriction, ligation enzymes and buffers | New England Biolabs | Various |
| Ribonuclease A | Sigma Aldrich | R6513 |
| Rompun® (Xylazine) | Oxford University Veterinary Services | N/A |
| RPMI-1640 medium | Sigma Aldrich | R0883 |
| SOC medium | Clontech | ST0215 |
| SOC outgrowth medium | New England Biolabs | B9020S |
| Sodium azide | Sigma Aldrich | S2002 |
| Sodium bicarbonate solution 7.5% | Life Technologies (Thermo Fisher Scientific) | 1423629 |
| Stellar™ Competent Cells | Clontech | ST0213 |
| SuperSignal® West Pico Chemiluminescent Substrate | Thermo Fisher Scientific | 34087 |
| SYBR Safe in DMSO | Invitrogen (Thermo Fisher Scientific) | S33102 |
| T175 Cell culture flask Corning | Fisher, Inc. | TKV123061C |
| T25 Cell culture flask Corning | Fisher, Inc. | TKV123011R |
| T75 Cell culture flask Corning | Fisher, Inc. | TKV123031L |
| Trans-Blot® Turbo™ Transfer Pack | Bio-Rad Laboratories | 170-4158 |
| Transfer pipettes | Thermo Fisher Scientific | FB55348 |
| Tris-acetate-EDTA (TAE) | Thermo Fisher Scientific | BP1332-1 |
| Triton™ X-100 | Sigma Aldrich | X100 |
| Trizma® HCL buffer solution (pH 7.8) | Sigma Aldrich | T-2569 |
| Trizma® HCL buffer solution (pH 8) | Sigma Aldrich | T2694 |
| Trypan Blue | Sigma Aldrich | T8154 |
| TrypLE™ Express Enzyme (1X) | Life Technologies (Thermo Fisher Scientific) | 12605-010 |
| Ultra-centrifuge polycarbonate 1.6 mL tubes | Beckman Coulter | 362305 |
| SuperSignal™ West Pico Chemiluminescent Substrate | Thermo Fisher Scientific | 34077 |
| XT Sample Buffer, 4x | Bio-Rad Laboratories | 161-0791 |
| XT Tricine | Bio-Rad Laboratories | 161-0790 |

## B1.2 Solutions and Buffers

| Solution or Buffer | Recipe / Ingredients |
|---|---|
| 1% BSA/PBS | ▪ 500 mL D-PBS<br>+ 5 g BSA |

| Solution or Buffer | Recipe / Ingredients |
|---|---|
| 3% BSA/PBS | ▪ 500 mL D-PBS<br>+ 15 g BSA |
| ACK Lysis Buffer | ▪ 800 mL $dH_2O$<br>+ 8.29 g $NH_4Cl$ (0.15 M)<br>+ 1 g $KHCO_3$ (1 mM)<br>+ 37.2 mg $Na_2EDTA$<br>▪ pH adjustment with HCl (1 M) to pH 7.2–7.4<br>▪ + $dH_2O$ to final volume of 1 L |
| Buffer A | ▪ $dH_2O$<br>+ 50 mM Tris<br>+ 100 mM NaCl<br>+ 5 mM $MgCl_2$<br>+ 1% Triton X-100 |
| Cell Lysis Buffer | ▪ $dH_2O$<br>+ 50 mM Tris HCl (pH7.5)<br>+ 150 mM NaCl<br>+ 1% Triton X-100<br>+ 0.1% sodium dodecyl sulfate<br>+ 0.5% sodium deoxycholate<br>▪ Added just before use:<br>+ Protease inhibitor (cOmplete, Mini, EDTA-free, Roche):<br>1 tbl per 25 mL |
| Coating Buffer (ELISpot) | ▪ $dH_2O$<br>+ 15 mM sodium carbonate<br>+ 35 mM sodium bicarbonate<br>▪ autoclavation |
| Complete α-MEM Medium | ▪ 500 mL MEM α-modification<br>+ 5 mL L-glutamine (2 mM)<br>+ 5 mL pen/strep (100 U penicillin, 100 µg streptomycin)<br>± 500 µL 2-mercaptoethanol (→ 50 µM)<br>+ 50 mL of heat inactivated FCS (10%) |
| Complete RPMI | ▪ 500 mL MEM α-modification<br>+ 5 mL L-glutamine (2 mM)<br>+ 5 mL pen/strep (100 U penicillin, 100 µg streptomycin)<br>+ 50 mL of heat inactivated FCS (10%) |
| Exflagellation Medium | ▪ RPMI-1640<br>+ 25 mM HEPES<br>+ 20% FCS<br>+ 10 mM sodium bicarbonate<br>+ 50 µM xanthurenic acid<br>▪ pH adjustment to pH 7.6 |
| Giemsa Solution | ▪ $dH_2O$<br>+ 10% Giemsa |
| LB Agar/Broth | ▪ $dH_2O$<br>+ LB tablets (1 tablet per 50 mL)<br>▪ Antibiotics were added in the following concentrations:<br>○ 100 µg/mL ampicillin<br>○ 25 µg/mL kanamycin<br>○ 12.5 µg/mL chloramphenicol |

| Solution or Buffer | Recipe / Ingredients |
|---|---|
| Mowiol | ▪ 6 mL $dH_2O$<br>+ 6 g glycerol<br>+ 2.4 g polyvinyl alcohol 4-88<br>▪ Incubation for 2 h at 50°C with agitation<br>▪ + 12 mL Tris pH 8.5 (0.2 M)<br>▪ Dissolving for 3 h at 50°C with agitation<br>▪ Centrifugation at 2500 rpm for 5 min to remove any undissolved solids<br>▪ + DAPI at final concentration of 0.1 µg/mL |
| Parasite Freezing Medium | ▪ 96 mL RPMI-1640<br>+ 11 mL FCS<br>+ 4.2 mL 5% $NaHCO_3$<br>+ 5.5 mg neomycin<br>Or:<br>▪ D-PBS<br>+ glycerol (30% of total V)<br>+ 10 IU Heparin/mL |
| PBS (0.1 M) | ▪ $dH_2O$<br>+ dissolving tablets according to the manufacturer´s instructions ( = 0.138 M NaCl, 0.0027 M KCl, pH 7.4) |
| PBS/Tween (PBS/T) (0.1 M) | ▪ $dH_2O$<br>+ dissolving tablets according to the manufacturer´s instructions ( = 0.138 M NaCl, 0.0027 M KCl, Tween 0.05%, pH 7.4) |
| Perm/Wash | ▪ 10x Perm/Wash buffer diluted in $dH_2O$ to 1x prior to use |
| TAE Buffer | ▪ 50x concentrate diluted to 1x with $dH_2O$ |
| Triton X-100 (0.2%) | ▪ 50 mL sterile PBS<br>+ 100 µL Triton X-100 |

# B2 Methods

## B2.1 Molecular Biology

### B2.1.1 Software

DNA maps were designed and cloning steps prepared using the DNASTAR Lasergene Suite (DNASTAR, Inc., Madison, Wisconsin, USA).

### B2.1.2 Agarose Gel Electrophoresis

Unless stated otherwise, DNA samples were prepared with 6× DNA Gel Loading Dye (Thermo Fisher Scientific, Waltham, Massachusetts, USA) and analysed using electrophoresis (100 V, 50 min) with 1% agarose (Sigma Aldrich, St. Louis, Missouri, USA) gels prepared with in Tris-acetate-EDTA (TAE) (Sigma-Aldrich) buffer and SYBR® Safe (1:10,000) (Thermo Fisher Scientific). Band sizes and approximate quantification was determined by comparison with GeneRuler 1 kb DNA ladder (Thermo Fisher Scientific) on a transilluminator (UVP, Jena, Germany). For cloning or sequencing, bands were excised and purified with the QIAquick Gel Extraction Kit (Qiagen, Hilden, Germany) according to the manufacturer´s instructions.

### B2.1.3 Restriction Endonuclease Digest

DNA samples were digested using restriction endonucleases from New England Biolabs (NEB, Ipswich, Massachusetts, USA) with the appropriate NEB buffer (with or without BSA) at 37°C for 2–4 h according to the manufacturer´s recommendations in a microcentrifuge tube as summarised in Table B-1.

**Table B-1.** Standard restriction endonuclease digest.

| Reagent | Quantity |
|---|---|
| NEB Restriction Enzyme | 10 U (usually equals 1 µL) |
| NEB Restriction Buffer (10×) | 2 µL |

| Reagent | Quantity |
|---|---|
| (BSA 10×) | (2 µL) |
| DNA sample | 0.5–2.0 µg |
| Nuclease-free $H_2O$ | to total volume of 20 µL |

### B2.1.4 DNA Ligation

DNA fragments were inserted into vector DNA with T4 DNA Ligase (NEB) according to the manufacturer´s instructions. Briefly, the ligation reaction was set up as outlined in Table B-2 and incubated at 16°C overnight or at room temperature (RT) for 10 min (cohesive ends) or 2 h (blunt ends), respectively.

**Table B-2.** Standard ligation reaction.

| Reagent | Quantity |
|---|---|
| NEB T4 DNA Ligase | 1 µL |
| NEB T4 DNA Ligase Buffer (10×) | 2 µL |
| Vector DNA | 100 ng |
| Insert DNA | Molar ratio of 1:3 (vector to insert; calculated with NEBioCalculator, http://nebiocalculator.neb.com/#!/ligation) |
| Nuclease-free $H_2O$ | to total volume of 20 µL |

### B2.1.5 In-Fusion® Cloning

When cloning was not possible using traditional cloning techniques, such as restriction enzyme digestion and ligation, the In-Fusion® HD Cloning Kit (Takara Bio Europe, Saint-Germain-en-Laye, France) was used according to the manufacturer´s instructions. The protocol included several steps:

1) The base vector was linearised by restriction enzyme digest and purified by agarose gel electrophoresis as well as the QIAquick Gel Extraction Kit (Qiagen) according to the manufacturer´s instructions. If there was no suitable restriction site close to the area of interest, the base vector was linearised using Polymerase Chain Reaction (PCR), the template DNA then digested with the restriction enzyme DpnI, and the linearised PCR

product purified using the QIAquick® PCR Purification Kit (Qiagen) according to the manufacturer´s instructions.

2) The insert (gene of interest) was designed with 15 base pair (bp) extensions (5´) that were complementary to the ends of the linearised vector. This was achieved by PCR with accordingly designed PCR primers and purifying the product with a DpnI digest and QIAquick® PCR Purification Kit (Qiagen) or by ordering custom-made uncloned, double-stranded linear DNA fragments (GeneArt™ Strings from Thermo Fisher Scientific).
3) The In-Fusion® cloning reaction was set up according to Table B-3, incubated for 15 min at 50°C, and then placed on ice prior to transforming the reaction mixture into competent cells.

**Table B-3.** In-Fusion® cloning reaction.

| Reagent | Quantity |
|---|---|
| 5× In-Fusion® HD Enzyme Premix | 2 µL |
| Linearised vector | 200 ng |
| Insert DNA fragment | 25 ng |
| Nuclease-free $H_2O$ | to total volume of 10 µL |

### B2.1.6 Polymerase Chain Reaction

The Phusion High-Fidelity PCR Master Mix with HF Buffer (Thermo Fisher Scientific) was used for PCR in a TProfessional Thermocycler (Biometra, Göttingen, Germany) to amplify or modify specific DNA sequences. Typical reaction components and cycling conditions are described in Table B-4 and Table B-5, respectively. The optimal annealing temperatures were determined using instructions and the Tm calculator and on www.thermofisher.com.

**Table B-4.** PCR components.

| Reagent | Quantity (20 µL reaction) | Quantity (50 µL reaction) |
|---|---|---|
| 2× Phusion Mastermix | 10 µL | 25 µL |
| Forward Primer | 0.5 µM | 0.5 µM |
| Reverse Primer | 0.5 µM | 0.5 µM |
| Template DNA | 10 ng | 10 ng |
| Betaine (5M) | 4 µL | 10 µL |
| Nuclease-free $H_2O$ | to total volume of 20 µL | to total volume of 50 µL |

**Table B-5.** PCR cycling conditions.

| Step | Procedure | Temperature | Duration |
|---|---|---|---|
| 1) | Initial denaturation | 98°C | 30 sec |
| 2) | Denaturation | 98°C | 10 sec |
| 3) | Annealing | Tm calculator | 20 sec |
| 4) | Extension | 72°C | 25 sec/kb |
| 5) | 30 cycles of steps 2–4 | | |
| 6) | Final extension | 72°C | 8 min |
| 7) | Hold | 4°C | ≤ overnight |

### B2.1.7 Site-Directed Mutagenesis

To introduce site-directed mutations, the plasmid of interest was amplified using PCR (B2.1.6) with primers which met, but did not overlap, and carried mutations in their 5´ends. Primers were 18–30 bp in length with annealing temperatures (Ta) of 55–68°C and designed to keep mispriming and hairpins to a minimum. Following the PCR, 5 µL of the PCR product were visualised as a control by gel electrophoresis. DpnI (1 µL) was added directly to the remaining PCR reaction and incubated at 37°C for 30 min to digest the template plasmid DNA. The mutated, linearised, and amplified plasmid DNA was phosphorylated using T4 DNA kinase (NEB) and ligated with T4 Polynucleotide Kinase (NEB) in one reaction at RT for 20 min (Table B-6) and then transformed into competent cells.

**Table B-6.** Ligation protocol for linearised, mutated plasmid DNA.

| Reagent | Quantity |
|---|---|
| Nuclease-free $H_2O$ | 6 µL |
| PCR mix following DpnI digestion | 10 µL |
| 10× T4 DNA Ligase Buffer | 2 µL |
| T4 Polynucleotide Kinase | 1 µL |
| T4 DNA Ligase | 1 µL |

### B2.1.8 Bacterial Transformation

Cloning products were transformed either into NEB® 5-α Competent E. coli (NEB) or into Stellar™ Competent Cells (Clontech, Mountain View, California, USA). Briefly, 2–5 µL of DNA was added to 50 µL of NEB® 5-α (in a microcentrifuge tube) or 50 µL of Stellar™ cells (in 14 mL Falcon® round-bottom tubes) and incubated on ice for 30 min. Subsequently, cells were heat shocked at 42°C for 30 seconds in case of NEB® 5-α, or 45 seconds in case of Stellar™ cells, and then placed back on ice for 2–5 min. After adding 950 µL of Super Optimal Broth with Catabolite Repression (SOC) media, cells were incubated at 37°C and 230 rpm in the shaking incubator for 60–90 min. Then, cells were plated onto LB agar plates containing the relevant antibiotic for selection and incubated at 37°C overnight.

### B2.1.9 DNA Preparation

**Initial DNA preparation.** Individual bacterial colonies were transferred from culture plates into 4 mL LB broth containing the relevant selection antibiotics and incubated overnight at 37°C and 230 rpm. The following day, purified DNA was extracted using the QIAprep Spin Miniprep Kit (Qiagen) according to the manufacturer´s instructions and quantified with a NanoDrop Spectrophotometer (Thermo Fisher Scientific). The correct sequence was either confirmed by analytical restriction enzyme digest and/or Sanger sequencing services (Source BioScience, Nottingham, UK).

**Plasmid DNA preparation.** To prepare greater quantities of purified plasmid DNA, the relevant bacteria were incubated in 40 mL of LB broth containing selection antibiotics and incubated at 37°C and 230 rpm overnight. The following day, a bacterial stock was made by spinning 1.5 mL of the bacterial culture (2500 g, 2 min), resuspending in LB broth containing 10% glycerol (Sigma-Aldrich) and stored at −80°C. The rest of the bacterial culture was used to extract plasmid DNA using the QIAGEN Plasmid Plus Midi Kit (Qiagen) according to the manufacturer´s instructions and quantified with a NanoDrop Spectrophotometer. The insert sequence was then confirmed by Sanger sequencing services, if not done before.

**Preparation of bacterial artificial chromosomes (BAC).** ChAdOX1 constructs were encoded in BAC rather than bacterial plasmids. Bacteria expressing the ChAdOX1 BAC were grown in 200 mL LB broth containing chloramphenicol overnight at 37°C and 230 rpm. The following day, a bacterial stock was made by spinning 1.5 mL of the bacterial culture (2500 g, 2 min), resuspending in LB broth containing 10% glycerol (Sigma-Aldrich) and stored at −80°C. The rest of the bacterial culture was centrifuged (6000 g, 15 min, 4°C), resuspended in buffer P1 (Qiagen), and lysed by gently adding 10 mL of buffer P2 (Qiagen). After 2 min 10 mL of ice-cold buffer P3 (Qiagen) was added and mixed. After centrifuging the cell debris at 10,000 g for 15 min at 4°C, the supernatant was transferred into a fresh tube and centrifuged again. Then the BAC was precipitated in 35% isopropanol (Sigma-Aldrich), centrifuged (15,000 g, 4°C, 30 min) and washed with cold 70% ethanol. After another spin (15,000 g, 4°C, 15 min), BAC were dissolved in 400 µL buffer QF (Qiagen) for 10 min. After adding 2 mL of buffer QBT (Qiagen), the DNA was pipetted on Qiagen-20 columns (pre-equilibrated with buffer QBT), washed twice with buffer QC (Qiagen), and eluted with 800 µL of buffer QF (preheated to 65°C). The DNA was again precipitated with 35% isopropanol and washed with 70% ethanol as described

above. Finally, the BAC was dissolved in 50 µL of sterile endonuclease free water and quantified using a NanoDrop Spectrophotometer.

### B2.1.10 Viral Vector Cloning

The recombinant ChAd63 and ChAdOX1 vaccines were cloned using the Invitrogen™ Gateway™ cloning technology (Thermo Fisher Scientific) to simplify the cloning procedure.

**Entry vectors.** As entry vectors pENTR4/LPTOS (Jenner Institute plasmid number p1990) was used for all constructs encoding ME-TRAP and pENTR4/Mono (p2022) for constructs encoding LSA1 or LSAP2. Both vectors contain the bovine growth hormone poly(A) transcription termination sequence, but differ in the human CMV immediate-early (IE) promotor that is used to drive transcription. Whereas pENTR4/LPTOS contains the "long" version of the promotor including intron A, pENTR4/Mono contains the intron-less and non-splicing version. The vector inserts were cloned between the Gateway™ attachment L (attL) sites using either restriction endonuclease digest (B2.1.3) and DNA ligation (B2.1.4) or In-Fusion® reactions (B2.1.5). The pENTR4/Mono-[insert] and pENTR4/LPTOS-[insert] vectors were then transformed into E. coli bacteria (B2.1.8) and the plasmid DNA produced as described in section B2.1.9. The correct insert sequence of all entry vectors was confirmed by Sanger sequencing services.

**Adenoviral destination vectors.** The entry vectors were subsequently inserted into the E1 locus of an E1 and E3-deleted adenoviral genome, either ChAd63 (p1916) or ChAdOX1 (p2563), by site-specific recombination using the Gateway® LR Clonase® II Enzyme mix (Thermo Fisher Scientific) according to the manufacturer´s instructions. After termination of the reaction with proteinase K (Thermo Fisher Scientific), DNA was transformed into competent *E. coli* bacteria (B2.1.8) and the plasmid DNA produced as

described in section B2.1.9. The correct length of the insert DNA was confirmed by restriction enzyme digest using *KpnI* (NEB) (B2.1.3). The expression vector was then linearised using the restriction enzyme *PmeI* (NEB) and delivered to the Viral Vector Core Facility of the Jenner Institute for production of viral vectors (B2.2.1, p. 41).

**Modified Vaccinia Ankara (MVA) vectors.** For production of MVA vaccines, the vaccine antigen was inserted into the thymidine kinase (TK) locus under the control of the p7.5 promoter of a markerless MVA plasmid (MVA/TD/GFP) with classic restriction endonuclease digest and DNA ligation methods. The antigen insert was extracted from the pENTR4 plasmid using the restriction enzymes Acc65I and NotI as described in B2.1.2–B2.1.4. The final MVA vector was then transformed into E. coli bacteria (B2.1.8) and the plasmid DNA produced as described in section B2.1.9. The correct length of the insert DNA was confirmed by restriction enzyme digest using KpnI (NEB) (B2.1.3). The expression vector was passed over to the Viral Vector Core Facility of the Jenner Institute for production of viral vectors.

### B2.1.11 Summary of Cloned Plasmids

Supplemental Table I-1 (p. 215) lists of all plasmids cloned in this work.

## B2.2 Vaccine Production

All recombinant adenoviral vectors (ChAd63, ChAdOX1, and MVA) were kindly produced by the Viral Vector Core Facility of the Jenner Institute, led by Dr Alison Turner.

### B2.2.1 Adenoviral Vectors

The linearised recombinant adenoviral vector (B2.1.10) was transfected into pre-prepared T-REx™ 293 cells and incubated at 37°C (5% $CO_2$) until an optimal cytopathic effect was monitored. The T-REx™ 293 cell line is based on primary human embryonic kidney cells

and is permissive for replication-incompetent E1 and E3 deleted adenoviruses, as it provides the E1 gene product *in trans*. Furthermore, in T-REx™ 293, cells the inserted antigen is silenced during virus production due to the expression of the tetracycline repressor protein that bind to two tetracycline repressor-operator complexes in the CMV promoter. Then, cells were harvested and purified by density centrifugation using a caesium chloride gradient. Virus titre was determined by plaque immunostaining and identity was confirmed by PCR.

### B2.2.2 Modified Vaccinia Ankara (MVA) Vectors

Chick Embryo Fibroblasts (CEF) (Pirbright Institute, Compton, UK) were infected with MVA expressing red fluorescent protein (RFP). 90 min later, the same cells were transfected with the MVA-TD-GFP-[insert] plasmids (B2.1.10) to allow homologous recombination to occur between the MVA virus and the newly cloned plasmid. After incubation, unstable intermediate products expressing both, GFP and RFP, cells were sorted at the Jenner Institute Flow Cytometry Facility (led by Andrew Worth) using a MoFlo Legacy MLS High Speed Cell Sorter (Beckman Coulter, Brea, California, USA). Lysates of collected cells were used to infect CEF again. Successful recombinant MVA encoding the antigen were selected by plaque picking. The virus was then bulked up, purified, analysed by identity and purity PCR, and finally titrated to determine the concentration of viruses in plaque forming units (PFU).

### B2.2.3 Summary of Viral Vectors

Supplemental Table I-2 (p. 223) lists of all viral vectors used in this work.

## B2.3 Animals and Animal Handling

### B2.3.1 Ethics and Laboratory Mice

All mice procedures were conducted in accordance with the UK Animals (Scientific Procedures) Act 1986 and approved by the University of Oxford Animal Care and Ethical Review Committee for use under Project License 30/2889. Animals were maintained at the Wellcome Trust Centre for Human Genetics Functional Genetics Facility in a specific-pathogen-free environment with individually ventilated cages. A 12 h light-dark cycle was used and temperature, as well as humidity, were kept constant. For *in vivo* imaging studies (B2.3.9), mice were temporarily moved to the Radiobiology Research Institute. In this thesis, studies were performed in various inbred and outbred mouse strains from Envigo (Harlan, UK) as listed in Table B-7.

**Table B-7.** Laboratory Mice.

| Laboratory Mouse Strain | | MHC Haplotype |
|---|---|---|
| Inbred | BALB/c | H-$2^d$ (H-$2K^d$, H-$2D^d$, H-$2L^d$, H-$2A^d$, H-$2E^d$) |
| Inbred | C57BL/6 | H-$2^b$ (H-$2K^b$, H-$2D^b$, H-$2L^b$, H-$2A^b$, H-$2E^b$) |
| Inbred | CBA | H-$2^k$ (H-$2K^k$, H-$2D^k$, H-$2L^{null}$, H-$2A^k$, H-$2E^k$) |
| Outbred | CD-1 | N/A |
| Outbred | TO | N/A |

### B2.3.2 Immunisation of Mice

Mice were anaesthetised with 3.5% isoflurane carried by medical oxygen (2 L/min) and immunised intramuscularly (IM) into the *M. tibialis* in a total volume of 50 µL per injection site using a 29-gauge needle (Becton Dickinson, Franklin Lakes, New Jersey, USA). As stated in the relevant text and figure legends, ChAd63 were injected at a dose of either $10^8$ or $10^7$ infectious units (IU). MVA was given at a dose of $10^6$ or $10^7$ PFU. For dilutions endotoxin-free PBS (Sigma-Aldrich) was used.

### B2.3.3 Intraperitoneal Injections

Intraperitoneal (IP) injections (100–300 µL) were administered using a 28-gauge needle (Becton Dickinson).

### B2.3.4 Blood and Serum Samples

For blood samples, 6–10 drops of peripheral blood were collected from the lateral tail vein into a sterile 1.5 mL microcentrifuge tube containing 200 µL EDTA/PBS (10 mM EDTA) and mixed instantly. Then, 1 mL of ammonium-chloride-potassium (ACK) lysis buffer was added, incubated for 5 min, and centrifuged at 1,500 g for 4 min. The cell pellet was resuspended in 1 mL of ACK lysis buffer, again incubated for 5 min, centrifuged (1,500 g, 4 min), and resuspended in a sufficient volume of complete α-MEM medium for downstream processing (325 µL if one peptide pool was analysed, 475 µL if two peptide pools were analysed).

For collection of mouse sera, a small amount of mouse blood was collected from the lateral tail vein using a microvette tube (Sarstedt, Nümbrecht, Germany) and stored at 4°C overnight to allow clotting. The following day, the filled microvette tubes were centrifuged at 7,000 g for 7 min. The serum was then transferred into a sterile 1.5 mL microcentrifuge and stored at −20°C until required for analysis.

### B2.3.5 Spleen Samples

For analysis of mouse splenocytes, mice were sacrificed by cervical dislocation prior to dissection of the spleen. Spleens were crushed with the back of the plunger from a 5 mL syringe (BD Plastipak™, Becton Dickinson) in a 6-well tissue culture plate (Corning Inc., Corning, New York, USA) and 2–5 mL PBS. Cells were then filtered through a 70 µm cell strainer (Thermo Fisher Scientific) and centrifuged at 400 g for 5 min. Subsequently, cell pellets were resuspended in 5 mL ACK lysis buffer (chemicals from Sigma-Aldrich) for

5 min to lyse RBC. Lysis reaction was stopped by adding 25 mL PBS before centrifugation (400 g, 5 min). Splenocytes were then resuspended in 5 mL complete α-MEM and counted by a CASY counter (Schärfe System, Reutlingen, Germany) before using in immunological assays.

### B2.3.6 Liver Samples

To isolate liver mononuclear cells, mice were sacrificed by cervical dislocation. The circulating blood was flushed out of the liver by injecting sterile PBS into the hepatic portal vein prior to excising the liver. The liver was crushed and mashed through a 70 µm cell strainer with the plunger of a 2 mL syringe (Becton Dickinson) in a petri dish. PBS was used to flush the cell strainer and petri dish and collect the filtered cells in a 15 mL tube. After centrifugation (500 g, 7 min) cells were resuspended in 10 mL of 33% isotonic percoll solution (Sigma Aldrich). Cells were then centrifuged without brakes at 693 g for 12 min. Subsequently, the upper layers were removed with a pipette before resuspending the remaining cell pellet in 1 mL ACK lysis buffer for 4 min at RT. After incubation, 10 mL complete α-MEM was added and the sample was centrifuged again (500 g, 5 min). Finally, cells were resuspended in up to 500 µL complete α-MEM, counted by a CASY counter, and used in immunological assays.

### B2.3.7 Sporozoite Challenge

Efficacy of malaria vaccines was tested by challenging immunised mice and naïve control mice with 1,000 sporozoites injected into the lateral tail vein. Mouse parasitaemia was monitored from day 4 or 5 post challenge by thin blood smears (B2.3.8). Mice were sacrificed when parasitaemia levels reached 1%, provided positive parasitaemia was confirmed on three consecutive days. The parasitaemia level from three blood smears allowed calculation of the time to 1% parasitaemia via linear regression. On day 15 post

challenge, all remaining mice (negative thin blood films) were classed as protected and sacrificed by cervical dislocation.

### B2.3.8 Thin Blood Smears

To monitor parasitaemia in mice after sporozoite challenge, thin blood smears were prepared by snipping the very end of the mouse´s tail, collecting a small mount (< 1 drop) of blood on a microscope slide (Menzel Gläser, Braunschweig, Germany), and smearing the blood with the end of another clean microscope slide. After air-drying, the blood smear was fixed in 100% methanol (Sigma-Aldrich) for > 1 min and then stained in 10% Giemsa (Sigma-Aldrich) diluted in 18 mΩ $H_2O$ for 20 min. The slide was then washed with tap water, air-dried and analysed on a light microscope at 100× magnification with an oil immersion objective. The percentage of infected RBC was counted in at least 10 fields of view.

### B2.3.9 In Vivo Imaging

Four double-transgenic parasites had not been used in challenge experiments in our institute before. To verify their ability to infect mouse hepatocytes, an in vivo imaging experiment was performed using the IVIS 200 imaging system (Perkin Elmer, Waltham, MA, USA) as previously described [189] in collaboration with Dr Ahmed Salman (The Jenner Institute, University of Oxford). 44 hours post infection, the level of liver-stage burden was assayed via bioluminescence of the parasite, which expressed the luciferase reporter gene. The mice were shaved in the liver area, anaesthetised (3.5% isoflurane, 2 L/min oxygen), and injected with 50 µL of D-luciferin substrate (50 mg/mL) subcutaneously (SC) into the scruff of the neck. Exactly eight min after injection, mice were imaged with an exposure time of 2 min. Quantification of bioluminescence was

performed using the Living Image® 4.2 (Perkin Elmer, Waltham, Massachusetts, U.S.) and expressed as total flux of photons emitted per second of exposure time.

## B2.4 Immunology

### B2.4.1 Peptides

Peptides used in immunological assays were acquired from commercial suppliers (NeoScientific, Woburn, Massachusetts, USA; Mimotopes, Wirral, UK; or Thermo Fisher Scientific). Crude 20mer peptides overlapping by ten amino acids (aa) for the entire protein sequence of *P. falciparum* TRAP, TRIP, CSP, LSA1, LSAP2, UIS3, Falstatin, or the human Ii were used. Peptides were reconstituted in DMSO at 50–100 mg/mL depending on their solubility and combined into a final peptide pool for cellular assays. Peptide sequences are provided in the appendix (I3, p. 228). For the human Ii, several sub-pools were prepared: hIi-Cytplasmic-Tail (Ii-1 to Ii-11), hIi-TMD (Ii-12 to Ii-16), and hIi-Luminal-Tail (Ii-17 to Ii-56).

### B2.4.2 Intracellular Cytokine Staining (ICS) of PBMC and Splenocytes

Mouse peripheral blood mononuclear cells (PBMC) or splenocytes were plated in 96-well round bottom plates (V = 150 µL) and stimulated by the addition of 50 µL of individual peptides or pools of overlapping 20mers covering the whole protein (TRAP, LSA1, LSAP2, UIS3, Falstatin, or Ii as indicated) at a final concentration of 2 µg/mL in the presence of 1 µg/mL BD GolgiPlug™, and incubated for 6 hours (37°C, 5% $CO_2$) before overnight storage at 4°C. The following day, cell surfaces were labelled with anti-CD4-e450 and anti-CD8-PerCP/Cy5.5 antibodies (Affymetrix eBioscience, San Diego, California, USA) as well as LIVE/DEAD® Fixable Aqua Dead Cell Stain Kit (Thermo Fisher Scientific) in 50 µL PBS containing 1% bovine serum albumin (Sigma-Aldrich) at 4°C for 30 min. Then, cells were spun down (600g, 4 min) and fixed by resuspending in 100 µL of neutral buffered

formalin solution containing 4% formaldehyde (Sigma-Aldrich) at 4°C for 5 min. After adding 100 µL of 1× BD Perm/Wash™ buffer (Becton Dickinson), cells were centrifuged as above. Then, intracellular staining was performed with anti-TNF-Alexa488, anti-IL-2-PE and anti-IFN-γ-Alexa647 antibodies (Affymetrix eBioscience) diluted in 50 µL BD Perm/Wash™ buffer for 30 min at 4°C. Cells were washed with BD™ Perm/Wash™ buffer and again with PBS and then analysed using a BD™ LSR II Flow Cytometer with BD FACSDIVA™ (Becton Dickinson) and FlowJo (Tree Star Inc., Ashland, Oregon, USA) software. The gating strategy used for all ICS experiments is shown in Figure B-1. Background responses in unstimulated wells were subtracted from responses of stimulated T cells.

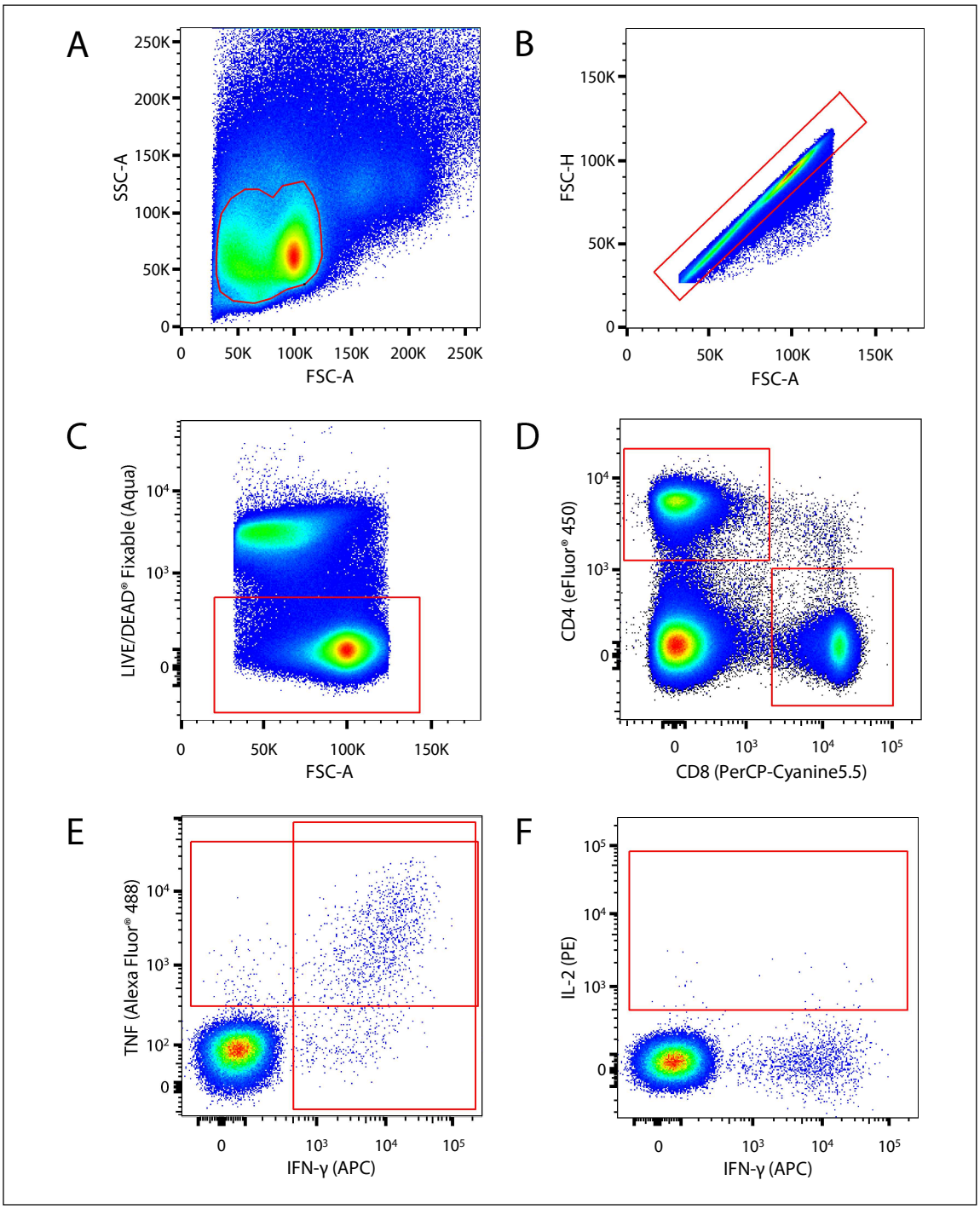



**Figure B-1. Gating Strategy.** The initial gate was set on the lymphocyte population by analysing the forward scatter (FSC) and side scatter (SSC) data (A), followed by a gate to exclude cell doublets (B). After excluding dead cells (C), lymphocytes were separated into $CD4^+$ or $CD8^+$ T-cell subsets. Finally, cytokine positive cells were gated from those subsets (E and F).

### B2.4.3 ELISpot Assay

A day before analysis of mouse samples, ELISpot plates (Mabtech AB, Nacka Strand, Sweden) were coated with 50 µL of purified anti-IFN-γ monoclonal Ab AN18 (Mabtech) (5 µg/mL in coating buffer) at 4°C overnight. The following day, plates were washed 3× with PBS and blocked with 100 µL complete α-MEM for ≥ 1 hour (37°C, 5% $CO_2$) before seeding 50 µL of mouse splenocytes in duplicates and serially (1:1) diluted to achieve different plating cell concentrations. 50 µL of stimulating peptides (1 µg/mL in complete α-MEM) were added and incubated for 18–20 h (37°C, 5% $CO_2$); wells containing splenocytes plus complete α-MEM (without peptides) served as unstimulated controls.

After incubation, plates were washed 6× with PBS using an automated plate washer (Dynex Technologies, Chantilly, Virginia, USA) and incubated with 50 µL of biotinylated rat anti-mouse IFN-γ diluted in PBS (final concentration of 1 µg/mL) for 2 h at RT. Subsequently, plates were washed 6x and incubated with 50 µL of alkaline phosphatase (AP) conjugate development buffer (Bio-Rad) for 5–10 min until spots appeared clearly visible. The reaction was stopped by washing the plate with tap water. After air-drying, spots were counted using an ELISpot plate counter (AID, Strassberg, Germany) and expressed as spot forming units (SFU) per million splenocytes. Responses in unstimulated wells were subtracted from the result in peptide-stimulated wells.

### B2.4.4 Luminescence Immunoprecipitation Assay (LIPS)

Antibody responses to TRAP, LSA1, LSAP2, or Falstatin were measured using a luciferase immunoprecipitation system as previously described [190]. The assay is based on binding of immobilised antibodies to a fusion protein of the relevant antigen to *Renilla* luciferase (rLuc). Briefly, serum samples were incubated with a cell lysate from HEK 293 cells transfected with an [antigen]-rLuc expression plasmid for 1 hour, prior to incubation with Protein A/G UltraLink Resin beads (Thermo Fisher Scientific) in MultiScreen HTS

membrane Barex plates (EMD Millipore, Billerica, Massachusetts, USA) for 1 h. Unbound lysate and antibodies were removed by washing the plates prior to quantification of bound rLuc activity using Renilla luciferase assay system (Promega, Madison, Wisconsin, United States) and a Varioskan™ Flash luminometer (Thermo Fisher Scientific). Antibody levels are expressed as log10 luminescence units (LU) and background response to each antigen was defined as the average of six naïve replicates plus twice the standard deviation.

## B2.5 Microscopy and Protein Expression

### B2.5.1 Cell Transfection

A549 cells (human adenocarcinoma epithelial cell line) or HEK 293 cells (cell line originally derived from human embryonic kidney cells) were used for transfection experiments. When cells were used for fluorescence imaging, 48-well or 6-well flat bottom plates were prepared with sterile coverslips (VWR International, Radnor, Pennsylvania, USA). Then, 35,000 cells per well (in 48-well plates) or 400,000 cells per well (in 6-well plates) were seeded in complete RPMI and incubated overnight at 37°C and 5% $CO_2$. The following day, plasmid DNA was transfected using Lipofectamine® 2000 (Thermo Fisher Scientific) according to the manufacturer´s protocol. Briefly, 300 ng (in 48-well plates) or 3 µg (in 6-well plates) of plasmid DNA was diluted in Opti-MEM (Thermo Fisher Scientific) and incubated for 20 min at RT before incubation with cultured cells for 3 hours at 37°C. Then, the transfection media was replaced with complete RPMI and cells incubated overnight (37°C, 5% $CO_2$).

### B2.5.2 Fluorescence Microscopy

A549 cells were washed with PBS, fixed with 4% paraformaldehyde (Sigma-Aldrich) for 30 min (10 min on ice, 20 min at RT), washed again, and quenched with 50 mM $NH_4Cl$ (Sigma-Aldrich) in PBS for 5 min. After another washing step, cells were permeabilised

with 0.2% Triton in PBS for 5 min. Subsequently, cells were blocked with 1% bovine serum albumin (Sigma-Aldrich) in PBS (1% BSA) for 30 min and incubated with mouse polyclonal serum against ME-TRAP diluted in 1% BSA for 30 min. Then, after washing, cells were incubated a donkey-anti-mouse-AlexaFluor488 antibody (Thermo Fisher Scientific) as secondary antibody for further 30 min. A549 cells were washed again and coverslips were then mounted on microscope slides (Menzel-Gläser) with Mowiol mounting medium (Mowiol 4-88, Glycerol, Tris-Cl, DABCO; all from Sigma-Aldrich) that was prepared with 1 µg/mL DAPI (Sigma-Aldrich).

### B2.5.3 Cell Lysis and Western Blots

HEK293A cells were seeded in 6-well plates (400,000 cells/well in 2 mL) and transfected with 3 µg plasmid DNA as described in section B2.5.1. The following day, media was removed and cells were harvested using the plunger of a 5 mL syringe and PBS as washing medium. After centrifugation (500 g, 5 min), cells were washed twice with 1 mL PBS. Then, cells were lysed in 250 µL cell lysis buffer (incl. proteinase inhibitor) for 20 min on ice and centrifuged at 16,000 g for 10 min (Heareus BioFuge Pico). The supernatant was stored at −20°C and used in Western Blot analysis within 10 days.

For Western Blot analyses, lysates were thawed on ice, mixed with 4× LDS loading buffer ± 10% 2-Mercaptoethanol (for reducing conditions, Sigma) and incubated at 85°C for 5 min. Samples and protein ladder (HiMark™ Pre-Stained HMW Protein Standard, Thermo Fisher Scientific) were then run in NuPAGE™ Novex™ 4-12% Bis-Tris Midi Protein Gels (Thermo Fisher Scientific) according to the manufacturer´s instructions.

Proteins were then blotted using Trans-Blot® Turbo™ Midi Nitrocellulose Transfer Packs (Bio-Rad) and the Trans-Blot® Turbo™ Transfer System (Bio-Rad) according to the manufacturer´s instructions. Subsequently, the membrane was incubated in 3% BSA/PBS for 1 h at RT, followed by incubation with primary antibodies diluted in 3% BSA for 1 h

at RT. Membranes were then incubated with mouse polyclonal serum against ME-TRAP (1:1,000 in 3% BSA), washed twice with PBS-Tween (10 min each), and incubated with Peroxidase AffiniPure Donkey Anti-Mouse IgG (H+L) (Jackson ImmunoResearch Laboratories Inc., West Grove, PA, USA) diluted 1:10,000 in 3% BSA. Membranes were washed 3× with PBS-Tween (10 min each) and with 18 mΩ $H_2O$ once (10 min), before developing with Thermo Scientific™ SuperSignal™ West Pico Chemiluminescent Substrate (Thermo Fisher Scientific) and imaging using a ChemiDoc™ MP System (Bio-Rad) according to the manufacturers´ instructions.

## B2.6 Insectary and Parasites

### B2.6.1 Parasite Strains

All parasite strains, which were used in this thesis are listed in Table B-8. These were generated by Dr Ahmed Salman (Jenner Institute, University of Oxford).

**Table B-8.** Transgenic parasites used in this thesis.

| Parasite No | Parasite Name | Abbreviated Name | Description |
|---|---|---|---|
| 2230 clone 1 | PfLSA-1$_{Pbuis4}$ GFP::Luc$_{Pbeef1a}$ | *Pb*(*Pf*LSA1) | *P. berghei* parasite expressing LSA1 of *P. falciparum* |
| 2394 clone 1 | PfTRAP$_{Pbuis4_230p}$ PfLSA1$_{Pbuis4_S1}$ GFP::Luc$_{Pbeef1a}$ | *Pb*(*Pf*TRAP+*Pf*LSA1) | *P. berghei* parasite expressing TRAP and LSA1 of *P. falciparum* |
| 2395 clone 1 | PfTRAP$_{Pbuis4_230p}$ PfUIS3$_{Pbuis4_S1}$ GFP::Luc$_{Pbeef1a}$ | *Pb*(PfTRAP+*Pf*UIS3) | *P. berghei* parasite expressing TRAP and UIS3 of *P. falciparum* |
| 2398 clone 4 | PfTRAP$_{Pbuis4_230p}$ PfLSAP2$_{Pbuis4_S1}$ GFP::Luc$_{Pbeef1a}$ | *Pb*(*Pf*TRAP+*Pf*LSAP2) | *P. berghei* parasite expressing TRAP and LSAP2 of *P. falciparum* |
| 2400 clone 1 | PfTRAP$_{Pbuis4_230p}$ PfFalstatin$_{Pbuis4_S1}$ GFP::Luc$_{Pbeef1a}$ | *Pb*(PfTRAP+*Pf*Falstatin) | *P. berghei* parasite expressing TRAP and Falstatin of *P. falciparum* |
| 2403 clone 1 | PfLSA1$_{Pbuis4_230p}$ PfLSAP2$_{Pbuis4_S1}$ GFP::Luc$_{Pbeef1a}$ | *Pb*(*Pf*TRAP+*Pf*LSAP2) | *P. berghei* parasite expressing LSA1 and LSAP2 of *P. falciparum* |

### B2.6.2 Preparation of Sporozoites

To prepare infectious sporozoites for mouse challenge experiments, 100 µL of frozen blood stocks of chimeric *P. berghei* parasites (see Table B-8) were injected intraperitoneally (IP) into BALB/c or TO outbred mice. Parasitaemia was monitored by manually counting infected erythrocytes of Giemsa stained blood smears (Sigma-Aldrich). After 4–7 days, infected mice were anaesthetised and fed to a pot of starved female *Anopheles stephensi* mosquitos for 15 min. Infected mosquitos were then maintained for 21 days at 20–24°C in a humidified incubator and fed on a fructose solution. In some experiments, infected mosquitos were fed a second time with a naïve BALB/c mouse 7–10 days after the initial feed to increase the sporozoite yield. Sporozoites were isolated from infected mosquitoes by dissecting out salivary glands and homogenising prior to IV injection into the mouse tail vein.

### B2.6.3 Cryopreservation of Blood-Stage Parasites

Blood from infected mice with high parasitaemia (5–10%) was collected by cardiac puncture and mixed 1:1 with Parasite Freezing Buffer (B1.2) and stored in cryotubes in liquid nitrogen tanks.

## B2.7 Data analysis

### B2.7.1 Software

Preparation of graphs and statistical analysis was performed in GraphPad Prism 6 (GraphPad Software, Inc., La Jolla, California, USA). Analysis of fluorescence images was performed with ImageJ v1.49 (developed by NIH, Bethesda, MD, USA).

### B2.7.2 Statistical Tests

All statistical analyses were performed using Graphpad Prism 6 (Graphpad Software, Inc.). LIPS data were log transformed prior to analyses. The Mann-Whitney rank test was used to compare two non-parametric groups and the Kruskal-Wallis test (One-Way ANOVA) with Dunn´s Multiple Comparison post-test was used to compare medians between more than two groups. Protective efficacy and mouse survival in malaria challenge experiments were shown using Kaplan-Meier plots and analysed with the Log-Rank (Mantel-Cox) test.

# Chapter C

# Combination of Liver-Stage Antigens

# C1 Introduction

The most advanced viral vectored vaccine in clinical development is based on a ChAd63 prime and MVA boost regimen with both vectors encoding ME-TRAP, a multiple epitope string fused to TRAP. Using this regimen, only moderate efficacy against *P. falciparum* sporozoites could be achieved in naïve adults [148] with higher though still limited efficacy in a malaria-endemic region [191]. Given that this liver-stage vaccine and other currently explored single-component vaccines lack sufficient efficacy justifying mass deployment, there is now general consensus that a truly effective vaccine will need to contain a combination of several parasite antigens.

However, to this date, only a few candidate liver-stage malaria antigens other than CSP or ME-TRAP have been tested extensively. As many more parasite antigens are now being identified using modern fields of study in biology, such as genomics, proteomics, or metabolomics, better candidate antigens could be identified. Longley et al. recently analysed a variety of viral vectors encoding a number of different liver-stage antigens and compared their immunogenicity and efficacy with those induced by the historical vaccine candidate antigens CSP and TRAP [10]. Most importantly, they showed that two of those antigens, LSA1 and LSAP2, were capable of inducing high levels of protection when challenged with chimeric *P. berghei* parasites. As a result, these two antigens have been considered as very interesting candidate antigens for a future liver-stage malaria vaccine.

As combining antigens might be beneficial for vaccine efficacy, the purpose of this study was to assess the immunogenicity and efficacy of selected antigens when administered together using viral vectored vaccines. Previous reports suggest that the interaction can be complex and effect antigen dependent, with some evidence that combining sub-unit vaccines can result in immune interference or competition between antigens and thereby reduce vaccine immunogenicity [192, 193], but in other studies combining vaccines led to no apparent interference [194, 195]. It is therefore absolutely

essential not only to search for new antigen candidates, but also to analyse their interaction with each other and existing vaccine candidates.

## C1.1 Liver-Stage Antigens

### C1.1.1 Thrombospondin Related Adhesive Protein (TRAP)

The thrombospondin related adhesive protein (TRAP) is encoded in one of the most advanced liver-stage vaccines in clinical development, named ME-TRAP. This vaccine encodes TRAP fused to a multiple epitope (ME) string, made of T- and B-cell epitopes from pre-erythrocytic *P. falciparum* antigens [133]. It has been thoroughly investigated in numerous preclinical experiments as well as phase I and II clinical studies and is therefore used as benchmark in these studies.

In this chapter, a modified version of TRAP was used instead of the clinical ME-TRAP construct (denoted as TRIP) for two reasons. Firstly, the ME string of the clinical construct contains a strong immunodominant H-$2^d$ restricted epitope from CSP (Pb9), which prohibits the analysis of TRAP-specific immunogenicity and efficacy in BALB/c mice. Secondly, in contrast to the ME-TRAP construct, which encodes the TRAP protein sequence of the *P. falciparum* T9/96 strain [136], TRIP uses the sequence of the *P. falciparum* 3D7 strain (PlasmoDB PF3D7_1335900), which matches the strain of parasites used in challenge studies (B2.6, p. 53). Furthermore, the predicted transmembrane helix and cytoplasmic domains, as well as 15 aa encoding five repeats of PNP were removed from the TRAP gene. The remaining sequence, denoted as TRIP, was codon optimised for expression in human cells.

### C1.1.2 Liver-Stage Antigen 1 (LSA1)

Liver-Stage Antigen 1 (LSA1) was one of the first and, at that time, one of the only known liver-stage specific proteins [196]. Two characteristics of this antigen are promising for its

usage in a malaria vaccine: LSA1 is strongly conserved between *P. falciparum* strains [197] and it seems to be essential for late liver-stage development, as parasites with deleted LSA1 show a severe defect in late liver-stage differentiation [198]. While the exact function of LSA1 has yet to be determined, its abundant expression in the parasitophorous vacuole as flocculent material surrounding merozoites make it likely that it is involved in the parasite´s transition from liver-stages to blood-stages. Importantly, studies of natural immunity [61–64] and volunteers vaccinated with irradiated sporozoites [199] have revealed that cellular responses to LSA1 are associated with protection. In 1992, Hill et al. described HLA-B53 restricted cytotoxic T cells recognising a conserved LSA1 epitope among malaria-immune Africans that indicated a possible molecular basis for the protective association between HLA-B53 and reduced severe malaria in Africa [200]. Despite these promising data, clinical usage of LSA1 as a protein-based vaccine antigen has not succeeded. For instance, recombinant LSA1 formulated with AS01 or AS02 as adjuvants was shown to be safe and elicit $CD4^+$ T cells and high titres of antibodies, but it did not protect against homologous malaria challenge [201]. However, this could be due to the lack of $CD8^+$ T-cell induction in this vaccination regimen. Another clinical trial examining a viral vectored prime-boost vaccination regimen with FP9 and MVA expressing a polyprotein which consisted of six P. *falciparum* antigens (incl. LSA1) also failed to show substantial immunogenicity [202]. According to the authors, this could be due to antigen competition or the very large size of the polyprotein gene (> 3000 aa), which may have resulted in limited antigen expression. Therefore, efficacy of LSA1-specific immunity induced by viral vectors remains to be investigated.

As LSA1 of the *P. falciparum* 3D7 strain contains 43 degenerative seventeen amino acid repeats, which can be deleterious because of the size increase and the higher likelihood of homologous recombination events when inserted into viral vectors, the sequence was modified before vector production (by Dr Rhea Longley [10]): One copy of

the most representative repeats (DLEGERLAKEKLWWR) and one copy of the most different repeats (DLERTKASTETLHEQQS) were expressed in the vaccine, while all other repeat regions were deleted. Furthermore, the sequence was codon optimised for expression in human cells and the tPA leader sequence [203] was added to the N-terminal end of LSA1 to improve expression and immunogenicity [204–206]. It was recently shown that a prime-boost regimen with ChAd63 and MVA vectors expressing this LSA1 construct protects BALB/c as well as CD1 mice with an efficacy of 87.5% against challenge with chimeric *P. berghei* parasites expressing LSA1 of *P. falciparum* (*Pf*LSA1) [10].

### C1.1.3 Liver-Stage Associated Protein 2 (LSAP2)

The liver-stage associated protein 2 (LSAP2) was identified by transcriptomic profiling of proteins, which were upregulated in sporozoites while co-culturing with hepatocytes [207]. It was shown that LSAP2 is not present in sporozoites, but is increasingly expressed throughout liver-stage development with the highest expression observed in the late liver-stages and moderate expression in the following erythrocytic stages of the parasite. Although the function of LSAP2 is still unknown, immunostaining suggests that LSAP2 is part of the parasitophorous vacuole membrane (PVM) and therefore is involved in parasite-hepatocyte interaction [208].

The *P. falciparum* LSAP2 sequence encoded in viral vectors used in this thesis was only slightly modified compared to its native sequence (plasmids were cloned by Dr Rhea Longley [10]). For better expression and immunogenicity, the tPA leader sequence [203] was added to the N-terminal end of LSAP2 [204–206]. Furthermore, the whole sequence was codon optimised for expression in human cells. ChAd63 and MVA vectors encoding this construct administered in a prime-boost regimen achieved 87.5% efficacy in BALB/c mice and 70% efficacy in CD1 mice when challenged with chimeric *P. berghei* parasites expressing *Pf*LSAP2 [10].

### C1.1.4 Upregulated in Infectious Sporozoites 3 (UIS3)

Upregulated in Infectious Sporozoites 3 (UIS3) was identified more recently by transcriptomic profiling of *P. berghei* and *P. yoelii* sporozoites that were isolated from mosquito salivary glands [209, 210]. It appears to be essential for early liver-stage development, as UIS3-deficient sporozoites infect hepatocytes, but are unable to progress to blood-stages *in vivo* [102]. These genetically attenuated parasites also conferred complete protection against sporozoite challenge with wild-type parasites in mice [102, 211]. Interestingly, in irradiated sporozoites, which also lack the ability to progress to blood stages, UIS3 expression is substantially reduced [212]. However, the exact function of UIS3 is still unknown: Mikolajczak et al. discovered a direct interaction between *P. berghei* UIS3, which is located in the PVM, and the liver-fatty acid binding protein (L-FABP) of the hepatocyte [213]. This most likely enables the parasite to import essential fatty acids and lipids. Reduced expression of hepatocyte L-FABP severely impairs parasite growth and vice versa. UIS3 of *P. falciparum* has also been shown to bind L-FABP [214], but a more recent study using NMR spectroscopy challenges this hypothesis [215].

A prime-boost vaccination regimen with DNA and vaccinia encoding UIS3 showed only limited protection (7%) against subsequent *P. yoelii* challenge, but when UIS3 vaccines were co-administered in combination with the *P. yoelii* homologue of Falstatin 43% sterile protection was achieved [216].

As UIS3 contains two predicted transmembrane domains and it was considered that adding a signal sequence could drastically alter the structure of the protein, a tPA leader sequence was not added to UIS3 in the ChAd63 and MVA vectors used in this thesis [38]. Administered in a prime-boost regimen, those vectors protected 12.5% of BALB/c mice, but none of the CD1 mice, when challenged with *P. berghei* parasites expressing *Pf*UIS3 [10].

### C1.1.5 Falstatin

Falstatin is an inhibitor of cysteine proteases (ICP) expressed by the parasite. It seems to facilitate hepatocyte invasion by sporozoites and also inhibits programmed cell death of the hepatocyte after parasite infection [217]. Similarly, the invasion of asexual merozoites into red blood cells is facilitated by inhibiting parasite and/or host cysteine proteases [218]. It was also shown that loss of ICP function by targeted gene disruption in the parasites does not affect their growth inside mammalian host cells. However, a defect in gliding motility and an impaired ability to infect of mosquito salivary glands could be observed [219].

As mentioned above, a prime-boost regimen using DNA and MVA vectors encoding the *P. yoelii* homologue of Falstatin showed 43% sterile protection against homologous parasite challenge when co-administered with vaccines encoding *Py*UIS3 [216].

In the viral vectors used in this thesis, the tPA leader sequence [203] was added to the N-terminal end of *P. falciparum* Falstatin [204–206] in addition to codon optimisation for expression in human cells. Longley et al. showed that administration of this construct in a ChAd63-MVA prime-boost regimen protected 10% of CD1 mice (but none of the BALB/c mice) against challenge with *P. berghei* parasites expressing *Pf*Falstatin [10].

# C2 Results

## C2.1 Combination of Novel Antigens with TRIP

### C2.1.1 Experimental Setup

To determine whether combinations of novel liver-stage antigens (LSA1, LSAP2, UIS3, and Falstatin) with TRIP encoded in ChAd63 and MVA vaccines could improve protection, sporozoite challenge experiments were conducted as outlined in Figure C-1. For each experiment, thirty BALB/c mice were divided into five groups. (1) Group 1 was vaccinated intramuscularly (IM) with $10^8$ IU ChAd63-TRIP followed by $10^7$ PFU MVA-TRIP six weeks later. (2) The second group of BALB/c mice was vaccinated with the same ChAd63-MVA prime-boost regimen, but viral vectors contained the LSA1, LSAP2, UIS3, or Falstatin insert. (3) The third group of mice was administered with both ChAd63 vaccines of group 1 and 2, each vaccine separately administered in the left or right *M. tibialis* of the mice. Six weeks later the corresponding MVA vaccines were administered, again separately in both legs. (4) For group 4, both vaccines were mixed in a tube before administration into both legs. (5) The fifth group of mice were not vaccinated and served as a negative control.

One week after MVA boost, a blood sample was taken from each mouse and blood PBMC were analysed for cytokine production after stimulation with either a peptide pool of overlapping 20mers covering the whole TRIP sequence or the relevant second antigen (B2.4.2, p. 47). Additionally, serum samples were analysed for antibodies via LIPS assay in week seven (B2.4.4, p. 50). Ten days after MVA boost, mice were challenged IV with 1,000 chimeric *P. berghei* sporozoites expressing *P. falciparum* TRIP and the relevant second vaccine antigen (B2.3.7, p. 45). After sporozoite challenge, thin blood smears were taken on a daily basis (starting four days after challenge), stained with Giemsa stain, and analysed by light microscopy to determine parasitaemia (B2.3.8, p. 46).

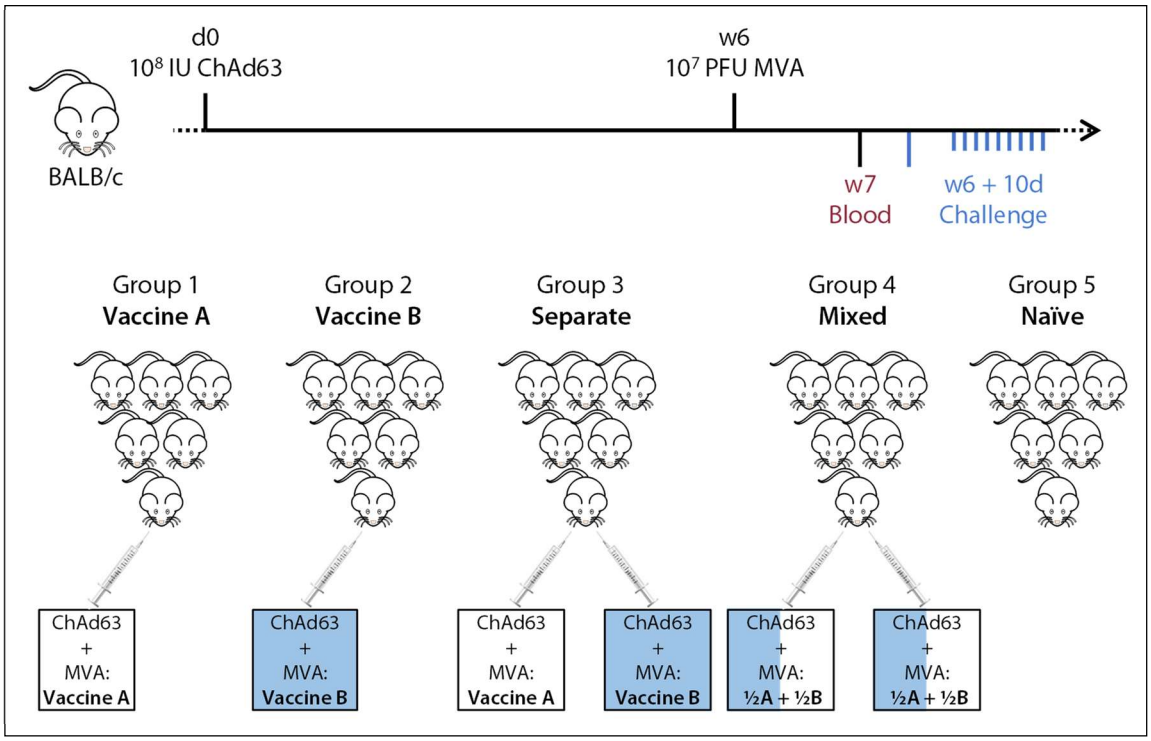



Figure C-1. Experimental setup to analyse immunogenicity and efficacy of antigen combinations.

### C2.1.2 Immunogenicity of Vaccine Combinations

Blood samples were taken one week after MVA boost and PBMC were stimulated with a single pool of overlapping peptides covering either the full TRIP sequence or the relevant second vaccine antigen (B2.4.1) to measure intracellular production of IFN-γ, IL-2, and TNF by ICS (B2.4.2). Only the IFN-γ responses are shown in Figure C-2 and following immunogenicity figures, as differences between groups were similar when IL-2 and TNF were analysed. All tested vaccines were immunogenic in BALB/c mice. Most importantly, combination of antigens did not lead to a significant reduction in immunogenicity because of antigenic competition. Interestingly, mixing TRIP and UIS3 induced a stronger UIS3-specific $CD8^+$ T-cell response in comparison to separate administration or UIS3 alone (Figure C-2C). However, this was not significant after adjusting for multiple comparisons. Inexplicably, there was a measurable $CD4^+$ and $CD8^+$ T-cell response in the TRIP

vaccinated group when stimulated with a Falstatin peptide pool. Even though, this was most likely a false positive result (presumably due to a contaminated peptide pool), the experiment was not repeated due to the lack of efficacy with this particular antigen combination (Figure C-4).

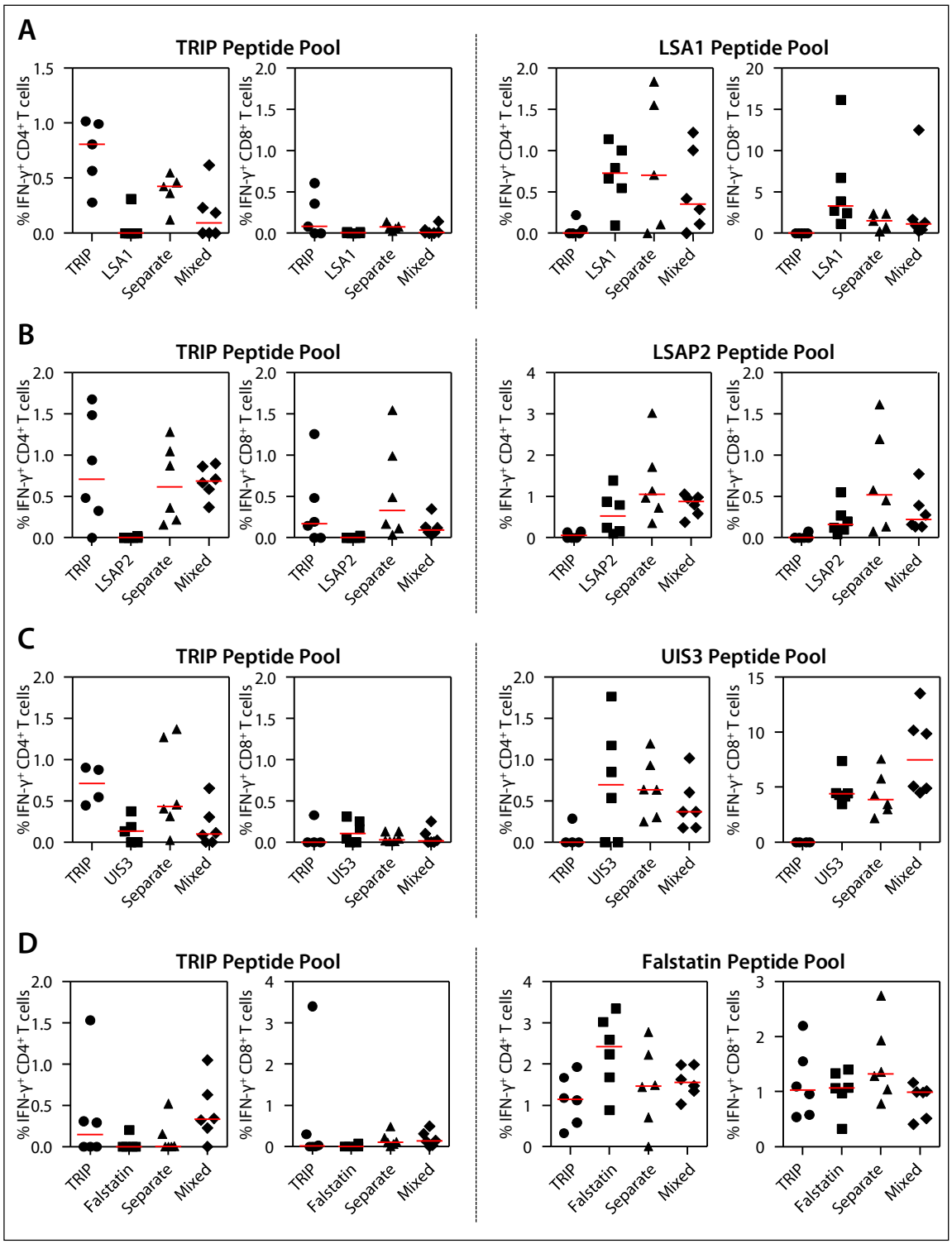



**Figure C-2. Post boost T-cell immunogenicity of co-administered liver-stage vaccines.** BALB/c mice were vaccinated with a ChAd63-MVA prime-boost regimen (C2.1.1) with antigens indicated on the x-axes. When two vaccines were given, mice were vaccinated with a full dose of each vaccine administered in separate legs ("Separate") or mixed prior to administration in both legs ("Mixed"). One week post MVA boost (week 7), a blood sample was taken and PBMC were analysed by ICS after stimulation with a TRIP peptide pool or a (A) LSA1, (B) LSAP2, (C) UIS3, or (D) Falstatin peptide pool, respectively. Graphs represent the frequency of $CD4^+IFN\text{-}\gamma^+$ or $CD8^+IFN\text{-}\gamma^+$ T cells. Single points indicate T-cell responses of individual mice and red lines show the median response per group.

One week after the administration of MVA booster vaccines, antibody responses were analysed in serum samples using the LIPS assay (B2.4.4, p. 50). Importantly, antibodies were detected against all antigens encoded by the relevant vaccines (Figure C-3). Levels of antibody responses were similar between vaccine groups and no difference was observed when vaccines were administered in separate injection sites or mixed together prior to injection.

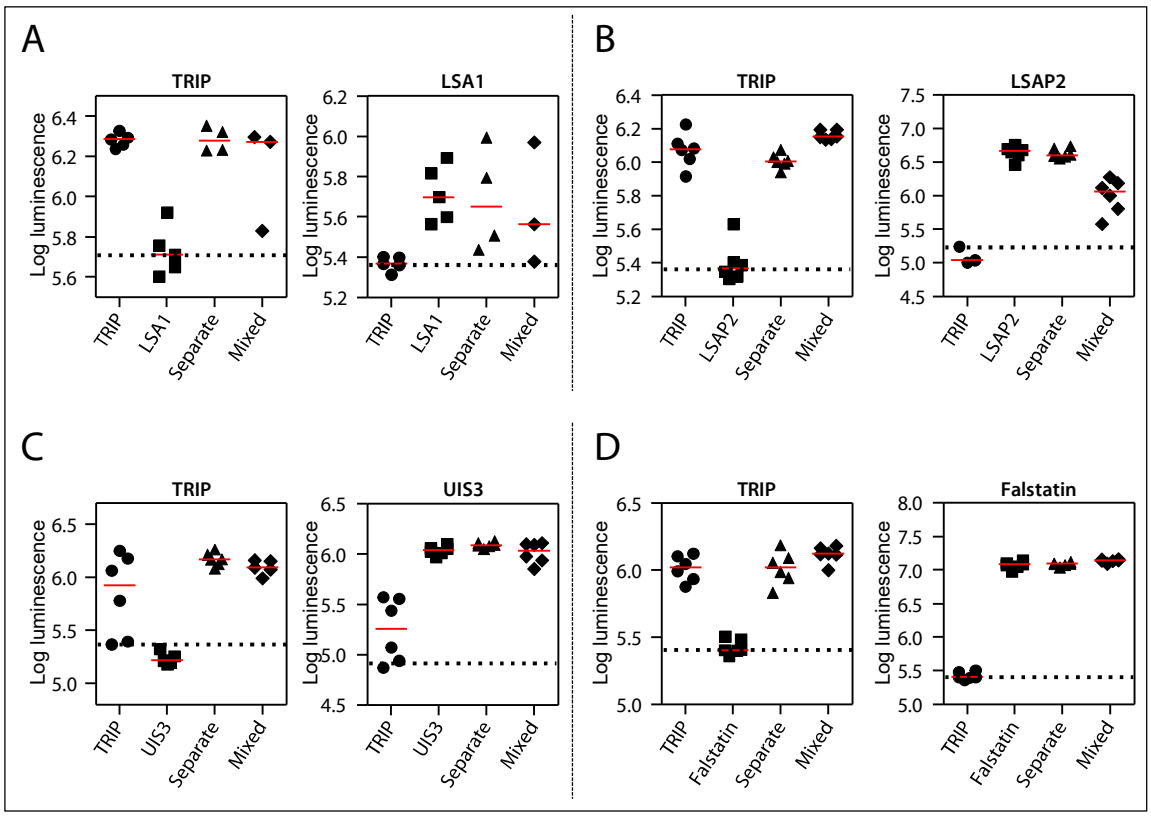



**Figure C-3. Assessment of antibody responses in BALB/c mice after co-administration of liver-stage vaccines.** BALB/c mice were vaccinated in a ChAd63-MVA prime-boost regime (C2.1.1) and antibody levels measured by the LIPS assay one week post-boost using a TRIP or (A) LSA1, (B) LSAP2, (C) UIS3, or (D) Falstatin lysate. The background response to each antigen was defined as the average of six naïve replicates plus two standard deviations and is shown with dotted lines. Log luminescence (light units) of individual data (points) and median of the corresponding group (red lines) are indicated.

### C2.1.3 Efficacy of Vaccine Combinations

To measure protective efficacy of antigen combinations, vaccinated BALB/c mice were challenged 10 days after administration of the booster MVA vaccine with 1,000 *P. berghei*

parasites expressing the relevant two *P. falciparum* vaccine antigens (C2.1.1 and B2.6.1). Liver infectivity of mice by these double transgenic parasites was initially confirmed by *in vivo* imaging (Supplemental Figure I-1, p. 200).

Consistent with previously published data [10], all BALB/c mice vaccinated with the single antigen TRIP succumbed to malaria, while vaccination with LSAP2 or UIS3 vaccines resulted in a delay to 1% parasitaemia, but not sterile protection (Figure C-4). Vaccination with LSA1 sterilely protected 33% (2/6) and an overall delay in time to 1% parasitaemia. Combination of TRIP with UIS3 (administered separately) protected two of six mice. Importantly, mixing of viral vectors prior to administration led to greatest efficacy: 33% of mice were protected with a combination of TRIP and LSAP2, and 100% of mice vaccinated with TRIP and LSA1 or TRIP and UIS3 were sterilely protected.

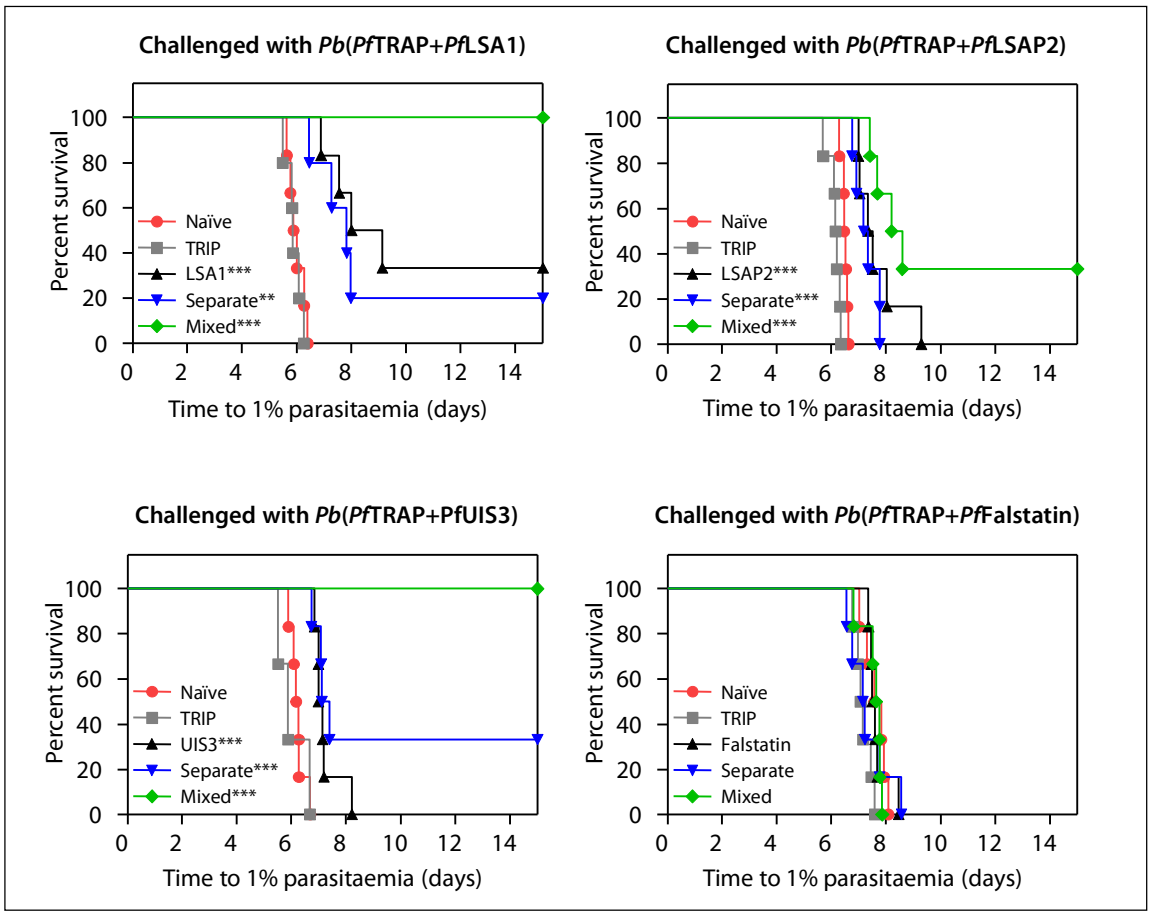



**Figure C-4. Efficacy of vaccine combinations after sporozoite challenge.** BALB/c mice were vaccinated with a ChAd63-MVA prime-boost regimen as described in section C2.1.1. Ten days after MVA boost, mice were challenged with 1,000 *P. berghei* sporozoites expressing the relevant *P. falciparum* vaccine antigens. Post challenge, blood smears were taken daily from four days after sporozoite challenge and analysed via Giemsa staining and light microscopy to determine the percentage of infected red blood cells (parasitaemia). Mice that were negative for blood-stage malaria until 15 days after sporozoite challenge were considered to be sterilely protected. Linear regression was used to determine the time of each individual mouse to reach 1% parasitaemia, which is plotted on Kaplan-Meier Curves. Data was analysed with the log-rank (Mantel-Cox) test. Asterisks denote the level of statistical significance when compared to the naïve control group (**p<0.01, ***p<0.001).

## C2.1.4 Immunogenicity in Lymph Nodes, Spleen, and Liver

To gain a more detailed understanding of the immunogenicity of viral vectors encoding TRIP or LSA1 when administered in combination, T-cell responses were investigated in specific organs (lymph node, spleen, and liver). Six weeks after administration of the ChAd63 vectors, BALB/c mice were boosted with MVA vectors (C2.1.1) with mice sacrificed in week 7 of the experiment (Figure C-5) and T cells in the popliteal lymph node,

spleen, and liver analysed by flow cytometry (B2.4.2, p. 47). In all organs tested, there was no statistically significant difference in the $CD8^+$ T-cell response between group 3 (both vaccines administered separately) and group 4 (vaccines mixed before administration in both legs). However, a (non-significant) trend towards an increased LSA1-specific $CD4^+$ T-cell response was observed in the liver for group 4 compared to group 3.

Subsequently, the functionality of antigen-specific T cells in the liver was analysed (Figure C-6). When vaccinated with both vaccines ("Separate" and "Mixed" groups), the vast majority of activated $CD8^+$ T cells were LSA1-specific (Figure C-6B) and produced IFN-γ and/or TNF, but not IL-2 (Figure C-6C). More detailed analyses showed that antigen-specifc $CD4^+$ T cells either produced exclusively IFN-γ, IFN-γ and TNF, or all of the three tested cytokines (IFN-γ, IL-2, and TNF) (Figure C-6D). Antigen-specific $CD8^+$ T cells were mainly IFN-$\gamma^+$IL-$2^-$TN$F^-$ or IFN-$\gamma^+$IL-$2^-$TN$F^+$.

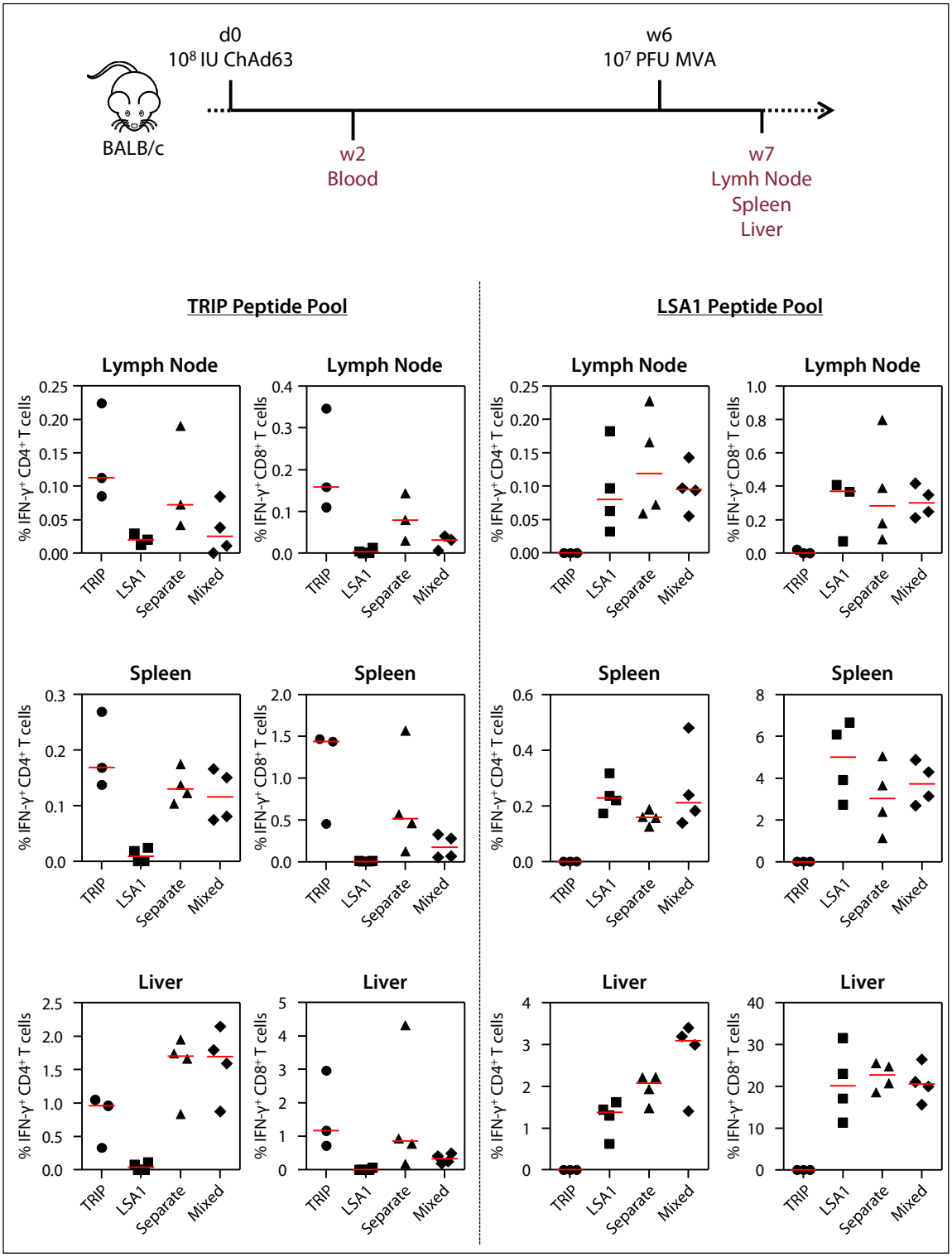



**Figure C-5. T-cell responses in lymph nodes, spleen, and liver after vaccine co-administration.** BALB/c mice were vaccinated with a ChAd63-MVA prime-boost regimen (C2.1.1) and with antigens indicated on the x-axes. When two vaccines were given, mice were vaccinated with a full dose of each vaccine administered in separate legs ("Separate") or mixed prior to administration in both legs ("Mixed"). One week post MVA boost (week 7), mice were sacrificed and the popliteal lymph node, spleen, and liver were processed and analysed by ICS after stimulation with a TRIP or LSA1 peptide pool. Graphs represent the frequency of $CD4^+IFN\text{-}\gamma^+$ or $CD8^+IFN\text{-}\gamma^+$ T cells. Single points indicate T-cell responses of individual mice and red lines show the median response per group.

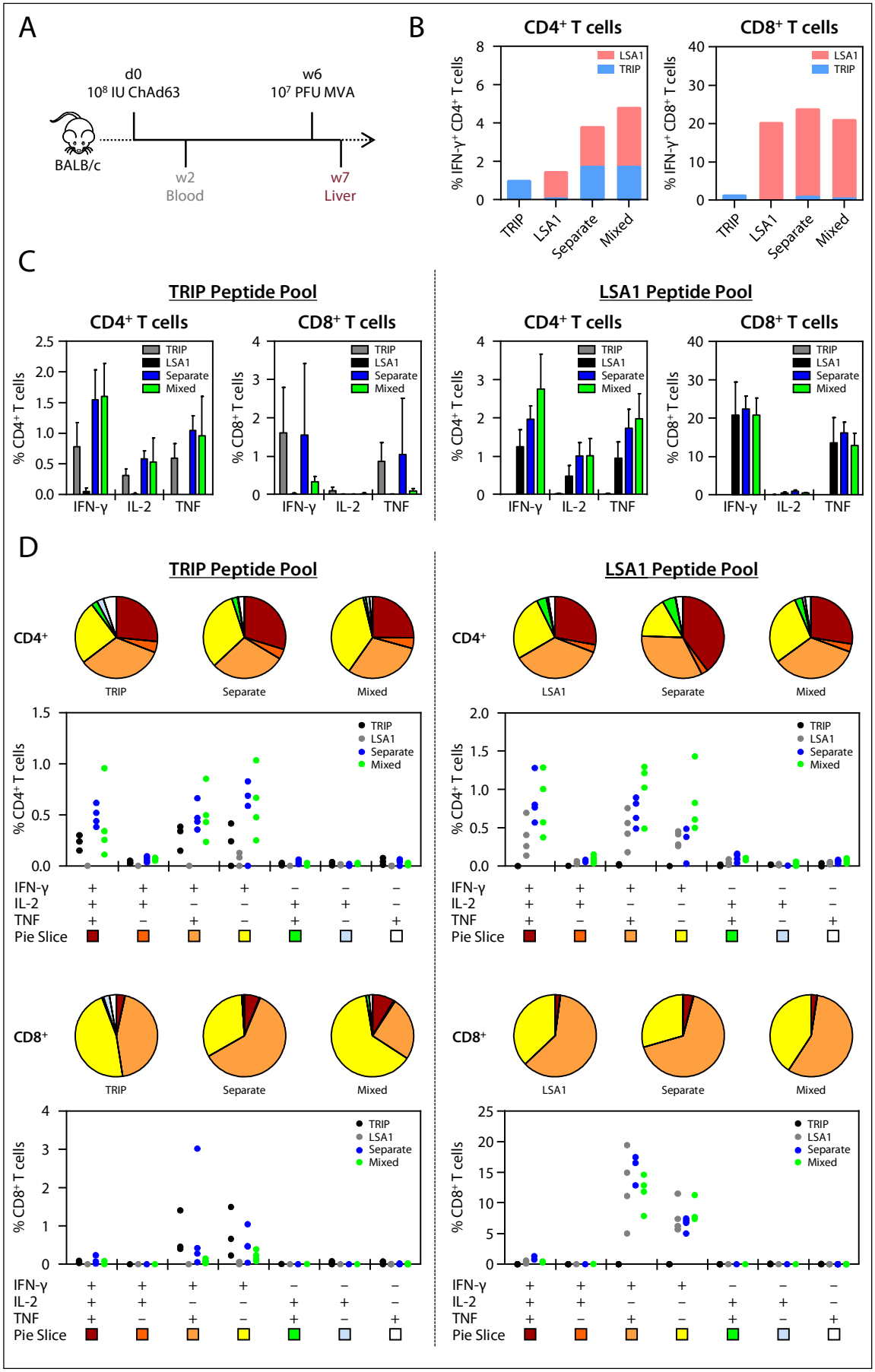

A
d0
10⁸ IU ChAd63
w6
10⁷ PFU MVA
BALB/c
w2
Blood
w7
Liver
B
CD4⁺ T cells
CD8⁺ T cells
% IFN-γ⁺ CD4⁺ T cells
% IFN-γ⁺ CD8⁺ T cells
LSA1
TRIP
TRIP
LSA1
Separate
Mixed
C
TRIP Peptide Pool
LSA1 Peptide Pool
CD4⁺ T cells
CD8⁺ T cells
% CD4⁺ T cells
% CD8⁺ T cells
TRIP
LSA1
Separate
Mixed
IFN-γ
IL-2
TNF
D
TRIP Peptide Pool
LSA1 Peptide Pool
CD4⁺
CD8⁺
TRIP
LSA1
Separate
Mixed
% CD4⁺ T cells
% CD8⁺ T cells
IFN-γ
IL-2
TNF
Pie Slice

**Figure C-6. Functionality of antigen-specific $CD4^+$ and $CD8^+$ T cells in the liver.** (A) Outline of the experimental setup. After immunising four BALB/c mice per group with $10^8$ IU of ChAd63 and $10^7$ PFU MVA vectors encoding LSA1, LSAP2, or both vaccines ("Separate" and "Mixed"), mice were sacrificed in week 7. Livers were processed and analysed by ICS after stimulation with a TRIP or LSA1 peptide pool. (B) Columns represent the median frequency of TRIP- and LSA1-specific $CD4^+IFN\text{-}\gamma^+$ or $CD8^+IFN\text{-}\gamma^+$ T cells as indicated in the figure legend. (C) Mean frequencies (with the standard error of the mean, SEM) of IFN-γ, IL-2, or TNF secreting $CD4^+$ and $CD8^+$ T cells are shown. (D) Pie charts summarise the fractions of $CD4^+$ or $CD8^+$ T-cells that are positive for one, two, or three cytokines. All possible combinations are shown in the bar chart stratified by vaccination groups, with the ordinate showing the percentage of $CD4^+$ or $CD8^+$ T cells. Single points indicate T-cell responses of individual mice.

## C2.2 Combination of Novel Liver-Stage Antigens (LSA1 + LSAP2)

### C2.2.1 Efficacy of a Prime-Boost Regimen

Having found a positive effect on efficacy when combining TRIP with novel antigens LSA1, LSAP2, or UIS3, the combination of the two novel antigens LSA1 and LSAP2 was investigated. In one experiment, conducted by Dr Ahmed Salman (The Jenner Institute, University of Oxford), BALB/c mice were vaccinated (similarly to Figure B-1, p. 64) with LSA1 and LSAP2 as vaccine antigens: group 1 was vaccinated with viral vectors ($10^8$ IU ChAd63 and $10^7$ PFU MVA) encoding LSA1; in group 2 viral vectors encoded LSAP2; in group 3 both vaccines were administered with a full dose of both vaccines separately in both legs; in group 4 vaccines were mixed before administration in both legs; and group 5 served as a unvaccinated control group. Ten days post boost, all mice were challenged with 1,000 chimeric *P. berghei* parasites expressing both *P. falciparum* LSA1 and LSAP2 intravenously. Importantly, in this experiment, all mice that were co-administered with LSA1 and LSAP2 vaccines (mice of "Separate" and "Mixed" groups) were fully protected against sporozoite challenge (Supplemental Figure I-2, p. 201). However, in this particular experiment, LSA1 alone and LSAP2 alone also showed high levels of sterile efficacy (87.5% and 75%, respectively).

### C2.2.2 Immunogenicity and Efficacy after ChAd63 Prime-Only

Given the high efficacy observed after ChAd63-MVA vaccination, the efficacy of combination antigens after a single dose of adenoviral vectors was assessed. Eight BALB/c mice per group were vaccinated with $10^8$ IU of ChAd63 expressing either LSA1 or LSAP2 and another group ("Mixed") was co-administered with a full dose of both vaccines. Naïve mice served as infection controls. Two weeks post immunisation, at the peak of the immune response [144], a blood sample was analysed for immunogenicity and mice were challenged with double transgenic *P. berghei* parasites *Pb(Pf*LSA1+*Pf*LSAP2) (Figure C-7A). Encouragingly, while all naïve control mice reached 1% parasitaemia between 6–8 days, 25% (2/8), 50% (4/8), and 75% (6/8) of mice vaccinated with LSA1, LSAP2, or both vaccines ("Mixed") were protected (Figure C-7B). A statistically significant improvement in efficacy was observed in mice vaccinated with LSA1 ($p<0.05$) and "Mixed" ($p<0.001$) when compared to the naïve control group. Interestingly, there was no statistically significant difference in the cellular immune response when mice were vaccinated with a single antigen (LSA1 or LSAP2) compared to mice immunised with both vaccines ("Mixed") (Figure C-7C).

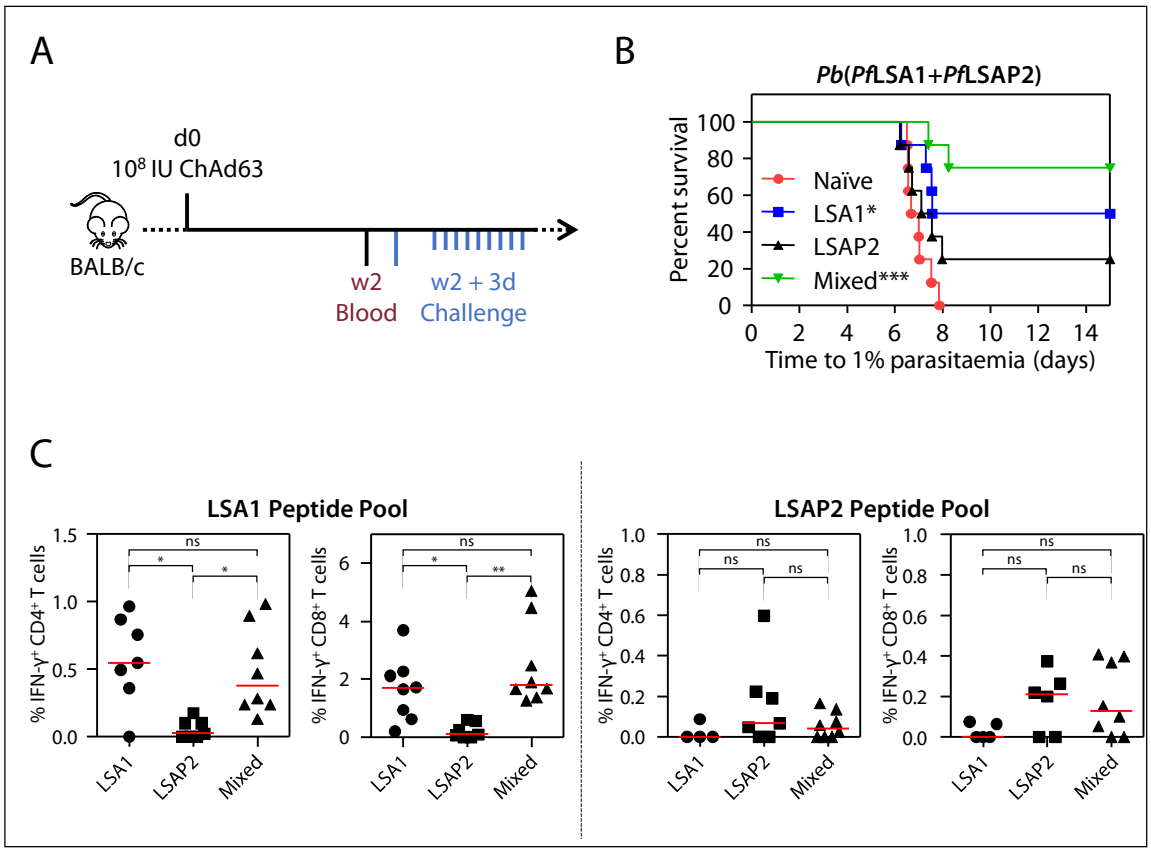



**Figure C-7. Combination of LSA1 and LSAP2 in a prime-only regimen.** (A) Outline of the experimental setup. After immunising eight BALB/c mice per group with $10^8$ IU of ChAd63 vectors encoding LSA1, LSAP2, or both vaccines ("Mixed"), a blood sample was taken on day 14 with mice challenged on day 17. (B) Efficacy data. Mice were challenged with 1,000 chimeric *P. berghei* sporozoites expressing *P. falciparum* LSA1 and LSAP2 on day 17 post immunisation. Blood smears were taken on a daily basis from four days after sporozoite challenge and analysed by Giemsa staining and light microscopy to determine parasitaemia. Mice that were negative for blood-stage malaria until 15 days after sporozoite challenge were considered to be sterilely protected. Time to 1% parasitaemia is plotted on a Kaplan-Meier Curve. Data was analysed with the log-rank (Mantel-Cox) test. Asterisks denote the level of statistical significance when compared to the naïve control group (*, $p<0.05$; ***, $p<0.001$). (C) Immunogenicity data. A blood sample was taken on day 14 post immunisation and analysed by ICS after stimulation with an LSA1 or LSAP2 peptide pool. Graphs represent the frequency of $CD4^+IFN\text{-}\gamma^+$ or $CD8^+IFN\text{-}\gamma^+$ T cells. Single points indicate T-cell responses of individual mice and red lines show the median response per group. Data was analysed with a one-way analysis of variance with Dunn's multiple comparison post-test. Asterisks denote the level of statistical significance when compared to each other (*, $p<0.05$; **, $p<0.01$; ns, non-significant).

### C2.2.3 Long-Term Immunogenicity

Long-term T-cell immunogenicity after co-administration of LSA1 and LSAP2 was analysed by immunising ten BALB/c mice per group in a ChAd63-MVA prime-boost regimen and measuring immunogenicity by flow cytometry of blood PBMC two weeks

post-prime (w2), one week post-boost (month 2 post-prime, m2), as well as at time points m3, m4, m5, and m6 with groups as outlined in Figure C-8. Mice were challenged 5 months post-boost (m7) with 1,000 chimeric *P. berghei* sporozoites expressing *P. falciparum* LSA1 and LSAP2 to investigate long-term vaccine efficacy.

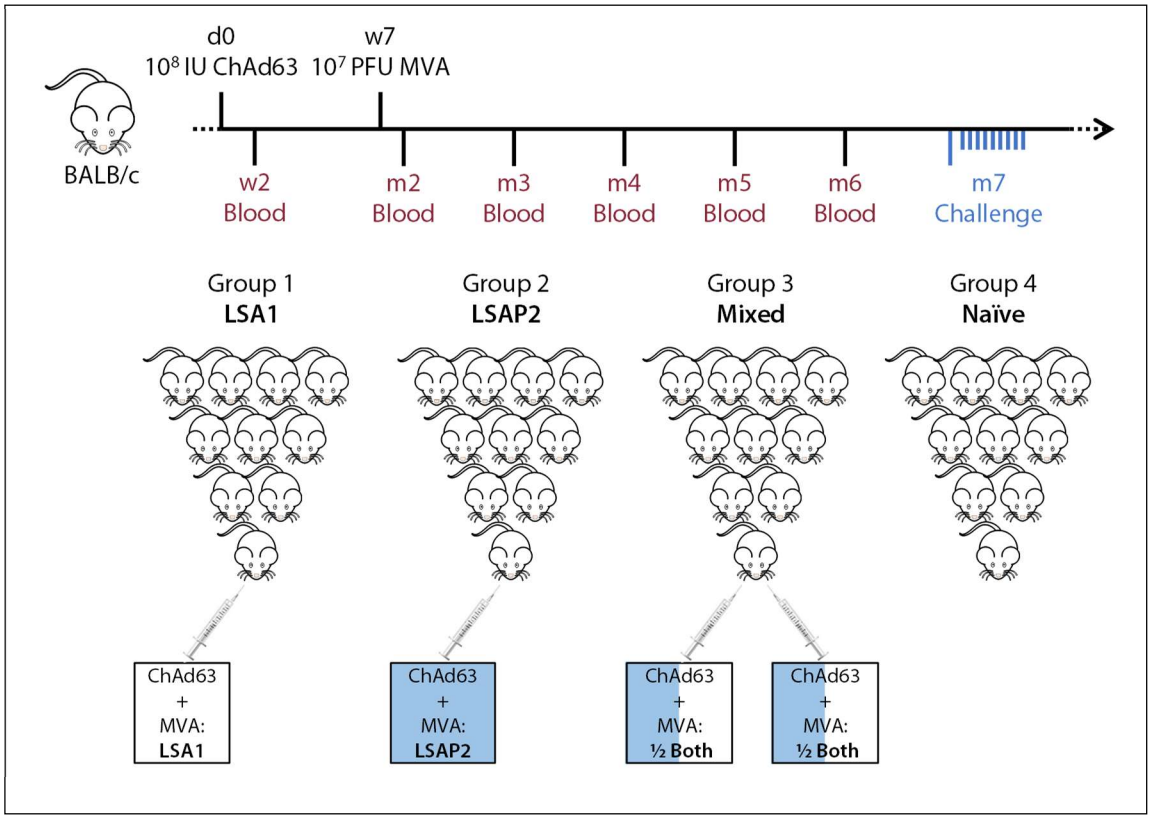



**Figure C-8. Setup of the long-term immunogenicity experiment.** (1) Group 1 was vaccinated IM with $10^8$ IU ChAd63-LSA1 followed by $10^7$ PFU MVA-LSA1 seven weeks later. (2) The second group of BALB/c mice was vaccinated with the same ChAd63-MVA prime-boost regimen, but vectors contained the LSAP2 insert. (3) The third group of mice was administered with a full dose of both vaccines, which were mixed in a tube before administration. (4) The fourth group was not vaccinated and served as a infection control. Two weeks post-prime (w2), one week post-boost (m2), at months 3 (m3), 4 (m4), 5 (m5), and 6 (m6), a blood sample was taken from each mouse and PBMC were analysed for cytokine production after stimulation with either an LSA1 or LSAP2 peptide pool. Ten days after MVA boost, mice were challenged IV with 1,000 chimeric *P. berghei* sporozoites expressing *P. falciparum* LSA1 and LSAP2. After sporozoite challenge, blood smears were taken on a daily basis (starting four days after sporozoite challenge), stained with Giemsa stain and analysed by light microscopy to determine parasitaemia.

Two weeks post immunisation with ChAd63 vaccines (at the peak of the immune response [144]), a strong T-cell response against LSA1 was observed when mice were vaccinated with ChAd63-LSA1 or both (ChAd63-LSA1 and Chad63-LSAP2) mixed together (Figure

C-9A). Similarly, a strong LSAP2-specific T-cell response was measured when mice were immunised with LSAP2 or co-administered with both vaccines ("Mixed"). Importantly, there was no statistically significant effect on the cellular immune response of either vaccine when administered alone compared to co-administration ("Mixed").

One week post MVA-boost, LSA1 and LSAP2-specific $CD4^+$ and $CD8^+$ T-cell responses were generally higher (Figure C-9B) compared to results two week post-prime (Figure C-9A). Again, no statistically significant difference was found between the group immunised with one vaccine only (LSA1 or LSAP2) and the group co-administered with both vaccines ("Mixed").

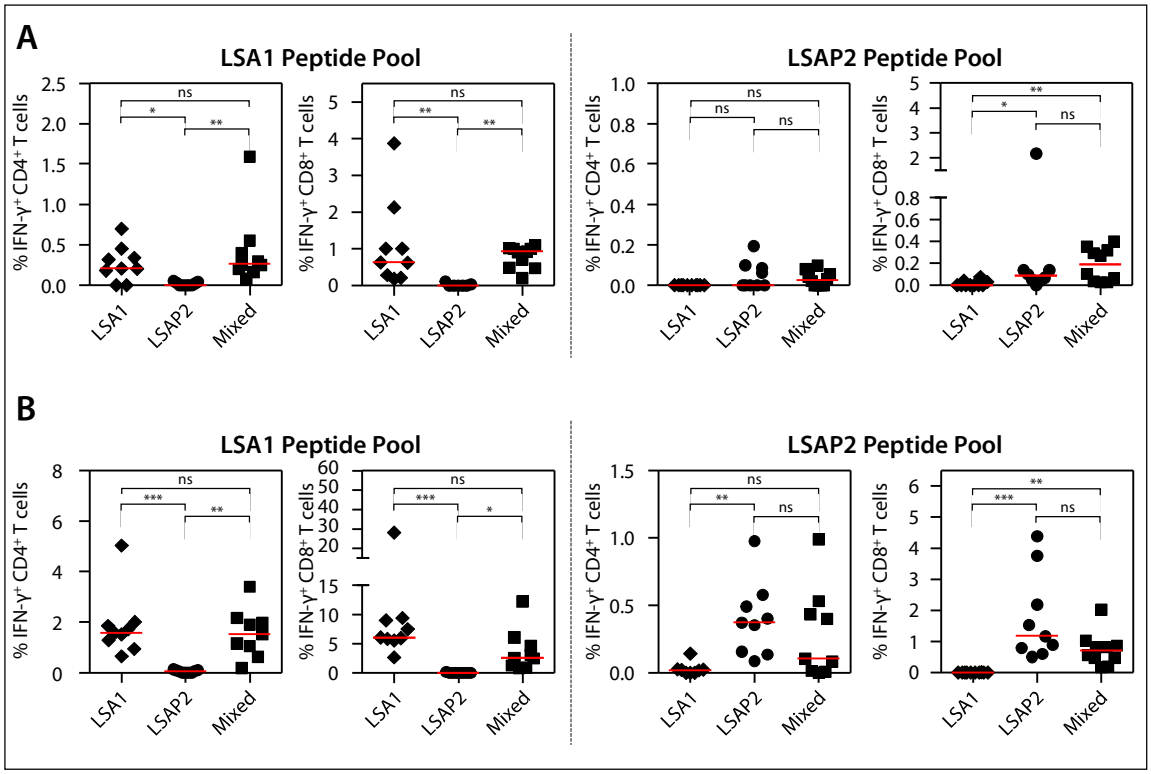



**Figure C-9. Post-prime and post-boost immunogenicity.** A blood sample was taken on day 14 post immunisation (A) or 7 days post boost (B) and analysed by ICS after stimulation with an LSA1 or LSAP2 peptide pool. Graphs represent the frequency of $CD4^+IFN\text{-}\gamma^+$ or $CD8^+IFN\text{-}\gamma^+$ T cells. Single points indicate T-cell responses of individual mice and red lines show the median response per group. Data was analysed with a one-way analysis of variance with Dunn's multiple comparison post-test. Asterisks denote the level of statistical significance when compared to each other (*, $p<0.05$; **, $p<0.01$; ***, $p<0.001$; ns, non-significant).

T-cell responses were monitored monthly over a period of 6 months (Figure C-8) to evaluate the durability of the immune response. LSA1-specific $CD4^+$ and $CD8^+$ T-cell responses peaked at month 2 when immunised with LSA1 only (Figure C-10A) and remained at a similar level until month 4, before declining in months 5 and 6. When co-administered with LSA1 and LSAP2 ("Mixed"), the immune response also peaked after the MVA boost (month 2), but appeared to decline earlier.

LSAP2-specific T-cell responses were generally lower compared with those induced by LSA1, but also peaked in month 2 after administration of the MVA boost (Figure C-10B). Whereas a low-level $CD4^+$ T cell response seemed to be maintained during the analysis period of 6 months, LSAP2-specific $CD8^+$ T-cell responses were clearly reduced in month 3 when vaccinated with LSAP2 only and slightly later (months 3–4) when immunised with both vaccines ("Mixed"). T-cell responses of months 3–6 are shown in detail in Supplemental Figure I-3 (p. 202).

Five months after MVA boost (month 7), mice were challenged IV with 1,000 infectious *P. berghei* parasites expressing *P. falciparum* LSA1 and LSAP2 to investigate long-term efficacy (Figure C-10D). All naïve BALB/c mice reached 1% parasitaemia before day 7 post challenge. Vaccinated mice showed a delay in the time to 1% parasitaemia (LSA1 $p<0.05$; LSAP2 $p<0.001$; Mixed $p<0.001$) with one sterilely protected mouse in the LSA1 as well as the "Mixed" group.

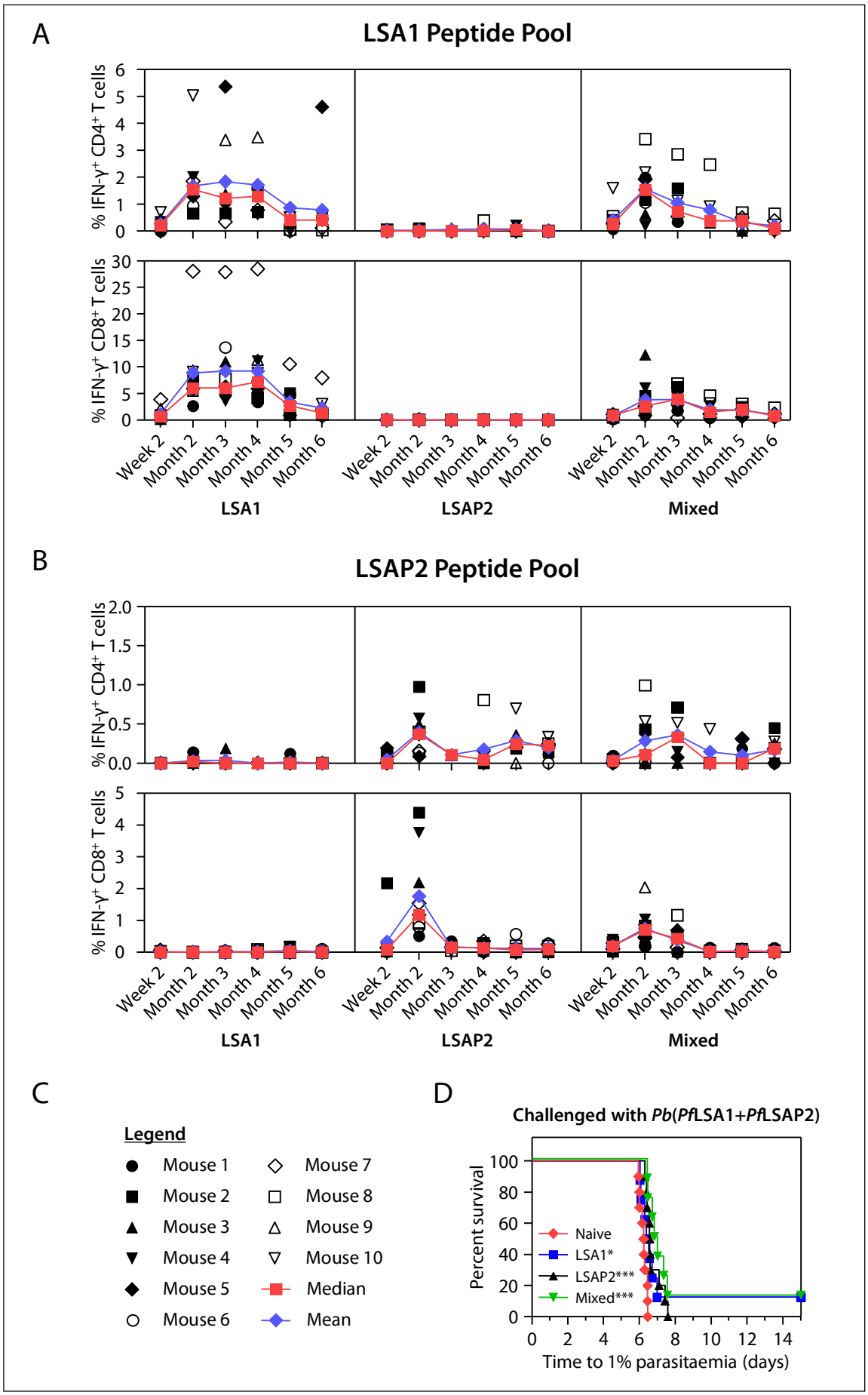

A
LSA1 Peptide Pool
% IFN-γ+ CD4+ T cells
% IFN-γ+ CD8+ T cells
Week 2
Month 2
Month 3
Month 4
Month 5
Month 6
LSA1
LSAP2
Mixed
B
LSAP2 Peptide Pool
C
Legend
Mouse 1
Mouse 2
Mouse 3
Mouse 4
Mouse 5
Mouse 6
Mouse 7
Mouse 8
Mouse 9
Mouse 10
Median
Mean
D
Challenged with Pb(PfLSA1+PfLSAP2)
Percent survival
Naive
LSA1*
LSAP2***
Mixed***
Time to 1% parasitaemia (days)

**Figure C-10. Long-term immunogenicity and efficacy.** (A–C) Blood samples were taken at various time points as indicated on the x-axes and analysed by ICS after stimulation with a (A) LSA1 or (B) LSAP2 peptide pool. Graphs represent the frequency of $CD4^+IFN\text{-}\gamma^+$ or $CD8^+IFN\text{-}\gamma^+$ T cells. Single points indicate T-cell responses of individual mice and red and blue lines show the median and mean response per group. (C) Legend explaining data points in A and B. (D) Efficacy data. Mice were challenged with 1,000 chimeric *P. berghei* sporozoites expressing *P. falciparum* LSA1 and LSAP2 at month 7. Blood smears were taken daily from four days after sporozoite challenge and analysed by Giemsa staining and light microscopy to determine parasitaemia. Mice that were negative for blood-stage malaria until 15 days after sporozoite challenge were considered to be sterilely protected. Time to 1% parasitaemia is plotted on a Kaplan-Meier Survival Curve. Data was analysed with the log-rank (Mantel-Cox) test. Asterisks denote the level of statistical significance when compared to the naïve control group (*, $p<0.05$; ***, $p<0.001$).

## C2.3 Assessment of Novel Dual Antigen Expressing Adenoviral Vectors

Having shown that the combination of two liver-stage antigens can be beneficial for the protective efficacy of a malaria vaccine, we wanted to investigate the possibilities to express multiple antigens in adenoviral vectors. Dr Sarah Sebastian (The Jenner Institute, University of Oxford) cloned two novel ChAd63 constructs, which encoded two liver-stage antigens, the N-terminal domain of CSP (denoted CSN) and ME-TRAP. The ChAd63 vectors were then produced by the viral vector core facility of the Jenner Institute (B2.2, p. 41). One construct used a bidirectional CMV derived promoter to express ME-TRAP and CSN (denoted as "Bidirectional"), whereas the other (E1-E3) encoded ME-TRAP in the E1 locus of the adenovirus under a long CMV promoter and CSN in the E3 locus under a short CMV promoter (Figure C-11, p. 82).

To investigate their immunogenicity, four BALB/c mice per group were immunised IM with $10^7$ IU or $10^8$ IU of ChAd63 expressing either ME-TRAP or CSN, both vaccines ("Mixed"), the bidirectional, or the E1-E3 construct, with spleens harvested two weeks later (which represents the peak in the immune response [144]). Splenocytes were then stimulated with the immunodominant $H\text{-}2^d$ restricted epitope of ME-TRAP (Pb9) or a single pool of overlapping peptides covering the full CSP sequence (B2.4.1, p. 47) to measure intracellular production of IFN-γ (IL-2, and TNF) by ICS (B2.4.2, p. 47).

Strong Pb9-specific $CD8^+$ T-cell responses could be measured in all groups of mice that were immunised with $10^7$ IU or $10^8$ IU ChAd63 vectors encoding ME-TRAP (ME-TRAP, Mixed, Bidirectional, E1-E3) (Figure C-11B and Figure C-11C). However, CSP-specific $CD8^+$ T-cell responses were only detected by CSN and the "Mixed" group. Both novel dual antigen expressing ChAd63 ("Bidirectional" and "E1-E3") failed to induce a strong $CD8^+$ T-cell response to the level observed with the single CSP vector, even when vaccinated with the higher dose of $10^8$ IU ChAd63 vectors (Figure C-11C). No $CD4^+$ T-cell responses could be measured when stimulated with Pb9 (which has been described to be a H-$2^d$ restricted epitope) or CSP.

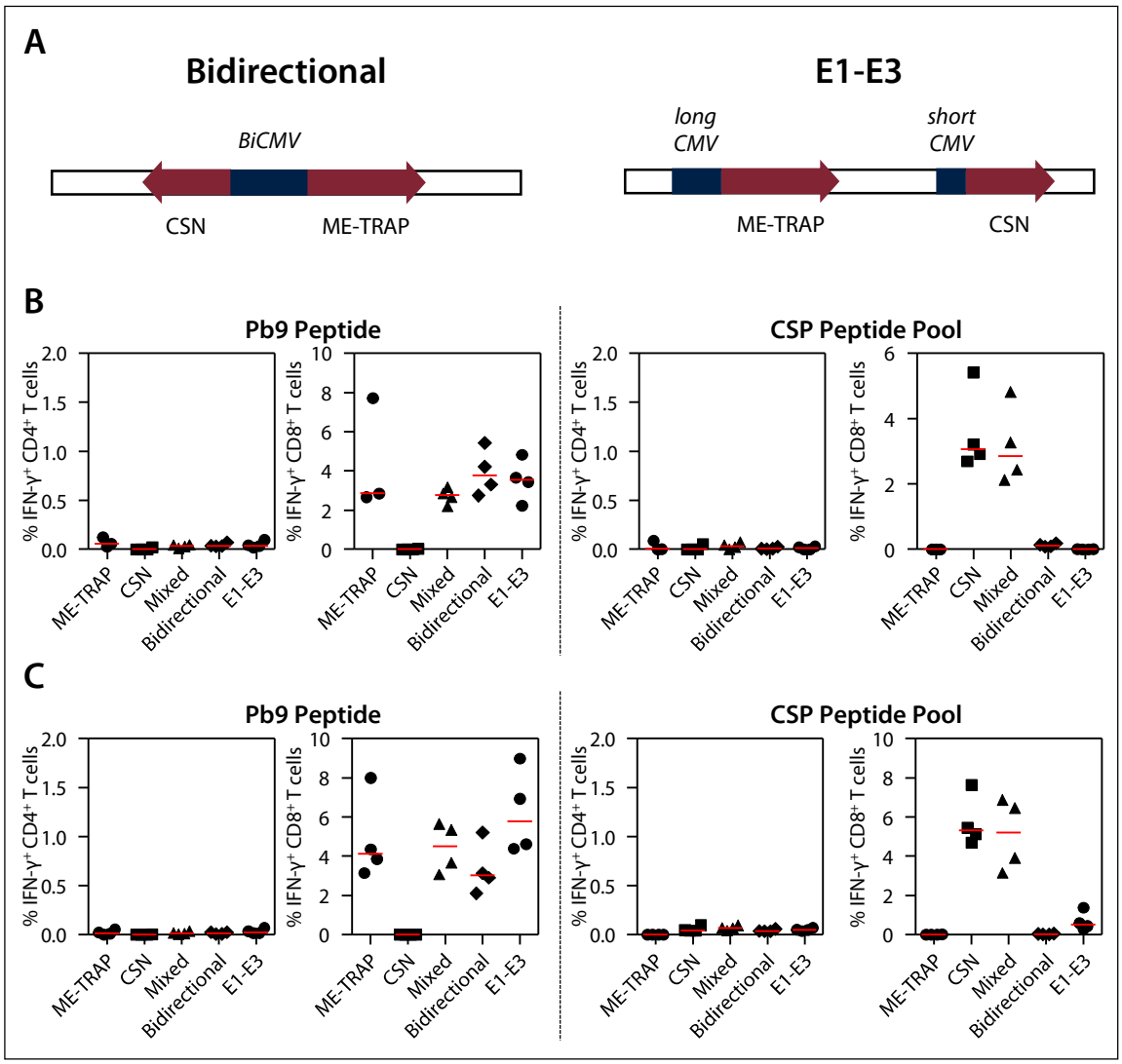



**Figure C-11. Immunogenicity of dual antigen expressing ChAd63 in BALB/c.** (A) Two novel ChAd63 vectors expressing ME-TRAP and CSN were produced – one encoding a bidirectional CMV promoter and the other encoding ME-TRAP under a long CMV promoter in the E1 locus and CSN under a short CMV promoter in the E3 locus of ChAd63. (B–C) BALB/c mice were immunised with (B) $10^7$ IU or (C) $10^8$ IU of ChAd63-ME-TRAP, ChAd63-CSN, a mix of the latter two vaccines ("Mixed") or dual antigen expressing ChAd63 vectors. Spleens were harvested two weeks later. $CD4^+$ and $CD8^+$ T-cell responses to the Pb9 peptide (a dominant H-$2^d$ restricted epitope) and a CSP peptide pool were measured by intracellular IFN-γ staining (B2.4.2, p. 47). Single points represent T-cell responses of individual mice and red lines indicate the median response per group.

## C3 Discussion

Pre-erythrocytic subunit malaria vaccines in clinical development are based on a small handful of historical candidate antigens, mainly CSP and TRAP, but success in clinical trials has been limited. As evidence suggests that antigens other than CSP and TRAP contribute to protective immunity [220–223], it is likely that the inclusion of multiple antigens in a vaccine will be necessary to reach sufficient levels of protection. Encouragingly, with science progressing into the –omic era, many more potential liver-stage vaccine antigen candidates have been identified from the parasite's genome. Preclinical assessment of these antigens has been difficult due to the fact that *P. falciparum* (which causes highest malaria burden in humans) does not naturally infect standard laboratory animals. However, in a recent publication, Longley et al. have described an elegant solution to this problem by challenging vaccinated mice with a murine parasite strain (*P. berghei*), which expresses the relevant *P. falciparum* vaccine antigen as a transgene [10]. This is especially useful when there is no known orthologue of the *P. falciparum* vaccine antigen present in the murine plasmodium species. Two of the liver-stage antigen candidates tested in this study, LSA1 and LSAP2, have been shown to induce significantly better protection compared to TRAP or CSP.

In this study, immunogenicity and efficacy of the combination of ChAd63-MVA prime boost vaccinations with vectors encoding a modified TRAP antigen (TRIP) and one of the four more protective liver-stage antigens (LSA1, LSAP2, UIS3, or Falstatin) compared to CSP or TRAP, were assessed in a BALB/c mouse model. In order to investigate efficacy, murine challenge parasites expressing two *P. falciparum* transgenes were generated by Dr Ahmed Salman (The Jenner Institute, University of Oxford). Despite theoretical concerns that administration of more than one antigen would result in competition between antigens [192, 193], no detrimental effect was observed when any of

these liver-stage vaccine candidate antigens were administered in combination with a TRAP encoding vaccine. Most importantly, the addition of LSA1, LSAP2, and UIS3 to TRIP vaccination increased protective efficacy against double chimeric *P. berghei* parasites expressing *P. falciparum* TRAP and the relevant second liver-stage antigen (LSA1, LSAP2, or UIS3; see Figure C-4, p. 69). Strikingly, when LSA1 or UIS3 vaccines were mixed with vectors encoding TRIP before administration, 100% of vaccinated mice were sterilely protected against parasite challenge. This was a very encouraging result as such high levels of efficacy have not been seen in our BALB/c challenge model before.

Another observation was that efficacy was higher when vaccines were mixed before administration compared to injection of both vaccines into separate sites. This was somewhat surprising, as the amount of injected vectors was identical between "Separate" and "Mixed" groups and previous studies with multiple antigen combinations suggested that a mixture of vaccines can be detrimental to T-cell priming [192, 224]. Analyses of antibody (Figure C-3, p. 67) and T-cell responses (Figure C-2, p. 66) did not explain our observation. All vaccines and vaccine combinations induced antigen-specific $CD4^+$ and $CD8^+$ T-cell as well as antibody responses comparable with previous publications [10], but there was no significant difference between the "Separate" and "Mixed" groups. As T-cell responses of PBMC do not necessarily reflect tissue specific immunity, liver-resident T cells were analysed. These could act much quicker after parasite infection compared to T cells recruited from the periphery. In fact, the liver is known to be an immunological organ capable of priming naïve T cells [56] and the presence of liver-resident antigen-specific T-cells has been demonstrated following immunisation with malaria vaccine candidates in previous studies [145, 225–228].

However, when T-cell responses in the draining lymph node, spleen, and the liver were analysed following ChAd63-MVA prime-boost immunisation with TRIP and LSA1 encoding vectors, there was no clear difference in the antigen-specific $CD8^+$ T-cell

responses between the groups, but LSA1-specific $CD4^+$ T-cell responses in the liver were higher in the "Mixed" group compared to the "Separate" group (Figure C-5, p. 71). As previous $CD4^+$ and $CD8^+$ T-cell depletion experiments suggested at least some protective efficacy of the LSA1-specific $CD4^+$ T-cell population in BALB/c mice, a significance of this finding cannot be ruled out. However, a more likely reason for the increased protective immunity induced by the "Mixed" group is that viral vectors encoding both antigens reach more lymphatic tissue (two injection sites for both vaccines) compared to the separate administration (one injection site per vaccine). This hypothesis can be tested easily by immunising mice with equal amount of viral vectors, but varying the number of injection sites. An initial experiment did not arrive at conclusions, because of full protection in all study groups (most likely caused by reduced fitness of the challenge parasites) and has to be repeated (data not shown).

Having shown that co-administration of viral vectors encoding second generation liver-stage antigens with well-studied TRAP containing vaccines can be beneficial for protection against parasite challenge, it was of similarly high interest to analyse the combination of LSA1 and LSAP2. Both have previously been shown to protect 87.5% of BALB/c mice against parasite challenge with *P. berghei* parasites expressing *Pf*LSA1 or *Pf*LSAP2 [10] or, as described in this thesis, 33% against double-chimeric *Pb*(*Pf*TRAP+*Pf*LSA1). Being located in the PVM [207, 229], epitopes of both antigens are likely to be presented more easily compared to other proteins, which are encapsulated inside the parasitophorous vacuole [208, 230], and therefore have the potential to induce a more efficacious T-cell response. An initial ChAd63-MVA prime-boost experiment performed by Dr Ahmed Salman (The Jenner Institute, University of Oxford) with vectors encoding LSA1 and LSAP2 mixed together prior to administration induced 100% sterile efficacy in BALB/c mice against challenge with double transgenic *Pb*(*Pf*LSA1+*Pf*LSAP2) parasites (Supplemental Figure I-2, p. 201). Based on these results, it was investigated

whether the administration of ChAd63 vectors alone encoding LSA1 and LSAP2 (without following MVA boost) can induce some levels of protective immunity. Strikingly, when challenged with double transgenic parasites 14 days after immunisation, 80% of BALB/c mice immunised with both vaccines ("Mixed") were protected (Figure C-7, p. 75). Even though mice were challenged at the peak of the immune response following ChAd63 vaccination [144] and therefore at an ideal, but somewhat artificial time point, the results were striking, as we had not seen such a high level of protective efficacy in a prime-only regimen in this model before.

Despite these promising data, it is difficult to predict how translatable these results are to human clinical trials. BALB/c mice are inbred mice and therefore present only a small number of MHC restricted epitopes leading to marked immunodominance, which does not reflect the diversity of antigen presentation in human populations. The combination of viral vectors should therefore also be tested in outbred mice, such as CD1 mice. Encouragingly, both antigens individually (LSA1 and LSAP2) have been shown to induce strong protective efficacy in CD1 mice when administered in a ChAd63-MVA prime-boost regimen [10].

Another limitation of the challenge model used in this study is that the *P. falciparum* antigens of the transgenic murine parasites are expressed under the control of the *P. berghei* UIS4 promoter and are therefore not matched with their native expression levels. The generation of parasites, which have their *P. berghei* genes replaced by their *P. falciparum* orthologues, might improve this challenge model. However, as for many antigen candidates (such as LSA1) no *P. berghei* orthologues are presently known, this strategy is not always applicable. Furthermore, analyses of the immune response kinetics induced by viral vectors encoding LSA1 and LSAP2 individually as well as mixed together revealed that antigen-specific immunity has limited durability (Figure C-10, p. 80). Antigen-specific T-cell responses peaked one week after administration of the MVA boost

with no significant differences between study groups, but started to decline 3 months after administration of the MVA booster vaccines. No sterile efficacy was observed 5 months post boost, but liver parasite burden was still reduced as suggested by the significant delay to patent parasitaemia.

Lastly, to reduce production costs of viral vectors, the possibility to encode two different liver-stage vaccine antigens in one adenoviral vector was investigated. The capacity to uptake gene inserts is limited in viral vectors: whereas MVAs are capable of encoding antigens of up to 10 kb, gene inserts in adenoviral vectors are limited to about 5–6.5 kB. This is still enough to accommodate multiple liver-stage antigens. Two dual antigen expressing ChAd63 vectors, one with a bidirectional CMV derived promoter, the other with two antigens encoded in two different loci of the virus genome (E1 and E3), were generated by Dr Sarah Sebastian (The Jenner Institute, University of Oxford) and analysed for immunogenicity in this thesis. Results suggested that neither of those novel vectors had the ability to induce strong immune response against both encoded antigens (ME-TRAP and CSN). Instead, only ME-TRAP, but not CSN, seemed to be immunogenic when encoded in these dual antigen-expressing vectors (Figure C-11, p. 82). The cause for this lack of immunogenicity against the second antigen remains unclear. It would be of interest to analyse if this is based on restricted protein expression (via western blot or quantitative PCR) or immune interference caused by the simultaneous presentation of epitopes from both antigens on the same APC (as suggested previously [231]). This might be less efficient, as the space around the APC is restricted, possibly limiting access to survival factors and costimulatory molecules [192].

In summary, this study has shown that the combination of certain liver-stage vaccine antigens in a ChAd63-MVA prime-boost regimen can have a positive effect on vaccine efficacy in the BALB/c mouse model. Unlike findings of previous publications [192, 224], the mixture of vaccine vectors before injection led to improved vaccine protection

compared to vaccine administration at separate sites. As immunogenicity data did not explain our finding, the underlying mechanisms remain unclear. Regardless of this obscurity, the efficacy of the combination of LSA1 and LSAP2 (two antigens that have recently been shown to be highly efficacious when administered individually [10]) was particularly promising with all vaccinated mice sterilely protected against subsequent parasite challenge. Prospective clinical trials analysing immunogenicity and efficacy are required to find out if these results obtained in murine models can be confirmed in humans. As durability of vaccine immunogenicity and sterile efficacy was limited in our BALB/c challenge model, future clinical vaccine trials should include a careful monitoring of antigen-specific $CD4^+$ and $CD8^+$ T cells over time. Vaccination regimens could then be adjusted accordingly to achieve long-lasting immunity.

# Chapter D

# Development of a Molecular Adjuvant

# D1 Introduction

Genetically engineered viral vectors are excellent inducers of strong $CD8^+$ T-cell responses and recent progress in liver-stage malaria vaccine development with ChAd63-MVA vaccination regimens is very encouraging with some degree of clinical efficacy in both malaria naïve and pre-exposed individuals [148, 191]. Since protection against the liver-stage of malaria has been strongly associated with high numbers of antigen specific $CD8^+$ T-cell responses, it has been a priority to further increase immunogenicity of viral vectors. Numerous approaches, often using well-known adjuvants, have been explored, but failed. However, several groups have now reported that genetic fusion of the vaccine antigen to the invariant chain (Ii) of MHC class II and expression from viral vectors enhances antigen-specific $CD8^+$ T-cell responses across various animal species, including non-human primates (NHP) [150, 232]. One of the last potential obstacles before clinical testing of the Ii as molecular adjuvant are safety concerns, as the expression of a self-antigen from a highly immunogenic viral vector could theoretically break immune-tolerance and induce an auto-immune response. These concerns will be addressed in this chapter.

## D1.1 Structure and Isoforms

The HLA class II associated invariant chain (Ii, also called γ-chain of HLA class II or CD74) is, as its name implies, non-polymorphic, and encoded on the human chromosome 5 [233]. However, expression of the Ii can be started at two translation initiation sites of the human Ii mRNA leading to the low expression of a 35 kDa form (hIi-p35) as well as a highly expressed smaller Ii molecule of 33 kDa (hIi-p33), which uses the second translation initiation site located further downstream. In addition, two larger isoforms, hIi-p41 and hIi-p43, can be generated by alternative mRNA splicing which leads to the expression of an additional 8 kDa large exon (Figure D-1) [234]. The use of the

upstream alternative translation initiation site seems to be unique to primates, mice only express the mIi-p31 and mIi-p41 isoforms. The shortest Ii isoforms (hIi-p33 in humans and mIi-p31 in mice) are most prominently expressed [235].

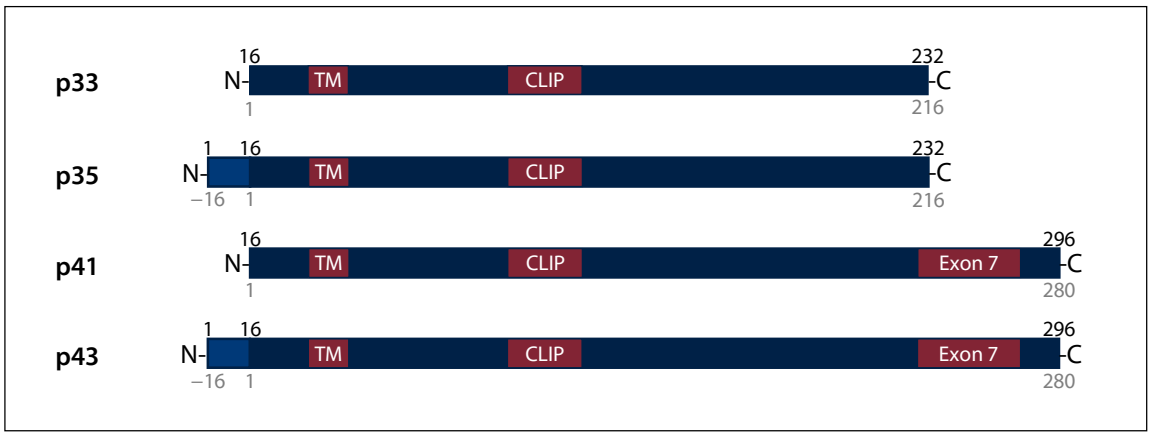



**Figure D-1. Isotypes of the human Ii.** Due to the existence of two sites of translation initiation and alternative mRNA splicing, four isoforms of the human Ii can be expressed. Adapted from [234].

As a type II transmembrane glycoprotein, the hIi-p35 isotype has an N-terminal cytoplasmic tail (aa 1–46), a transmembrane domain (aa 47–72), and a C-terminal luminal end (aa 73–232) (Figure D-2).

The cytoplasmic domain (aa 01–46) encodes two leucine based sorting signals (L23I24 and M32L33G34), which are described to direct the Ii-MHC-class-II-complex to endocytic compartments [236–238]. The human Ii isoforms hIi-p35 and hIi-p43 also contain an N-terminal ER retention motif, consisting of three consecutive arginine residues (R3R4R5) [239, 240].

The luminal domain of the hIi-p35 (aa 73–232) consists of a trimerisation domain (aa 136–207) [241, 242] as well as the MHC class II associated invariant chain peptide (CLIP, aa 103–117) which binds to the MHC class II binding groove, thereby prohibiting endogenous peptides binding to it during protein synthesis. Despite enormous variability in the affinity of CLIP-MHC-class-II-interactions due to the extremely high polymorphism of the MHC class II binding groove [243, 244], effective binding is

accomplished by additional low-affinity sites of interaction between Ii regions outside the CLIP domain and MHC class II [245–249]. A four-amino-acid sequence (LRMK), denoted as Ii-key, is known to bind to an allosteric site just outside the MHC class II binding groove [250–253].

The Ii transmembrane region (aa 47–72) has an intrinsic capacity to form a trimer [254], caused by a hydrophilic patch of polar amino acids, which form an α-helical left-handed coiled coil [255, 256]. Furthermore, the Ii transmembrane region interacts and is thought to stabilise MHC class II molecules in endosomes after the majority of Ii has been degraded in the luminal region [249].

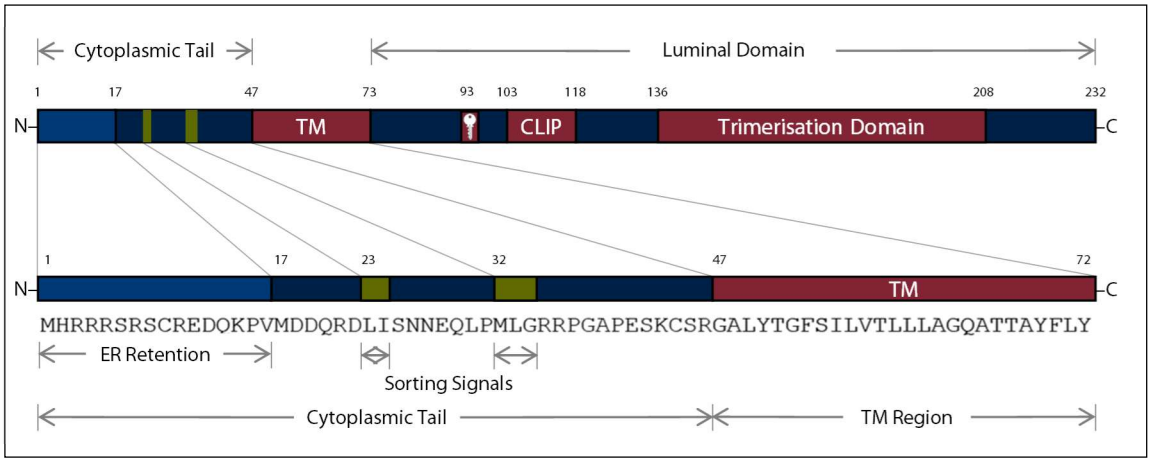



**Figure D-2. Subdomains of the human Ii.** The hIi-p35 isotype of the human Ii consists of an N-terminal cytoplasmic tail encoding an ER retention site as well as two sorting signals, a transmembrane domain, and a luminal domain encoding the Ii-key, CLIP, and C-terminal trimerisation domains.

## D1.2 Invariant Chain HLA class II Interaction

The interaction between HLA class II and Ii is well-described. The multiple functions of Ii can be viewed as scaffold, guardian, and leader [257].

**Scaffold.** The invariant chain is synthesised alongside the MHC class II α and β chains in the endoplasmic reticulum (ER), where it self-assembles into trimers and then

chaperones the assembly of MHC class II by associating sequentially with MHC class II α and β chains to form MHC-class-II-Ii complexes [258, 259].

**Guardian.** The formation of these MHC-class-II-Ii complexes ensures that the binding groove of MHC class II is occupied by the class II-associated invariant chain peptide (CLIP). This prevents endogenous peptides from binding during early intracellular transport [260]. To ensure Ii rather than peptide binding, Ii is normally synthesised in excess over MHC class II [235, 261–263, 263].

**Leader.** Leucine based sorting signals in the cytoplasmic domain of the Ii direct MHC-class-II-Ii complexes to endo/lysosomal compartments directly via the Golgi apparatus or by recycling from the cell surface membrane [256].

Inside late endosomes, specific enzymes (such as cathepsin S) process the Ii by sequential proteolysis until only the CLIP domain remains bound to MHC class II. In a final step, CLIP is released to be replaced by a (mostly) exogenous peptide. This is facilitated by the MHC-II-related chaperone, known as HLA-DM (H2-M in mice), which induces a conformational change in the MHC-II molecule and thereby CLIP displacement. Exogenous peptides are derived from antigens that have reached the late endo/lysosomal compartments by phagocytosis, pinocytosis, or endocytosis, and have been processed by cathepsins or the γ-interferon-inducible lysosomal thiol [235, 260].

The MHC-II-peptide-complex is then transported to the cell surface membrane for presentation to $CD4^+$ T cells [260] (Figure D-3).

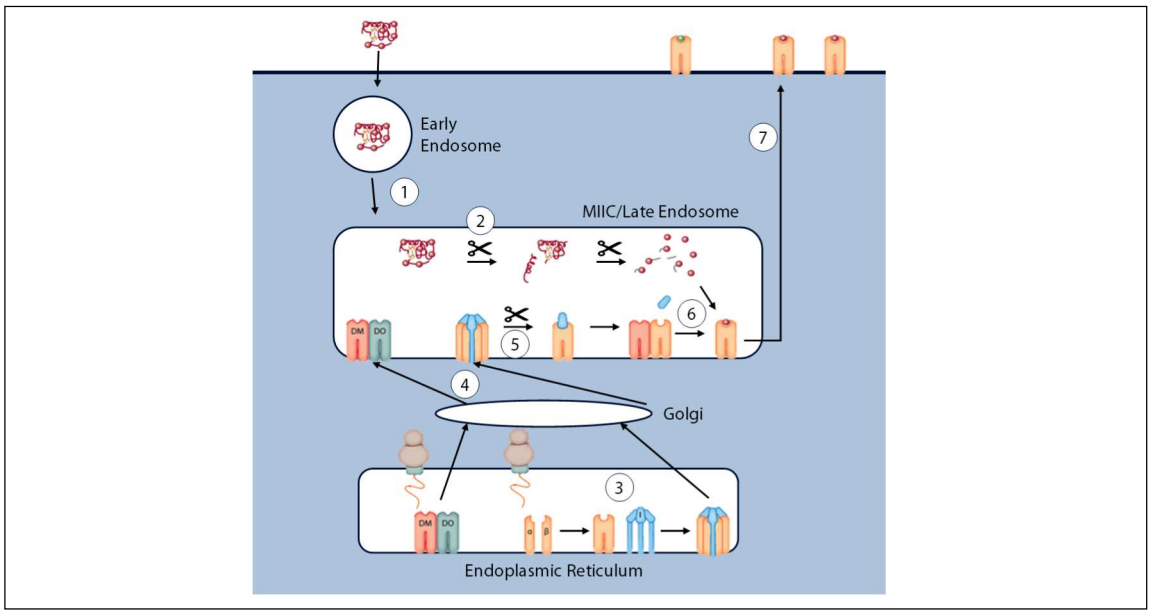



**Figure D-3. Processing and presentation of exogenous antigens on MHC class II molecules.** Adapted from [260]. (1) An exogenous antigen is internalised and located in an early endosome. (2) Endosomal proteases digest exogenous proteins. (3) After production of the α and β chain of MHC class II, it associates with the invariant chain (Ii) and trimerises. (4) HLA-DM, HLA-DO and MHC-II-trimers are transported to late endosome via Golgi. (5) Ii is degraded to a residual CLIP that still blocks the MHC binding groove. (6) The exchange of CLIP for an exogenous peptide is facilitated by HLA-DM. (7) Presentation of the MHC-II-peptide-complex on the cell surface.

## D1.3 Invariant Chain MHC class I Interaction

An interaction between MHC class I, especially β2-microglobulin, and Ii as well as their co-localisation in endocytic compartments has been known since the 1990s [264–267]. In 2002, Reber et al. demonstrated that transfection of HeLa cells with Ii leads to much higher surface expression of MHC class I, suggesting a functional importance of the Ii-MHC-class-I-interaction [268, 269]. This physiological significance in cross-presentation was then creatively demonstrated by Basha et al. in 2012 [269]. The Ii binds a fraction of newly synthesised MHC class I and directs them to endolysosomal compartments, thereby facilitating the binding of peptides which are derived from exogenous antigen [270]. Interestingly, the Ii therefore seems to interact with MHC II and MHC I molecules in a very similar way [271, 272].

## D1.4 Evidence for Ii-Adjuvanticity

Ii fusion to a vaccine antigen of interest to enhance antigen presentation to $CD4^+$ T cells has already been demonstrated by several researchers since the 1990s [150, 232, 273–279]. However, an additional effect on $CD8^+$ T-cell induction was not described until 2006 when Rowe et al. induced an improved CTL response by immunising mice with a lentiviral vector encoding an Ii-ovalbumin fusion construct (Ii-OVA) [277]. Numerous reports from the University of Copenhagen then confirmed the $CD8^+$ T-cell adjuvanticity of the Ii by immunising several inbred mouse strains with various vector systems, such as plasmid DNA or human adenovirus 5, and different viral antigens, such Lymphocytic Choriomeningitis Virus (LCMV)-derived glycoprotein [278, 279] or the non-structural protein 3 (NS3) of Hepatitis C Virus (HCV) [280]. Ii linkage of *Listeria monocytogenes*-derived antigens also improved protection against these intracellular bacteria [281]. As this effect is preserved in MHC class II-deficient mice, it seems to be independent from $CD4^+$ T-cell help [282]. More recent reports also document enhanced $CD8^+$ T-cell induction in non-human primates (NHP) by vaccination with chimpanzee adenoviral vectors, ChAd3 [232] and ChAd63 [150], expressing HCV non-structural proteins [232] or the malaria antigen ME-TRAP [150] (see Table D-1).

**Table D-1.** Literature documenting Ii adjuvanticity.

| | **CD4s** | **CD8s** |
|---|---|---|
| 1990s | ▪ cDNA-OVA [273]: Ii truncated to 80 aa<br>▪ cDNA-tetanus toxoid [274]: Site-specific insertion into the CLIP region<br>▪ cDNA-HEL [275]: Hen egg lysozyme | |
| 2000s | ▪ HAd5/PEI/DNA-OVA complex [276]<br>▪ Lentivirus-OVA [277]<br>▪ HAd5-GP (GP of LCMV) [278]<br>▪ cDNA-GP (GP of LCMV) [279] | ▪ Lentivirus-OVA [277]<br>▪ HAd5-GP (GP of LCMV) [278]<br>▪ HAd5-NP (NP of LCMV) [278]<br>▪ cDNA-GP (GP of LCMV) [279] |

| | CD4s | CD8s |
|---|---|---|
| 2010s | ▪ (HAd5-LLO and HAd5-p60 [281]: Antigens of *L. monocytogenes*)<br>▪ ChAd3-NS + MVA-NS [232]: NS of HCV also in NHP<br>▪ ChAd63-ME-TRAP + MVA-ME-TRAP [150]: also in NHP | ▪ HAd5-OVA; HAd5-GP (GP of LCMV) in MHC II deficient mice [282]<br>▪ HAd5-NS3 [280]: (NS3 of HCV)<br>▪ HAd5-LLO and HAd5-p60 [281]: Antigens of *L. monocytogenes*<br>▪ ChAd3-NS + MVA-NS [232]: NS of HCV also in NHP<br>▪ ChAd63-ME-TRAP + MVA-ME-TRAP [150]: also in NHP |

## D1.5 Development of Ii for Clinical Usage

Despite encouraging progress in the development of an efficacious liver-stage malaria vaccine, a greater number of circulating antigen-specific $CD8^+$ T cells will be required to achieve levels of efficacy justifying mass vaccine deployment. Hence, Spencer et al. investigated the fusion of ME-TRAP to the C-terminal end of the full-length human Ii sequence and reported increased antigen-specific $CD8^+$ T-cell responses in mice as well as rhesus macaques [150]. Progress of this approach into human clinical trials would therefore be of highest interest. However, because concerns were raised that tolerance against the Ii, a self-antigen, could be broken by inclusion of the antigen in a strong T-cell inducing vaccination regimen, this vaccine has not translated to clinical testing. These concerns were brought to attention when two publications documented autoantibodies targeting the CLIP region of the Ii [283, 284]. To minimise this potential risk, two strategies were pursued in this thesis:

- **Truncation approach**: The Ii was truncated to determine essential parts of the Ii for adjuvanticity.
- **Xenogenisation approach:** The Ii sequence was "xenogenised" by using Ii sequences of animal species that are distinct from the human Ii sequence.

# D2 Results

## D2.1 Truncation of Ii

### D2.1.1 Design and Cloning of Truncated Ii-ME-TRAP Constructs

The ME-TRAP antigen construct, which has already been used in clinical trials, comprises a human codon-optimised multi-epitope string (ME) fused to the native *P. falciparum* T9/96 strain sequence of TRAP. When fused to Ii sequences, the nucleotides 1–75 of TRAP were deleted from the construct, which encodes a predicted signal peptide in order to prevent hydrolysis of the Ii from TRAP (if signal peptide binding were to occur). This deletion within ME-TRAP itself did not have an impact on immunogenicity when expressed in ChAd63 vectors as shown in Supplemental Figure I-4 (p. 203). ME-TRAP was then fused to the C-terminal end of the full-length human p35 isoform of the invariant chain, named (fl)human/Ii-ME-TRAP, and subcloned into the entry vector pENTR4-LPTOS, which contains the human cytomegalovirus immediate-early promoter and the bovine growth hormone poly(A) transcription termination sequence (B2.1.10, p. 40). To identify the essential parts of Ii for its adjuvanticity, the Ii sequence was truncated systematically. In the first novel Ii-ME-TRAP constructs, (tr)human98/Ii-ME-TRAP, (tr)human92/Ii-ME-TRAP, and (tr)human72/Ii-ME-TRAP, the Ii was truncated to its N-terminal 98 aa, 92 aa, or 72 aa, respectively (Figure D-4).

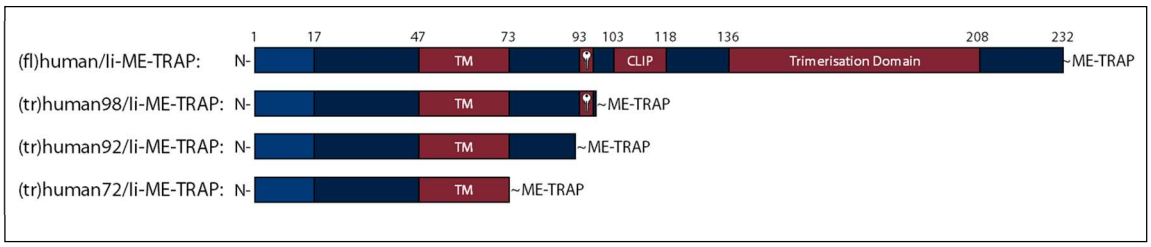



**Figure D-4. Initial truncation of Ii in Ii-ME-TRAP constructs.** The DNA sequence of the liver-stage antigen ME-TRAP was fused to the C-terminal end of either the full-length human p35 isoform of the invariant chain or Ii truncations of 98, 92, or 72 amino acid length and subcloned into the entry vector

pENTR4-LPTOS. The full-length Ii encodes a transmembrane domain (TM, aa 47–72), the Ii-Key domain (aa 93–96), the CLIP domain (aa 103–117), as well as the C-terminal trimerisation domain (aa 136–207).

After positive initial results (chapter D2.1.2), further Ii constructs were designed. One encodes only the Ii TMD (humanTM/Ii-ME-TRAP), another only its cytoplasmic tail (humanCT/Ii-ME-TRAP). Three more spare either the ER retention site (humanV1/Ii-ME-TRAP) or one of the sorting signals (humanV2/Ii-ME-TRAP and humanV3/Ii-ME-TRAP) (Figure D-5). Cloning and following production steps of ChAd63 vectors encoding these Ii-ME-TRAP constructs are described in sections B2.1.10ff (p. 40ff).

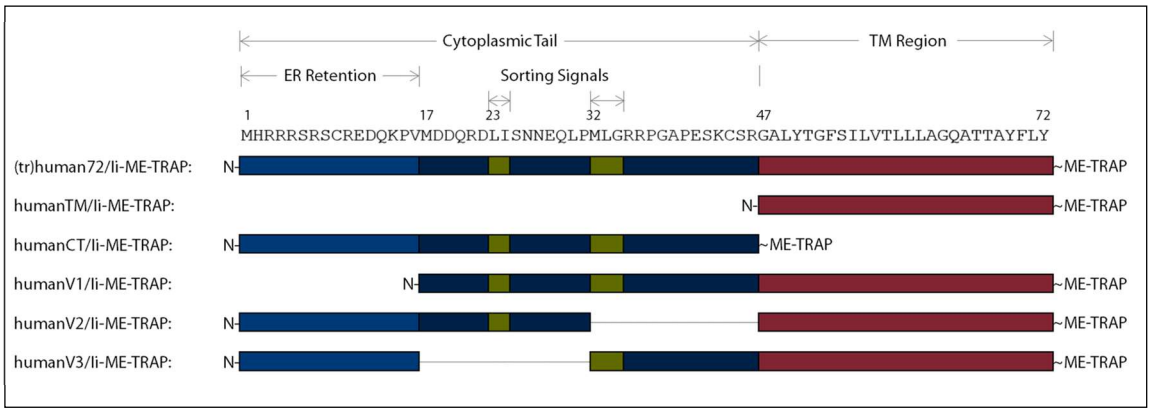



**Figure D-5. Further truncation of the Ii.** The DNA sequence of the liver-stage antigen ME-TRAP was fused to further truncated human invariant chain sequences. As prior results indicated that strong $CD8^+$ T-cell responses could be induced with a 72 amino acid long sequence of the Ii chain, new constructs with further truncations were designed as indicated.

## D2.1.2 Immunogenicity of Truncated Ii-ME-TRAP Fusion Constructs

To determine whether vaccination with ChAd63 vectors encoding ME-TRAP fused to the described Ii truncations could enhance antigen-specific T-cell responses, C57BL/6 mice were vaccinated IM with spleens harvested 14 days later, which represents the peak in the immune response [144], and splenocytes stimulated with a single pool of overlapping peptides covering the full TRAP sequence (B2.4.1, p. 47) to measure intracellular production of IFN-γ, IL-2, and TNF by ICS (B2.4.2, p. 47).

First, the immunogenicity of unfused ME-TRAP was compared to (fl)human/Ii-ME-TRAP and 98, 92, and 72 aa-long truncated variants of the Ii-ME-TRAP constructs by Dr Alex Spencer (Figure D-4 and Supplemental Figure I-5, p. 204). All investigated Ii-ME-

TRAP vectors induced a higher immune response compared to unfused ME-TRAP. Remarkably, (tr)human72/Ii-ME-TRAP induced a similar TRAP-specific $CD4^+$ T cells response as well as an increased $CD8^+$ T-cell response when compared to (fl)human/Ii-ME-TRAP. This difference was not statistically significant in this particular experiment. An additional experiment showed that the TRAP-specific $CD8^+$ T-cell response could be further enhanced by boosting mice with an MVA vector encoding the same antigen sequence (MVA-(tr)human72/Ii-ME-TRAP) (Supplemental Figure I-5, p. 204).

Based on these encouraging results, the Ii sequence in Ii-ME-TRAP constructs was further truncated (D2.1.1), produced in ChAd63 vectors and immunogenicity was analysed by ICS (IFN-γ, IL-2, and TNF) of splenocytes from C57BL/6 mice two weeks after vaccination. Methods and gating strategy are described in section B2.4.2 (p. 47f). The data was analysed with a one-way analysis of variance with Dunn's multiple comparison post-test.

The highest $CD8^+$ T-cell responses were observed when ME-TRAP was fused to (tr)human72/Ii or humanTM/Ii. Both induced an approximately 5.5-fold and statistically significant increase in the frequency of IFN-γ producing $CD8^+$ T cells compared to unfused ME-TRAP. In the absence of the transmembrane domain (humanCT/Ii-ME-TRAP), no difference to the unfused ME-TRAP construct was observed (Figure D-6). The remaining three constructs, humanV1-Ii-ME-TRAP, humanV2-Ii-ME-TRAP, and humanV3-Ii-ME-TRAP induced a significantly higher number of antigen-specific $CD8^+$ T cells compared to unfused ME-TRAP, but a lower number than humanTM/Ii-ME-TRAP. The frequency of TNF-producing $CD8^+$ T cells was comparable to IFN-γ, but IL-2 production was generally much lower (Supplemental Figure I-6, p. 205).

In contrast to results in $CD8^+$ T cells, (fl)human/Ii-ME-TRAP induced superior $CD4^+$ T-cell responses to all truncated versions of Ii. Even though the frequency of the cytokine producing $CD4^+$ T-cell population was generally low, all truncated Ii-ME-TRAP fusion

constructs were equal or slightly better than unfused ME-TRAP (albeit not statistically significant with the exception of (fl)human/Ii-ME-TRAP).

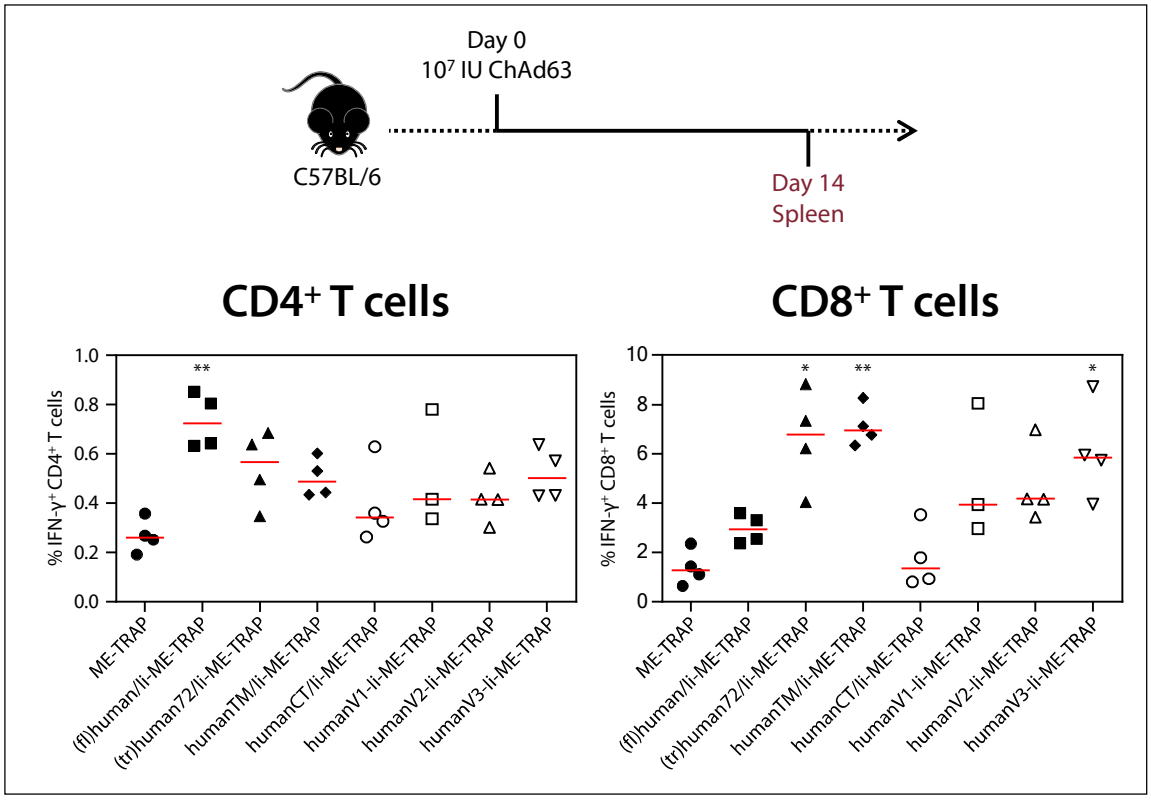



**Figure D-6. Effect of truncated Ii sequences as adjuvant for ME-TRAP in mice vaccinated with ChAd63 vectors.** C57BL/6 mice were immunised with $10^7$ IU ChAd63 vectors and spleens were harvested two weeks later. T-cell responses to a TRAP peptide pool were analysed by ICS. The percentage of $CD4^+$ and $CD8^+$ T cells positive for IFN-γ are shown. Single points indicate T-cell responses of individual mice and red lines denote the median response per group. Data was analysed with a one-way analysis of variance with Dunn's multiple comparison post-test. Asterisks denote the level of statistical significance when compared to the control ME-TRAP vaccinated group (*, $p<0.05$; **, $p<0.01$).

The experiment was repeated with selected viral vectors to confirm that only the transmembrane domain of the human Ii (humanTM/Ii) was needed for CD8-adjuvanticity (Supplemental Figure I-7, p. 206). Again, humanTM/Ii-ME-TRAP (as well as (tr)human72/Ii-ME-TRAP), but not (fl)human/Ii-ME-TRAP induced a significantly higher TRAP-specific $CD8^+$ T-cell response compared to unfused ME-TRAP.

## D2.2 Understanding the Positive Effect of Ii Truncation on Adjuvanticity

As shown in section D2.1.2, when (fl)human/Ii was truncated to the 72 aa long (tr)human72/Ii and fused to ME-TRAP, the induced antigen-specific $CD8^+$ T-cell response was considerably higher compared to (fl)human/Ii-ME-TRAP. One possible explanation is that there is a competing $CD8^+$ T-cell response against the xenogenic (fl)human/Ii, which is directed against parts of the human Ii that are not expressed in the (tr)human72/Ii version. In the case of the non-truncated version, there is competition between the response to the Ii chain and TRAP, overall leading to a reduction in the TRAP-specific response. To test this hypothesis two different strategies were pursued.

Firstly, full-length and truncated versions of mouse Ii sequences were fused to ME-TRAP and produced in ChAd63 viral vectors as described in sections B2.1.10ff (p. 40ff). C57BL/6 mice were vaccinated with $10^7$ IU of ChAd63 encoding either ME-TRAP or adjuvanted versions in which ME-TRAP was fused to either full-length or truncated human Ii sequences, or full-length or truncated mouse Ii sequence, respectively. Splenocytes were analysed two weeks later by ICS. Both vectors that were adjuvanted with full-length Ii sequences, (fl)human/Ii-ME-TRAP or (fl)mouse/Ii-ME-TRAP, induced similarly strong TRAP-specific $CD4^+$ T-cell responses, which were significantly higher compared to the response induced by unfused ME-TRAP (Figure D-7). In contrast, both (tr)human72/Ii-ME-TRAP and (tr)mouse/Ii-ME-TRAP only induced a slightly but not significantly higher TRAP-specific $CD4^+$ T cell response. Consistent with previous observations, a stronger antigen-specific $CD8^+$ T-cell response was induced by (tr)human72/Ii-ME-TRAP compared to (fl)human/Ii-ME-TRAP. Interestingly, both vectors that were adjuvanted by full-length or truncated mouse Ii induced the highest TRAP-specific $CD8^+$ T cell responses with no significant difference between the constructs.

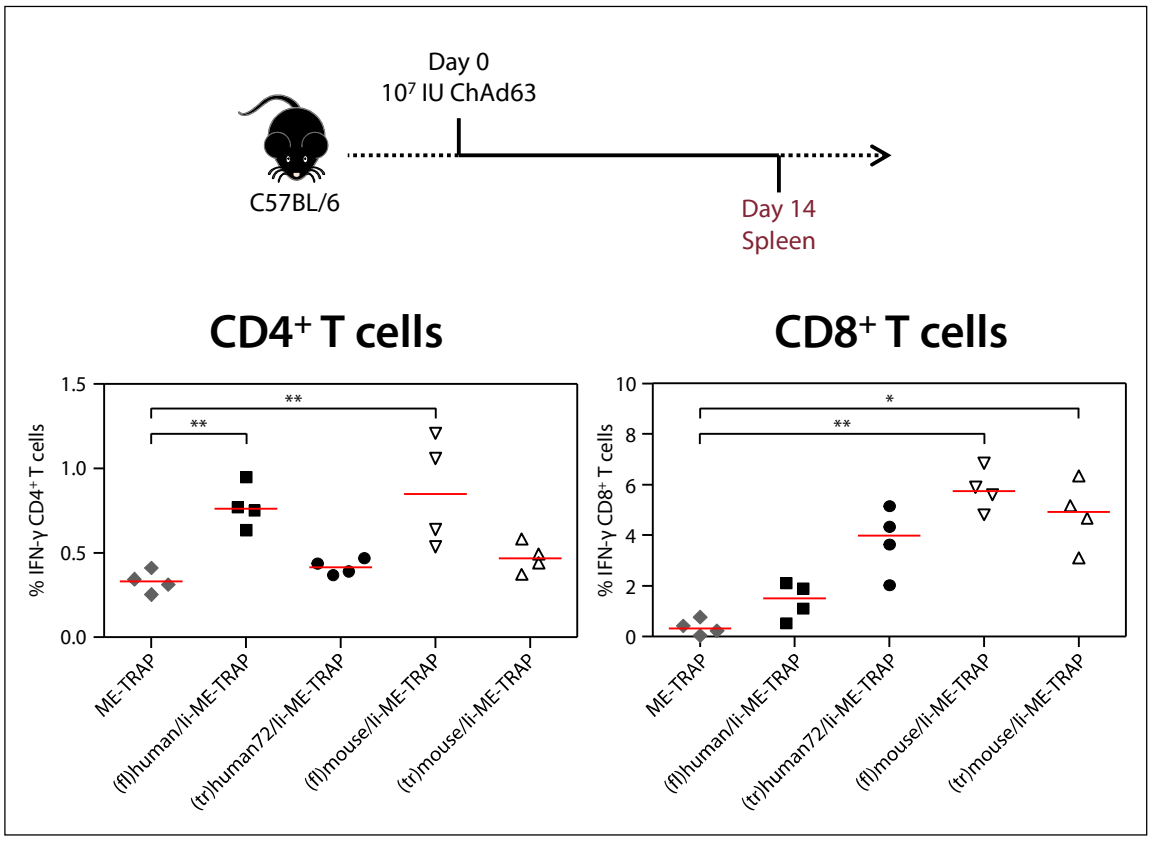



**Figure D-7. Adjuvanticity of homogenic mouse Ii.** C57BL/6 mice were immunised with $10^7$ IU ChAd63 vectors and spleens were harvested two weeks later. T-cell responses to a TRAP peptide pool were analysed by ICS. The percentage of $CD4^+$ and $CD8^+$ T cells positive for IFN-γ are shown. Single points indicate T-cell responses of individual mice and red lines denote the median response per group. Data was analysed with a one-way analysis of variance with Dunn's multiple comparison post-test. Asterisks denote the level of statistical significance between indicated groups (*, $p<0.05$; **, $p<0.01$).

In a separate experiment, whether immunisation with Ii adjuvanted vaccines induces an immune response directed against the Ii sequence was investigated (Figure D-8). C57BL/6 mice were vaccinated with ChAd63 vectors expressing unfused ME-TRAP or ME-TRAP fused to either full-length human Ii [(fl)human/Ii], the truncated 72 aa long version of human Ii [(tr)human72/Ii] or the transmembrane domain of human Ii [humanTM/Ii] with spleens analysed by ICS two weeks post immunisation. Splenocytes were stimulated with a single pool of overlapping peptides covering the full TRAP sequence (B) or the full human Ii sequence (C). Additionally, splenocytes were stimulated with peptide pools covering only the N-terminal cytoplasmic tail (D), only the transmembrane domain (E), or only the C-terminal luminal domain (F) of the human Ii. Lastly, splenocytes were also

stimulated with a pool of peptides covering the transmembrane sequence of the mouse Ii (G). All vaccines induced an immune response against the vaccine antigen TRAP (Figure D-8B). The highest fraction of TRAP-specific IFN-$\gamma^+$ T cells was induced by ME-TRAP fused to (fl)human/Ii (for $CD4^+$ T cells) or humanTM/Ii (for $CD8^+$ T cells). An immune response directed against the human Ii was only observed when mice were immunised with ME-TRAP fused to the full-length human Ii sequence (Figure D-8C). Ii-specific $CD4^+$ and $CD8^+$ T-cell responses appeared to be primarily directed against epitopes within the luminal domain of the Ii (Figure D-8F). However, a low $CD8^+$ T-cell response against the Ii cytoplasmic tail and TMD was also detected when mice were immunised with (fl)human/Ii-ME-TRAP (Figure D-8D). Taken together the data would suggest that immune response to the Ii chain can impact on its ability to enhance the $CD8^+$ T cell response, therefore truncated versions of non-homologous Ii chain sequences would not only reduce theoretical safety concerns, but may show greater adjuvant capacity than their full-length equivalents.

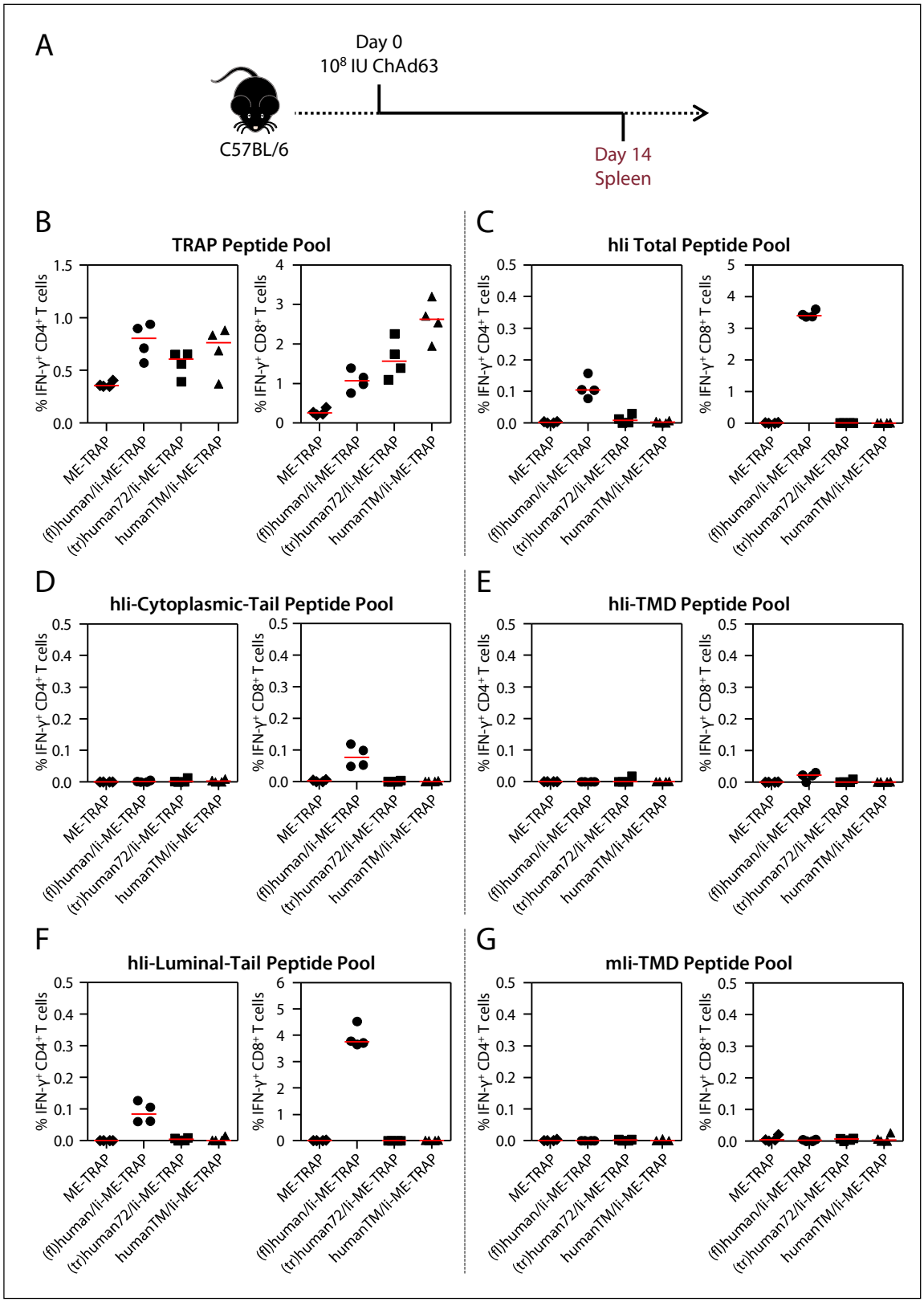



**Figure D-8. Immunogenicity against the Ii adjuvant.** C57BL/6 mice were immunised with $10^8$ IU ChAd63 vectors and spleens were harvested two weeks later. T-cell responses against peptide pools covering TRAP (B), the full human Ii sequence (C), only its cytoplasmic tail (D), only its TMD (E), only its luminal domain (F), or the mouse Ii TMD sequence (G) were analysed by ICS. The percentage of $CD4^+$ and $CD8^+$ T cells positive for IFN-γ are shown. Single points indicate T-cell responses of individual mice and red lines denote the median response per group.

## D2.3 Xenogenisation of Ii

### D2.3.1 Design and Cloning of Xenogenised Ii sequences

The second strategy to reduce the potential risk of breaking immuno-tolerance by vaccination of man with human Ii sequence was to design Ii-[antigen] constructs expressing Ii aa sequences with low homology to the human Ii. The NCBI protein database was screened for Ii sequences from a large variety of animal species and sub-groups, such as birds, fish, mammals, or amphibians. Sequences were compared to the full-length (fl) human and mouse Ii sequences to determine their homology using the ClustalW algorithm in DNAStar® Megalign. Supplemental Table I-3 (p. 227) lists the alignment analyses of the selected animal species. The two Ii sequences with the lowest homology to (fl)human/Ii, namely (fl)trout/Ii and (fl)shark/Ii, were fused to the N-terminal end of ME-TRAP and produced in ChAd63 viral vectors as described in sections B2.1.10ff (p. 40ff).

As initial immunogenicity data suggested that the luminal domain of the Ii is not needed for adjuvanticity, Ii sequences from various animal species were truncated (tr) according to the equivalent length of (tr)human72/Ii and analysed for homology to (tr)human72/Ii or (tr)mouse/Ii using the ClustalW algorithm in DNAStar® Megalign (Table D-2). Constructs with high sequence homology with (tr)human72/Ii (grey font) were not further considered. The sequences in black or red font were fused to the N-terminal end of ME-TRAP and cloned into the pENTR4-LPTOS entry vector and only used for *in vitro* analysis. Sequences in red font were also produced in ChAd63 vectors to obtain *in vivo* immunogenicity data.

**Table D-2. Homology analysis of Ii sequences.** Full-length Ii sequences from a variety of animal species were compared for homology to human Ii and truncated corresponding to the length of (tr)human72/Ii. Entitled name, GenBank identifier/NCBI Reference Sequence, and sequence homology with (tr)human72/Ii or (tr)mouse/Ii sequence are listed. Homology was analysed using the ClustalW algorithm in DNAStar® Megalign. Due to high homology to human Ii, constructs in grey font were not considered further. All constructs in black and red were fused to the N-terminal end of ME-TRAP and cloned into

pENTR4-LPTOS. Constructs in red font were also produced in ChAd63 vectors. tr denotes truncated sequences, fl denotes full-length sequences.

| Name | GenBank Identifier/ NCBI Reference Sequence | Homology with (tr)human72/li | Homology with (tr)mouse/li |
|---|---|---|---|
| (tr)human72/li | NP_004346 | 100% | 83.6% |
| (tr)orangutan/li | NP_001124630 | 98.6% | 81.8% |
| (tr)boar/li | NP_998939 | 91.1% | 87.3% |
| (tr)macaque/li | XP_002804624 | 90.3% | 81.8% |
| (tr)cattle/li | BAA12156 | 89.3% | 85.5% |
| (tr)dolphin/li | XP_004326859 | 89.3% | 81.8% |
| (tr)cat/li | XP_003981534 | 87.5% | 89.1% |
| (tr)rabbit/li | XP_002710211 | 87.5% | 87.3% |
| (tr)sheep/li | XP_004009025 | 87.5% | 87.3% |
| (tr)walrus/li | XP_004402873 | 87.5% | 85.5% |
| (tr)whale/li | XP_004280397 | 87.5% | 81.8% |
| (tr)floridamantee/li | XP_004384950 | 85.7% | 89.1% |
| (tr)mouse/li | NP_034675 | 83.6% | 100% |
| (tr)rat/li | NP_037201 | 78.6% | 87.3% |
| (tr)pigeon/li | AAX47311 | 50.0% | 52.0% |
| (tr)duck/li | AEB71788 | 49.1% | 55.8% |
| (tr)quail/li | ADG01642 | 43.6% | 40.0% |
| (tr)chicken/li | NP_001001613 | 42.9% | 40.0% |
| (tr)goose/li | ADK11994 | 41.8% | 53.8% |
| (tr)zebrafish/li | NP_571447 | 37.0% | 37.3% |
| (tr)mallard/li | XP_005010602 | 32.8% | 40.0% |
| (tr)zebrafish65/li | NP_571665 | 32.8% | 38.9% |
| (tr)trout/li | NP_001117913 | 31.6% | 34.5% |
| (tr)carp/li | AEZ67439 | 31.6% | 50.0% |
| (tr)grouper/li | AEA39679 | 30.0% | 33.3% |
| (tr)mandarinfish/li | AAS77256 | 27.9% | 29.6% |
| (tr)frog/li | NP_001184041 | 27.6% | 37.0% |
| (tr)shark/li | AEX34752 | 24.6% | 36.4% |

### D2.3.2 Immunogenicity of Vectors Encoding Xenogenised Ii

ChAd63 vectors encoding a full-length or truncated xenogenised Ii-ME-TRAP fusion constructs were administered IM to C57BL/6 mice and T-cell responses to a TRAP peptide pool were analysed two weeks later by ICS. All Ii-ME-TRAP fusion constructs induced stronger TRAP-specific $CD4^+$ or $CD8^+$ T-cell responses compared to unfused ME-TRAP (Figure D-9). In comparison to unfused ME-TRAP, significantly higher frequencies of $CD8^+IFN\text{-}\gamma^+$ T cells were induced when ME-TRAP was fused to (fl)trout/Ii ($p<0.05$), (tr)human72/Ii ($p<0.01$), (tr)shark/Ii ($p<0.01$), or (tr)chicken/Ii ($p<0.05$), respectively. TRAP-specific $CD4^+IFN\text{-}\gamma^+$ T-cell responses were highest when ME-TRAP was fused to (fl)human/Ii ($p<0.01$), (fl)trout/Ii ($p<0.05$), or (tr)frog/Ii ($p<0.01$), respectively. The frequency of TNF-producing $CD8^+$ T cells was comparable to IFN-γ, but IL-2 production of $CD8^+$ T cells was generally much lower (Supplemental Figure I-8, p. 207).

To confirm these results, the experiment was repeated with selected vectors expressing truncated and xenogenised Ii sequences as molecular adjuvant and was consistent with the previous data. When C57BL/6 mice were immunised with ChAd63 vectors encoding ME-TRAP fused to truncated and xenogenised Ii sequences, a higher number of TRAP-specific $CD4^+$ or $CD8^+$ T-cell responses were induced compared to mice vaccinated with vectors expressing unfused ME-TRAP. These results were significant for (tr)trout/Ii-ME-TRAP (CD4 and CD8) and (tr)chicken/Ii (CD8) (Supplemental Figure I-9, p. 233).

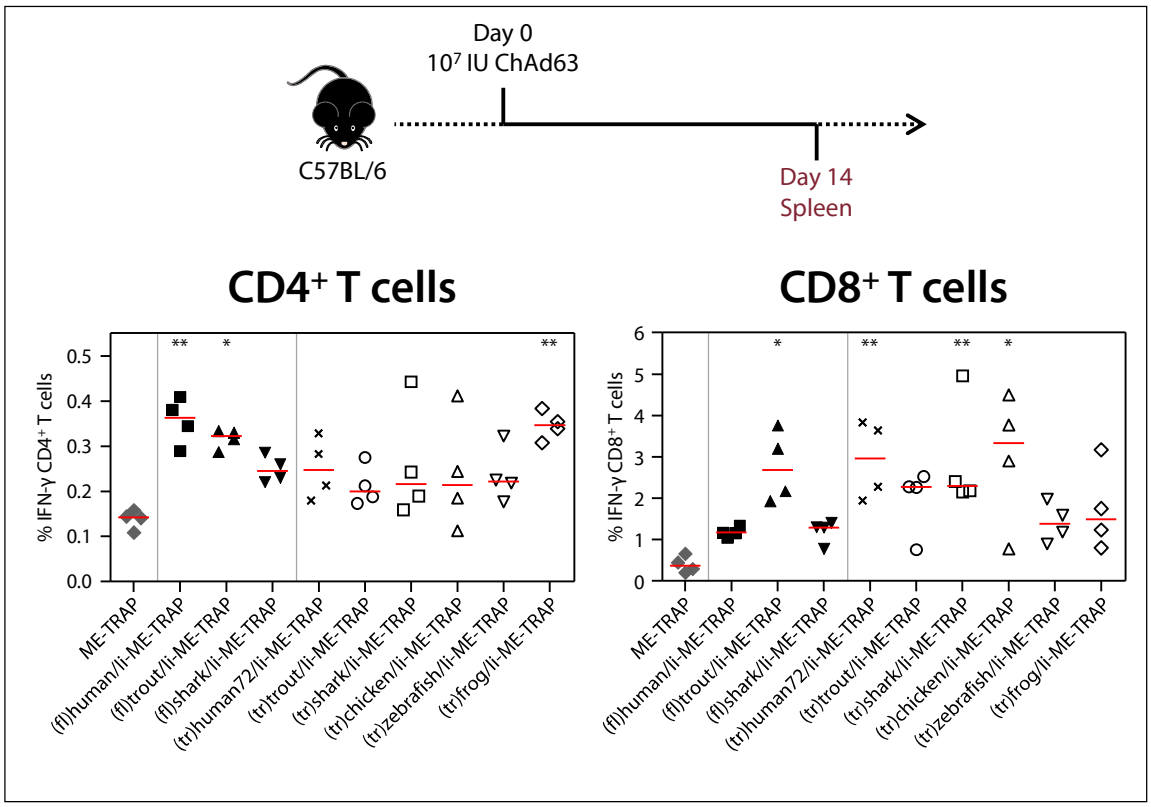



**Figure D-9. Adjuvanticity of xenogenised Ii.** C57BL/6 mice were immunised with $10^7$ IU ChAd63 vectors encoding ME-TRAP adjuvanted by full-length or truncated sequences of xenogenised Ii or unfused ME-TRAP as control. Spleens were harvested two weeks later and T-cell responses to a TRAP peptide pool analysed by ICS. The percentage of $CD4^+$ and $CD8^+$ T cells positive for IFN-γ are shown. Single points indicate T-cell responses of individual mice and red lines denote the median response per group. Data was analysed with a one-way analysis of variance with Dunn's multiple comparison post-test. Asterisks denote the level of statistical significance when compared to the control ME-TRAP vaccinated group (*, $p<0.05$; **, $p<0.01$).

# D3 Discussion

The clinically most advanced viral vector liver-stage malaria vaccine is based on a heterologous vaccination regimen with ChAd63 and MVA encoding ME-TRAP. In contrast to most licensed vaccines, protection is correlated with the magnitude of antigen-specific $CD8^+$ T cells [148]. Hence, for further improvement of vaccine efficacy, higher levels of cytotoxic T cells may be required. As the carrier viruses themselves have an adjuvantation effect [285], it is difficult to further increase antigen-specific T-cell responses by adding classic adjuvants. In our institute many potential adjuvants have been considered, such as TLR signalling molecules (TRAF, TRAM, TAK1) [286], classical co-stimulatory molecules (4-1BBL, CD80, Raet1e) [287], or cytokines (IL-15, IL-7, GM-CSF), but none sufficiently increased vaccine immunogenicity to a level that would merit progression to clinical testing.

In this chapter, the HLA class II associated invariant chain (Ii) was analysed and modified to improve immunogenicity and efficacy of viral vectored vaccines. During production of MHC class II proteins in the rough endoplasmic reticulum, a fragment of the Ii, the so-called 'class II-associated invariant chain peptide' (CLIP), binds the peptide binding groove of MHC class II to prevent binding of self-antigens. Furthermore, special trafficking sequences at the N-terminal end of the Ii are responsible for directing the entire MHC-II-Ii-complex to late endosomal compartments where the Ii is gradually degraded by endosomal enzymes (e.g. cathepsin S) and subsequently replaced by an exogenous peptide. The resulting MHC-II-peptide-complex is then presented on the cell surface in association with co-stimulatory molecules [288]. Several groups demonstrated that an extension of the C-terminal end of Ii with an antigenic sequence can facilitate enhanced activation of naïve $CD4^+$ T cells [274–276]. Further investigations revealed that this strategy could also induce improved $CD8^+$ T-cell responses [277, 279–282, 289], even though the exact mechanism by which this occurs remains to be fully understood. Prime-

boost vaccination regimens with ChAd63 and MVA encoding ME-TRAP fused to the C-terminal end of the full-length human Ii have been reported to enhance $CD4^+$ and $CD8^+$ T-cell responses in mice and NHP [150]. However, concerns that expressing the human Ii in viral vectors would break self-tolerance has slowed progression to clinical trial. These ideas were reinforced with recent data suggesting autoantibodies against the CLIP domain of the Ii are associated with axial spondylitis [283, 284]. To address these concerns, two strategies were pursued in this chapter: Ii truncation and Ii xenogenisation.

Initially, the Ii was truncated in a stepwise manner from its C-terminal end to a 72 aa long "truncated" Ii version and fused to the N-terminal end of ME-TRAP. These constructs were then encoded in ChAd63 vectors and compared in terms of their ability to induce antigen-specific T-cell responses in C57BL/6 mice. This mouse strain was selected, as the ME string of ME-TRAP contains a strong immunodominant H-$2^d$ restricted epitope from CSP (Pb9), which prohibits the analysis of TRAP-specific immunogenicity in BALB/c mice because of the very low level of immunogenicity observed against TRAP [144]. Strikingly, Ii truncation did not hinder its ability to enhance TRAP specific $CD8^+$ T cell responses (Supplemental Figure I-5, p. 204), suggesting that essential parts of Ii adjuvanticity are located in its N-terminal 72 aa. Subsequently, the Ii was further truncated and *in vivo* immunogenicity assessed after vaccination with ChAd63 vectors. These experiments revealed that only the TMD of Ii, a peptide sequence of only 26 aa length, is needed for its adjuvanting effect: (tr)human72/Ii-ME-TRAP as well as humanTM/Ii-ME-TRAP induced TRAP-specific $CD8^+$ T-cell responses which were around 5.5-fold higher than the response induced by unfused ME-TRAP (Figure D-6, p. 100). If the transmembrane domain of the Ii was not expressed in the fusion construct (humanCT/Ii-ME-TRAP), the Ii adjuvantation effect was completely lost. TRAP-specific $CD4^+$ T-cell responses were generally lower compared to $CD8^+$ T-cell responses, but fusion of ME-TRAP to all Ii truncations (except humanCT/Ii-ME-TRAP) improved $CD4^+$

T-cell immunogenicity. The highest $CD4^+$ T-cell responses were achieved with (fl)human/Ii-ME-TRAP, suggesting that including the C-terminal end of Ii is slightly beneficial for $CD4^+$ T-cell immunogenicity.

An unexpected finding was that truncated Ii versions, namely (tr)human72/Ii-ME-TRAP and humanTM/Ii-ME-TRAP induced 2–3-fold higher antigen-specific $CD8^+$ T-cell responses compared to the construct encoding the untruncated, full-length Ii [(fl)human/Ii-ME-TRAP]. The data suggest this is due to T-cell responses against the C-terminal end of the human Ii sequence outcompeting TRAP-specific response (Figure D-8, p. 104). Chopping off the immunogenic C-terminal end of the Ii revealed the full adjuvantation capacity of the Ii, as no response to Ii chain peptides were observed in parallel to improved TRAP specific $CD8^+$ T-cell responses. In line with this finding, full-length mouse Ii was equally potent in increasing TRAP-specific $CD8^+$ T-cell responses as truncated mouse Ii in C57BL/6 mice (Figure D-7, p. 102), suggesting that no competing Ii-specific T-cell responses were induced.

The other strategy to minimise the potential risk of breaking self-tolerance to human Ii in man was to design Ii-[antigen] constructs expressing Ii chain sequences of distant animal species. A similar approach was recently described by Ogun et al. who developed a minimal human homology adjuvant based on the oligomerisation domain of C4-binding protein [290]. The NCBI protein database was screened for Ii sequences of various animal species (birds, fish, mammals, amphibians) with low homology compared to the full-length and truncated human and mouse Ii sequences. Truncated and xenogenised Ii sequences fused to ME-TRAP and encoded in ChAd63 vectors were shown to retain vaccine adjuvantation effects in the C57BL/6 mouse model (Figure C-9, p. 77). ChAd63 encoding (tr)frog/Ii-ME-TRAP induced particularly high numbers of TRAP-specific $CD4^+$ T cells, whereas (tr)trout/Ii-ME-TRAP, (tr)shark/Ii-ME-TRAP and (tr)chicken/Ii-ME-TRAP induced high levels of $CD8^+$ T-cell responses. Taking into account that the very

low sequence homology to human/Ii reduces the risk for autoimmunity and that $CD8^+$ T cells are most important in mediating sterile immunity against malaria [291], (tr)trout/Ii and (tr)shark/Ii are highly promising adjuvant candidates for future viral-vectored liver-stage vaccines. Further truncation of their sequences was considered, as truncation experiments (described above) revealed that in case of the human Ii only the TMD is needed for full $CD8^+$ T-cell adjuvanticity.

Using the viral vector platform in heterologous ChAd63-MVA prime-boost regimens, remarkably high frequencies of antigen-specific T-cells were observed with some degree of efficacy [148] and therefore to achieve higher T-cell levels may still be required to achieve sterile efficacy. Whereas most classic adjuvants failed to achieve continued immune enhancement during progression to clinical trial, the Ii as a molecular adjuvant has consistently proven its adjuvanticity with a diverse range of vaccine antigens and in various inbred mouse strains, outbred mice, and also NHP. The results of this chapter show that (1) the 26 aa long segment of the human Ii (the TMD of its sequence) is sufficient for its adjuvantation effect and (2) xenogenised Ii sequences can be used instead of the human sequence. As the induction of strong $CD8^+$ T-cell responses is crucial for liver-stage immunity, this study strongly supports the progression of Ii-ME-TRAP fusion constructs to human clinical safety, immunogenicity, and efficacy trials. Furthermore, since cell mediated responses are important for the prevention of many diseases other than malaria, the fusion of Ii to other vaccine antigens may also pursue to clinical trials.

In an attempt to utilise the findings of this chapter in the design of a novel clinical liver-stage vaccine candidate, Chapter E investigates the adjuvantation capacity of the shark and trout Ii TMD sequences when fused to LSA1 or LSAP2 and encoded in viral vectors.

# Chapter E

# Development of Adjuvanted Multi-Antigen Liver-Stage Malaria Vaccines

# E1 Introduction

Despite encouraging progress in liver-stage malaria vaccine development using viral vectored prime-boost regimens, even higher levels of protective efficacy have to be achieved to justify mass deployment of such a vaccine. Two possible ways to increase immunogenicity and efficacy of viral vectored liver-stage malaria vaccines have been discussed in previous chapters. (1) The first option is described in Chapter C and investigated the development of vaccines containing a combination of liver-stage antigens. The combination of vaccine antigens clearly improved protective efficacy in a mouse challenge model. (2) Secondly, immunogenicity of the viral vector platform can be increased by including a suitable adjuvant. This has been a rather difficult challenge, but truncated and xenogenised versions of the MHC class II invariant chain as a molecular adjuvant showed promising results in Chapter D.

The aim of this this chapter was to generate adjuvanted viral vectors expressing LSA1, LSAP, or both as a fusion protein, and rank them in terms of their immunogenicity and protective efficacy in inbred and outbred mouse strains. The most promising vaccine candidates were then chosen for manufacturing to clinical grade (GMP) and progress to clinical trials.

In contrast to all previous chapters, ChAdOX1 [292] (a simian adenoviral vector developed by our group) was used instead of ChAd63, as some intellectual property rights of the latter may be owned by GlaxoSmithKline (GSK) as well as the University of Oxford. ChAdOX1 is based on a simian adenovirus and has been found to exhibit comparable immunogenicity to ChAd63 [292], and importantly demonstrates good safety, immunogenicity and efficacy in numerous pre-clinical and clinical studies [293–298].

# E2 Results

## E2.1 Cloning of Clinical Vaccine Candidates

The inserts of LSA1 and LSAP2 (described in C1.1, p. 58) were both cloned into ChAdOX1 and denoted ChAdOX1-tPA-LSA1 or ChAdOX1-tPA-LSAP2 to highlight the fact that the tPA leader sequence [203] was expressed at the N-terminal end of the antigens to improve expression and immunogenicity [204–206]. Additionally, a fusion construct expressing both, LSA1 and LSAP2, with a peptide linker (GGGPGGG) separating both antigens was cloned to the C-terminus of tPA leader sequence and denoted ChAdOX1-tPA-LSA1-LSAP2.

Furthermore, adjuvanted versions of these viral vectors were produced. Based on the positive results in Chapter D, the xenogenised and truncated Ii sequences (tr)shark/Ii and (tr)trout/Ii were chosen and fused N-terminally to the above mentioned antigens (LSA1, LSAP2, and LSA1-LSAP2). As the transmembrane domain of the human Ii showed a similarly strong adjuvanticity compared to (tr)human72/Ii (Figure D-6, p. 100), Ii transmembrane domains of numerous animal species were compared. The analysis revealed that the Ii TMD sequence is highly conserved between animal species. This becomes obvious when amino acids with similar biochemical characteristics are colour coded in groups as in Supplemental Figure I-10 (p. 209). Still, when compared to the humanTM/Ii using the MUSCLE or ClustalW algorithm, troutTM/Ii and sharkTM/Ii have a very low sequence homology of 50% and 35% (Table E-1, below). Importantly, both xenogenised TMD have only three or four identical consecutive amino acids in common with the humanTM/Ii. For this reason, troutTM/Ii and sharkTM/Ii were also fused N-terminally to LSA1, LSAP2, and LSA1-LSAP2 to investigate their adjuvant effect.

Lastly, several MVA constructs expressing LSA1, LSAP2, or the LSA1-LSAP2 fusion construct were cloned, either fused to the C-terminal end of the leader sequence of tPA or the Ii TMD (troutTM/Ii or sharkTM/Ii).

Cloning and subsequent production steps of ChAdOX1 and MVA vectors encoding these constructs are described in sections B2.1.10ff (p. 40ff). All viruses considered for clinical production are listed in Table E-2.

**Table E-1.** Comparison of Ii transmembrane domains. Percent identity and number of identical consecutive amino acids compared to the human TMD of Ii.

| Species | Sequence | Percent Identity | | Number of identical consecutive amino acids |
|---|---|---|---|---|
| | | ClustalW | MUSCLE | |
| Human | GALYTGFSILVTLLLAGQATTAYFLY | - | - | |
| Trout | RAFKIAGFTLLACLLIAGQALTAYFVL | 53.8% | 50.0% | 4 |
| Shark | SLLWGGVTVLAAMLIAGQVASVVFLV | 36.0% | 35.0% | 3 |

**Table E-2.** List of ChAdOX1 and MVA vectors.

| ChAdOX1 vectors | MVA vectors |
|---|---|
| ChAdOX1/Mono-tPA-LSA1 | MVA/TD/GFP-tPA-LSA1 |
| ChAdOX1/Mono-(tr)trout/Ii-LSA1 | MVA/TD/GFP-sharkTM/Ii-LSA1 |
| ChAdOX1/Mono-(tr)shark/Ii-LSA1 | |
| ChAdOX1/Mono-troutTM/Ii-LSA1 | |
| ChAdOX1/Mono-sharkTM/Ii-LSA1 | |
| ChAdOX1/Mono-tPA-LSAP2 | MVA/TD/GFP-tPA-LSAP2 |
| ChAdOX1/Mono-(tr)trout/Ii-LSAP2 | MVA/TD/GFP-sharkTM/Ii-LSAP2 |
| ChAdOX1/Mono-(tr)shark/Ii-LSAP2 | |
| ChAdOX1/Mono-troutTM/Ii-LSAP2 | |
| ChAdOX1/Mono-sharkTM/Ii-LSAP2 | |
| ChAdOX1/Mono-tPA-LSA1-LSAP2 | MVA/TD/GFP-tPA-LSA1-LSAP2 |
| ChAdOX1/Mono-(tr)trout/Ii-LSA1-LSAP2 | MVA/TD/GFP-troutTM/Ii-LSA1-LSAP2 |
| ChAdOX1/Mono-(tr)shark/Ii-LSA1-LSAP2 | MVA/TD/GFP-sharkTM/Ii-LSA1-LSAP2 |
| ChAdOX1/Mono-troutTM/Ii-LSA1-LSAP2 | |
| ChAdOX1/Mono-sharkTM/Ii-LSA1-LSAP2 | |

## E2.2 Comparison of Immunogenicity: ChAd63 vs ChAdOX1

As ChAdOX1 was used instead of ChAd63, the LSA1 and LSAP2 expressing vectors of both origins were compared in terms of their immunogenicity.

Four BALB/c mice per group were vaccinated IM with spleens harvested 14 days later and splenocytes stimulated with a single pool of overlapping peptides covering either the full LSA1 or LSAP2 sequence (B2.4.1, p. 47) to measure intracellular production of IFN-γ, IL-2, and TNF by ICS (B2.4.2, p. 47). Only IFN-γ responses are shown in Figure E-1 (below), as IL-2 and TNF showed similar results. No statistical difference could be found between ChAdOX1 and ChAd63 in terms of inducing $CD4^+$ or $CD8^+$ T-cell against either LSA1 or LSAP2. However, a non-statistical trend of a higher LSA1-specific $CD8^+$ T-cell response in ChAd63 and LSAP2-specific $CD8^+$ T-cell response in ChAdOX1 was observed.

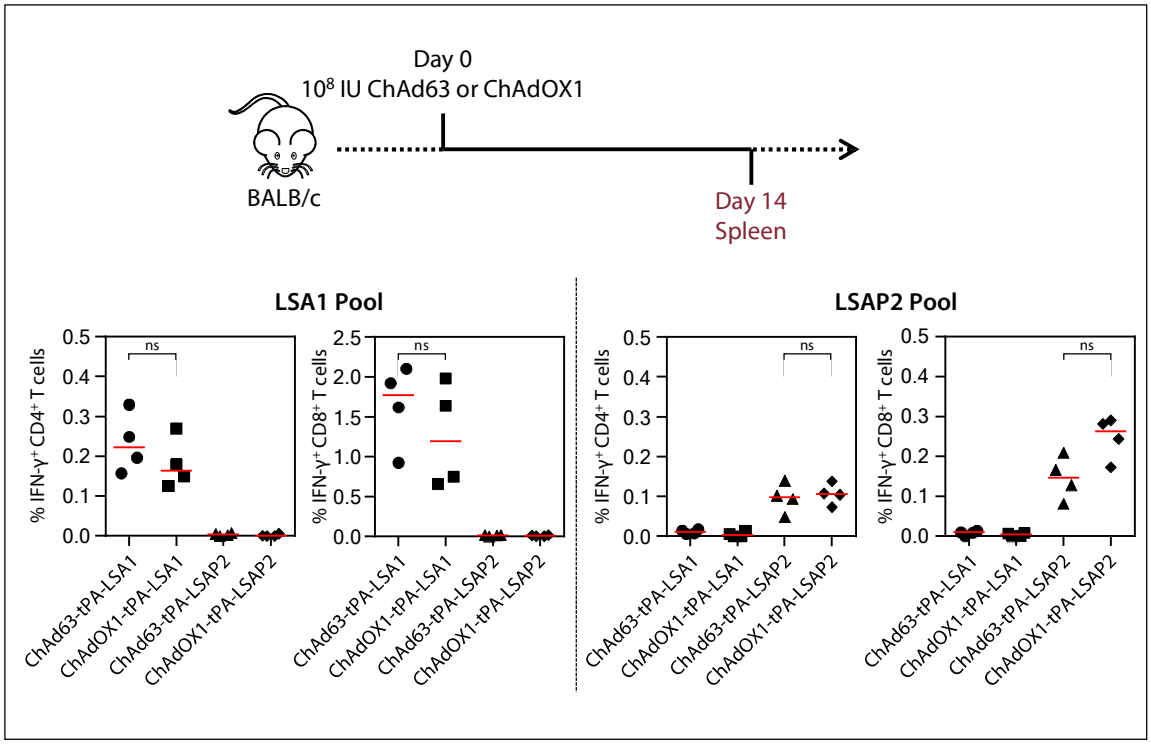



**Figure E-1. Immunogenicity of ChAd63 and ChAdOX1.** BALB/c mice (4 per group) were immunised with $10^8$ IU ChAd63 or ChAdOX1 vectors and spleens harvested two weeks later. T-cell responses to an LSA1 or LSAP2 peptide pool were analysed by ICS. The percentage of $CD4^+$ and $CD8^+$ T cells positive for IFN-γ are shown. Single points indicate T-cell responses of individual mice and red lines denote the median

response per group. Data was analysed with a one-way analysis of variance with Dunn's multiple comparison post-test. ns, non-significant.

## E2.3 Comparison of Vaccine Candidates in Inbred Mice

### E2.3.1 Analyses of ChAdOX1 vaccines

To provide a first overview of the potency of the different vaccine candidates, the immunogenicity of all ChAdOX1 vectors were compared in the BALB/c mouse model. In three separate experiments, the adjuvanticity of the five leader sequences – tPA, (tr)trout/Ii, (tr)shark/Ii, troutTM/Ii, and sharkTM/Ii – was compared when fused to LSA1, LSAP2 or the LSA1-LSAP2 fusion construct. BALB/c mice (6 per group) were immunised with $10^7$ IU of adenoviral vectors IM with mice sacrificed and spleens harvested two weeks post vaccination with antigen specific production of IFN-g measured by ICS (Figure E-2).

When vaccinated with ChAdOX1 vectors expressing LSA1, there was no statistical difference in the LSA1-specific $CD4^+$ or $CD8^+$ T-cell response between the study groups. However, there was a non-significant trend towards a higher LSA1-specific $CD8^+$ T-cell response when mice were immunised with LSA1 fused to the sharkTM/Ii (Figure E-2B).

When mice were immunised with adenoviral vectors encoding LSAP2, a very similar T-cell response was observed (Figure E-2C): there was no significant difference between tPA or Ii adjuvants, but sharkTM/Ii showed a non-significant trend to induce the highest $CD8^+$ T-cell responses.

In Figure E-2D, mice were vaccinated with the different versions of the LSA1-LSAP2 fusion construct. Both, LSA1- and LSAP2-specific $CD4^+$ T-cell responses were similar to those induced by ChAdOX1 vectors expressing only one of the two antigens (B and C). However, the $CD8^+$ T-cell responses against LSA1 and LSAP2 appeared reduced when mice were immunised with the LSA1-LSAP2 constructs. Fusion to any Ii variant did not result in an increased $CD8^+$ T-cell response.

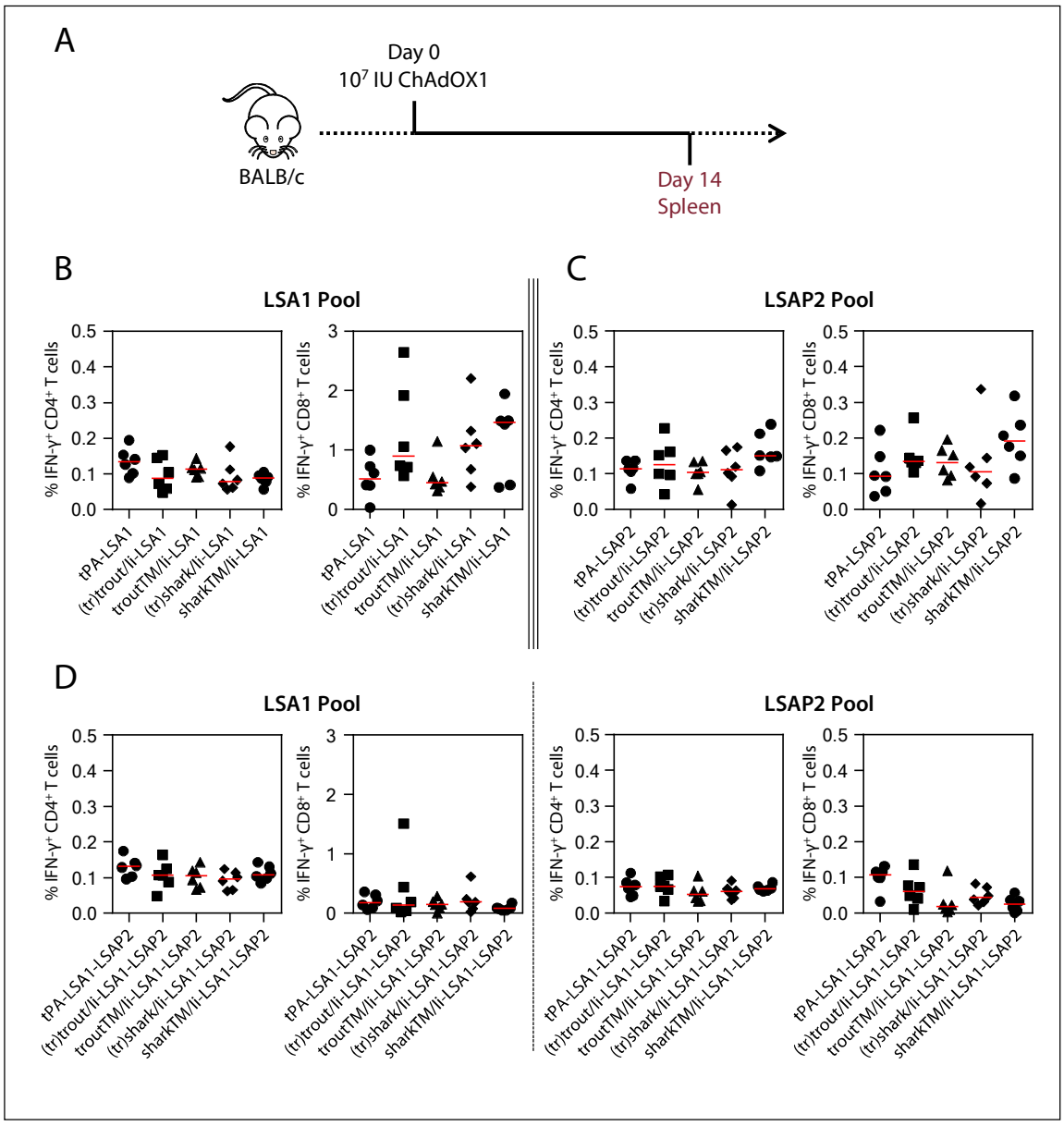



**Figure E-2. Immunogenicity of ChAdOX1 vaccine candidates in BALB/c mice.** BALB/c mice (6 per group) were immunised with $10^7$ IU ChAdOX1 vectors as indicated on the x-axes and spleens were harvested two weeks later. T-cell responses to an LSA1 or LSAP2 peptide pool were analysed by ICS. The percentage of $CD4^+$ and $CD8^+$ T cells positive for IFN-γ are shown. Single points indicate T-cell responses of individual mice and red lines denote the median response per group.

Next, sharkTM/Ii adjuvanted single antigen expressing ChAdOX1 vectors (sharkTM/Ii-LSA1 and sharkTM/Ii-LSAP2) were compared with the equivalent dual antigen expressing vector (sharkTM/Ii-LSA1-LSAP2). Five mice per group were immunised and analysed as per the previous experiment. As indicated on the x-axes (Figure E-3), groups 1 and 2 were immunised with $10^8$ IU of ChAdOX1 expressing sharkTM/Ii-LSA1 or sharkTM/Ii-LSAP2,

respectively. In group 3, mice received the full dose of sharkTM/Ii-LSA1 in the right leg, whilst sharkTM/Ii-LSAP2 was administered in the left leg. In group 4, full doses of both vaccines were mixed in a vial before administration in both legs. Group 5 was administered with $10^8$ IU of the dual antigen expressing vector (sharkTM/Ii-LSA1-LSAP2), and group 6 received two doses of this vaccine in the left and right leg ($2 \times 10^8$ IU) to match the total amount of infectious virus administered in groups 3 and 4.

LSA1- and LSAP2-specific $CD4^+$ T-cell responses and LSAP2-specific $CD8^+$ T-cell responses of all groups were similarly strong. The doubled dose of sharkTM/Ii-LSA1-LSAP2 only marginally increased T-cell responses. Interestingly, LSA1-specific $CD8^+$ T-cell responses were considerably reduced in dual antigen vector vaccinated mice compared to single antigen controls. Doubling the dose of sharkTM/Ii-LSA1-LSAP2 did not compensate for the reduction in LSA1-specific $CD8^+$ T cell immunogenicity.

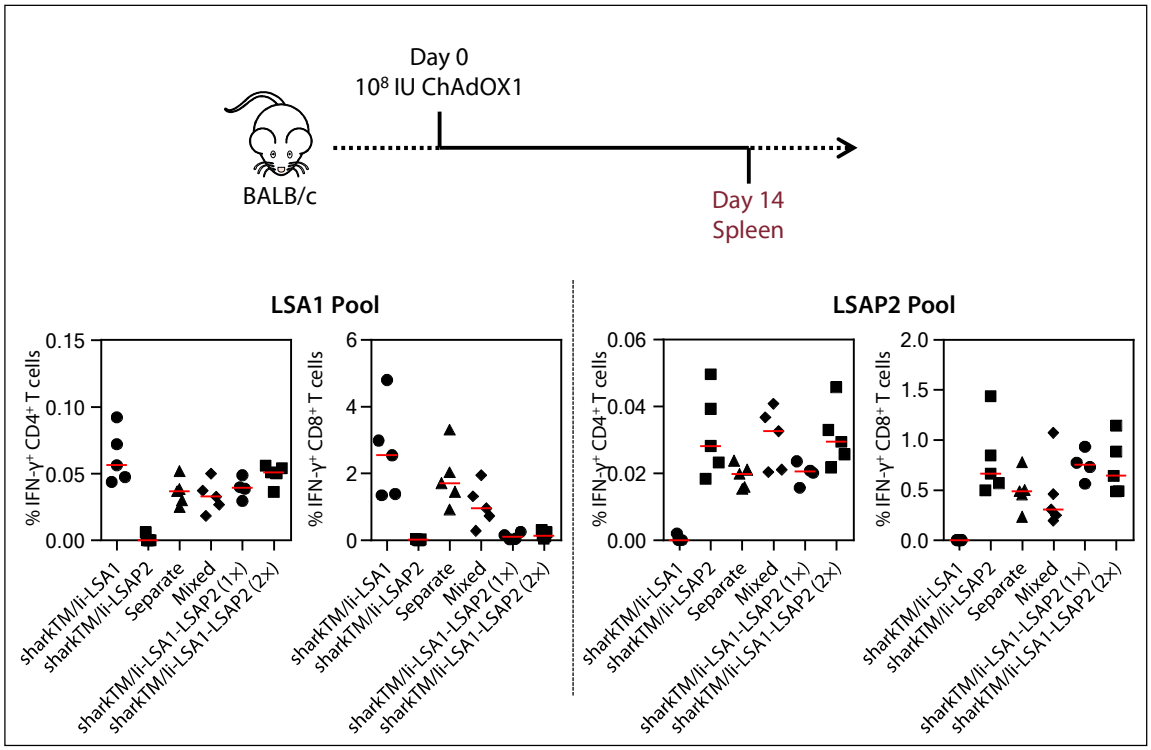



**Figure E-3. Immunogenicity of adjuvanted single vs dual antigen expressing vectors.** BALB/c mice (5 per group) were immunised with $10^8$ IU ChAdOX1 vectors as indicated on the x-axes and spleens were harvested two weeks later. T-cell responses to an LSA1 or LSAP2 peptide pool were analysed by ICS. The percentage of $CD4^+$ and $CD8^+$ T cells positive for IFN-γ are shown. Single points indicate T-cell responses of individual mice and red lines denote the median response per group.

The reduced LSA1-specific $CD8^+$ T-cell response induced by dual antigen expressing vectors compared to ChAdOX1 expressing LSA1 only was somewhat surprising, given that LSA1-specific $CD4^+$ T-cell responses were similar. To investigate if this result can also be found in mice with an MHC haplotype different to $H\text{-}2^d$, single and dual antigen expressing ChAdOX1 vectors were also analysed in another inbred mouse strain with an $H\text{-}2^k$ MHC haplotype. Four CBA mice per group were immunised with $10^8$ IU of ChAdOX1 expressing LSA1, LSAP2, or the fusion construct LSA1-LSAP2, either fused to tPA or sharkTM/Ii as adjuvant (as indicated on the x-axes in Figure E-4). Two weeks post immunisation mice were sacrificed and spleens were analysed by ICS (Figure E-4, below).

LSA1 as well as LSAP2-specific T-cell responses were generally very low and difficult to analyse. Results suggested that LSA1-specific $CD4^+$ and $CD8^+$ T-cell responses were highest in mice immunised with tPA-LSA1. Fusion of the antigen to sharkTM/Ii did not have a beneficial effect. LSA1-specific $CD8^+$ T-cell responses appeared to be even lower when ChAdOX1 expressed the LSA1-LSAP2 fusion construct compared to LSA1 only. LSAP2-specific $CD4^+$ T-cell responses were similarly low in all mouse groups vaccinated with LSAP2 expressing vectors. There was no measureable $CD8^+$ T-cell responses against LSAP2 in any of the vaccinated mice.

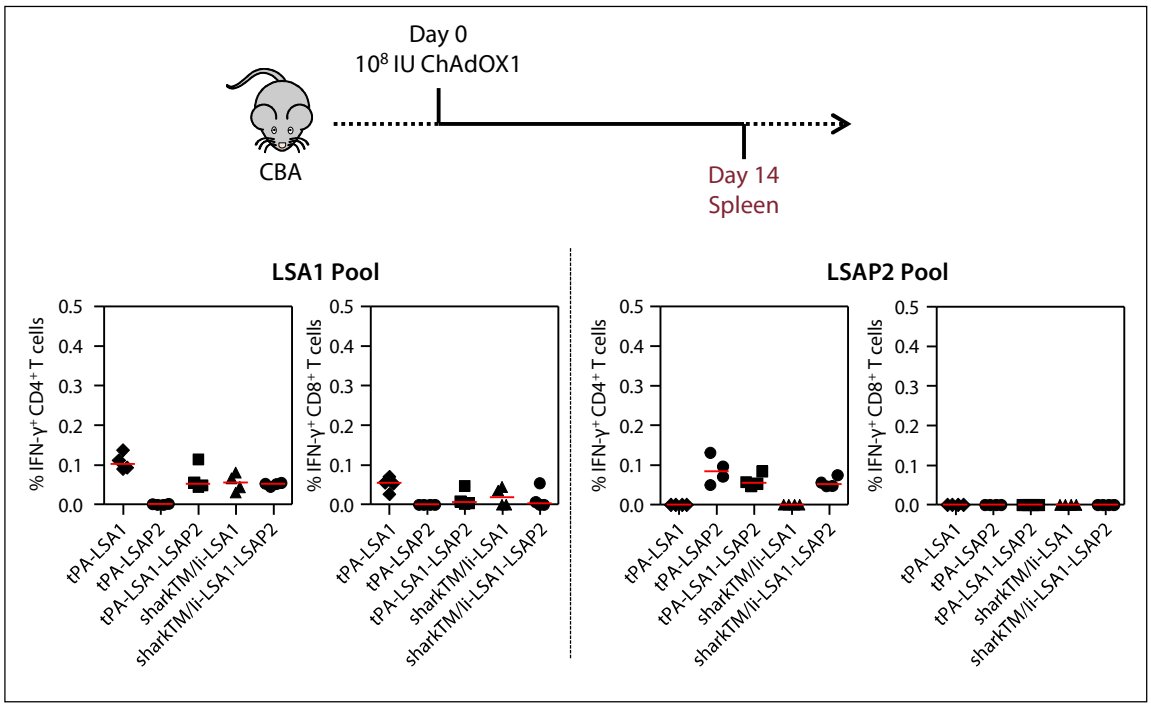



**Figure E-4. Immunogenicity in CBA mice.** CBA mice (4 per group) were immunised with $10^8$ IU ChAdOX1 vectors as indicated on the x-axes and spleens were harvested two weeks later. T-cell responses to an LSA1 or LSAP2 peptide pool were analysed by ICS. The percentage of $CD4^+$ and $CD8^+$ T cells positive for IFN-γ are shown. Single points indicate T-cell responses of individual mice and red lines denote the median response per group.

To assess whether the fusion of sharkTM/Ii to LSA1 had a positive impact on protective efficacy, BALB/c mice were immunised with $10^8$ IU ChAdOX1 encoding tPA-LSA1 or adjuvanted sharkTM/Ii-LSA1 and challenged with 1,000 chimeric *P. berghei* sporozoites expressing *P. falciparum* LSA1 (Figure E-5A). Before sporozoite challenge, a blood sample was taken and T cells were analysed for antigen-specific intracellular production of IFN-γ (IL-2 and TNF, data not shown) by ICS. LSA1-specific $CD4^+$ T-cell responses in the blood were consistent between groups when mice were immunised with tPA-LSA1 or sharkTM/Ii-LSA1 (Figure E-5B). However, $CD8^+$ T-cell responses against LSA1 were significantly higher in the group of mice vaccinated with sharkTM/Ii-LSA1. After sporozoite challenge, all naïve control mice reached 1% parasitaemia within 7 days. One mouse immunised with tPA-LSA1 was protected (Figure E-5C). Vaccination with the

adjuvanted vaccine (sharkTM/Ii-LSA1) resulted in a significant delay to 1% parasitaemia ($p<0.01$) and one mouse was sterilely protected.

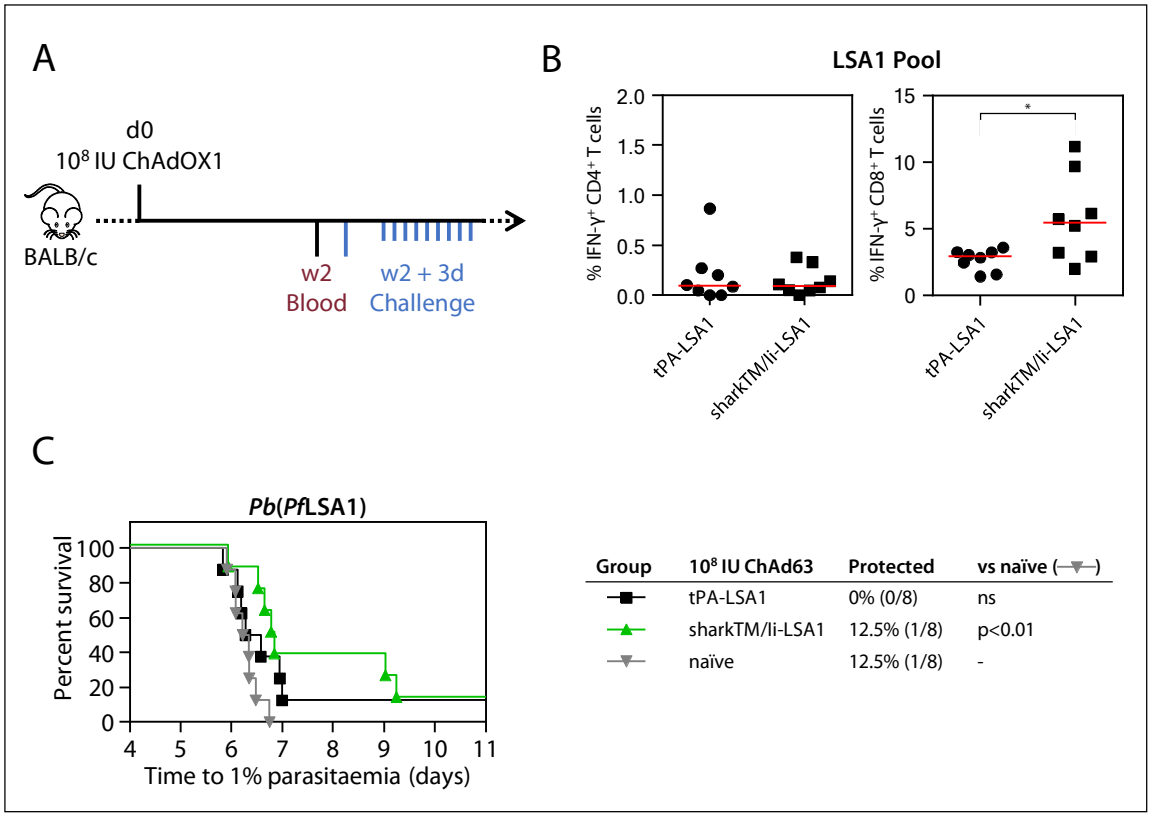



**Figure E-5. Immunogenicity and efficacy of LSA1 expressing ChAdOX1 vectors in BALB/c.** (A) Outline of the experimental setup. After immunising eight BALB/c mice per group with $10^8$ IU of ChAdOX1 vectors encoding tPA-LSA1 or sharkTM/Ii-LSA1 a blood sample was taken on day 14 and mice challenged on day 17. (B) Immunogenicity data. Blood PBMC were analysed by ICS after stimulation with an LSA1 peptide pool. Graphs represent the frequency of $CD4^+IFN\text{-}\gamma^+$ or $CD8^+IFN\text{-}\gamma^+$ T cells. Single points indicate T-cell responses of individual mice and red lines show the median response per group. Data was analysed with a one-way analysis of variance with Dunn's multiple comparison post-test. The asterisk denotes the level of statistical significance when compared to each other (*, $p<0.05$). (C) Efficacy data. Mice were challenged with 1,000 chimeric *P. berghei* sporozoites expressing *P. falciparum* LSA1 on day 17 post immunisation. Blood smears were taken daily from four days after sporozoite challenge and analysed by Giemsa staining and light microscopy to determine parasitaemia. Mice that were negative for blood-stage malaria until 15 days after sporozoite challenge were considered to be sterilely protected. Time to 1% parasitaemia is plotted on a Kaplan-Meier Survival Curve. Data was analysed with the log-rank (Mantel-Cox) test. Number of protected animals and levels of statistical significance when compared to the naïve control group are shown in the table. There was no statistical difference between groups immunised with tPA-LSA1 and sharkTM/Ii-LSA1.

To compare efficacy of adjuvanted single antigen and dual antigen expressing viral vectors (Figure E-6), eight BALB/c mice per group were immunised with $10^8$ IU of ChAdOX1 vectors expressing sharkTM/Ii-LSA1 (group 1), sharkTM/Ii-LSAP2 (group 2), or sharkTM/Ii-LSA1-LSAP2 (group 4). A further group of mice was vaccinated with both

single antigen expressing vectors (group 3), and a naïve group of mice served as an infection control for parasite challenge with *Pb*(*Pf*LSA1+LSAP2) at day 17 (group 5). Two weeks post immunisation antigen-specific production of IFN-γ on blood T-cells was analysed by ICS (Figure E-6B). The LSAP2-specific $CD4^+$ and $CD8^+$ T-cell response as well as the LSA1-specific $CD4^+$ T-cell response were low in all study groups. The highest LSA1-specific $CD8^+$ T-cell response was observed in mice immunised with sharkTM/Ii-LSA1 or both single antigen expressing vectors ("Mixed"). The percentage of LSA1-specific T cells in mice vaccinated with sharkTM/Ii-LSA1-LSAP2 was visibly (but not significantly) lower. Post parasite challenge, all naïve control mice and all mice immunised with sharkTM/Ii-LSAP2 reached 1% parasitaemia within 7 or 8 days, respectively (Figure E-6C). The observed difference in the vaccinated groups was marginal. There was a delay in time to 1% parasitaemia when mice were immunised with sharkTM/Ii-LSA1 ($p<0.05$) and with both single antigen expressing vectors ("Mixed", $p<0.001$) and one mouse was sterilely protected in both study groups. When mice were vaccinated with the dual antigen expressing construct (sharkTM/Ii-LSA1-LSAP2) one mouse was protected, but no delay in parasitaemia could be observed in the other mice of the group.

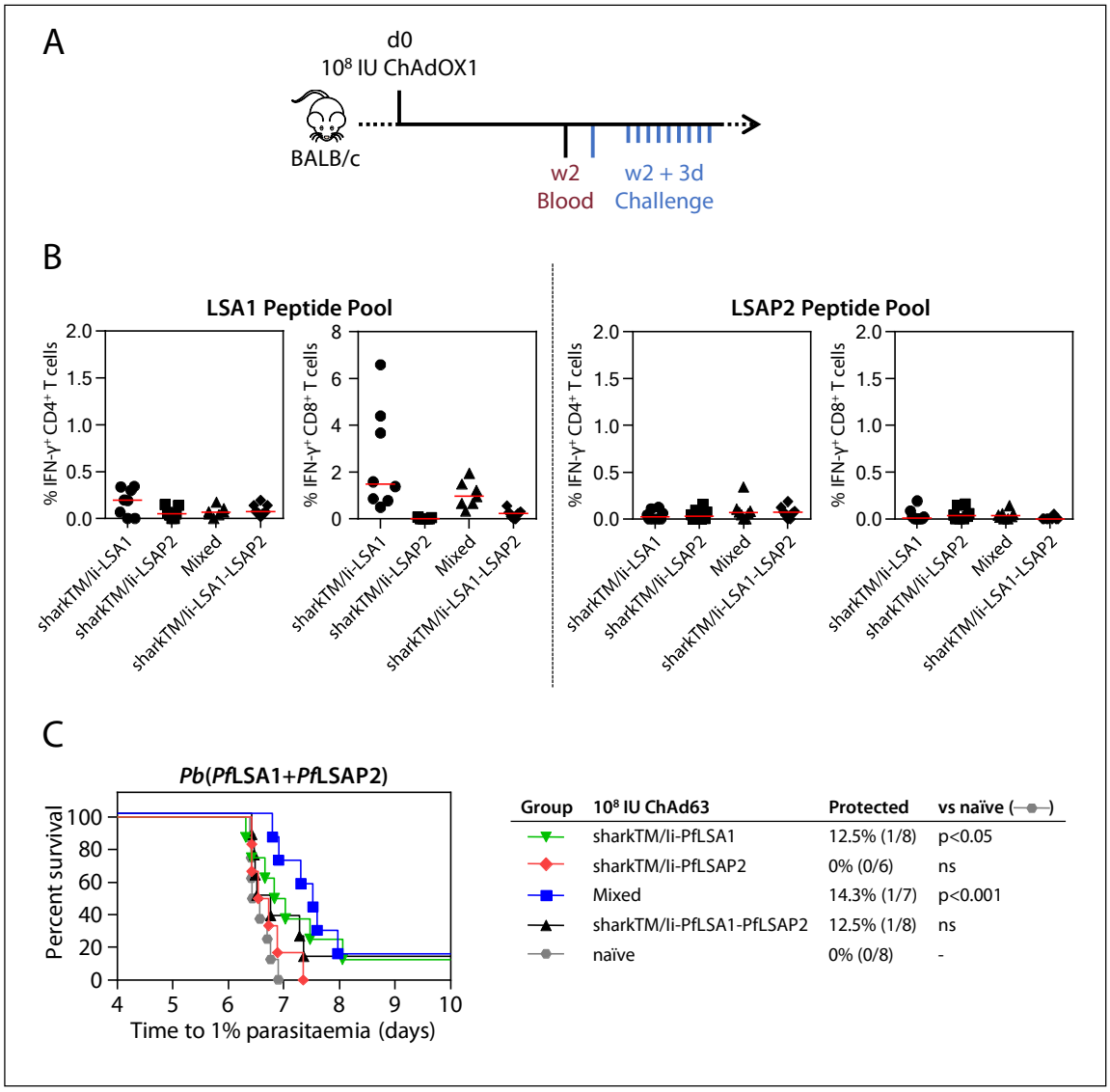



**Figure E-6. Immunogenicity and efficacy of dual antigen expressing ChAdOX1 in BALB/c.** A) Outline of the experimental setup. After immunising eight BALB/c mice per group with $10^8$ IU of ChAdOX1 vectors, a blood sample was taken on day 14 and mice challenged on day 17. (B) Immunogenicity data. Blood PBMC were analysed by ICS after stimulation with an LSA1 or LSAP2 peptide pool. Graphs represent the frequency of $CD4^+IFN\text{-}\gamma^+$ or $CD8^+IFN\text{-}\gamma^+$ T cells. Single points indicate T-cell responses of individual mice and red lines show the median response per group. (C) Efficacy data. Mice were challenged with 1,000 chimeric *P. berghei* sporozoites expressing *P. falciparum* LSA1 and LSAP2. Time to 1% parasitaemia is plotted on a Kaplan-Meier Survival Curve. Data was analysed with the log-rank (Mantel-Cox) test. Number of protected animals and levels of statistical significance when compared to the naïve control group are shown in the table.

## E2.3.2 Analyses of MVA vectors

Immunogenicity of newly produced MVA vectors was investigated in BALB/c mice without prior priming of the immune response with adenoviral vectors. Four BALB/c mice per group were immunised with $10^7$ PFU MVA expressing tPA-LSA1, tPA-LSAP2, tPA-

LSA1-LSAP2, sharkTM/Ii-LSA1-LSAP2, or troutTM/Ii-LSA1-LSAP2. A naïve group of mice served as an unvaccinated control group. Seven days post vaccination, mice were sacrificed and splenocytes analysed via an IFN-γ ELISpot assay (as described in B2.4.3, p. 50) or ICS for IFN-γ (as well as IL-2 and TNF, data not shown). As expected, LSA1- and LSAP2-specific T-cell responses were low when measured by flow cytometry (Figure E-7C). However, measuring IFN-γ production by an ELISpot assay (which is known to be more sensitive compared to ICS/flow cytometry) revealed that all five MVA vaccines were immunogenic, but no significant difference between groups was observed for either antigen (Figure E-7B).

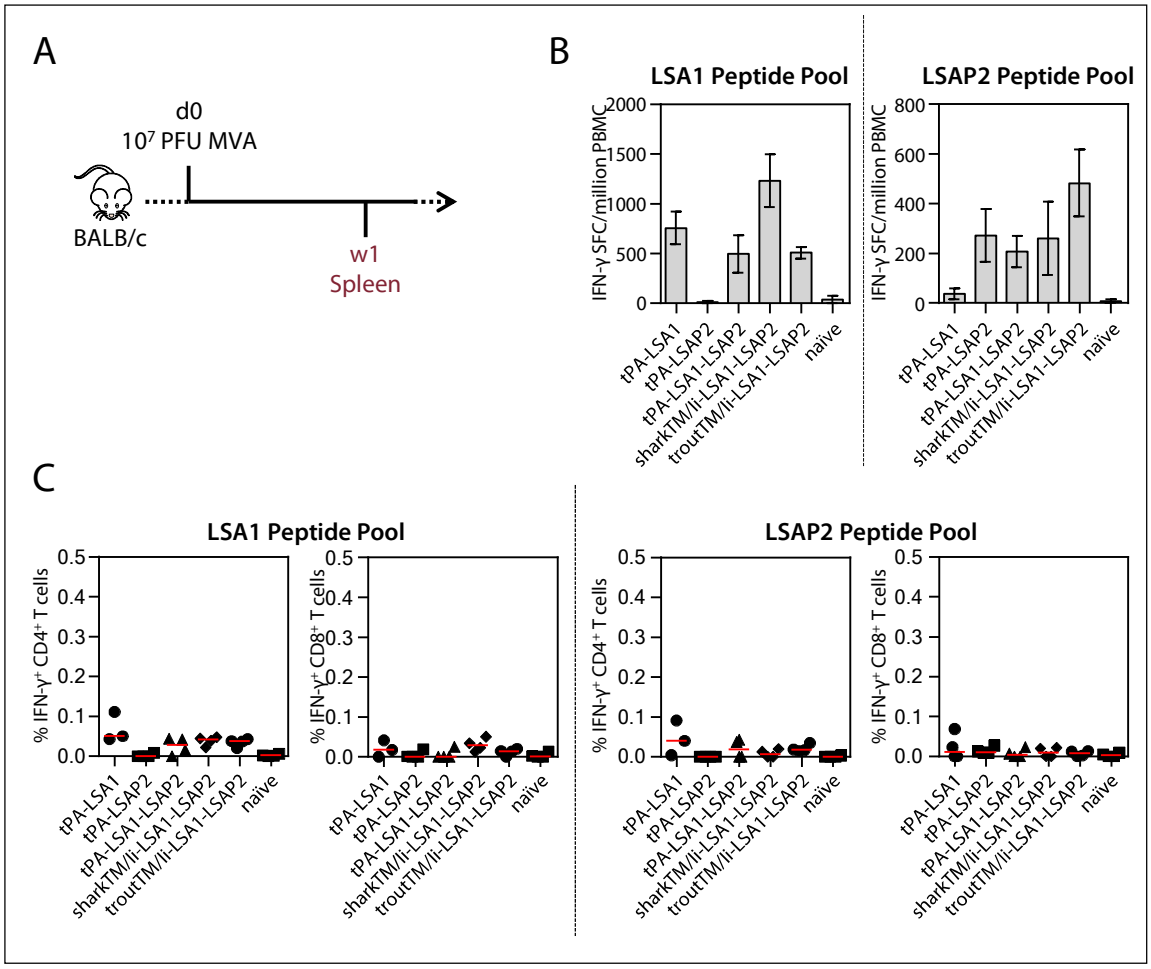



**Figure E-7. Immunogenicity of novel MVA encoding LSA1 and/or LSAP2.** (A) Outline of the experimental setup. BALB/c mice (4 per group) were immunised with $10^7$ PFU of MVA and spleens were harvested seven days later. (B) Graphs represent the number of IFN-γ producing cells per million splenocytes as measured by ELISpot. Columns denote the mean response per group. Error bars indicate the standard error of the mean (SEM) (C) T-cell responses to an LSA1 or LSAP2 peptide pool were

analysed by ICS. The percentage of $CD4^+$ and $CD8^+$ T cells positive for IFN-γ are shown. Single points indicate T-cell responses of individual mice and red lines denote the median response per group.

### E2.3.3 Analyses of ChAdOX1-MVA Prime-Boost Regimens

Having established immunogenicity of both, ChAdOX1 and MVA vectors, it was of interest to assess immunogenicity and efficacy of those vaccines in prime-boost regimens.

In a first experiment, all BALB/c mice were immunised with $10^8$ IU ChAdOX1-sharkTM/Ii-LSA1 and boosted after 7 days with $10^6$ PFU MVA expressing either tPA-LSA1, tPA-LSA1-LSAP2, or sharkTM/Ii-LSA-LSAP2 (Figure E-8, below). A blood sample was taken on day 14 (with PBMC analysed by ICS) and mice challenged with *Pb*(*Pf*LSA1+*Pf*LSAP2) three days later (Figure E-8). The frequency of LSA1-specific $CD4^+$ and $CD8^+$ T cells was increased when mice where boosted with MVA encoding the tPA leader sequence (tPA-LSA1, tPA-LSA1-LSAP2). However, no increase in LSA1-specific T-cell responses were observed in mice vaccinated with the adjuvanted MVA (sharkTM/Ii-LSA1-LSAP2). LSAP2-specific T-cell responses were generally low with no obvious differences between study groups. After challenge with 1,000 *Pb*(*Pf*LSA1+*Pf*LSAP2) sporozoites, very few mice were protected from developing blood stage malaria (a maximum of 1/6 mice survived per group, Figure E-8C). Receiving an MVA booster vaccine only slightly improved time to patent parasitaemia compared to the prime-only control group (group 1), but the difference was not statistically significant. Compared to the naïve control group, all immunisation regimens conferred a delay to patent parasitaemia ($p<0.01$ for prime-only, $p<0.001$ for all prime-boost regimens).

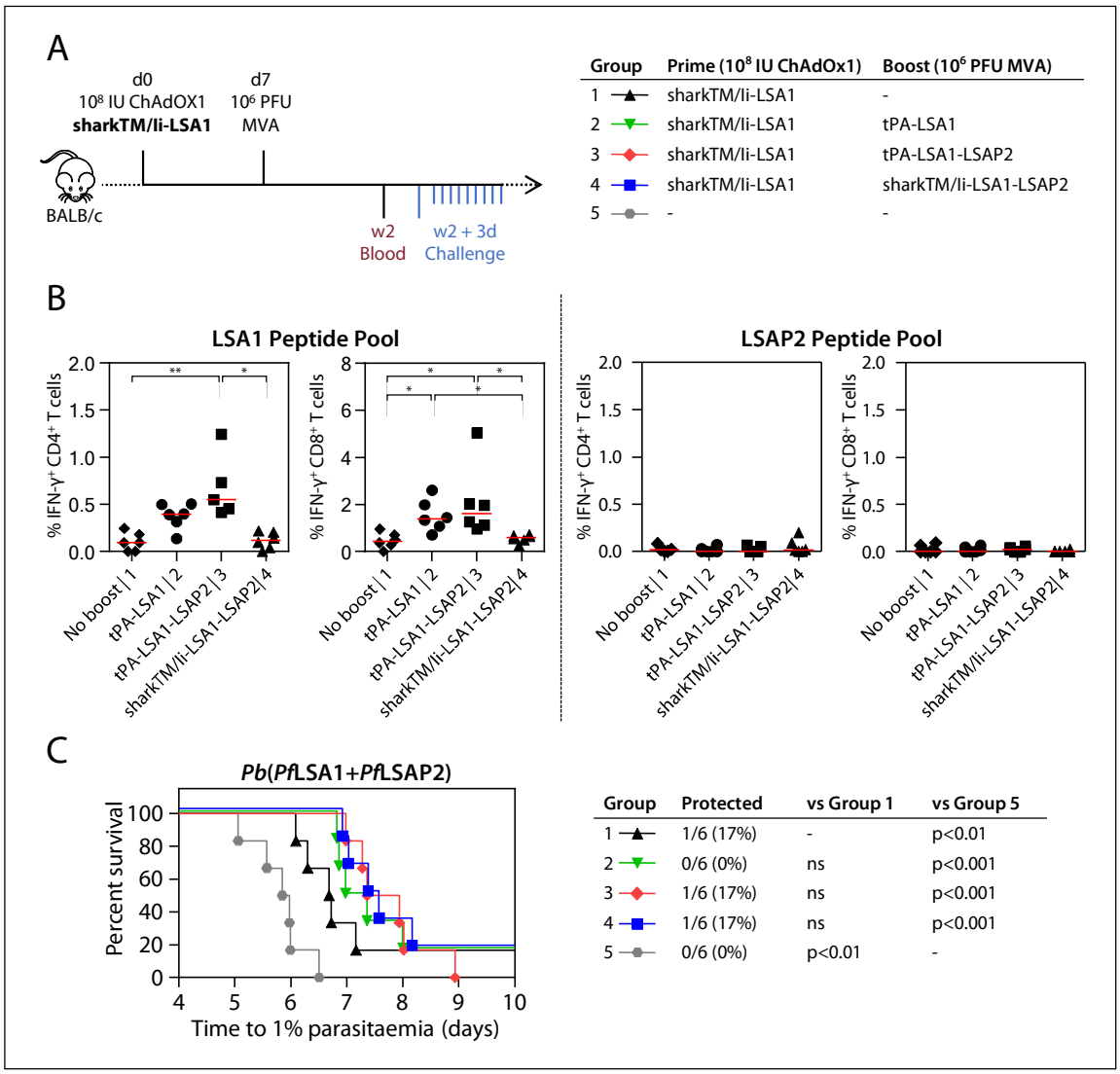



**Figure E-8. Immunogenicity and efficacy of a 1-week ChAdOX1-MVA prime-boost regimen in BALB/c.** (A) Outline of the experimental setup. After immunising six BALB/c mice per group with $10^8$ IU of ChAdOX1 encoding sharkTM/li-LSA1, the immune response was boosted with $10^6$ PFU MVA as indicated in the table. A blood sample was taken on day 14; three days later mice were challenged with 1,000 chimeric *P. berghei* sporozoites expressing *P. falciparum* LSA1 and LSAP2. (B) Immunogenicity data. Blood PBMC were analysed by ICS after stimulation with an LSA1 or LSAP2 peptide pool. Graphs represent the frequency of $CD4^+IFN\text{-}\gamma^+$ or $CD8^+IFN\text{-}\gamma^+$ T cells. Single points indicate T-cell responses of individual mice and red lines show the median response per group. Data was analysed with a one-way analysis of variance with Dunn's multiple comparison post-test. The asterisks denote the level of statistical significance when compared to each other (*, $p<0.05$; **, $p<0.01$). (C) Efficacy data. Blood smears were taken daily from four days after sporozoite challenge and analysed by Giemsa staining and light microscopy to determine parasitaemia. Mice that were negative for blood-stage malaria until 14 days after sporozoite challenge were considered to be sterilely protected. Time to 1% parasitaemia is plotted on a Kaplan-Meier Survival Curve. Data was analysed with the log-rank (Mantel-Cox) test. P-values when compared to the naïve control group (Group 5) and the group that did not receive an MVA booster vaccine (group 1) are presented in the table.

In a final experiment, immunogenicity and efficacy of novel ChAdOX1 and MVA vectors expressing LSA1, LSAP2, or LSA1-LSAP2 were investigated in a 6-week prime-boost

vaccination regimen (Figure E-9A). A blood sample was taken two weeks after administration of ChAdOX1 and one-week post MVA boost, and analysed for antigen specific production of IFN-γ by ICS (Figure E-9B). Comparing both time points showed that administration of MVA vaccines increased the fraction of mice with detectable antigen-specific immunity, as well as the magnitude of the individual T-cell responses (Supplemental Figure I-11, p. 210). One week post boost (Figure E-9B), the frequency of $CD4^+$ T cells against LSA1 was similar between all study groups that received a vaccine component expressing LSA1, but highest in group 1 that received vectors expressing LSA1 only. As seen previously (Figure E-3, p. 121), the LSA1-specific $CD8^+$ T-cell response was lower in mice immunised with vectors expressing the LSA1-LSAP2 fusion construct (group 5) compared to mice vaccinated with single LSA1 expressing vectors. LSAP2-specific T-cell responses were generally lower with no significant differences between groups. A detailed analysis of the functionality of antigen-specific T cells is shown in Supplemental Figure I-12 (p. 211). When challenged with 1,000 *Pb*(*Pf*LSA1+*Pf*LSAP2) sporozoites ten days after receiving the booster vaccination, the time to patent parasitaemia was significantly delayed in vaccinated mice. All mice (6/6) of group 4 (2×; primed with $10^8$ IU ChAdOX1-sharkTM/Ii-LSA1 mixed with $10^8$ IU ChAdOX1-sharkTM/Ii-LSAP2 and boosted with $10^7$ PFU tPA-LSA1 mixed with $10^7$ PFU tPA-LSAP2) were protected against parasite challenge. Five of six mice were protected in group 3 (1×; primed with $0.5\times10^8$ IU ChAdOX1-sharkTM/Ii-LSA1 mixed with $0.5\times10^8$ IU ChAdOX1-sharkTM/Ii-LSAP2 and boosted with $0.5\times10^7$ PFU tPA-LSA1 mixed with $0.5\times10^7$ PFU tPA-LSAP2). When mice were immunised with vectors expressing LSA1 only (group 1) or vectors expressing the LSA1-LSAP2 fusion construct (group 5), four of six mice survived. Lowest protection (1/6) was seen in group 2, which was vaccinated with vaccines expressing LSAP2 only.

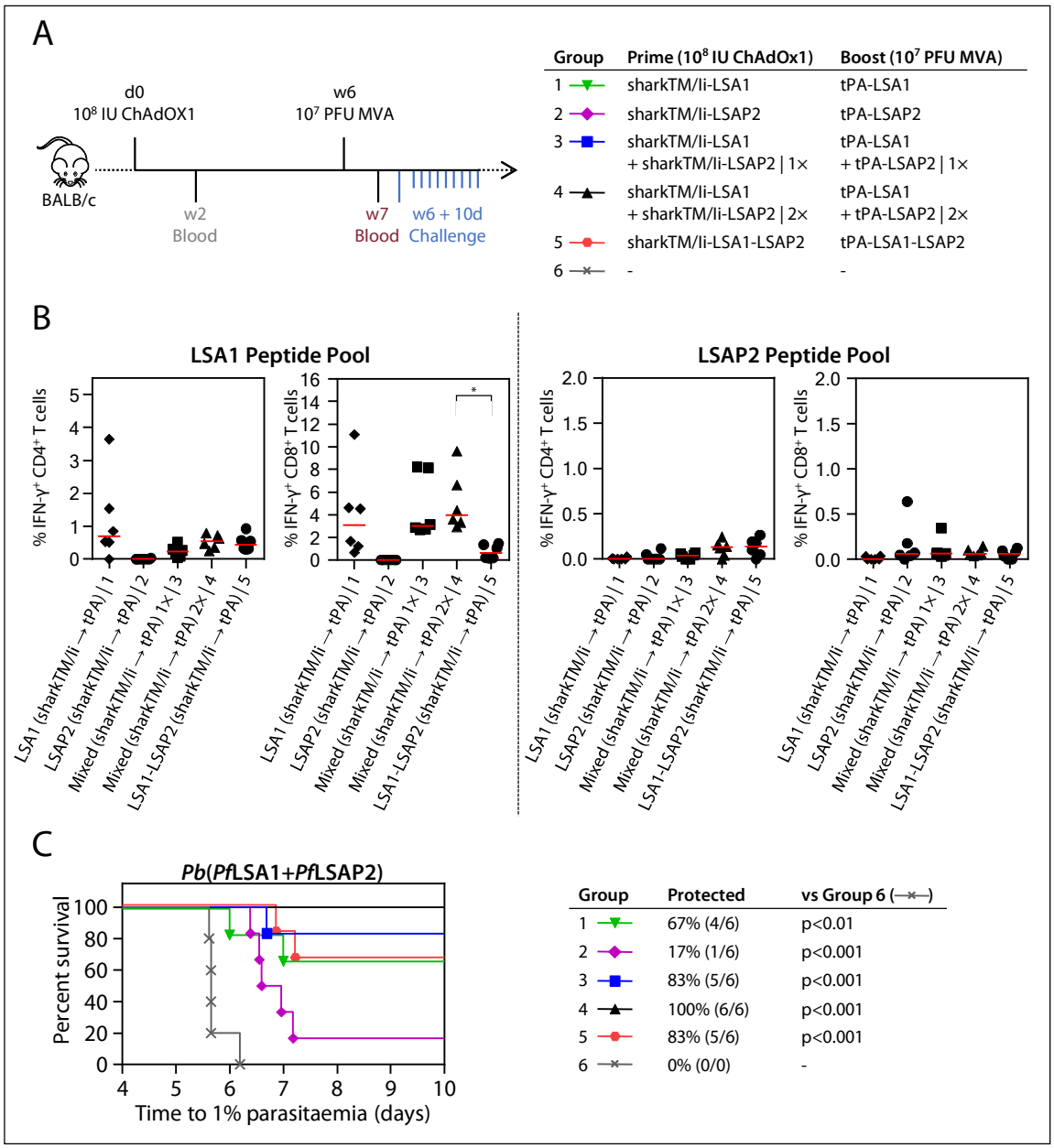



**Figure E-9. Immunogenicity and efficacy of a 6-week ChAdOX1-MVA prime-boost regimen in BALB/c.** (A) Experimental setup. After immunising six BALB/c mice per group with $10^8$ IU of ChAdOX1 (group 4 received $2\times10^8$ IU in total), mice were boosted with $10^7$ PFU MVA (group 4 received $2\times$ $10^7$ PFU) as indicated in the table. In ChAdOX1 vectors, the antigen was fused to the adjuvant sharkTM/Ii, in MVA vectors the antigen was fused to tPA (sharkTM/Ii → tPA). A blood sample was taken in week 7; three days later mice were challenged. (B) Immunogenicity data. Blood PBMC were analysed by ICS after stimulation with an LSA1 or LSAP2 peptide pool. Graphs represent the frequency of $CD4^+IFN\text{-}\gamma^+$ or $CD8^+IFN\text{-}\gamma^+$ T cells. Single points indicate T-cell responses of individual mice and red lines show the median response per group. Groups 1–4 were compared to group 5 with a one-way analysis of variance with Dunn's multiple comparison post-test. The asterisk denotes the level of statistical significance (*, $p<0.05$). (C) Efficacy data. Mice were challenged with 1,000 chimeric *P. berghei* sporozoites expressing *P. falciparum* LSA1 and LSAP2. Blood smears were taken daily from four days after sporozoite challenge and analysed by Giemsa staining and light microscopy to determine parasitaemia. Mice that were negative for blood-stage malaria until 15 days after sporozoite challenge were considered to be sterilely protected. Time to 1% parasitaemia is plotted on a Kaplan-Meier Survival Curve. Data was analysed with the log-rank (Mantel-Cox) test. Number of protected animals and levels of statistical significance when compared to the naïve control group are shown in the table.

## E2.4 Comparison of Vaccine Candidates in Outbred Mice

Many of the experiments described above were repeated in CD1 mice, which are more representative of an outbred human population than inbred BALB/c or CBA mice with their limited MHC repertoire (B2.3.1, p. 43).

### E2.4.1 Analyses of ChAdOX1 vaccines

First, sharkTM/Ii adjuvanted ChAdOX1 vectors (sharkTM/Ii-LSA1, sharkTM/Ii-LSAP2, and sharkTM/Ii-LSA1-LSAP2) were compared. Thirty CD1 mice were divided into six groups. Group 1 was immunised with $10^8$ IU ChAdOX1 encoding LSA1. Group 2 received the same dose of LSAP2 encoding vectors. In group 3, a full dose of LSA1 and a full dose of LSAP2 were administered into separate legs. For immunisation of group 4, $10^8$ IU of each vector were mixed in a vial before administration into both legs of the mice. Group 5 was administered with the $10^8$ IU of ChAdOX1-LSA1-LSAP2 and group 6 received $2\times10^8$ IU of the same vaccine to match the total amount of injected infectious adenovirus with that of groups 3 and 4.

Two weeks after vaccination, mice were sacrificed, spleens processed, and antigen-specific T-cell responses measured by ICS. T-cell responses to both antigens LSA1 and LSAP2 were generally low with no substantial differences between groups (Figure E-10). To induce a measureable immune response in this outbred mouse model, an MVA booster vaccine was included in subsequent experiments.

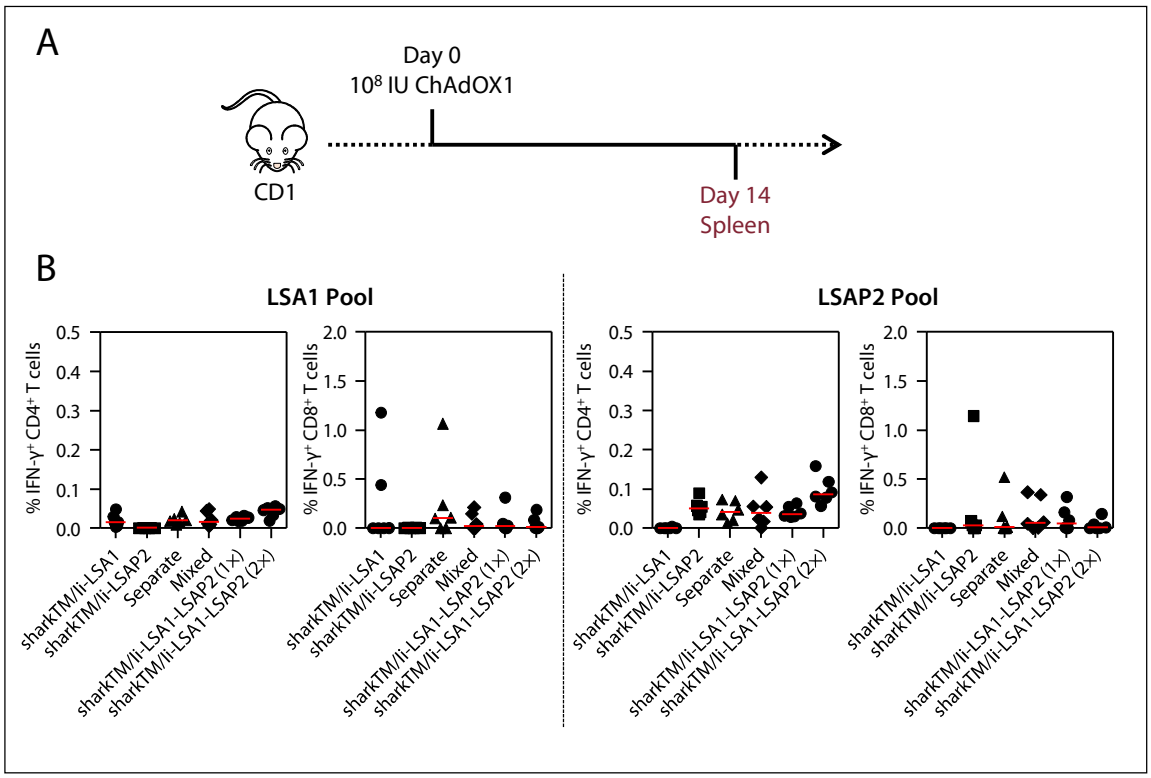



**Figure E-10. Immunogenicity of adjuvanted single vs dual antigen expressing vectors.** (A) Experimental setup. CD1 mice (6 per group) were immunised with $10^8$ IU ChAdOX1 vectors as indicated on the x-axes in B with spleens harvested two weeks later. (B) Immunogenicity data. T-cell responses to an LSA1 or LSAP2 peptide pool were analysed by ICS. The percentage of $CD4^+$ and $CD8^+$ T cells positive for IFN-γ are shown. Single points indicate T-cell responses of individual mice and red lines denote the median response per group.

### E2.4.2 Analyses of ChAdOX1-MVA Prime-Boost Regimens

In a first prime-boost experiment, all CD1 mice were immunised with $10^8$ IU ChAdOX1-sharkTM/Ii-LSA1 and then boosted after 7 days with $10^6$ PFU MVA expressing either tPA-LSA1, tPA-LSA1-LSAP2, or sharkTM/Ii-LSA-LSAP2 as indicated on the x-axes of Figure E-11. At day 14, mice were sacrificed and spleen T-cell responses analysed by flow cytometry. LSA1-specific $CD4^+$ T-cell responses were only marginally boosted (if at all) by either of the MVA vaccines. In contrast, LSA1-specific $CD8^+$ T-cell responses were increased by vaccinating with MVA encoding tPA-LSA1 or tPA-LSA1-LSAP2. However, this difference in $CD8^+$ T-cell induction was not statistically significant. The adjuvanted MVA (sharkTM/Ii-LSA1-LSAP) did not improve LSA1-specific T-cell responses. LSAP2-specfic T-cell responses were generally lower. Only $CD4^+$ T-cell responses against LSAP2

were slightly boosted by the administration of MVA vectors encoding tPA-LSA1-LSAP2 (not significant) or sharkTM/Ii-LSA1-LSAP2 ($p<0.05$).

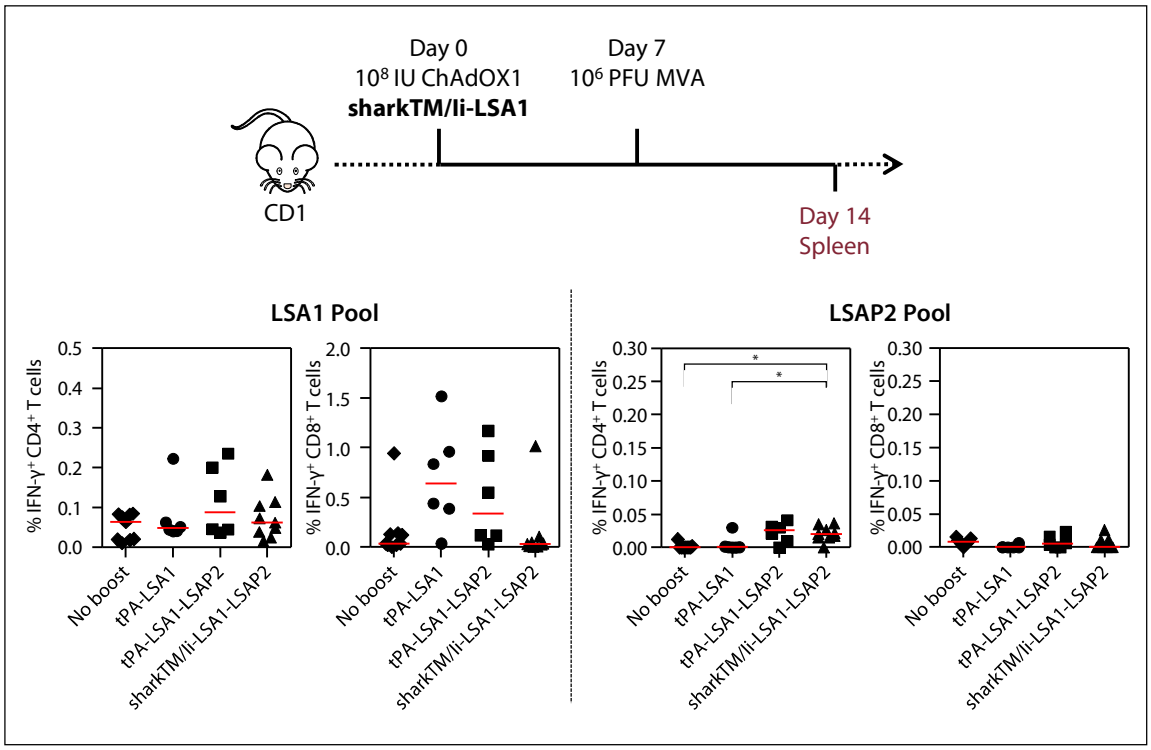



**Figure E-11. Immunogenicity of a 1-week ChAdOX1-MVA prime-boost regimen in outbred mice.** CD1 mice (6 per group) were immunised with $10^8$ IU ChAdOX1-sharkTM/Ii-LSA1 and boosted one week later with $10^6$ PFU MVA vectors as indicated on the x-axes. Spleens were harvested at day 14. T-cell responses to an LSA1 or LSAP2 peptide pool were analysed by ICS. The percentage of $CD4^+$ and $CD8^+$ T cells positive for IFN-γ are shown. Single points indicate T-cell responses of individual mice and red lines denote the median response per group. Data was analysed with a one-way analysis of variance with Dunn's multiple comparison post-test. The asterisk denotes the level of statistical significance when compared to each other (*, $p<0.05$).

Next, efficacy of a 1-week ChAdOX1-MVA prime-boost vaccination regimen was investigated in CD1 mice. As outlined in Figure E-12A, mice were immunised with $10^8$ IU ChAdOX1 and boosted after 7 days with $10^7$ PFU MVA. The antigens encoded by these vaccines are outlined in the table.

On day 17, mice were challenged with 1,000 *Pb*(*Pf*LSA1+*Pf*LSAP2) sporozoites. Fusion of the dual antigen construct to shark/TM did not enhance vaccine efficacy, as only mice that received a non-adjuvanted MVA were sterilely protected from malaria. Three of the nine mice in groups 1 (boosted with MVA-tPA-LSA1) and 2 (boosted with MVA-tPA-

LSA1-LSAP2) were protected against parasite challenge. However, the highest level of protection (50%) was observed when mice were primed with ChAdOX1-sharkTM/Ii-LSA1-LSAP2 and boosted with MVA-tPA-LSA1-LSAP2.

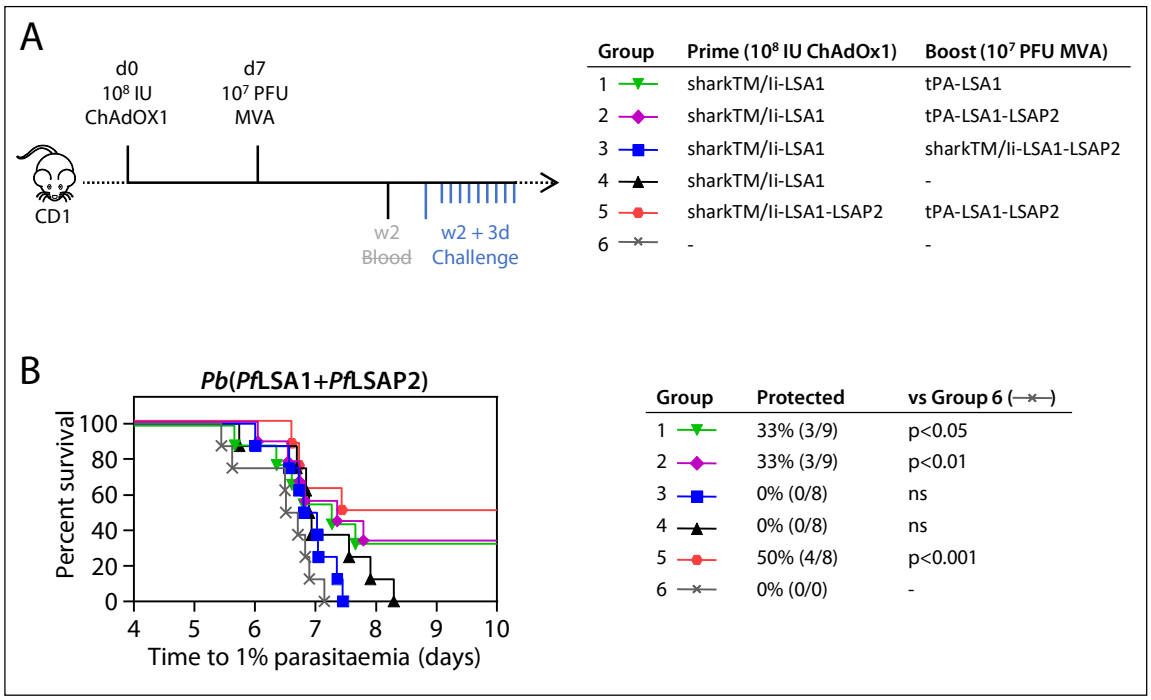



**Figure E-12. Efficacy of a 1-week ChAdOX1-MVA prime-boost regimen in CD1 mice.** (A) Experimental setup. After immunising eight or nine CD1 mice per group with $10^8$ IU of ChAdOX1 encoding sharkTM/Ii-LSA1, or sharkTM/Ii-LSA1-LSAP2 the immune response was boosted with $10^7$ PFU MVA as indicated in the table. A blood sample was taken on day 14, but could not be analysed due to a technical error of the flow cytometer; three days later mice were challenged. (B) Efficacy data. Mice were challenged with 1,000 chimeric *P. berghei* sporozoites expressing *P. falciparum* LSA1 and LSAP2 on day 17 post immunisation. Blood smears were taken daily from four days after sporozoite challenge and analysed by Giemsa staining and light microscopy to determine parasitaemia. Mice that were negative for blood-stage malaria until 14 days after sporozoite challenge were considered to be sterilely protected. Time to 1% parasitaemia is plotted on a Kaplan-Meier Survival Curve. Data was analysed with the log-rank (Mantel-Cox) test. Number of protected animals and levels of statistical significance when compared to the naïve control group are shown in the table.

Having established that the inclusion of sharkTM/Ii in MVA vectors did not confer any additional protection, another experiment comparing adjuvanted and non-adjuvanted ChAdOX1 vectors in a prime-boost regimen with non-adjuvanted MVA was performed. 32 CD1 mice were divided into four groups and immunised as outlined in Figure E-13A. The first two groups were vaccinated with ChAdOX1 vectors encoding non-adjuvanted (group 1) or adjuvanted (group 2) LSA1, the second two groups were immunised with

ChAdOX1 vectors encoding the non-adjuvanted (group 3) or adjuvanted (group 4) LSA1-LSAP2 fusion construct. T-cell responses from spleens dissected on day 14 were analysed by ICS and flow cytometry. Surprisingly, LSA1-specific $CD4^+$ T-cell responses were significantly lower when mice were primed with the adjuvanted ChAdOX1-sharkTM/Ii-LSA1-LSAP2 vector. As seen previously, the frequency of LSA1-specific $CD8^+$ T cells was lower in mice vaccinated with the LSA1-LSAP2 fusion construct (groups 3 and 4). LSAP2-specific T-cell responses were only observed in the groups that were immunised with a LSAP2 component (groups 3 and 4) with no significant difference between them.

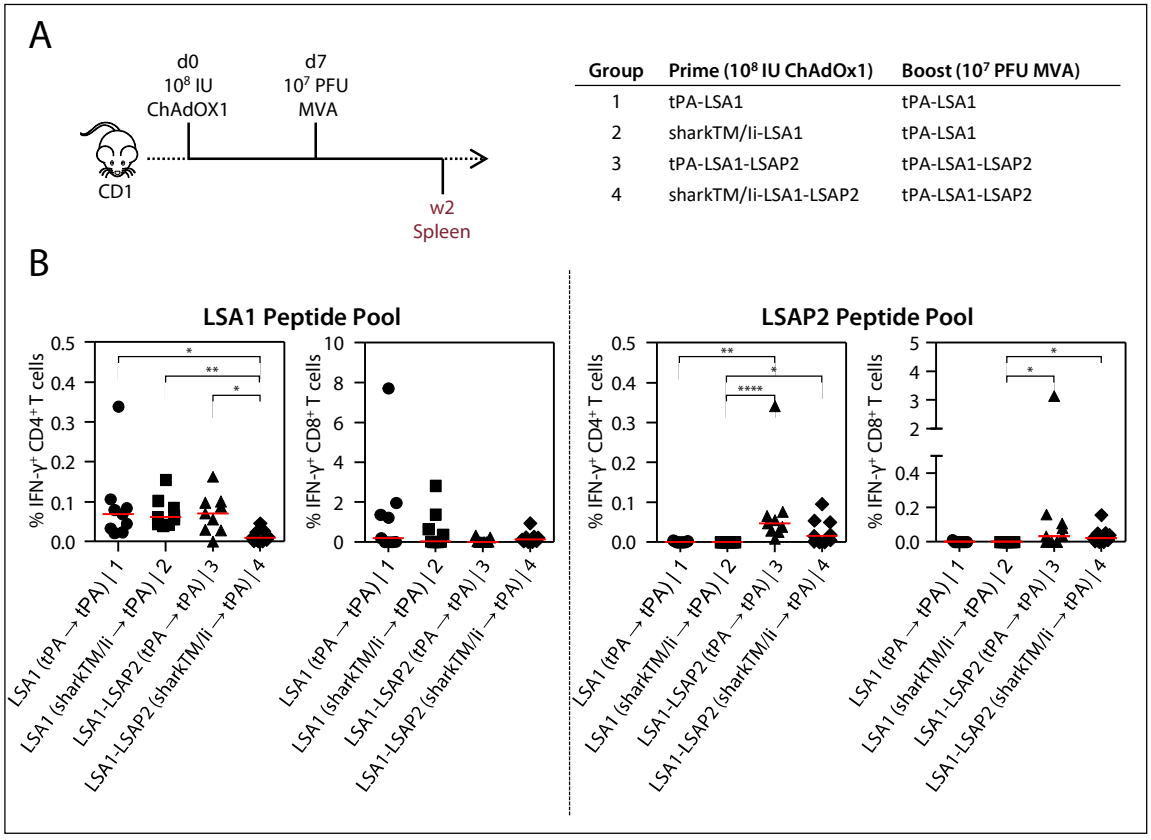



**Figure E-13. Comparison of immunogenicity of ChAdOX1 expressing tPA or sharkTM/Ii as a leader sequence in a 1-week ChAdOX1-MVA prime-boost regimen in outbred mice.** (A) Experimental outline. CD1 mice (8 per group) were immunised with $10^8$ IU ChAdOX1 and boosted one week later with $10^6$ PFU MVA vectors as indicated in the table. Spleens were harvested at day 14. (B) Immunogenicity data. T-cell responses to an LSA1 or LSAP2 peptide pool were analysed by ICS. The percentage of $CD4^+$ and $CD8^+$ T cells positive for IFN-γ are shown. Single points indicate T-cell responses of individual mice and red lines denote the median response per group. Data was analysed with a one-way analysis of variance with Dunn's multiple comparison post-test. The asterisks denote the level of statistical significance when compared to each other (*, $p<0.05$; **, $p<0.01$, ****, $p<0.0001$).

In a similar experiment, CD1 mice were immunised with non-adjuvanted and adjuvanted ChAdOX1 vectors encoding LSA1, LSAP2, or LSA1-LSAP2 and boosted with the corresponding non-adjuvanted MVA vaccines one week later as outlined in Figure E-14A. On day 14, a blood sample was taken and analysed by ICS and flow cytometry; on day 18 mice were challenged with 1,000 *Pb*(*Pf*LSA1+*Pf*LSAP2) sporozoites.

While LSA1-specific $CD4^+$ T-cell responses in the blood were similar between groups (Figure E-14B), yet again, the frequency of $CD8^+$ T cells specific for LSA1 was lower in mice vaccinated with the LSA1-LSAP2 fusion construct compared to those immunised with LSA1 only. However, in this experiment, the non-adjuvanted ChAdOX1-tPA-LSA1-LSAP vaccine (group 5) did not induce a higher $CD4^+$ T-cell response compared to the adjuvanted ChAdOX1-sharkTM/Ii-LSA1-LSAP2. LSAP2-specific $CD4^+$ T-cell responses were generally low, but highest in the group 4, which had received the ChAdOX1 vector expressing adjuvanted LSAP2. There was a large spread in the levels of LSAP2-specific $CD8^+$ T-cell responses between individual mice per group with some exceptionally high responders. This was most likely a result of the diverse MHC repertoire of the CD1 outbred population.

Sporozoite challenge revealed that most of the vaccination regimens did not confer significant delay in patent parasitaemia (Figure E-14C). The highest level of protection (38%) was observed in groups 1 (ChAdOX1-tPA-LSA1 → MVA-tPA-LSA1) and 6 (ChAdOX1-sharkTM/Ii-LSA1-LSAP2 → MVA-tPA-LSA1-LSAP2). However, only the efficacy of group 6 was statistically significant compared to the naïve control group (group 7), as unprotected mice of group 1 did not show a delay to patent parasitaemia.

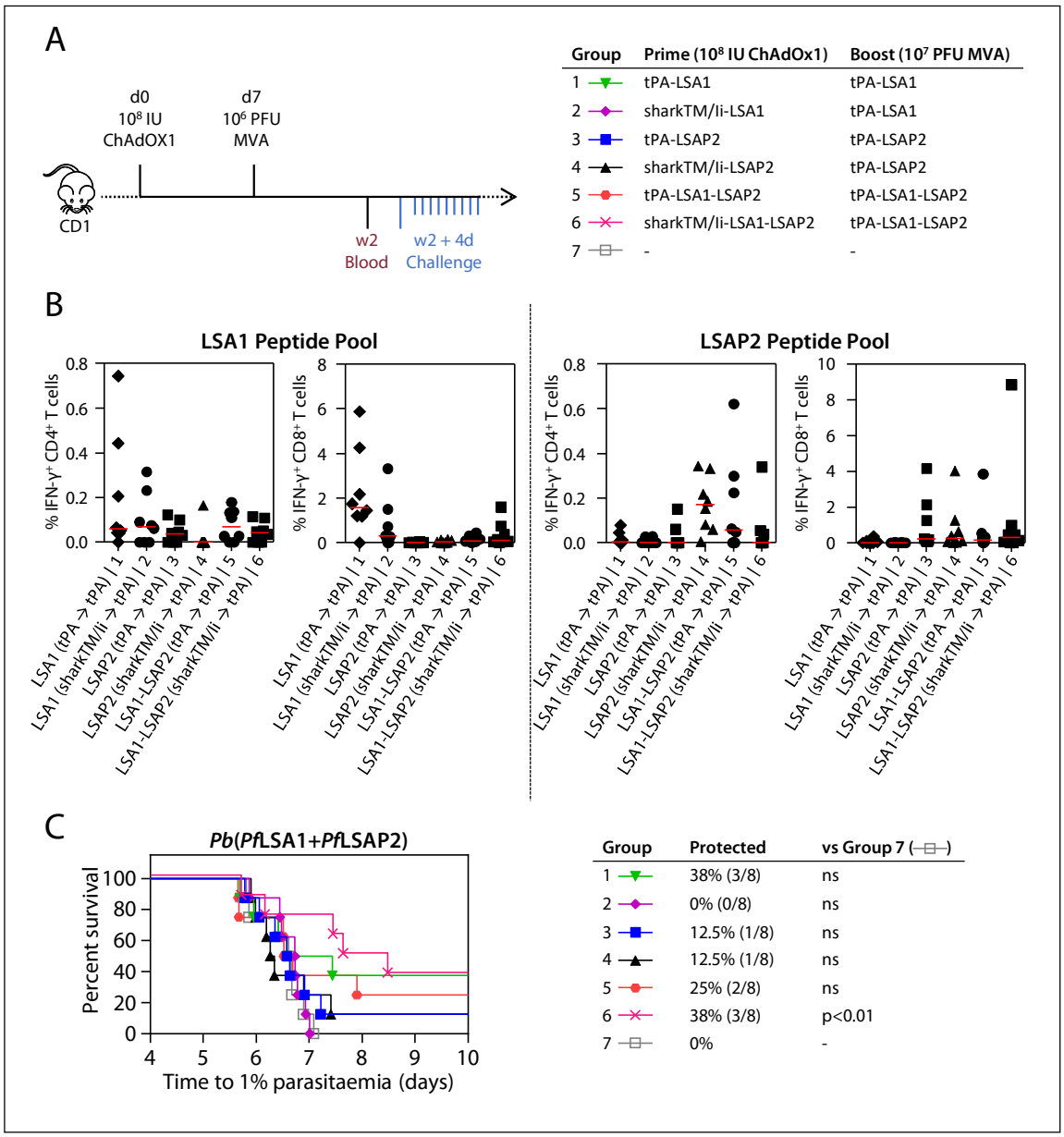



**Figure E-14. Comparison (immunogenicity and efficacy) of mono and dual antigen expressing vectors in CD1.** (A) Outline of the experimental setup. After immunising eight CD1 mice per group with $10^8$ IU of ChAdOX1, the immune response was boosted with $10^6$ PFU MVA as indicated in the table. A blood sample was taken on day 14; four days later mice were challenged. (B) Immunogenicity data. T-cell responses of blood PBMC to an LSA1 or LSAP2 peptide pool were analysed by ICS. The percentage of $CD4^+$ and $CD8^+$ T cells positive for IFN-γ are shown. Single points indicate T-cell responses of individual mice and red lines denote the median response per group. (C) Efficacy data. Mice were challenged with 1,000 chimeric *P. berghei* sporozoites expressing *P. falciparum* LSA1 and LSAP2 on day 18 post immunisation. Blood smears were taken daily from four days after sporozoite challenge and analysed by Giemsa staining and light microscopy to determine parasitaemia. Mice that were negative for blood-stage malaria until 14 days after sporozoite challenge were considered to be sterilely protected. Time to 1% parasitaemia is plotted on a Kaplan-Meier Survival Curve. Data was analysed with the log-rank (Mantel-Cox) test. Number of protected animals and levels of statistical significance when compared to the naïve control group are shown in the table.

Another experiment was set up to analyse efficacy of this vaccination regimen against *P. berghei* parasites expressing *Pf*LSA1 only. Immunogenicity data were similar to the previously described experiment. Unfortunately, in this particular experiment, all mice, apart from one CD1 mouse (vaccinated with ChAdOX1-sharkTM/Ii-LSA1 and MVA-tPA-LSA1), developed blood stage parasitaemia (Supplemental Figure I-13, p. 213).

Lastly, immunogenicity and efficacy of LSA1-, LSAP2-, or LSA1-LSAP2- expressing vectors were investigated in a 6-week prime-boost ChAdOX1-MVA vaccination regimen in CD1 mice (Figure E-15A). Two weeks after administration of ChAdOX1 vectors and one week after administration of booster vaccines, a blood sample was taken and analysed by ICS. Comparing both time points showed that injection of MVA vaccines increased the number of mice with detectable antigen-specific immunity, as well as the magnitude of the individual T-cell responses (Supplemental Figure I-14, p. 214). As described repeatedly, LSA1-specific $CD8^+$ T-cell responses appeared to be (non-significantly) lower if mice were vaccinated with viral vectors encoding the LSA1-LSAP2 fusion construct (Figure E-15B). Ten days after administration of booster vaccines, mice were challenged with 1,000 double-chimeric *Pb*(*Pf*LSA1+*Pf*LSAP2) sporozoites. Surprisingly, vaccinating mice with viral vectors encoding LSAP2 only (group 2, $p<0.01$) conferred the highest level of protection (4/10). However, the difference to the naïve control group was not as statistically significant as the efficacy of group 5 (vaccinated with viral vectors encoding the LSA1-LSAP2 fusion construct), as in this group all mice showed a delay to patent parasitaemia.

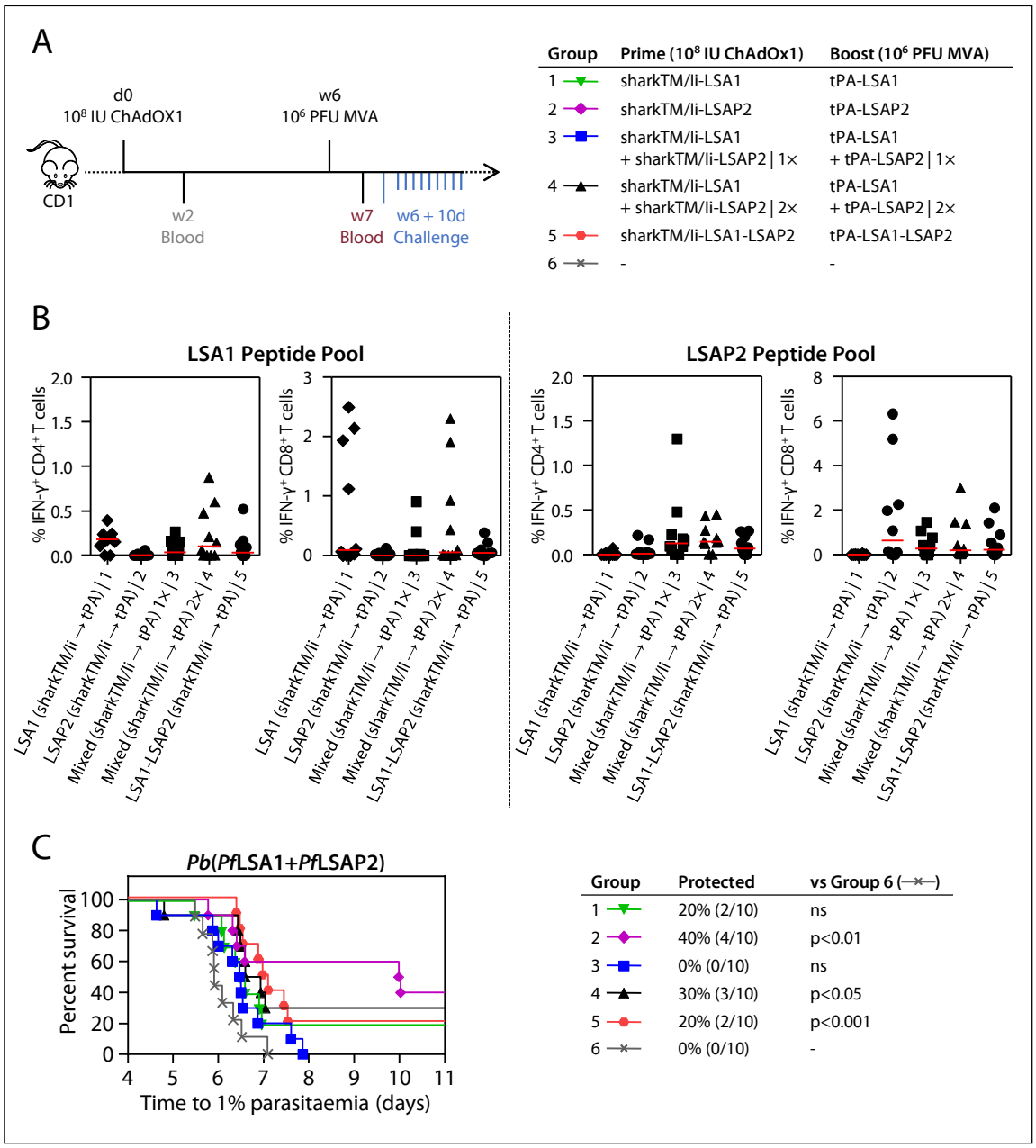



**Figure E-15. Immunogenicity and efficacy of a 6-week ChAdOX1-MVA prime-boost regimen in CD1.** (A) Experimental setup. After immunising eight CD1 mice per group with $10^8$ IU of ChAdOX1, the immune response was boosted with $10^6$ PFU MVA as indicated in the table. A blood sample was taken in week 7; three days later mice were challenged. (B) Immunogenicity data. T-cell responses of blood PBMC to an LSA1 or LSAP2 peptide pool were analysed by ICS. The percentage of $CD4^+$ and $CD8^+$ T cells positive for IFN-γ are shown. Single points indicate T-cell responses of individual mice and red lines denote the median response per group. (C) Efficacy data. Mice were challenged with 1,000 chimeric *P. berghei* sporozoites expressing *P. falciparum* LSA1 and LSAP2 on day 10 post boost. Blood smears were taken daily from four days after sporozoite challenge and analysed by Giemsa staining and light microscopy to determine parasitaemia. Mice that were negative for blood-stage malaria until 15 days after sporozoite challenge were considered to be sterilely protected. Time to 1% parasitaemia is plotted on a Kaplan-Meier Survival Curve. Data was analysed with the log-rank (Mantel-Cox) test. Number of protected animals and levels of statistical significance when compared to the naïve control group are shown in the table.

# E3 Discussion

Current liver-stage vaccination strategies still have to be further optimised to achieve reasonable levels of protective efficacy justifying mass vaccine production and deployment. In the previous chapters, LSA1 and LSAP2 as well as the combination of both antigens were analysed, and vaccine adjuvantation by fusion of antigens to Ii variants were discussed. In order to generate the most immunogenic and efficacious vaccine candidates, both strategies were combined in this chapter and adjuvanted LSA1 and/or LSAP2 encoding ChAdOX1 vectors produced. This viral vector was chosen instead of ChAd63, as some intellectual property rights of the latter are owned by GSK, potentially restricting or slowing clinical development. Both viral vectors were compared when encoding LSA1 or LSAP2 and found to be similarly immunogenic (Figure E-1, p. 117). This was in accordance with previous publications that reported ChAdOX1 to be comparably immunogenic in preclinical as well as clinical vaccine trials [292–298].

In total, fifteen different ChAdOX1 vectors were produced expressing either LSA1, LSAP2, or both antigens. An attempt to encode two antigens separately in different loci of an adenoviral vector or using a bidirectional CMV derived promotor failed to induce strong immunogenicity against both antigens (C2.3, p. 80). Therefore, an LSA1-LSAP2 fusion construct, which encoded LSAP2 fused to the C-terminal of LSA1 with a peptide linker separating both antigens (LSA1-LSAP2) was produced. The encoded antigen – LSA1 (461 aa), LSAP2 (302 aa), or LSA1-LSAP2 (770 aa incl. peptide linker) – was fused to the tPA leader sequence (which is known to improve expression and immunogenicity [204–206]), or to one of four Ii based adjuvants (tr)trout/Ii, (tr)shark/Ii, troutTM/Ii, or sharkTM/Ii. Furthermore, several corresponding non-adjuvanted (tPA) and adjuvanted (troutTM/Ii or sharkTM/Ii) MVA vectors were produced (Table E-2, p. 116).

All novel adjuvanted and non-adjuvanted vectors were then analysed in prime-only and ChAdOX1-MVA prime-boost regimens for immunogenicity and efficacy in inbred (BALB/c and CBA) as well as outbred (CD1) mice.

Direct comparison of spleen T-cell immunogenicity between LSA1 encoding ChAdOX1 vectors in BALB/c mice two weeks after vaccination, showed the highest LSA1-specific $CD8^+$ T-cell responses was elicited when LSA1 was fused to the shark/TM adjuvant (Figure E-2B, p. 120). However, compared to the T-cell response induced by the non-adjuvanted tPA-LSA1 vector, this increase was subtle and not statistically significant. To determine whether this enhanced immunogenicity would translate into improved efficacy, BALB/c mice were vaccinated with $10^8$ IU ChAdOX1 expressing tPA-LSA1 or sharkTM/Ii-LSA1 and challenged with transgenic *Pb*(*Pf*LSA1) parasites at the peak of the immune response. With this immunisation dose, the ChAdOX1-sharkTM/Ii-LSA1 induced a significantly ($p<0.05$) higher LSA1-specific $CD8^+$ T-cell response compared to the non-adjuvanted ChAdOX1-tPA-LSA1, which translated into a slightly improved protection against parasite challenge (Figure E-5, p. 124). However, levels of protective efficacy induced by ChAdOX1-tPA-LSA1 were much lower compared to the prime-only efficacy experiments conducted with ChAd63-tPA-LSA1 in chapter C (Figure C-7, p. 75). This could have been due to the slightly (but not significantly) reduced immunogenicity of the ChAdOX1 vectors expressing LSA1 (compared to corresponding ChAd63, Figure E-1, p. 117) or, more likely, a more vigorous parasite challenge, caused by the injection of more viable and therefore more infectious parasites. Parasite viability could be affected during the manual dissection process of the mosquito salivary glands or the storage time between mosquito dissection and IV injection. Therefore, comparisons of efficacy data between separate experiments have to be interpreted with caution. $CD8^+$ T-cell immunogenicity of viral vectors encoding LSAP2 were highest when adjuvanted with sharkTM/Ii, confirming the results obtained by LSA1 encoding ChAdOX1 (Figure E-2C,

p. 120). Immunogenicity of non-adjuvanted and adjuvanted vectors expressing the LSA1-LSAP2 fusion protein seemed to be generally lower compared to single antigen expressing vaccines (Figure E-2, p. 120). However, as single and dual antigen encoding vectors were investigated in separate experiments a definite conclusion was not possible. A separate immunogenicity experiment comparing all three inserts (adjuvanted with sharkTM/Ii) confirmed a dramatically reduced LSA1-specific $CD8^+$ T-cell response when mice were vaccinated with the vector expressing the LSA1-LSAP2 fusion construct (sharkTM/Ii-LSA1-LSAP2) (Figure E-3, p. 121). Remarkably, the LSA1-specific $CD4^+$ and LSAP2-specific $CD4^+$ and $CD8^+$ T-cell responses were not reduced when mice were vaccinated with the LSA1-LSAP2 fusion construct, suggesting protein expression was not affected. Instead, for some unknown reasons, the presentation of LSA1 $CD8^+$ T-cell epitopes on $H\text{-}2^d$, the MHC haplotype of BALB/c mice, seemed to be impaired in the presence of LSAP2 in one and the same APC. The reduced LSA1-specific $CD8^+$ T-cell response was also not detected when mice where vaccinated with both antigens, but encoded by two viral vectors individually ("Separate" and "Mixed" groups). In this scenario, at least some of the APC are likely to process and present epitopes of only one antigen. Notably, the low LSA1-specific $CD8^+$ T-cell response in mice immunised with the LSA1-LSAP2 fusion construct did not translate into reduced efficacy when challenged with *Pb*(*Pf*LSA1+*Pf*LSAP2) two weeks after immunisation. However, levels of sterile protection with this parasite were very low again, hampering a conclusion (Figure E-6, p. 126).

As the prime-only vaccination regimen described above appeared not to be sufficiently immunogenic to induce sterile efficacy, novel MVA encoding LSA1 or LSA1-LSAP2 fused to tPA or the sharkTM/Ii adjuvant were included in prime-boost regimens after their potency was confirmed in a short immunogenicity experiment (Figure E-7, p. 127). Immunogenicity measured in blood PBMC after a 1-week ChAdOX1-MVA prime-boost regimen revealed that only non-adjuvanted MVA (tPA-LSA1 or tPA-LSA1-LSAP2) had

the ability to boost the immune response primed by ChAdOX1-sharkTM/Ii-LSA1 (Figure E-8B, p. 129). Remarkably, in contrast to results obtained with ChAdOX1 vectors, the LSA1-LSAP2 fusion construct seemed to be as good as LSA1 in boosting LSA1-specific $CD8^+$ T-cell responses when expressed in MVA. Adjuvanted MVA (sharkTM/Ii-LSA1-LSAP2), however, did not further enhance LSA1-specific $CD4^+$ or $CD8^+$ T-cell responses. Experiments in CD1 mice confirmed this result (Figure E-11, p. 134). Given that non-adjuvanted MVA encoding the same fusion protein (tPA-LSA1-LSAP2) had the ability to boost LSA1-specific T-cell responses, this was quite unexpected. One possible explanation could be that priming the immune response with an adenoviral vector induced an immune response against the adjuvant (sharkTM/Ii), which then competed against antigen-specific immune responses and therefore hampered the booster effect. However, this seemed quite unlikely, since the adjuvant only consists of a short TMD. Another explanation could be the fact that cell types infected by MVA and its mechanisms of action are likely to be different compared to ChAdOX1. Therefore, sharkTM/Ii (as adjuvant) could have a positive adjuvantation affect with one vector (ChAdOX1) and be detrimental in a different vector (MVA). However, MVA encoding the full-length human Ii fused to ME-TRAP have been shown to have a positive effect on boosting the immune response [150]. Levels of sterile efficacy induced by these 1-week prime-boost regimens were still low and not significantly higher compared to mice immunised with ChAdOX1-sharkTM/Ii-LSA1 only (Figure E-8, p. 129). This was not surprising, as recent data in our group has shown that intervals shorter than six weeks between adenoviral vector prime and MVA boost is disadvantageous for the induction of cytotoxic T-cell responses (Spencer et al., in preparation). Vaccine immunogenicity and efficacy was then assessed using a 6-week prime-boost interval. BALB/c mice were primed with $10^8$ IU ChAdOX1 expressing adjuvanted LSA1, LSAP2, or LSA1-LSAP2 and were boosted with $10^7$ PFU MVA expressing the same vaccine antigen fused to tPA. Despite the reduced ability to induce

LSA1-specific $CD8^+$ T-cell responses (Figure E-9B, p. 131), the prime-boost vaccination regimen with ChAdOX1 and MVA expressing the LSA1-LSAP2 fusion construct induced similarly high levels of protective efficacy against parasite challenge as vectors encoding LSA1 only (Figure E-9C, p. 131). This was also seen in similar experiments using CD1 outbred mice (e.g. Figure E-12, p. 135). Only mixing viral vectors encoding LSA1 or LSAP2 individually resulted in higher levels of protection.

All these results strongly suggested that the best possible vaccination regimen would be the combination of an adjuvanted ChAdOX1 vaccine (ChAdOX1-sharkTM/Ii-LSA1 or ChAdOX1-sharkTM/Ii-LSA1-LSAP2) with an MVA encoding the antigen fused to tPA (MVA-tPA-LSA1 or MVA-tPA-LSA1-LSAP2). As the reduced LSA1-specific $CD8^+$ T-cell immunogenicity of the LSA1-LSAP2 fusion construct might be exceptional in the context of antigen processing and epitope presentation on $H\text{-}2^d$ (the MHC haplotype of BALB/c mice) and therefore vaccine efficacy might be even improved when presented on other MHC subtypes, the decision was made to prefer the LSA1-LSAP2 fusion construct. Both sharkTM/Ii-LSA1-LSAP2 and MVA-tPA-LSA1-LSAP2 are currently being produced to clinical grade (GMP) and will progress to clinical trials in the first half of 2017.

Many more experiments were conducted to confirm the results obtained in BALB/c mice. To determine whether the impaired LSA1-specific immunogenicity of adenoviral vectors encoding LSA1-LSAP2 is based on unknown mechanisms in the $H\text{-}2^d$ presentation pathway, immunogenicity of single and dual antigen encoding vectors were investigated in CBA mice, another inbred mouse strain with a different MHC haplotype ($H\text{-}2^k$). Unfortunately, $CD8^+$ T-cell responses in this mouse type were almost not detectable and therefore did not allow a conclusion.

Analyses in CD1 mice, an outbred mouse population with a diverse MHC repertoire, resulted in greater variability in vaccine immunogenicity and efficacy, but largely confirmed results obtained in BALB/c. This was very valuable, as CD1 are much more

representative of the diverse human population. Immunogenicity data in prime-only regimen did not induce high enough T-cell responses to detect differences between vaccine groups (Figure E-10, p. 133), but prime-boost regimens had the ability to strongly expand the LSA1-specific immune response (Figure E-11, p. 134). As mentioned above, it was confirmed that MVA expressing the antigen fused to sharkTM/Ii as adjuvant were not able to boost the LSA1-specific $CD8^+$ T-cell response induced by ChAdOX1-sharkTM/Ii-LSA1. This also translated into reduced levels of protective efficacy (Figure E-12, p. 135). Therefore, similar to results obtained in BALB/c mice, the combination of an adjuvanted ChAdOX1 with and non-adjuvanted MVA seemed to be most promising. Comparison of LSA1 with LSA1-LSAP2 encoding vectors in prime-boost regimens showed that LSA1-LSAP2 induced similar levels of vaccine efficacy (Figure E-14, p. 138; or Figure E-15, p. 140), if not higher (Figure E-12, p. 135) compared to LSA1-only.

As already discussed in Chapter C, the challenge model used in this study does not perfectly reflect natural infection, as the *P. falciparum* antigens of the transgenic murine parasites are expressed under the control of the *P. berghei* UIS4 promoter and are therefore not matched with their native expression levels. The replacement of *P. berghei* genes with their *P. falciparum* orthologues could improve this transgenic parasite challenge model, but as for many antigen candidates (such as LSA1 and LSAP2) no *P. berghei* orthologues are presently known, this strategy was not applicable.

In summary, this chapter provides robust support for the progression of ChAdOX1-sharkTM/Ii-LSA1-LSAP2 and MVA-tPA-LSA1-LSAP2 to clinical assessment, as administration of these vaccines in prime-boost vaccination regimens showed consistently highest levels of protective efficacy in inbred and outbred mouse strains. It has already been shown that viral vectors encoding LSA1 or LSAP2 induce high levels of efficacy in mice associated with just moderate levels of antigen-specific $CD8^+$ T cells which should therefore be achievable in humans [10]. Both, LSA1 and LSAP2, are surrounding the

developing merozoites either inside the parasitophorous vacuole or as part of the PVM and therefore might be presented by infected hepatocytes a lot more easily than merozoite proteins. LSA1 is also known to be highly conserved between *P. falciparum* strains [197], essential for late liver-stage development [198], and target of protective cellular immunity after natural infection [61–64] or vaccination with irradiated sporozoites [199]. As evidence suggests that the inclusion of multiple antigens in a vaccine will likely be necessary to reach sufficient levels of protection, immunising with viral vectors expressing two antigens (LSA1 and LSAP2), possibly in combination with existing ME-TRAP based liver-stage vaccines, therefore promises to increase protective immunity that is currently achieved in human liver-stage vaccination studies. Therefore, the adenoviral vaccine ChAdOX1-sharkTM/Ii-LSA1-LSAP2 and the MVA-tPA-LSA1-LSAP2 are currently being produced to clinical grade (GMP) and future clinical trials analysing their immunogenicity and efficacy in humans will provide final certainty.

# Chapter F

# Mechanisms of Ii Adjuvantation and a Search for Additional Adjuvants

# F1 Introduction

Despite the broad evidence of Ii adjuvanticity, very little is known about its mechanism of action. Bone-marrow derived DC transduced with viral vectors expressing antigen fused to Ii have been shown to induce increased antigen-specific $CD8^+$ T-cell proliferation *in vitro*, without any measurable difference in surface expression of MHC class I or costimulatory molecules [278]. It was also shown, that $CD4^+$ T-cell help is not necessary for this *in vitro* effect (equally not *in vivo*) [282].

These *in vitro* results suggest that the increased $CD8^+$ T-cell response is due to a direct effect on transduced DC leading to a more efficient presentation of antigen derived peptides on MHC class I (and II). To understand if antigen fusion to Ii has an impact on intracellular trafficking of the antigen, immunohistological analysis of transfected A549 cells (human adenocarcinoma epithelial cell line) was performed.

Conversely, one could argue that *in vivo* adjuvanticity is not caused by a direct effect of antigen processing in DC, as the majority of transduced cells after an intramuscular injection are not DC, but muscle cells or fibroblasts inside the muscle tissue. For T-cell priming, antigen stability would then be of higher importance in order to allow effective cross-presentation [299, 300]. Ii trimerisation could be crucial in this regard, as multimers tend to be more stable to proteolysis. *In vitro* and *in vivo* experiments were performed to analyse this hypothesis.

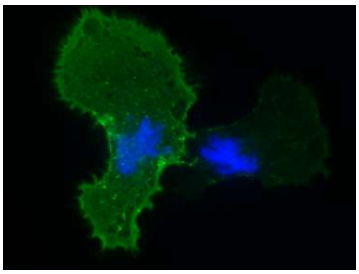
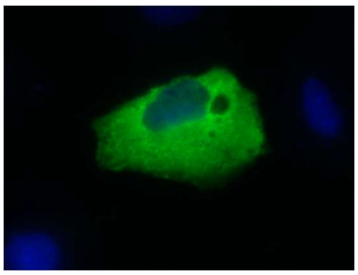
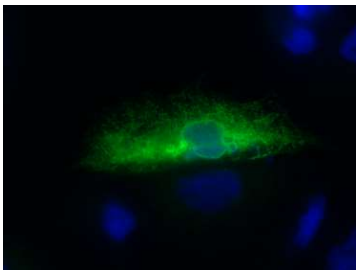
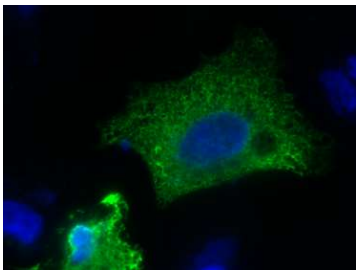
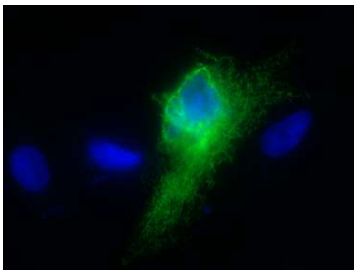
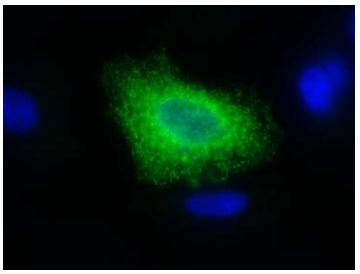
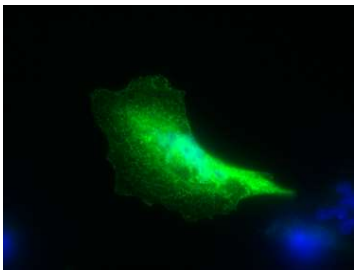
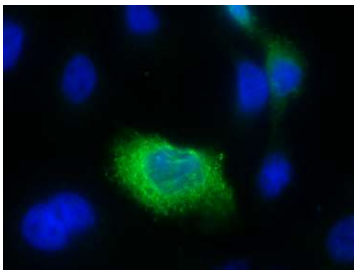
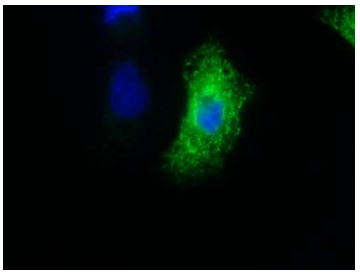
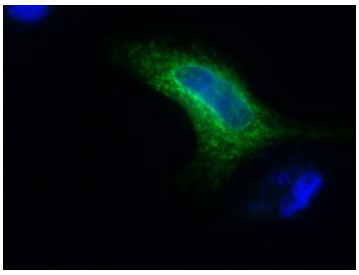
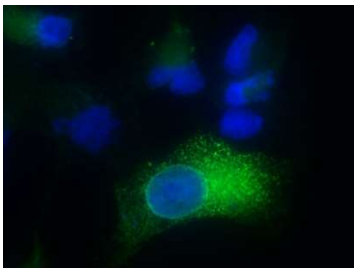
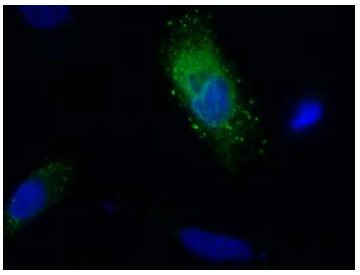
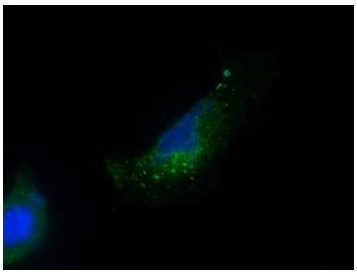
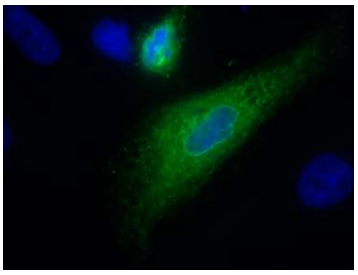
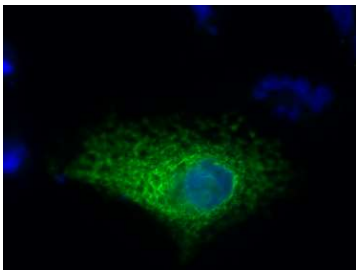
# F2 Results

## F2.1 Invariant Chain Fusion Alters Intracellular Antigen Trafficking

A variety of Ii-ME-TRAP fusion plasmids were screened in an *in vitro* imaging assay. After transfecting A549 cells with the various plasmids, antigen distribution within the cells was detected by immunofluorescent staining as described in in B2.5.1 and B2.5.2 (p. 51f).

Unfused ME-TRAP was primarily located on the cell surface (Figure F-1). When the predicted signal peptide of TRAP was deleted (w/o_eSP), TRAP was distributed diffusely across the cell. Fusion of ME-TRAP (which also lacks the TRAP signal peptide) to the full-length human Ii led to a significant alteration in TRAP expression, with the most intense fluorescence detected around the cell nucleus. This distinct localisation pattern was also observed when ME-TRAP was fused to other Ii truncations. A notable exception was humanCT/Ii-ME-TRAP. Even though the most intense fluorescence could still be detected intracellularly, staining of the plasma membrane was also more pronounced.

A549 cells were also transfected with plasmid DNA encoding truncated Ii sequences from various animal species (xenogenised Ii). In general, TRAP localisation was similar to (tr)human72/Ii-ME-TRAP. When cells were transfected with (tr)chicken/Ii-ME-TRAP or (tr)trout/Ii-ME-TRAP expressing constructs, TRAP expression was found to accumulate in small round-shaped conglomerations. Although this pattern of expression was not unique to these two constructs, it occurred at a higher frequency.

| | | |
|---|---|---|
| ME-TRAP  | ME-TRAP(w/o_eSP)  | (fl)human/li-ME-TRAP  |
| (tr)human72/li-ME-TRAP  | (tr)humanQ64A/li-ME-TRAP  | humanTM/li-ME-TRAP  |
| humanCT/li-ME-TRAP  | humanV1/li-ME-TRAP  | humanV2/li-ME-TRAP  |
| humanV3/li-ME-TRAP  | (tr)mouse/li-ME-TRAP  | (tr)chicken/li-ME-TRAP  |
| (tr)trout/li-ME-TRAP  | (tr)mallard-ME-TRAP  | (tr)zebrafish65-ME-TRAP  |

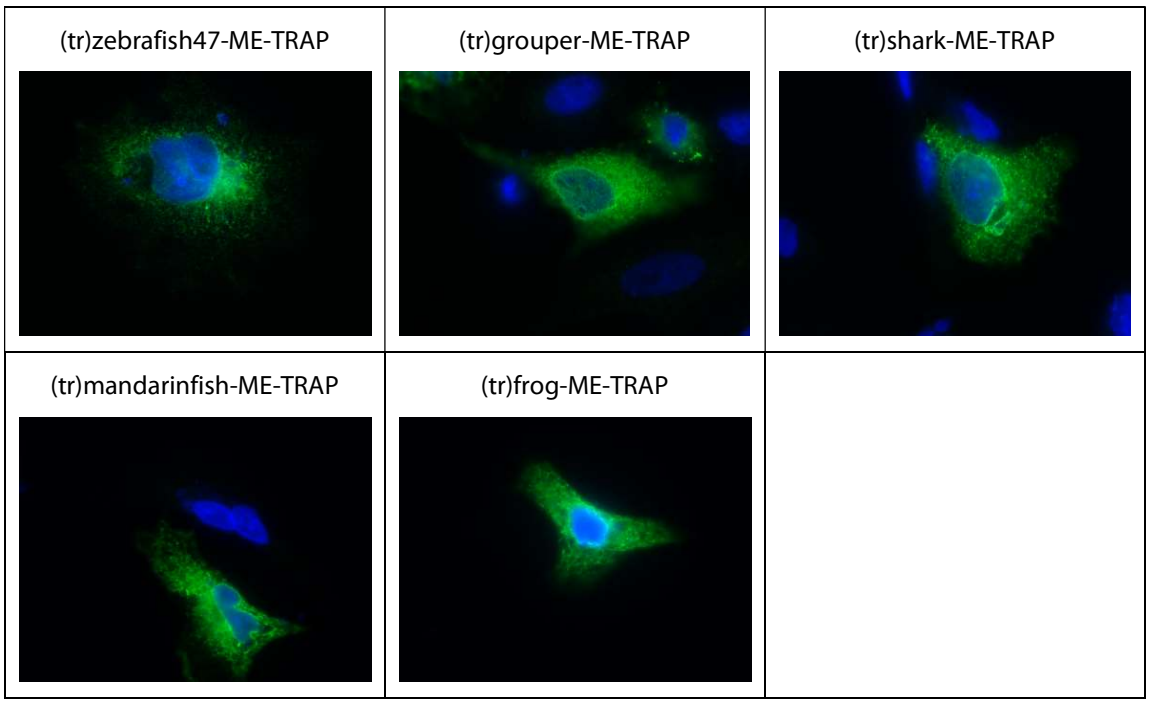



**Figure F-1. Invariant chain fusion alters the pattern of TRAP expression.** A549 cells were transfected with pENTR4-LPTOS plasmids encoding different Ii-ME-TRAP fusion constructs, incubated overnight prior to staining for TRAP expression (green). The nucleus was stained with DAPI (blue). Immunofluorescence images in 100× magnification are shown.

## F2.2 Importance of Ii Trimerisation

To investigate the importance of Ii trimerisation, a mutated version of (tr)human72/Ii-ME-TRAP was cloned, in which a glutamine was replaced by an alanine in position 64 by site directed mutagenesis (as described in B2.1.7, p. 37); the mutated construct was named (tr)humanQ64A/Ii-ME-TRAP. This mutation was previously shown to disrupt Ii trimerisation [301]. A ChAd63 vector encoding this mutated construct was produced (B2.2, p. 41) and its immunogenicity compared to the unmutated (tr)human72/Ii-ME-TRAP (Figure F-2). C57BL/6 mice were immunised with $10^7$ IU ChAd63 encoding unfused ME-TRAP or ME-TRAP fused to different Ii versions as indicated on the x-axes (Figure F-2B). Two weeks later, spleens were harvested and splenocytes stimulated with a single pool of overlapping peptides covering the full TRAP sequence (B2.4.1) to measure intracellular production of IFN-γ, IL-2, and TNF by ICS (B2.4.2); only IFN-γ responses

are shown. TRAP-specific CD4⁺ and CD8⁺ T-cell responses were of a similar magnitude when mice were vaccinated with ChAd63 vectors expressing the unmutated (tr)human72/Ii-ME-TRAP, mutated (tr)humanQ64A-ME-TRAP, or humanTM/Ii-ME-TRAP (Figure F-2B). Therefore, introducing the mutation within the Ii TMD did not impact on vaccine immunogenicity.

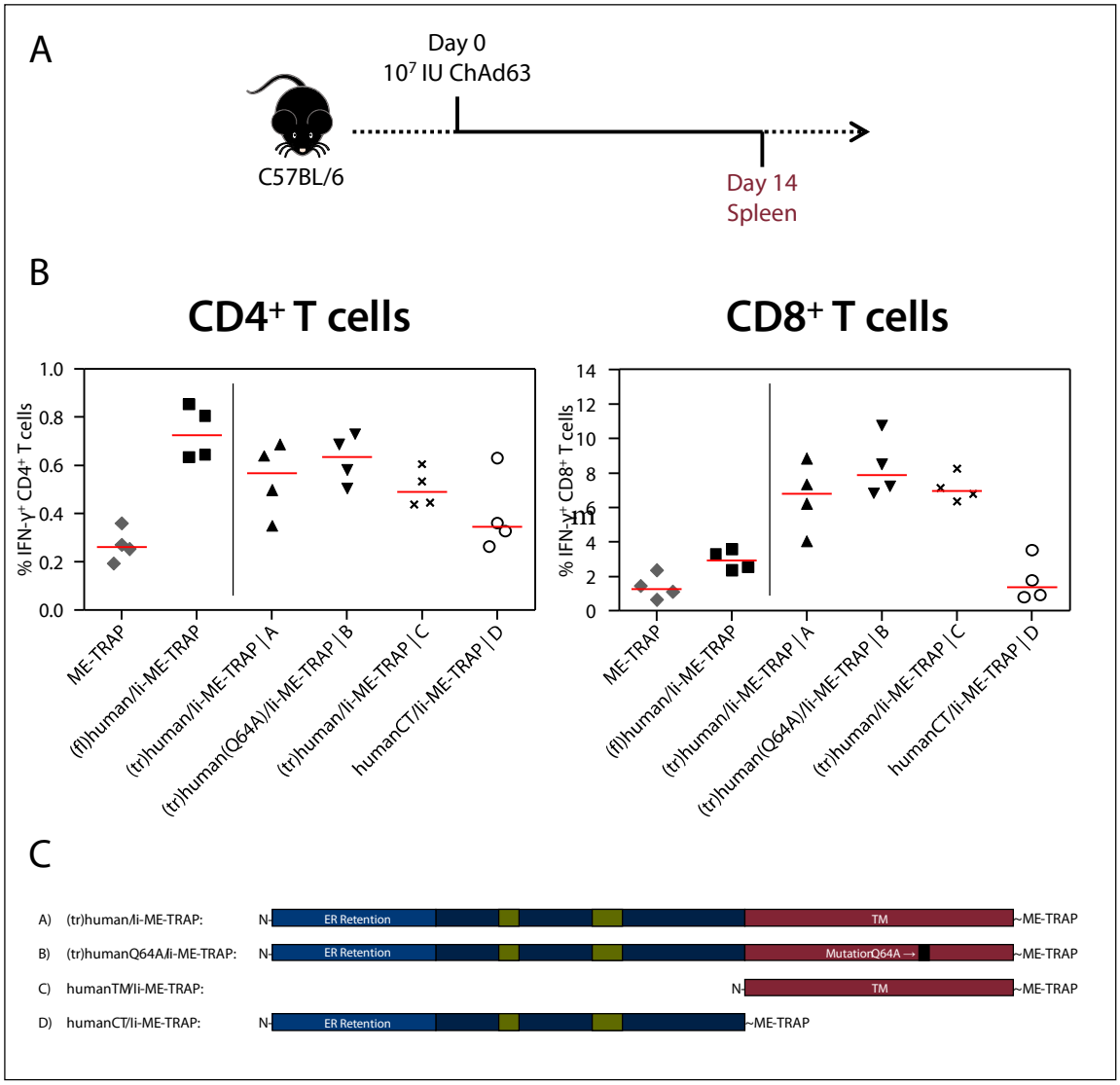



**Figure F-2. Immunogenicity of mutated (Q64A) Ii fused to ME-TRAP.** (A) Experimental outline. C57BL/6 mice were immunised with $10^7$ IU ChAd63 vectors and spleens were harvested two weeks later. T-cell responses to a TRAP peptide pool were analysed by ICS. (B) Immunogenicity data. The percentage of CD4⁺ and CD8⁺ T cells positive for IFN-γ are shown. Single points indicate T-cell responses of individual mice and red lines denote the median response per group. (C) Drawing of different Ii versions compared in this experiment.

In order to investigate whether the introduced mutation had an effect on antigen multimerisation, a western blot analysis was performed. HEK293 cells were transfected with pENTR4LPTOS-plasmids encoding unfused or adjuvanted ME-TRAP constructs, with cells harvested and lysed the following day (B2.5.3, p. 52). Lysate samples were then analysed under reducing and non-reducing conditions using polyacrylamide gels and western blot analyses with mouse polyclonal antibodies against ME-TRAP, HRP-conjugated anti-mouse antibodies, and a chemiluminescence detection system (B2.5.3, p. 52f). All lysate samples from cells transfected with ME-TRAP variants showed at least two bands – one of expected length and one slightly smaller (possibly due to partial post-translational modifications or expression from alternative translation initiation sites). Using non-reducing conditions, ME-TRAP appeared to multimerise/aggregate when fused to (fl)human/Ii, (tr)human72/Ii, humanTM/Ii, and also (tr)humanQ64A/Ii (Figure F-3A). Despite the reducing conditions (Figure F-3B), ME-TRAP still formed dimers when fused to these four Ii variants, suggesting an extraordinary multimer stability. Importantly, dimerisation was also seen when the Ii-TMD was mutated ((tr)humanQ64A/Ii-ME-TRAP). Multimerisation was therefore not disrupted by this mutation.

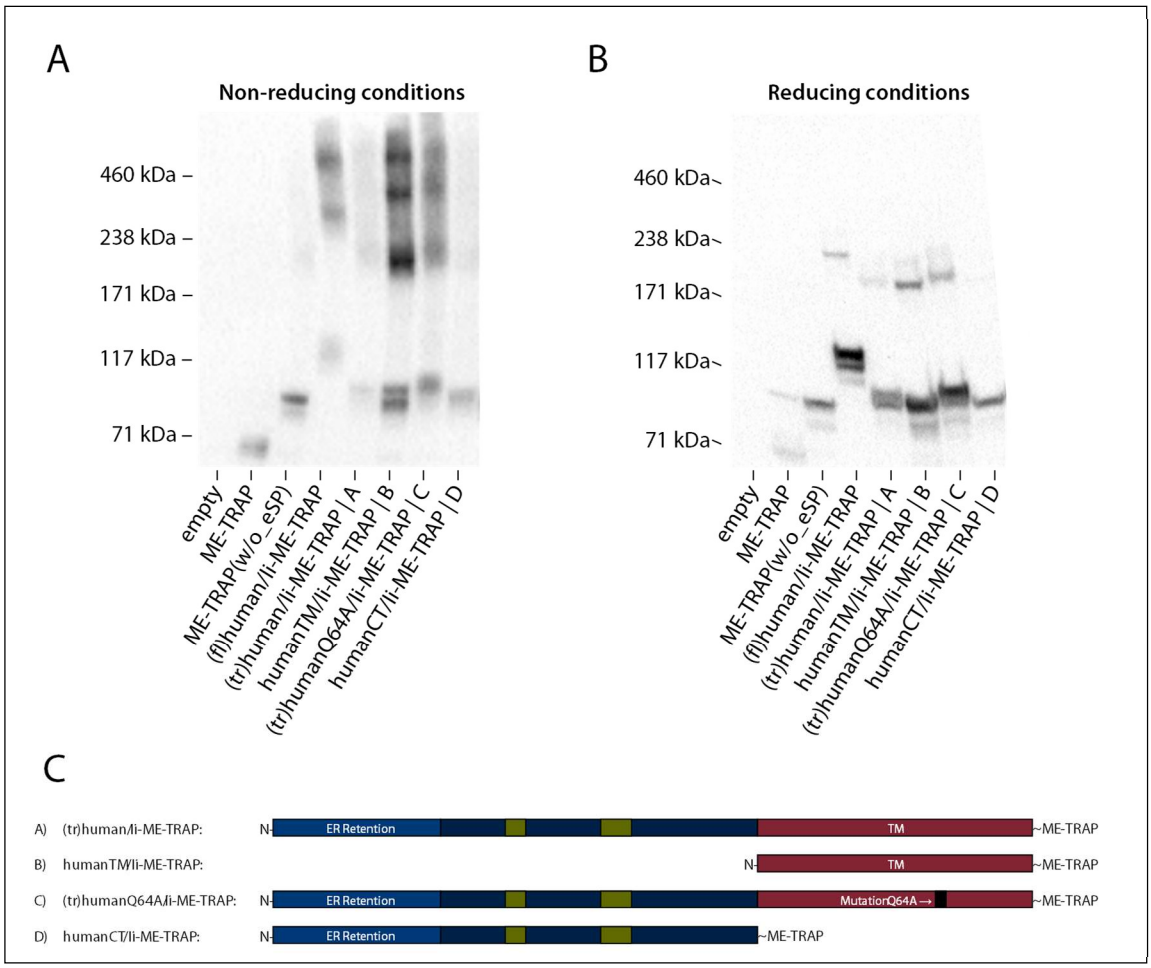
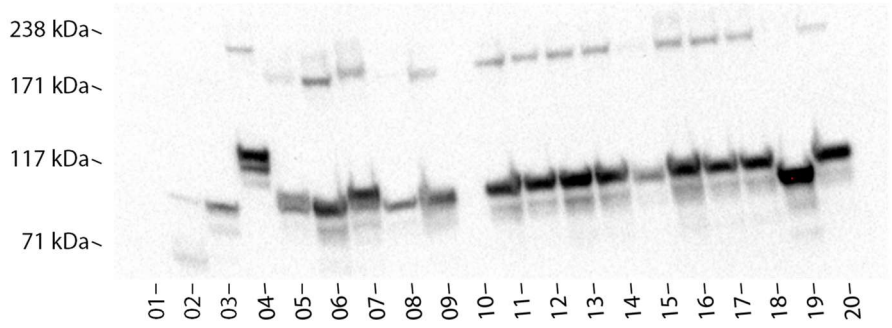



**Figure F-3. Western blot of unfused and adjuvanted ME-TRAP constructs.** HEK293 cells were transfected with plasmid DNA and lysed one day later. Lysates were then analysed using polyacrylamide gels and western blots stained with polyclonal serum against ME-TRAP (A) Western blot of lysates in non-reducing conditions: LDS loading buffer, 85°C, 5 min. (B) Western blot in reducing conditions: LDS loading buffer + 10% 2-Mercaptoethanol, 85°C, 5 min. (C) Drawing of different Ii versions compared in this experiment. Both plots were parts of a larger blot shown in Figure F-4 (below).

Based on these results, the TMD of humanTM/Ii-ME-TRAP in the pENTR4-LPTOS plasmid was systematically mutated (Figure F-4B, samples 11–20) by site-directed mutagenesis (B2.1.7, p. 37). HEK293 cells were transfected with these mutated plasmids, lysed, and analysed by western blots as described above. One of the mutated candidates, humanTM(ly71aa)/Ii-ME-TRAP, had a N-terminal deletion (as confirmed by Sanger sequencing), which resulted in translation of a smaller protein. Another construct (humanTM(lll59aaa)/Ii-ME-TRAP) attracted attention, as it showed a lower tendency to

multimerise. However, protein expression levels from this plasmid seemed to be lower compared to other plasmids, too.

A




B

| Sample | Plasmid Name | TMD sequence (if applicable) |
|---|---|---|
| 01 | empty | |
| 02 | ME-TRAP | |
| 03 | ME-TRAP(w/o_eSP) | |
| 04 | (fl)human/Ii-ME-TRAP | |
| 05 | (tr)human/Ii-ME-TRAP | |
| 06 | humanTM-Ii-ME-TRAP | galytgfsilvtlllagqattayfly |
| 07 | (tr)human(Q64A)/Ii-ME-TRAP | galytgfsilvtlllagAattayfly |
| 08 | humanCT/Ii-ME-TRAP | |
| 09 | NC/TMD-ME-TRAP | |
| 10 | Ladder | |
| 11 | humanTM(gal47aaa)/Ii-ME-TRAP | AAAytgfsilvtlllagqattayfly |
| 12 | humanTM(ytg50aaa)/Ii-ME-TRAP | galAAAfsilvtlllagqattayfly |
| 13 | humanTM(fsi53aaa)/Ii-ME-TRAP | galytgAAAlvtlllagqattayfly |
| 14 | humanTM(lvt56aaa)/Ii-ME-TRAP | galytgfsiAAAlllagqattayfly |
| 15 | humanTM(lll59aaa)/Ii-ME-TRAP | galytgfsilvtAAAagqattayfly |
| 16 | humanTM(agq62aaa)/Ii-ME-TRAP | galytgfsilvtlllAAAattayfly |
| 17 | humanTM(att65aaa)/Ii-ME-TRAP | galytgfsilvtlllagqAAAayfly |
| 18 | humanTM(ayf68aaa)/Ii-ME-TRAP | galytgfsilvtlllagqattAAAly |
| 19 | humanTM(ly71aa)/Ii-ME-TRAP | galytgfsilvtlllagqattayfAA |
| 20 | humanTM(Mut02)/Ii-ME-TRAP | galytgfAiAvtAllagAattaAfly |

**Figure F-4. Western blot of ME-TRAP constructs fused to mutated Ii-TMD.** (A) HEK293 cells were transfected with plasmid DNA as shown in B. Cell lysates were analysed in reducing conditions (LDS loading buffer + 10% 2-Mercaptoethanol, 85°C, 5 min) using a polyacrylamide gel and western blot stained with polyclonal serum against ME-TRAP. (B) Sample name and sequence of Ii TMD if applicable. Mutated amino acids are highlighted in red.

A ChAd63 viral vector encoding the mutated humanTM(lll59aaa)/Ii-ME-TRAP was produced by the viral vector core facility of the Jenner Institute (B2.2, p. 41) to investigate immunogenicity in C57BL/6 mice. Two weeks after immunising with $10^8$ IU ChAd63 encoding unfused ME-TRAP, humanTM/Ii-ME-TRAP, or mutated humanTM(lll59aaa)/Ii-ME-TRAP, spleens were harvested and T-cell responses against a

TRAP peptide pool analysed by ICS (Figure F-5A). TRAP-specific CD4$^+$ T-cell responses were (non-significantly) increased by fusing ME-TRAP to humanTM/Ii, but not by fusing ME-TRAP to the mutated humanTM(lll59aaa)/Ii-ME-TRAP. Similarly, antigen-specific CD8$^+$ T-cell responses were significantly increased when ME-TRAP was fused to humanTM/Ii, but only slightly and non-significantly increased when fused to mutated humanTM(lll59aaa)/Ii.

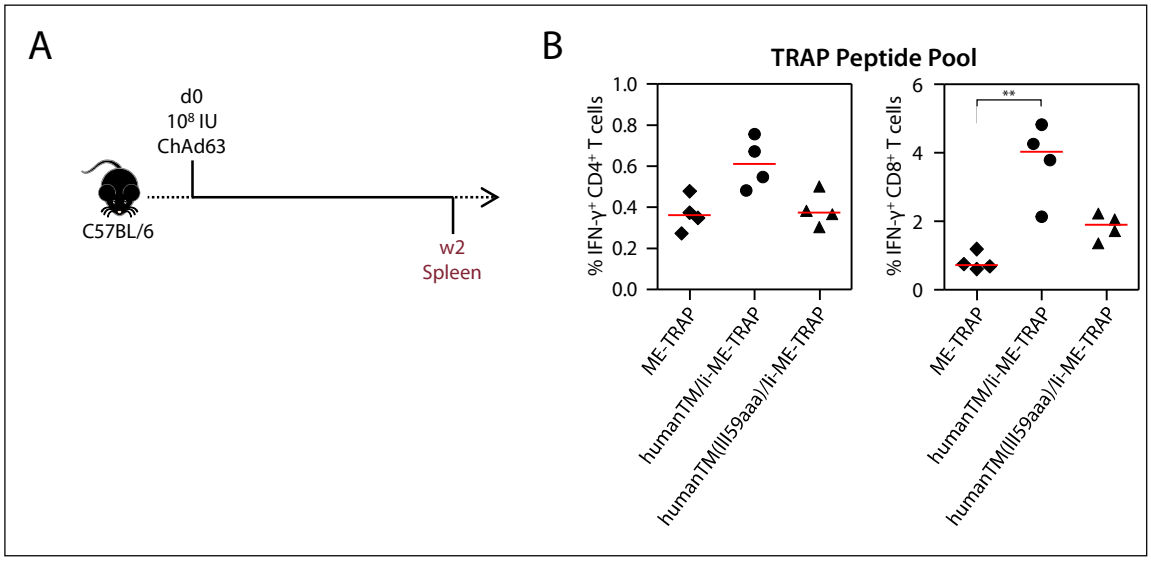



**Figure F-5. Immunogenicity of humanTM(lll59aaa)/Ii-ME-TRAP.** (A) Experimental outline. C57BL/6 mice were immunised with $10^8$ IU ChAd63 vectors and spleens were harvested two weeks later. T-cell responses to a TRAP peptide pool were analysed by ICS. (B) Immunogenicity data. The percentage of CD4$^+$ and CD8$^+$ T cells positive for IFN-γ are shown. Single points indicate T-cell responses of individual mice and red lines denote the median response per group. Data was analysed with a one-way analysis of variance with Dunn's multiple comparison post-test. Asterisks denote the level of statistical significance when compared to the control group vaccinated with ME-TRAP (**, $p<0.01$).

## F2.3 Newcastle Disease Virus Fusion Protein TMD as Molecular Adjuvant

Based on these findings, the literature was screened for TMD of non-human proteins, which are known to trimerise or at least multimerise. Excitingly, the TMD of paramyxoviridae fusion proteins have recently been described to self-associate into trimeric complexes in the absence of the rest of the protein [302] and therefore share the

most outstanding characteristic of the Ii TMD. To investigate if this similarity results in an equal effect on vector immunogenicity, the 21 aa long TMD sequence of the fusion protein of one paramyxovirus (Newcastle disease virus) was fused to the N-terminal end of ME-TRAP using In-Fusion cloning methods (B2.1.5, p. 35), and produced as a ChAd63 vector (B2.1.10 and B2.2) to compare its immunogenicity with existing unfused and adjuvanted ME-TRAP expressing vectors.

C57BL/6 mice were vaccinated with $10^7$ or $10^8$ IU ChAd63 encoding non-adjuvanted ME-TRAP, ME-TRAP fused to the TMD of Ii (humanTM/Ii) or the TMD of the Newcastle disease virus fusion protein (NC/TMD). Two weeks post vaccination, splenocytes were stimulated with a TRAP peptide pool and analysed by ICS. Having immunised mice with $10^7$ IU ChAd63 vectors, the resulting TRAP-specific $CD8^+$ T-cell response induced by NC/TMD-ME-TRAP was of similar magnitude compared to that induced by humanTM/Ii-ME-TRAP. There was no adjuvantation effect on $CD4^+$ T-cell responses when vaccinated with NC/TMD-ME-TRAP. However, when mice were immunised with $10^8$ IU ChAd63 vectors, both antigen-specific $CD4^+$ and $CD8^+$ T-cell responses were statistically significantly higher than the response in mice vaccinated with the non-adjuvanted ME-TRAP.

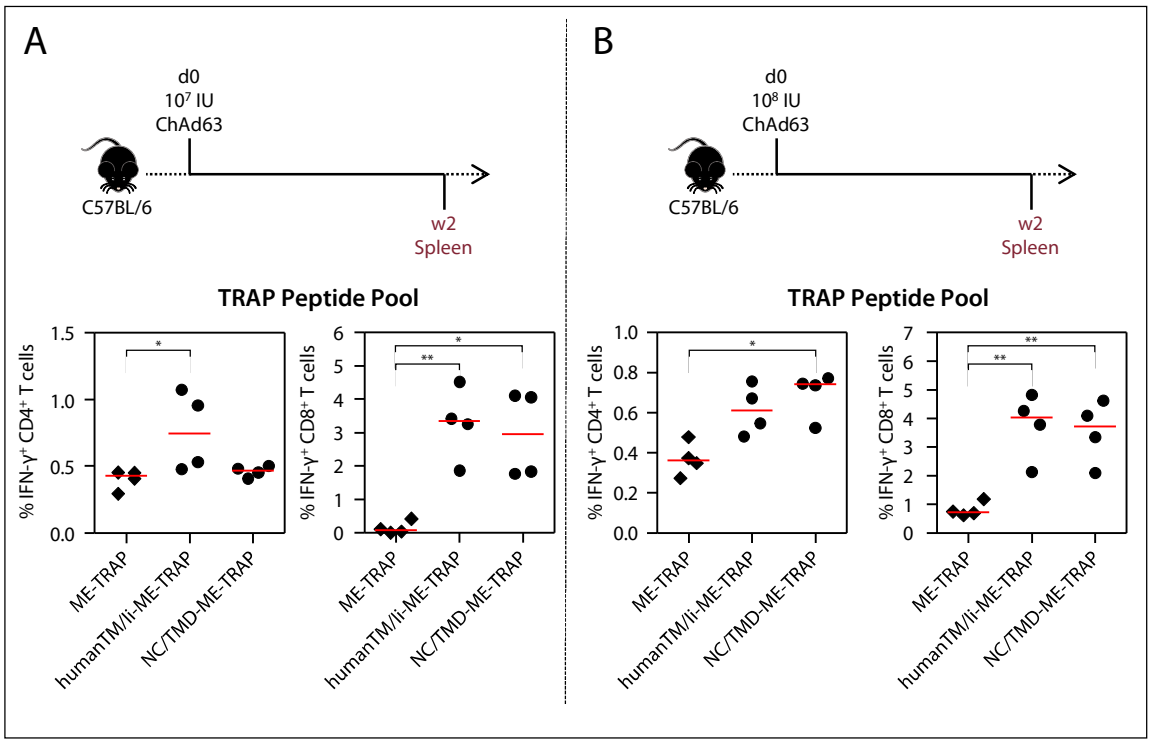



**Figure F-6. Immunogenicity of NC/TMD-ME-TRAP.** C57BL/6 mice were immunised with ChAd63 vectors ($10^7$ IU in A, $10^8$ IU in B) and spleens were harvested two weeks later. T-cell responses to a TRAP peptide pool were analysed by ICS. The percentage of $CD4^+$ and $CD8^+$ T cells positive for IFN-γ are shown. Single points indicate T-cell responses of individual mice and red lines denote the median response per group. Data was analysed with a one-way analysis of variance with Dunn's multiple comparison post-test. Asterisks denote the level of statistical significance when compared to the control group vaccinated with ME-TRAP (*, $p<0.05$; **, $p<0.01$).

## F3 Discussion

Ii adjuvanticity has been demonstrated repeatedly since the 1990s using various vaccine vectors and wide range of target antigens [150, 232, 273–282]. However, uncovering its mechanism of action has been difficult, given the multiple physiological functions of the invariant chain such as involvement in endosomal sorting, MHC class I and II association, or trimerisation (see Chapter D, p. 89). CD74 (Ii on the cell surface) has also been shown to have a role as an accessory-signalling molecule due to its high-affinity binding for the macrophage migration-inhibitory factor, a proinflammatory cytokine [303]. Its accessory role was also identified during T-cell responses through interactions with CD44 [304] and through regulation of B-cell differentiation [305].

In an attempt to understand $CD8^+$ T-cell immunogenicity, Holst et al. have shown that bone marrow derived DC transduced with adenoviruses expressing antigen fused to Ii have the ability to induce increased antigen-specific $CD8^+$ T-cell proliferation compared to vectors encoding non-adjuvanted antigen *in vitro*, without any measurable difference in surface expression of MHC class I or costimulatory molecules [278]. $CD4^+$ T-cell help was also not necessary for these results, suggesting that the increased $CD8^+$ T-cell response is due to a direct effect on transduced DC, leading to more efficient presentation of antigen peptides on MHC class I. In this chapter, A549 cells (human adenocarcinoma epithelial cell line) were transfected with Ii-ME-TRAP constructs and analysed for TRAP expression by immunohistochemistry to determine whether Ii has an impact on intracellular trafficking of the antigen (Figure F-1, p. 152). Indeed, fusion of ME-TRAP to full-length human Ii altered the intercellular localisation of the antigen from being primarily located on the cell surface (ME-TRAP) or being distributed diffusely across the cell (ME-TRAP(w/o_eSP)) to a more perinuclear location ((fl)human/Ii-ME-TRAP). Truncated and xenogenised Ii retained this characteristic expression pattern. However, this effect on intracellular antigen trafficking was reduced when cells were transfected with

humanCT/Ii-ME-TRAP, suggesting that the transmembrane domain of the Ii is essential for this effect. It would be of great interest to further analyse intracellular antigen location by conducting co-localisation experiments of transfected cells and collecting more detailed images using a confocal laser scanning microscope.

Another possible explanation for the adjuvantation effect of Ii when encoded in viral vectors is that many viruses (such as pox viruses) have developed the capability to downregulate Ii expression as part of their immune evasion strategy. In case this downregulation takes place after infection with viral vectors, the presentation of vaccine antigens could therefore be suboptimal. Encoding the Ii as a transgene in viral vectors could then replace the downregulated Ii (as shown in [306]) and contribute to improved antigen presentation. However, it was shown in this thesis, that it is not necessary to encode the full-length Ii as a transgene for a maximum $CD8^+$ T-cell adjuvanticity. Instead, the fusion of the Ii TMD (humanTM/Ii) to the vaccine antigen seems to be sufficient for this effect, suggesting that Ii replacement is not the mechanism of $CD8^+$ T-cell adjuvanticity (Figure D-6, p. 100). On the other hand, highest $CD4^+$ T-cell responses were induced by fusing ME-TRAP to the full-length Ii. A contribution of Ii replacement to the increased $CD4^+$ T-cell immunity therefore cannot be excluded.

As the majority of transduced cells after an intramuscular injection of viral vectors are most likely muscle cells or fibroblasts inside muscle tissue, the *in vivo* adjuvantation effect of Ii might not be caused by a direct effect on antigen processing in DC, but rather by a contribution to improved cross-presentation. To allow effective cross-presentation for T-cell priming, *in vivo* antigen accumulation and stability has shown to be crucial [299, 300]. As oligomers tend to be more stable to proteolysis, it was investigated if antigen trimerisation, caused by fusion to the Ii, contributes to $CD8^+$ T-cell adjuvanticity. This was a plausible explanation, as the TMD of Ii is known to form a trimer, even in the absence of the rest of the Ii protein. Based on the finding of Dixon et al. that mutation of one

particular aa inside the Ii TMD can disrupt trimerisation [301], (tr)human/Ii-ME-TRAP was modified to (tr)humanQ64A/Ii-ME-TRAP. However, when encoded in ChAd63 vectors and analysed in C57BL/6 mice, immunogenicity of this mutated construct was not reduced (Figure F-2, p. 153). A subsequent western blot analysis of lysates from HEK293 cells transfected with plasmids encoding unfused or adjuvanted ME-TRAP suggested that in fact the introduction of the mutation inside the Ii TMD did not have an effect on the tendency of the Ii-ME-TRAP protein to multimerise (Figure F-3, p. 155). Remarkably, dimer formation was still detectable in Ii-ME-TRAP lysates (that encoded the Ii TMD) even after treatment with 2-mercaptoethanol in SDS. On the contrary, unfused ME-TRAP or ME-TRAP fused to humanCT/Ii did not (or showed a largely reduced tendency to) multimerise. As these two constructs also failed to induce high levels of $CD8^+$ T-cell responses in C57BL/6 mice when encoded in ChAd63 vectors, the assumption was made that antigen multimerisation indeed contributes to the $CD8^+$ T-cell adjuvantation effect. The sequence of humanTM/Ii was then systematically mutated to generate variants of humanTM/Ii-ME-TRAP with reduced tendency to multimerise (Figure F-4, p. 156). The most promising candidate was produced in ChAd63 vectors and found to be much less immunogenic compared to unmutated multimerising humanTM/Ii-ME-TRAP (Figure F-5, p. 157).

Considering these data, it was hypothesised that $CD8^+$ T-cell adjuvanticity might be achieved by fusion of the vaccine antigen to any TMD with a strong tendency to multimerise. As the TMD of paramyxoviridae fusion proteins have recently been described to self-associate into trimeric complexes even in the absence of the rest of the protein [302], one representative sequence (the TMD sequence of the Newcastle disease virus fusion protein, named NC/TMD) was fused to ME-TRAP instead of the humanTM/Ii. Western blot analyses showed that this construct had a strong tendency to multimerise, very similar to the TMD of the Ii (humanTM/Ii) (Figure F-4, p. 156).

Strikingly, when NC/TMD-ME-TRAP was encoded in ChAd63 and immunogenicity was investigated in C57BL/6 mice, TRAP-specific $CD8^+$ T-cell responses were as high as those induced by humanTM/Ii-ME-TRAP (Figure F-6, p. 159), suggesting a similarly strong adjuvantation capacity. As this transmembrane domain has been derived from a viral protein, which does not have any closely related eukaryote proteins (as confirmed by a BLAST analysis), NC/TMD avoids the theoretical risk of autoimmunity associated with Ii derived adjuvants (D1.5, p. 96) and therefore warrants further investigations.

The knowledge that multimerising TMD seem to be advantageous for antigen-specific $CD8^+$ T-cell responses when encoded in viral vectors could lead to the discovery of a whole group of novel T-cell adjuvants. Adjuvanticity of the fusion protein TMD of another paramyxoviridae (avian metapneumovirus) as well as the TMD of the influenza A M2 protein, which is known to form a tetramer in the absence of the rest of the M2 protein, will be assessed shortly for confirmation of this hypothesis.

In summary, results described in this chapter provide evidence that the adjuvantation effect of the Ii is largely based on its TMD with its outstanding capability to self-associate into trimers, even in the absence of the rest of the Ii protein. This might lead to increased stability of the Ii-[antigen] to proteolysis when expressed in muscle resident cells after vaccination, thereby increasing the chances for effective cross-presentation in DC to $CD8^+$ T cells. A multimerising TMD derived from another transmembrane protein of non-eukaryote origin (the fusion protein TMD of the Newcastle disease virus), showed a T-cell adjuvantation effect, which was equally strong compared to humanTM/Ii, and a selection of other multimerising TMD adjuvants will be analysed shortly. If the positive adjuvantation results can be confirmed, protein data bases should be screened for more TMD candidates of non-eukaryotic origin. Their sequence could then be fused to ME-TRAP or other T-cell antigens for the development of viral vector vaccines against diseases, which can be protected by cell-mediated immunity. The adjuvants could then be

ranked in terms of their ability to increase antigen-specific immune responses with the best candidate progressing to clinical trials.

# Chapter G

# Concluding Remarks

# G1 Summary of Findings

Despite promising progress in the malaria vaccine field, a malaria vaccine with high-level efficacy that would justify mass deployment is yet to be licensed. The most advanced subunit vaccines in clinical development are RTS,S/AS01, which confers protection by inducing antibodies against CSP, and the ChAd63-MVA prime-boost vaccination regimen encoding ME-TRAP, which induces high levels of TRAP-specific $CD8^+$ T-cell responses targeting the liver-stage of the disease. Compared to WSV approaches (such as RAS, GAS, or ITV), these subunit vaccines do not achieve similarly high levels of efficacy in non-immunes, however, they appear to be better suited for mass deployment, as the use of attenuated whole sporozoites involves significant technical and logistical challenges. Subunit vaccines are easier to produce (by using commercially available and scalable vector platforms), are administered through a standard and easy route of vaccination, intramuscularly, (WSV have to be injected intravenously), and do not rely on storage in liquid nitrogen (which would hamper deployment in rural African areas). It is therefore highly desirable to further develop existing subunit vaccination approaches. One possibility to improve efficacy of subunit vaccines would be the coadministration of RTS,S with ME-TRAP in a combination regimen. This has already been investigated clinically and found to enhance vaccine efficacy to 72% sterile efficacy at six months post challenge [307]. Further clinical trials are under way to confirm these positive results (NCT02252640). Other multi-stage vaccination approaches, possibly including blood-stage and mosquito stage vaccine components, will likely be considered in the future.

Even though the parasite´s genome encodes more than 5,000 proteins, only a few candidate liver-stage malaria antigens other than CSP or ME-TRAP have been tested extensively. As many more parasite antigens are now being identified using modern omics technologies, this knowledge gap might be closed rapidly. In a recent preclinical mouse study, a comparative assessment of viral vectors encoding several novel liver-stage malaria

antigens identified a few very promising candidates [10]. Results of this thesis provide further support for the idea to include novel liver-stage antigens in current subunit vaccination approaches. Mouse experiments were performed to compare immunogenicity and efficacy of ChAd63-MVA prime-boost vaccinations with vectors encoding TRAP, one of four novel antigens (LSA1, LSAP2, UIS3, or Falstatin), or a combination of these antigens. Strikingly, when vectors encoding TRAP were mixed with vectors encoding LSA1, LSAP2, or UIS3 before administration, vaccine efficacy was significantly improved. Two of these combinations (TRAP and LSA1; TRAP and UIS3) induced 100% sterile efficacy against parasite challenge. The combination of LSA1 with LSAP2 also conferred full protection, regardless if vaccine vectors were mixed before administration or injected in separate sites. Furthermore, this combination also showed high levels of efficacy following a ChAd63 prime-only vaccination regimen, suggesting that these two antigens are highly protective. Hence, LSA1 and LSAP2 were considered as promising candidates for a future clinical vaccine.

Immunogenicity and efficacy of viral vectors could also be enhanced by the addition of an adjuvant. Numerous approaches, often using well-known adjuvants, have been explored, but failed. Nonetheless, one approach, the fusion of vaccine antigens to the Ii, was reported to enhance $CD4^+$ and $CD8^+$ T-cell responses to ME-TRAP when encoded in viral vectors and administered in a ChAd63-MVA prime-boost regimen [150]. However, concerns that human Ii expressed in viral vectors could break self-tolerance have stopped its progression to clinical trials. To address these concerns, the Ii was truncated and xenogenised, fused to ME-TRAP, and encoded in ChAd63 vectors to comparatively assess their adjuvanticity in mice. Strikingly, only the TMD of Ii (humanTM/Ii) was needed for the strong $CD8^+$ T-cell adjuvantation effect; the C-terminal end of the Ii was only needed to achieve highest $CD4^+$ adjuvanticity. Furthermore, Ii sequences from various animals

with low sequence homology compared to the human Ii (xenogenisation) also induced enhanced T-cell responses similar to human Ii.

In order to generate most immunogenic and efficacious vaccine candidates, all findings described above were combined in novel vaccine candidates. Fifteen different adjuvanted and non-adjuvanted ChAdOX1 and corresponding MVA vectors were produced, expressing either LSA1, LSAP2, or both antigens (as a LSA1-LSAP2 fusion construct with a peptide linker separating both antigens). ChAdOX1 was preferred to ChAd63, as the Jenner Institute has freedom to operate and possesses intellectual property rights for ChAdOX1. All candidates were then analysed in prime-only and ChAdOX1-MVA prime-boost regimens for immunogenicity and efficacy in inbred (BALB/c and CBA) followed by confirmation in outbred (CD1) mice. BALB/c mice have a defined MHC haplotype, which can lead to protective immunity caused by one immunodominant epitope. On the contrary, CD1 mice with their diverse MHC repertoire are much more representative of the heterogeneous human population. The results provided robust support for the progression of ChAdOX1-sharkTM/Ii-LSA1-LSAP2 and MVA-tPA-LSA1-LSAP2 to clinical assessment, as administration of these vaccines in prime-boost vaccination regimens showed consistently highest levels of protective efficacy in all mouse strains. Furthermore, these high levels of efficacy were achieved with moderate numbers of antigen-specific $CD8^+$ T cells (which are supposedly well-achievable in humans), making these vaccines ideal candidates for GMP production.

Last but not least, the data presented in this thesis provides evidence that Ii adjuvanticity is based on the exceptional capability of its TMD to self-associate into trimers, even in the absence of the rest of the Ii protein. This might lead to increased stability of the Ii-[antigen] protein to proteolysis when expressed in muscle resident cells after vaccination, thereby increasing the chances for effective cross-presentation in DC to $CD8^+$ T cells. On the basis of this finding, the TMD of the Newcastle disease virus fusion

protein (NC/TMD), which has recently been shown to self-aggregate into trimers [302], was assessed as potential molecular adjuvant by fusing it to ME-TRAP in an adenoviral vector. Strikingly, $CD8^+$ T-cell adjuvanticity was similarly high compared to viral vectors encoding the TMD of Ii. Given its derivation is from a viral protein not closely related to eukaryote proteins, NC/TMD avoids the potential risk of autoimmunity associated with Ii derived adjuvants (D1.5, p. 96) and therefore warrants further investigations. Future clinical vaccines could include NC/TMD as a molecular adjuvant, rather than sharkTM/Ii.

# G2 Future Directions

## G2.1 Viral Vectors Encoding LSA1-LSAP2 in Clinical Trials

The Jenner Institute has obtained funding for GMP compliant manufacture and clinical trials with viral vectors encoding LSA1-LSAP2. Based on the results in Chapter E, both ChAdOX1-sharkTM/Ii-LSA1-LSAP2 and MVA-tPA-LSA1-LSAP2 are currently being manufactured to GMP with a phase 1 trial in healthy UK adults planned to commence in 2017, with the primary aim of investigating safety and immunogenicity of both vaccines. This study could be followed by a phase IIa *P. falciparum* challenge study to assess their ability to confer protective efficacy in man.

## G2.2 Sequence Optimisation

Preliminary *in silico* analyses (not shown) of LSA1, LSAP2 and LSA1-LSAP2 constructs suggested that their protein sequence can be improved in future vaccine candidates. For instance, both, LSA1 and LSAP2, have a predicted TMD at their N-terminal end. The LSA1-LSAP2 fusion construct might therefore fold back during expression resulting in one protein on the cytoplasmic side of the ER membrane, and the other on the luminal side. Whether this is detrimental for protein expression remains to be investigated. However, fusion of a TMD-adjuvant (such as sharkTM/Ii or NC/TMD) to the N-terminal end of LSA1, LSAP2, or LSA1-LSAP2, which already encode a TMD at their very N-terminal end, is likely to have an effect on expression efficiency. The addition of a peptide linker between the adjuvant and antigen TMD, allowing the antigen TMD to flip back into the ER membrane might solve this issue. Another, and potentially easier possibility, is to delete the antigen's TMD. Both strategies will be assessed shortly.

## G2.3 Novel Adjuvants

Chapter F provided evidence that the adjuvantation effect conferred by the TMD of Ii is based on its intrinsic drive to self-aggregate into trimers, which might lead to increased Ii-[antigen] stability. Strikingly, fusion of ME-TRAP to a different trimerising TMD (the Newcastle disease virus fusion protein TMD; NC/TMD), showed a similarly high adjuvantation capacity compared to the Ii TMD, suggesting that many other TMD with similar characteristics could serve as potent molecular adjuvants. For example, fusion protein TMD of other members of the family of paramyxoviridae (such as the metapneumovirus) are obvious candidates, but initial screening of protein databases on the literature suggests that many more TMD should be considered. The TMD of influenza M2 proteins, for instance, has been shown to self-aggregate into tetramers even in the absence of the rest of the M2 protein [308]. These TMD sequences (and many more) could be analysed in future experiments to be ranked in terms of their ability to increase antigen-specific immune responses, with the best candidate progressing to clinical trials.

## G2.4 Multi-Stage Vaccination Regimens

It is very likely that an effective subunit malaria vaccine will have to contain targets from multiple stages of the parasite´s life cycle. If the number of parasites exiting the liver is reduced by pre-erythrocytic malaria vaccines, antibody-mediated blood-stage immunity conferred by blood-stage vaccines would have an increased chance to eliminate the remaining parasites. A transmission blocking component would further reduce the malaria burden, even if the multi-stage vaccine failed to protect 100% of the vaccinees. Nonetheless, vaccine candidates of multiple stages should not be pooled randomly, as immunogenicity to each individual component could be affected positively or negatively by the combination of antigenic targets. A first step towards a multi-component vaccine could be the combination of sporozoite vaccines, such as RTS,S, which aim to reduce (if

not eliminate) the number of sporozoites that infect hepatocytes, with a potent liver-stage vaccine that clears the remaining parasites inside infected liver cells by the induction of liver-stage specific $CD8^+$ T cells. Clinical trials to assess the efficacy of RTS,S or R21 (a more recent potentially improved version of RTS,S) in combination with a ChAd63-MVA regimen using vectors expressing ME-TRAP are under way. Future clinical trials should include the novel liver-stage vaccines described in this thesis (ChAdOX1-sharkTM/Ii-LSA1-LSAP2 and MVA-tPA-LSA1-LSAP2), if they are found to be superior to the currently leading ME-TRAP based vaccines in upcoming trials.

## G2.5 Administration Route: Prime-Target Approach

For liver-stage vaccination approaches, a high frequency of hepatic antigen-specific $CD8^+$ T cells is crucial for protection against parasite challenge, as the time window to recognise and kill the few infected hepatocytes is very limited. Recently, a novel vaccine strategy was described aiming to increase liver-stage specific $CD8^+$ T cells specifically in the hepatic tissue (Gola et al., submitted). This has been accomplished in several murine models with multiple different vaccine antigens by priming $CD8^+$ T cells in the periphery by immunisation with adenoviral vectors IM, followed by a secondary vaccination with nanoparticles or viral vectors, including the option of using the same adenoviral vector, given IV to target primed $CD8^+$ T cells to the liver. As vaccine efficacy was vastly improved by this administration regimen, future clinical trials with LSA1-LSAP2 encoding viral vectors should investigate if this can be translated in the clinical setting.

# G3 Final Remarks

The aim of this project was the development of adjuvanted multi-antigen liver-stage vaccines, which will progress to clinical trials. To achieve this, subtasks were identified (the assessment of combinations of liver-stage antigens and the development of a molecular adjuvant for the viral vector platform) and approached individually before merging all findings to make the most promising adjuvanted multi-antigen vectors. The liver-stage antigens LSA1 and LSAP2 were found to induce 100% sterile efficacy in mouse models against parasite challenge when mixed before administration and therefore included in the final vaccine candidate. Furthermore, immunogenicity analyses of adenoviral vectors with a liver-stage antigen fused to several different versions of Ii showed that its TMD alone has the ability to greatly improve antigen-specific $CD8^+$ T-cell responses and Ii xenogenisation can be done without losing adjuvanticity. Based on these results, fifteen novel ChAdOX1 vectors and several corresponding MVA vectors encoding adjuvanted and non-adjuvanted LSA1 and/or LSAP2 were generated and ranked in terms of their immunogenicity and efficacy. The viral vectors of the best combination (ChAdOX1-sharkTM/Ii-LSA1-LSAP2 and MVA-tPA-LSA1-LSAP2) are currently being produced to GMP grade and will progress to initial clinical trials shortly. Therefore, it is now more important than ever to continue to invest time and effort in the preclinical development to optimise these viral vectors and also to find efficacious combinations with subunit vaccines of other stages of the parasite´s life cycle.

# Chapter H

# References

1 WHO, *World malaria report 2015*. World Health Organization, [S.l.] 2016.
2 The RTS,S Clinical Trials Partnership, Efficacy and safety of the RTS,S/AS01 malaria vaccine during 18 months after vaccination: a phase 3 randomized, controlled trial in children and young infants at 11 African sites. *PLoS Med*. 2014. **11**: e1001685.
3 **Moorthy, V. S., Newman, R. D. and Okwo-Bele, J.-M.**, Malaria vaccine technology roadmap. *Lancet*. 2013. **382**: 1700–1701.
4 **Cao, Y., Zhang, D. and Pan, W.**, Construction of transgenic Plasmodium berghei as a model for evaluation of blood-stage vaccine candidate of Plasmodium falciparum chimeric protein 2.9. *PloS one*. 2009. **4**: e6894.
5 **Espinosa, D. A., Yadava, A., Angov, E., Maurizio, P. L., Ockenhouse, C. F. and Zavala, F.**, Development of a chimeric Plasmodium berghei strain expressing the repeat region of the P. vivax circumsporozoite protein for in vivo evaluation of vaccine efficacy. *Infection and immunity*. 2013. **81**: 2882–2887.
6 **Mlambo, G., Maciel, J. and Kumar, N.**, Murine model for assessment of Plasmodium falciparum transmission-blocking vaccine using transgenic Plasmodium berghei parasites expressing the target antigen Pfs25. *Infection and immunity*. 2008. **76**: 2018–2024.
7 **Persson, C., Oliveira, G. A., Sultan, A. A., Bhanot, P., Nussenzweig, V. and Nardin, E.**, Cutting edge: a new tool to evaluate human pre-erythrocytic malaria vaccines: rodent parasites bearing a hybrid Plasmodium falciparum circumsporozoite protein. *Journal of immunology (Baltimore, Md. 1950)*. 2002. **169**: 6681–6685.
8 **Porter, M. D., Nicki, J., Pool, C. D., DeBot, M., Illam, R. M. *et al.*, Dutta, S.**, Transgenic parasites stably expressing full-length Plasmodium falciparum circumsporozoite protein as a model for vaccine down-selection in mice using sterile protection as an endpoint. *Clinical and vaccine immunology CVI*. 2013. **20**: 803–810.
9 **Ramjanee, S., Robertson, J. S., Franke-Fayard, B., Sinha, R., Waters, A. P. *et al.*, Sinden, R. E.**, The use of transgenic Plasmodium berghei expressing the Plasmodium vivax antigen P25 to determine the transmission-blocking activity of sera from malaria vaccine trials. *Vaccine*. 2007. **25**: 886–894.
10 **Longley, R. J., Salman, A. M., Cottingham, M. G., Ewer, K., Janse, C. J. *et al.*,** Hill, Adrian V S, Comparative assessment of vaccine vectors encoding ten malaria antigens identifies two protective liver-stage candidates. *Scientific reports*. 2015. **5**: 11820.
11 **Tavares, J., Formaglio, P., Thiberge, S., Mordelet, E., van Rooijen, N. *et al.*, Amino, R.**, Role of host cell traversal by the malaria sporozoite during liver infection. *The Journal of experimental medicine*. 2013. **210**: 905–915.
12 **Mota, M. M., Pradel, G., Vanderberg, J. P., Hafalla, J. C., Frevert, U. *et al.*, Rodriguez, A.**, Migration of Plasmodium sporozoites through cells before infection. *Science (New York, N.Y.)*. 2001. **291**: 141–144.

13 **Richie, T. L., Billingsley, P. F., Sim, B. K. L., James, E. R., Chakravarty, S. *et al.,* Hoffman, S. L.**, Progress with Plasmodium falciparum sporozoite (PfSPZ)-based malaria vaccines. *Vaccine*. 2015. **33**: 7452–7461.

14 **Sturm, A., Amino, R., van de Sand, C., Regen, T., Retzlaff, S. *et al.,* Heussler, V. T.**, Manipulation of host hepatocytes by the malaria parasite for delivery into liver sinusoids. *Science (New York, N.Y.)*. 2006. **313**: 1287–1290.

15 **Reilly, H. B., Wang, H., Steuter, J. A., Marx, A. M. and Ferdig, M. T.**, Quantitative dissection of clone-specific growth rates in cultured malaria parasites. *International journal for parasitology*. 2007. **37**: 1599–1607.

16 **Hafalla, J. C., Silvie, O. and Matuschewski, K.**, Cell biology and immunology of malaria. *Immunological reviews*. 2011. **240**: 297–316.

17 CDC - Centers for Disease Control and Prevention, CDC - Malaria - About Malaria - Biology. http://www.cdc.gov/malaria/about/biology/. Accessed 14 June 2016.

18 **Koning-Ward, T. F.** de, **Speranca, M. A., Waters, A. P. and Janse, C. J.**, Analysis of stage specificity of promoters in Plasmodium berghei using luciferase as a reporter. *Molecular and biochemical parasitology*. 1999. **100**: 141–146.

19 **Koning-Ward, T. F.** de, **Thomas, A. W., Waters, A. P. and Janse, C. J.**, Stable expression of green fluorescent protein in blood and mosquito stages of Plasmodium berghei. *Molecular and biochemical parasitology*. 1998. **97**: 247–252.

20 **Tewari, R., Spaccapelo, R., Bistoni, F., Holder, A. A. and Crisanti, A.**, Function of region I and II adhesive motifs of Plasmodium falciparum circumsporozoite protein in sporozoite motility and infectivity. *The Journal of biological chemistry*. 2002. **277**: 47613–47618.

21 **Parkin, J. and Cohen, B.**, An overview of the immune system. *Lancet (London, England)*. 2001. **357**: 1777–1789.

22 **Delves, P. J. and Roitt, I. M.**, The immune system. First of two parts. *The New England journal of medicine*. 2000. **343**: 37–49.

23 **Poeggel, G.**, *Kurzlehrbuch Biologie: 9 Tabellen*. Thieme, Stuttgart [u.a.] 2005.

24 **O'Sullivan, T. E., Sun, J. C. and Lanier, L. L.**, Natural Killer Cell Memory. *Immunity*. 2015. **43**: 634–645.

25 **Murphy, K., Travers, P. and Walport, M.,** Janeway, Charles, *Janeway's immunobiology,* 8th edn. Garland Science, New York ©2012.

26 **Halbroth, B. R.**, *Novel Influenza Vaccines and Their Impact on Human Dendritic Cells In Vitro* 2015.

27 **Rink, L., Haase, H. and Kruse, A.**, *Immunologie für Einsteiger,* 2nd edn. Springer Spektrum, Berlin [u.a.] 2015.

28 **Sallusto, F., Geginat, J. and Lanzavecchia, A.**, Central memory and effector memory T cell subsets: function, generation, and maintenance. *Annual review of immunology*. 2004. **22**: 745–763.

29 **Gupta, S., Snow, R. W., Donnelly, C. A., Marsh, K. and Newbold, C.**, Immunity to non-cerebral severe malaria is acquired after one or two infections. *Nature medicine*. 1999. **5**: 340–343.

30 **Owusu-Agyei, S., Koram, K. A., Baird, J. K., Utz, G. C., Binka, F. N. *et al.,* Hoffman, S. L.**, Incidence of symptomatic and asymptomatic Plasmodium falciparum infection following curative therapy in adult residents of northern Ghana. *The American journal of tropical medicine and hygiene*. 2001. **65**: 197–203.
31 **Baird, J. K., Masbar, S., Basri, H., Tirtokusumo, S., Subianto, B. and Hoffman, S. L.**, Age-dependent susceptibility to severe disease with primary exposure to Plasmodium falciparum. *The Journal of infectious diseases*. 1998. **178**: 592–595.
32 **Okell, L. C., Ghani, A. C., Lyons, E. and Drakeley, C. J.**, Submicroscopic infection in Plasmodium falciparum-endemic populations: a systematic review and meta-analysis. *The Journal of infectious diseases*. 2009. **200**: 1509–1517.
33 **Finney, O. C., Riley, E. M. and Walther, M.**, Regulatory T cells in malaria - friend or foe? *Trends in immunology*. 2010. **31**: 63–70.
34 **Hansen, D. S. and Schofield, L.**, Natural regulatory T cells in malaria: host or parasite allies? *PLoS pathogens*. 2010. **6**: e1000771.
35 **Riley, E. M., Wahl, S., Perkins, D. J. and Schofield, L.**, Regulating immunity to malaria. *Parasite immunology*. 2006. **28**: 35–49.
36 **Liehl, P. and Mota, M. M.**, Innate recognition of malarial parasites by mammalian hosts. *International journal for parasitology*. 2012. **42**: 557–566.
37 **Riley, E. M. and Stewart, V. A.**, Immune mechanisms in malaria: new insights in vaccine development. *Nature medicine*. 2013. **19**: 168–178.
38 **Longley, R. J.**, *Liver-Stage Vaccines for Malaria* 2013.
39 **Sidjanski, S. and Vanderberg, J. P.**, Delayed migration of Plasmodium sporozoites from the mosquito bite site to the blood. *The American journal of tropical medicine and hygiene*. 1997. **57**: 426–429.
40 **Yamauchi, L. M., Coppi, A., Snounou, G. and Sinnis, P.**, Plasmodium sporozoites trickle out of the injection site. *Cell Microbiol*. 2007. **9**: 1215–1222.
41 **Usynin, I., Klotz, C. and Frevert, U.**, Malaria circumsporozoite protein inhibits the respiratory burst in Kupffer cells. *Cellular microbiology*. 2007. **9**: 2610–2628.
42 **Epiphanio, S., Mikolajczak, S. A., Goncalves, L. A., Pamplona, A., Portugal, S. *et al.,* Mota, M. M.**, Heme oxygenase-1 is an anti-inflammatory host factor that promotes murine plasmodium liver infection. *Cell host & microbe*. 2008. **3**: 331–338.
43 **Singh, A. P., Buscaglia, C. A., Wang, Q., Levay, A., Nussenzweig, D. R. *et al.,* Nussenzweig, V.**, Plasmodium circumsporozoite protein promotes the development of the liver stages of the parasite. *Cell*. 2007. **131**: 492–504.
44 **Amino, R., Thiberge, S., Martin, B., Celli, S., Shorte, S. *et al.,* Menard, R.**, Quantitative imaging of Plasmodium transmission from mosquito to mammal. *Nat Med*. 2006. **12**: 220–224.
45 **Khan, Z. M. and Vanderberg, J. P.**, Role of host cellular response in differential susceptibility of nonimmunized BALB/c mice to Plasmodium berghei and Plasmodium yoelii sporozoites. *Infection and immunity*. 1991. **59**: 2529–2534.
46 **van de Sand, C., Horstmann, S., Schmidt, A., Sturm, A., Bolte, S. *et al.,* Heussler, V. T.**, The liver stage of Plasmodium berghei inhibits host cell apoptosis. *Molecular microbiology*. 2005. **58**: 731–742.

47 **Khan, Z. M., Ng, C. and Vanderberg, J. P.**, Early hepatic stages of Plasmodium berghei: release of circumsporozoite protein and host cellular inflammatory response. *Infection and immunity*. 1992. **60**: 264–270.

48 **Scheller, L. F., Wirtz, R. A. and Azad, A. F.**, Susceptibility of different strains of mice to hepatic infection with Plasmodium berghei. *Infection and immunity*. 1994. **62**: 4844–4847.

49 **Ockenhouse, C. F., Hu, W.-c., Kester, K. E., Cummings, J. F., Stewart, A. *et al.*, Burke, D. S.**, Common and divergent immune response signaling pathways discovered in peripheral blood mononuclear cell gene expression patterns in presymptomatic and clinically apparent malaria. *Infection and immunity*. 2006. **74**: 5561–5573.

50 **Walther, M., Woodruff, J., Edele, F., Jeffries, D., Tongren, J. E. *et al.*, Riley, E. M.**, Innate immune responses to human malaria: heterogeneous cytokine responses to blood-stage Plasmodium falciparum correlate with parasitological and clinical outcomes. *J Immunol*. 2006. **177**: 5736–5745.

51 **Gazzinelli, R. T. and Denkers, E. Y.**, Protozoan encounters with Toll-like receptor signalling pathways: implications for host parasitism. *Nature reviews. Immunology*. 2006. **6**: 895–906.

52 **Krishnegowda, G., Hajjar, A. M., Zhu, J., Douglass, E. J., Uematsu, S. *et al.*, Gowda, D. C.**, Induction of proinflammatory responses in macrophages by the glycosylphosphatidylinositols of Plasmodium falciparum: cell signaling receptors, glycosylphosphatidylinositol (GPI) structural requirement, and regulation of GPI activity. *The Journal of biological chemistry*. 2005. **280**: 8606–8616.

53 **Coban, C., Ishii, K. J., Kawai, T., Hemmi, H., Sato, S. *et al.*, Akira, S.**, Toll-like receptor 9 mediates innate immune activation by the malaria pigment hemozoin. *The Journal of experimental medicine*. 2005. **201**: 19–25.

54 **Zhu, J., Krishnegowda, G. and Gowda, D. C.**, Induction of proinflammatory responses in macrophages by the glycosylphosphatidylinositols of Plasmodium falciparum: the requirement of extracellular signal-regulated kinase, p38, c-Jun N-terminal kinase and NF-kappaB pathways for the expression of proinflammatory cytokines and nitric oxide. *The Journal of biological chemistry*. 2005. **280**: 8617–8627.

55 **Parroche, P., Lauw, F. N., Goutagny, N., Latz, E., Monks, B. G. *et al.*, Golenbock, D. T.**, Malaria hemozoin is immunologically inert but radically enhances innate responses by presenting malaria DNA to Toll-like receptor 9. *Proceedings of the National Academy of Sciences of the United States of America*. 2007. **104**: 1919–1924.

56 **Jenne, C. N. and Kubes, P.**, Immune surveillance by the liver. *Nature immunology*. 2013. **14**: 996–1006.

57 **Klein, I. and Crispe, I. N.**, Complete differentiation of CD8+ T cells activated locally within the transplanted liver. *The Journal of experimental medicine*. 2006. **203**: 437–447.

58 **Winau, F., Hegasy, G., Weiskirchen, R., Weber, S., Cassan, C. *et al.,* Kaufmann, S. H. E.**, Ito cells are liver-resident antigen-presenting cells for activating T cell responses. *Immunity*. 2007. **26**: 117–129.

59 **Portugal, S., Carret, C., Recker, M., Armitage, A. E., Goncalves, L. A. *et al.,* Mota, M. M.**, Host-mediated regulation of superinfection in malaria. *Nature medicine*. 2011. **17**: 732–737.

60 **Vaughan, A. M. and Kappe, S. H. I.**, Malaria vaccine development: persistent challenges. *Curr Opin Immunol*. 2012. **24**: 324–331.

61 **John, C. C., Sumba, P. O., Ouma, J. H., Nahlen, B. L., King, C. L. and Kazura, J. W.**, Cytokine responses to Plasmodium falciparum liver-stage antigen 1 vary in rainy and dry seasons in highland Kenya. *Infection and immunity*. 2000. **68**: 5198–5204.

62 **Kurtis, J. D., Lanar, D. E., Opollo, M. and Duffy, P. E.**, Interleukin-10 responses to liver-stage antigen 1 predict human resistance to Plasmodium falciparum. *Infection and immunity*. 1999. **67**: 3424–3429.

63 **Luty, A. J., Lell, B., Schmidt-Ott, R., Lehman, L. G., Luckner, D. *et al.,* Kremsner, P. G.**, Parasite antigen-specific interleukin-10 and antibody reponses predict accelerated parasite clearance in Plasmodium falciparum malaria. *European cytokine network*. 1998. **9**: 639–646.

64 **Migot-Nabias, F., Deloron, P., Ringwald, P., Dubois, B., Mayombo, J. *et al.,* Luty, A.**, Immune response to Plasmodium falciparum liver stage antigen-1: geographical variations within Central Africa and their relationship with protection from clinical malaria. *Transactions of the Royal Society of Tropical Medicine and Hygiene*. 2000. **94**: 557–562.

65 **Todryk, S. M., Bejon, P., Mwangi, T., Plebanski, M., Urban, B. *et al.,* Flanagan, K. L.**, Correlation of memory T cell responses against TRAP with protection from clinical malaria, and CD4 CD25 high T cells with susceptibility in Kenyans. *PloS one*. 2008. **3**: e2027.

66 **Reece, W. H. H., Pinder, M., Gothard, P. K., Milligan, P., Bojang, K. *et al.,* Hill, A. V. S.**, A CD4(+) T-cell immune response to a conserved epitope in the circumsporozoite protein correlates with protection from natural Plasmodium falciparum infection and disease. *Nature medicine*. 2004. **10**: 406–410.

67 **Warren, A., Le Couteur, D. G., Fraser, R., Bowen, D. G., McCaughan, G. W. and Bertolino, P.**, T lymphocytes interact with hepatocytes through fenestrations in murine liver sinusoidal endothelial cells. *Hepatology (Baltimore, Md.)*. 2006. **44**: 1182–1190.

68 **Weiss, W. R., Mellouk, S., Houghten, R. A., Sedegah, M., Kumar, S. *et al.,* Hoffman, S. L.**, Cytotoxic T cells recognize a peptide from the circumsporozoite protein on malaria-infected hepatocytes. *The Journal of experimental medicine*. 1990. **171**: 763–773.

69 **Hoffman, S. L., Isenbarger, D., Long, G. W., Sedegah, M., Szarfman, A. *et al.,* Ballou, W. R.**, Sporozoite vaccine induces genetically restricted T cell elimination of malaria from hepatocytes. *Science (New York, N.Y.)*. 1989. **244**: 1078–1081.

70 **Renia, L., Grillot, D., Marussig, M., Corradin, G., Miltgen, F. *et al.,* Del Giudice, G.**, Effector functions of circumsporozoite peptide-primed CD4+ T cell clones against Plasmodium yoelii liver stages. *Journal of immunology (Baltimore, Md. 1950)*. 1993. **150**: 1471–1478.

71 **Renia, L., Marussig, M. S., Grillot, D., Pied, S., Corradin, G. *et al.,* Mazier, D.**, In vitro activity of CD4+ and CD8+ T lymphocytes from mice immunized with a synthetic malaria peptide. *Proceedings of the National Academy of Sciences of the United States of America*. 1991. **88**: 7963–7967.

72 **Trimnell, A., Takagi, A., Gupta, M., Richie, T. L., Kappe, S. H. and Wang, R.**, Genetically attenuated parasite vaccines induce contact-dependent CD8+ T cell killing of Plasmodium yoelii liver stage-infected hepatocytes. *Journal of immunology (Baltimore, Md. 1950)*. 2009. **183**: 5870–5878.

73 **Balam, S., Romero, J. F., Bongfen, S. E., Guillaume, P. and Corradin, G.**, CSP - a model for in vivo presentation of Plasmodium berghei sporozoite antigens by hepatocytes. *PloS one*. 2012. **7**: e51875.

74 **Leiriao, P., Mota, M. M. and Rodriguez, A.**, Apoptotic Plasmodium-infected hepatocytes provide antigens to liver dendritic cells. *The Journal of infectious diseases*. 2005. **191**: 1576–1581.

75 **Parker, G. A. and Picut, C. A.**, Liver immunobiology. *Toxicologic pathology*. 2005. **33**: 52–62.

76 **Elloso, M. M.,** van der Heyde, H C, **vande Waa, J. A., Manning, D. D. and Weidanz, W. P.**, Inhibition of Plasmodium falciparum in vitro by human gamma delta T cells. *Journal of immunology (Baltimore, Md. 1950)*. 1994. **153**: 1187–1194.

77 **Pombo, D. J., Lawrence, G., Hirunpetcharat, C., Rzepczyk, C., Bryden, M. *et al.,* Good, M. F.**, Immunity to malaria after administration of ultra-low doses of red cells infected with Plasmodium falciparum. *Lancet*. 2002. **360**: 610–617.

78 **Carvalho, L. H., Fontes, C. J. and Krettli, A. U.**, Cellular responses to Plasmodium falciparum major surface antigens and their relationship to human activities associated with malaria transmission. *The American journal of tropical medicine and hygiene*. 1999. **60**: 674–679.

79 **Riley, E. M., Allen, S. J., Wheeler, J. G., Blackman, M. J., Bennett, S. *et al.,* Greenwood, B. M.**, Naturally acquired cellular and humoral immune responses to the major merozoite surface antigen (PfMSP1) of Plasmodium falciparum are associated with reduced malaria morbidity. *Parasite immunology*. 1992. **14**: 321–337.

80 **Cohen, S., McGregor, I. A. and Carrington, S.**, Gamma-globulin and acquired immunity to human malaria. *Nature*. 1961. **192**: 733–737.

81 **Wipasa, J., Suphavilai, C., Okell, L. C., Cook, J., Corran, P. H. *et al.,* Hafalla, J. C. R.**, Long-lived antibody and B Cell memory responses to the human malaria parasites, Plasmodium falciparum and Plasmodium vivax. *PLoS pathogens*. 2010. **6**: e1000770.

82 **Sabchareon, A., Burnouf, T., Ouattara, D., Attanath, P., Bouharoun-Tayoun, H. *et al.,* Druilhe, P.**, Parasitologic and clinical human response to immunoglobulin

administration in falciparum malaria. *The American journal of tropical medicine and hygiene*. 1991. **45**: 297–308.

83 **Astagneau, P., Chougnet, C., Lepers, J. P., Danielle, M., Andriamangatiana-Rason, M. D. and Deloron, P.**, Antibodies to the 4-mer repeat of the ring-infected erythrocyte surface antigen (Pf155/RESA) protect against Plasmodium falciparum malaria. *International journal of epidemiology*. 1994. **23**: 169–175.

84 **Astagneau, P., Roberts, J. M., Steketee, R. W., Wirima, J. J., Lepers, J. P. and Deloron, P.**, Antibodies to a Plasmodium falciparum blood-stage antigen as a tool for predicting the protection levels of two malaria-exposed populations. *The American journal of tropical medicine and hygiene*. 1995. **53**: 23–28.

85 **Astagneau, P., Steketee, R. W., Wirima, J. J., Khoromana, C. O. and Millet, P.**, Antibodies to ring-infected erythrocyte surface antigen (Pf155/RESA) protect against P. falciparum parasitemia in highly exposed multigravidas women in Malawi. *Acta tropica*. 1994. **57**: 317–325.

86 **Bull, P. C., Lowe, B. S., Kortok, M., Molyneux, C. S., Newbold, C. I. and Marsh, K.**, Parasite antigens on the infected red cell surface are targets for naturally acquired immunity to malaria. *Nature medicine*. 1998. **4**: 358–360.

87 **Chizzolini, C., Dupont, A., Akue, J. P., Kaufmann, M. H., Verdini, A. S. *et al.*, Del Giudice, G.**, Natural antibodies against three distinct and defined antigens of Plasmodium falciparum in residents of a mesoendemic area in Gabon. *The American journal of tropical medicine and hygiene*. 1988. **39**: 150–156.

88 **Crompton, P. D., Kayala, M. A., Traore, B., Kayentao, K., Ongoiba, A. *et al.*, Pierce, S. K.**, A prospective analysis of the Ab response to Plasmodium falciparum before and after a malaria season by protein microarray. *Proceedings of the National Academy of Sciences of the United States of America*. 2010. **107**: 6958–6963.

89 **Marsh, K. and Kinyanjui, S.**, Immune effector mechanisms in malaria. *Parasite immunology*. 2006. **28**: 51–60.

90 **Polley, S. D., Mwangi, T., Kocken, C. H. M., Thomas, A. W., Dutta, S. *et al.*, Marsh, K.**, Human antibodies to recombinant protein constructs of Plasmodium falciparum Apical Membrane Antigen 1 (AMA1) and their associations with protection from malaria. *Vaccine*. 2004. **23**: 718–728.

91 **Schwartz, L., Brown, G. V., Genton, B. and Moorthy, V. S.**, A review of malaria vaccine clinical projects based on the WHO rainbow table. *Malaria journal*. 2012. **11**: 11.

92 **John, C. C., Tande, A. J., Moormann, A. M., Sumba, P. O., Lanar, D. E. *et al.*, Kazura, J. W.**, Antibodies to pre-erythrocytic Plasmodium falciparum antigens and risk of clinical malaria in Kenyan children. *The Journal of infectious diseases*. 2008. **197**: 519–526.

93 **Alger, N. E. and Harant, J.**, Plasmodium berghei: heat-treated sporozoite vaccination of mice. *Exp Parasitol*. 1976. **40**: 261–268.

94 **Nussenzweig, R. S., Vanderberg, J. P., Most, H. and Orton, C. G.**, Protective immunity produced by the injection of x-irradiated sporozoites of plasmodium berghei. *Nature*. 1967. **216**: 160–162.

95 **Clyde, D. F., Most, H., McCarthy, V. C. and Vanderberg, J. P.**, Immunization of man against sporozoite-induced falciparum malaria. *Am J Med Sci*. 1973. **266**: 169–177.

96 **Rieckmann, K. H., Beaudoin, R. L., Cassells, J. S. and Sell, K. W.**, Use of attenuated sporozoites in the immunization of human volunteers against falciparum malaria. *Bull World Health Organ*. 1979. **57 Suppl 1**: 261–265.

97 **Hoffman, S. L., Billingsley, P. F., James, E., Richman, A., Loyevsky, M. *et al.,*** Sim, B Kim Lee, Development of a metabolically active, non-replicating sporozoite vaccine to prevent Plasmodium falciparum malaria. *Hum Vaccin*. 2010. **6**: 97–106.

98 **Epstein, J. E., Tewari, K., Lyke, K. E., Sim, B. K. L., Billingsley, P. F. *et al.,* Hoffman, S. L.**, Live attenuated malaria vaccine designed to protect through hepatic $CD8^+$ T cell immunity. *Science*. 2011. **334**: 475–480.

99 **Seder, R. A., Chang, L.-J., Enama, M. E., Zephir, K. L., Sarwar, U. N. *et al.,* Hoffman, S. L.**, Protection against malaria by intravenous immunization with a nonreplicating sporozoite vaccine. *Science*. 2013. **341**: 1359–1365.

100 **Halbroth, B. R. and Draper, S. J.**, Recent developments in malaria vaccinology. *Advances in parasitology*. 2015. **88**: 1–49.

101 **Doll, K. L. and Harty, J. T.**, Correlates of protective immunity following whole sporozoite vaccination against malaria. *Immunol Res*. 2014. **59**: 166–176.

102 **Mueller, A.-K., Labaied, M., Kappe, S. H. I. and Matuschewski, K.**, Genetically modified Plasmodium parasites as a protective experimental malaria vaccine. *Nature*. 2005. **433**: 164–167.

103 **van Dijk, M. R., Douradinha, B., Franke-Fayard, B., Heussler, V., Janse, C. J. *et al.,* Waters, A. P.**, Genetically attenuated, P36p-deficient malarial sporozoites induce protective immunity and apoptosis of infected liver cells. *Proc Natl Acad Sci U S A*. 2005. **102**: 12194–12199.

104 **Khan, S. M., Janse, C. J., Kappe, S. H. I. and Mikolajczak, S. A.**, Genetic engineering of attenuated malaria parasites for vaccination. *Curr Opin Biotechnol*. 2012. **23**: 908–916.

105 **Labaied, M., Harupa, A., Dumpit, R. F., Coppens, I., Mikolajczak, S. A. and Kappe, S. H. I.**, Plasmodium yoelii sporozoites with simultaneous deletion of P52 and P36 are completely attenuated and confer sterile immunity against infection. *Infect Immun*. 2007. **75**: 3758–3768.

106 **Butler, N. S., Schmidt, N. W., Vaughan, A. M., Aly, A. S., Kappe, S. H. I. and Harty, J. T.**, Superior antimalarial immunity after vaccination with late liver stage-arresting genetically attenuated parasites. *Cell Host Microbe*. 2011. **9**: 451–462.

107 **Spring, M., Murphy, J., Nielsen, R., Dowler, M., Bennett, J. W. *et al.,* Kappe, S. H. I.**, First-in-human evaluation of genetically attenuated Plasmodium falciparum sporozoites administered by bite of Anopheles mosquitoes to adult volunteers. *Vaccine*. 2013. **31**: 4975–4983.

108 **Finney, O. C., Keitany, G. J., Smithers, H., Kaushansky, A., Kappe, S. H. I. and Wang, R.**, Immunization with genetically attenuated P. falciparum parasites induces

long-lived antibodies that efficiently block hepatocyte invasion by sporozoites. *Vaccine*. 2014. **32**: 2135–2138.

109 **Mikolajczak, S. A., Lakshmanan, V., Fishbaugher, M., Camargo, N., Harupa, A. *et al.,* Kappe, S. H. I.**, A Next-generation Genetically Attenuated Plasmodium falciparum Parasite Created by Triple Gene Deletion. *Mol Ther*. 2014. **22**: 1707–1715.

110 **Davie, B.**, MalarVx - News Page. http://malarvx.com/ct-menu-item-14. Accessed 16 June 2016.

111 **Belnoue, E., Costa, F. T. M., Frankenberg, T., Vigario, A. M., Voza, T. *et al.,* Renia, L.**, Protective T cell immunity against malaria liver stage after vaccination with live sporozoites under chloroquine treatment. *J Immunol*. 2004. **172**: 2487–2495.

112 **Roestenberg, M., McCall, M., Hopman, J., Wiersma, J., Luty, A. J. F. *et al.,* Sauerwein, R.**, Protection against a malaria challenge by sporozoite inoculation. *N Engl J Med*. 2009. **361**: 468–477.

113 **Bijker, E. M., Schats, R., Obiero, J. M., Behet, M. C., van Gemert, G.-J. *et al.,* Sauerwein, R. W.**, Sporozoite Immunization of Human Volunteers under Mefloquine Prophylaxis Is Safe, Immunogenic and Protective: A Double-Blind Randomized Controlled Clinical Trial. *PLoS One*. 2014. **9**: e112910.

114 **Friesen, J., Silvie, O., Putrianti, E. D., Hafalla, J. C. R., Matuschewski, K. and Borrmann, S.**, Natural immunization against malaria: causal prophylaxis with antibiotics. *Sci Transl Med*. 2010. **2**: 40.

115 **Pfeil, J., Sepp, K. J., Heiss, K., Meister, M., Mueller, A.-K. and Borrmann, S.**, Protection against malaria by immunization with non-attenuated sporozoites under single-dose piperaquine-tetraphosphate chemoprophylaxis. *Vaccine*. 2014. **32**: 6005–6011.

116 **Cohen, J., Nussenzweig, V., Nussenzweig, R., Vekemans, J. and Leach, A.**, From the circumsporozoite protein to the RTS, S/AS candidate vaccine. *Hum Vaccin*. 2010. **6**: 90–96.

117 **Stewart, V. A., McGrath, S. M., Walsh, D. S., Davis, S., Hess, A. S. *et al.,*** Heppner, D Gray Jr, Pre-clinical evaluation of new adjuvant formulations to improve the immunogenicity of the malaria vaccine RTS,S/AS02A. *Vaccine*. 2006. **24**: 6483–6492.

118 **Stewart, V. A., Walsh, D. S., McGrath, S. M., Kester, K. E., Cummings, J. F. *et al.,*** Heppner, D Gray Jr, Cutaneous delayed-type hypersensitivity (DTH) in a multi-formulation comparator trial of the anti-falciparum malaria vaccine candidate RTS,S in rhesus macaques. *Vaccine*. 2006. **24**: 6493–6502.

119 **Mettens, P., Dubois, P. M., Demoitie, M.-A., Bayat, B., Donner, M.-N. *et al.,* Cohen, J.**, Improved T cell responses to Plasmodium falciparum circumsporozoite protein in mice and monkeys induced by a novel formulation of RTS,S vaccine antigen. *Vaccine*. 2008. **26**: 1072–1082.

120 **Kester, K. E., Cummings, J. F., Ofori-Anyinam, O., Ockenhouse, C. F., Krzych, U. *et al.,*** Heppner, D Gray Jr, Randomized, double-blind, phase 2a trial of

falciparum malaria vaccines RTS,S/AS01B and RTS,S/AS02A in malaria-naive adults: safety, efficacy, and immunologic associates of protection. *J Infect Dis*. 2009. **200**: 337–346.

121 **Agnandji, S. T., Lell, B., Soulanoudjingar, S. S., Fernandes, J. F., Abossolo, B. P. *et al.,* Vansadia, P.**, First results of phase 3 trial of RTS,S/AS01 malaria vaccine in African children. *N Engl J Med*. 2011. **365**: 1863–1875.

122 **Agnandji, S. T., Lell, B., Fernandes, J. F., Abossolo, B. P., Methogo, B. G. N. O. *et al.,* Vansadia, P.**, A phase 3 trial of RTS,S/AS01 malaria vaccine in African infants. *N Engl J Med*. 2012. **367**: 2284–2295.

123 RTS,S Clinical Trials Partnership, Efficacy and safety of RTS,S/AS01 malaria vaccine with or without a booster dose in infants and children in Africa: final results of a phase 3, individually randomised, controlled trial. *Lancet (London, England)*. 2015. **386**: 31–45.

124 **Enosse, S., Dobano, C., Quelhas, D., Aponte, J. J., Lievens, M. *et al.,* Sutherland, C. J.**, RTS,S/AS02A malaria vaccine does not induce parasite CSP T cell epitope selection and reduces multiplicity of infection. *PLoS Clin Trials*. 2006. **1**: e5.

125 European Medicines Agency, First malaria vaccine receives positive scientific opinion from EMA. http://www.ema.europa.eu/ema/index.jsp?curl=pages/news_and_events/news/2015/07/news_detail_002376.jsp&mid=WC0b01ac058004d5c1. Accessed 16 June 2016.

126 **Schmidt, N. W., Butler, N. S., Badovinac, V. P. and Harty, J. T.**, Extreme CD8 T cell requirements for anti-malarial liver-stage immunity following immunization with radiation attenuated sporozoites. *PLoS Pathog*. 2010. **6**: e1000998.

127 **Weiss, W. R. and Jiang, C. G.**, Protective CD8+ T lymphocytes in primates immunized with malaria sporozoites. *PLoS One*. 2012. **7**: e31247.

128 **Moorthy, V. S. and Ballou, W. R.**, Immunological mechanisms underlying protection mediated by RTS,S: a review of the available data. *Malar J*. 2009. **8**: 312.

129 **Foquet, L., Hermsen, C. C., van Gemert, G.-J., van Braeckel, E., Weening, K. E. *et al.,* Leroux-Roels, G.**, Vaccine-induced monoclonal antibodies targeting circumsporozoite protein prevent Plasmodium falciparum infection. *J Clin Invest*. 2014. **124**: 140–144.

130 **Flanagan, K. L., Plebanski, M., Akinwunmi, P., Lee, E. A., Reece, W. H. *et al.,* Pinder, M.**, Broadly distributed T cell reactivity, with no immunodominant loci, to the pre-erythrocytic antigen thrombospondin-related adhesive protein of Plasmodium falciparum in West Africans. *Eur J Immunol*. 1999. **29**: 1943–1954.

131 **Moorthy, V. and Hill, A. V. S.**, Malaria vaccines. *Br Med Bull*. 2002. **62**: 59–72.

132 **Bodescot, M., Silvie, O., Siau, A., Refour, P., Pino, P. *et al.,* Mazier, D.**, Transcription status of vaccine candidate genes of Plasmodium falciparum during the hepatic phase of its life cycle. *Parasitol Res*. 2004. **92**: 449–452.

133 **Gilbert, S. C., Plebanski, M., Harris, S. J., Allsopp, C. E., Thomas, R. *et al.,* Hill, A. V. S.**, A protein particle vaccine containing multiple malaria epitopes. *Nat Biotechnol*. 1997. **15**: 1280–1284.

134 **Robson, K. J., Hall, J. R., Jennings, M. W., Harris, T. J., Marsh, K. *et al.*, Weatherall, D. J.**, A highly conserved amino-acid sequence in thrombospondin, properdin and in proteins from sporozoites and blood stages of a human malaria parasite. *Nature*. 1988. **335**: 79–82.

135 **Schneider, J., Gilbert, S. C., Blanchard, T. J., Hanke, T., Robson, K. J. *et al.*, Hill, A. V. S.**, Enhanced immunogenicity for CD8+ T cell induction and complete protective efficacy of malaria DNA vaccination by boosting with modified vaccinia virus Ankara. *Nat Med*. 1998. **4**: 397–402.

136 **McConkey, S. J., Reece, W. H. H., Moorthy, V. S., Webster, D., Dunachie, S. *et al.*, Hill, A. V. S.**, Enhanced T-cell immunogenicity of plasmid DNA vaccines boosted by recombinant modified vaccinia virus Ankara in humans. *Nat Med*. 2003. **9**: 729–735.

137 **Webster, D. P., Dunachie, S., Vuola, J. M., Berthoud, T., Keating, S. *et al.*, Hill, A. V. S.**, Enhanced T cell-mediated protection against malaria in human challenges by using the recombinant poxviruses FP9 and modified vaccinia virus Ankara. *Proc Natl Acad Sci U S A*. 2005. **102**: 4836–4841.

138 **Anderson, R. J., Hannan, C. M., Gilbert, S. C., Laidlaw, S. M., Sheu, E. G. *et al.*, Hill, A. V. S.**, Enhanced CD8+ T cell immune responses and protection elicited against Plasmodium berghei malaria by prime boost immunization regimens using a novel attenuated fowlpox virus. *J Immunol*. 2004. **172**: 3094–3100.

139 **Bejon, P., Mwacharo, J., Kai, O., Mwangi, T., Milligan, P. *et al.*, Hill, A. V. S.**, A phase 2b randomised trial of the candidate malaria vaccines FP9 ME-TRAP and MVA ME-TRAP among children in Kenya. *PLoS Clin Trials*. 2006. **1**: e29.

140 **Bejon, P., Ogada, E., Mwangi, T., Milligan, P., Lang, T. *et al.*, Hill, A. V. S.**, Extended follow-up following a phase 2b randomized trial of the candidate malaria vaccines FP9 ME-TRAP and MVA ME-TRAP among children in Kenya. *PLoS One*. 2007. **2**: e707.

141 **Rodrigues, E. G., Claassen, J., Lee, S., Wilson, J. M., Nussenzweig, R. S. and Tsuji, M.**, Interferon-gamma-independent CD8+ T cell-mediated protective anti-malaria immunity elicited by recombinant adenovirus. *Parasite Immunol*. 2000. **22**: 157–160.

142 **Gilbert, S. C., Schneider, J., Hannan, C. M., Hu, J. T., Plebanski, M. *et al.*, Hill, A. V. S.**, Enhanced CD8 T cell immunogenicity and protective efficacy in a mouse malaria model using a recombinant adenoviral vaccine in heterologous prime-boost immunisation regimes. *Vaccine*. 2002. **20**: 1039–1045.

143 **Sridhar, S., Reyes-Sandoval, A., Draper, S. J., Moore, A. C., Gilbert, S. C. *et al.*, Hill, A. V. S.**, Single-dose protection against Plasmodium berghei by a simian adenovirus vector using a human cytomegalovirus promoter containing intron A. *J Virol*. 2008. **82**: 3822–3833.

144 **Reyes-Sandoval, A., Sridhar, S., Berthoud, T., Moore, A. C., Harty, J. T. *et al.*, Hill, A. V. S.**, Single-dose immunogenicity and protective efficacy of simian adenoviral vectors against Plasmodium berghei. *Eur J Immunol*. 2008. **38**: 732–741.

145 **Reyes-Sandoval, A., Berthoud, T., Alder, N., Siani, L., Gilbert, S. C. *et al.,* Hill, A. V. S.**, Prime-boost immunization with adenoviral and modified vaccinia virus Ankara vectors enhances the durability and polyfunctionality of protective malaria CD8+ T-cell responses. *Infect Immun*. 2010. **78**: 145–153.

146 **Capone, S., Reyes-Sandoval, A., Naddeo, M., Siani, L., Ammendola, V. *et al.,* Hill, A. V. S.**, Immune responses against a liver-stage malaria antigen induced by simian adenoviral vector AdCh63 and MVA prime-boost immunisation in non-human primates. *Vaccine*. 2010. **29**: 256–265.

147 **O'Hara, G. A., Duncan, C. J. A., Ewer, K. J., Collins, K. A., Elias, S. C. *et al.,* Hill, A. V. S.**, Clinical assessment of a recombinant simian adenovirus ChAd63: a potent new vaccine vector. *J Infect Dis*. 2012. **205**: 772–781.

148 **Ewer, K. J., O'Hara, G. A., Duncan, C. J. A., Collins, K. A., Sheehy, S. H. *et al.,* Hill, A. V. S.**, Protective CD8+ T-cell immunity to human malaria induced by chimpanzee adenovirus-MVA immunisation. *Nat Commun*. 2013. **4**: 2836.

149 **Ogwang, C., Afolabi, M. O., Kimani, D., Jagne, Y. J., Sheehy, S. H. *et al.,* Bojang, K.**, Safety and immunogenicity of heterologous prime-boost immunisation with Plasmodium falciparum malaria candidate vaccines, ChAd63 ME-TRAP and MVA ME-TRAP, in healthy Gambian and Kenyan adults. *PLoS One*. 2013. **8**: e57726.

150 **Spencer, A. J., Cottingham, M. G., Jenks, J. A., Longley, R. J., Capone, S. *et al.,* Hill, A. V. S.**, Enhanced Vaccine-Induced CD8+ T Cell Responses to Malaria Antigen ME-TRAP by Fusion to MHC Class II Invariant Chain. *PLoS One*. 2014. **9**: e100538.

151 **Goodman, A. L. and Draper, S. J.**, Blood-stage malaria vaccines - recent progress and future challenges. *Ann Trop Med Parasitol*. 2010. **104**: 189–211.

152 **Sagara, I., Dicko, A., Ellis, R. D., Fay, M. P., Diawara, S. I. *et al.,* Saul, A.**, A randomized controlled phase 2 trial of the blood stage AMA1-C1/Alhydrogel malaria vaccine in children in Mali. *Vaccine*. 2009. **27**: 3090–3098.

153 **Thera, M. A., Doumbo, O. K., Coulibaly, D., Laurens, M. B., Ouattara, A. *et al.,* Plowe, C. V.**, A field trial to assess a blood-stage malaria vaccine. *N Engl J Med*. 2011. **365**: 1004–1013.

154 **Takala, S. L., Coulibaly, D., Thera, M. A., Batchelor, A. H., Cummings, M. P. *et al.,* Plowe, C. V.**, Extreme polymorphism in a vaccine antigen and risk of clinical malaria: implications for vaccine development. *Sci Transl Med*. 2009. **1**: 2.

155 **Stubbs, J., Simpson, K. M., Triglia, T., Plouffe, D., Tonkin, C. J. *et al.,* Cowman, A. F.**, Molecular mechanism for switching of P. falciparum invasion pathways into human erythrocytes. *Science*. 2005. **309**: 1384–1387.

156 **Lyon, J. A., Angov, E., Fay, M. P., Sullivan, J. S., Girourd, A. S. *et al.,* Barnwell, J. W.**, Protection induced by Plasmodium falciparum MSP1(42) is strain-specific, antigen and adjuvant dependent, and correlates with antibody responses. *PLoS One*. 2008. **3**: e2830.

157 **Dutta, S., Sullivan, J. S., Grady, K. K., Haynes, J. D., Komisar, J. *et al.,* Barnwell, J. W.**, High antibody titer against apical membrane antigen-1 is required to protect against malaria in the Aotus model. *PLoS One*. 2009. **4**: e8138.

158 **Miura, K., Zhou, H., Diouf, A., Moretz, S. E., Fay, M. P. *et al.,* Long, C. A.**, Anti-apical-membrane-antigen-1 antibody is more effective than anti-42-kilodalton-merozoite-surface-protein-1 antibody in inhibiting plasmodium falciparum growth, as determined by the in vitro growth inhibition assay. *Clin Vaccine Immunol*. 2009. **16**: 963–968.

159 **Genton, B., Betuela, I., Felger, I., Al-Yaman, F., Anders, R. F. *et al.,* Alpers, M. P.**, A recombinant blood-stage malaria vaccine reduces Plasmodium falciparum density and exerts selective pressure on parasite populations in a phase 1-2b trial in Papua New Guinea. *J Infect Dis*. 2002. **185**: 820–827.

160 **Chuang, I., Sedegah, M., Cicatelli, S., Spring, M., Polhemus, M. *et al.,* Richie, T. L.**, DNA prime/Adenovirus boost malaria vaccine encoding P. falciparum CSP and AMA1 induces sterile protection associated with cell-mediated immunity. *PLoS One*. 2013. **8**: e55571.

161 **Draper, S. J., Moore, A. C., Goodman, A. L., Long, C. A., Holder, A. A. *et al.,* Hill, A. V. S.**, Effective induction of high-titer antibodies by viral vector vaccines. *Nat Med*. 2008. **14**: 819–821.

162 **Douglas, A. D., de Cassan, S. C., Dicks, M. D. J., Gilbert, S. C., Hill, A. V. S. and Draper, S. J.**, Tailoring subunit vaccine immunogenicity: maximizing antibody and T cell responses by using combinations of adenovirus, poxvirus and protein-adjuvant vaccines against Plasmodium falciparum MSP1. *Vaccine*. 2010. **28**: 7167–7178.

163 **Biswas, S., Dicks, M. D. J., Long, C. A., Remarque, E. J., Siani, L. *et al.,* Draper, S. J.**, Transgene optimization, immunogenicity and in vitro efficacy of viral vectored vaccines expressing two alleles of Plasmodium falciparum AMA1. *PLoS One*. 2011. **6**: e20977.

164 **Goodman, A. L., Epp, C., Moss, D., Holder, A. A., Wilson, J. M. *et al.,* Draper, S. J.**, New candidate vaccines against blood-stage Plasmodium falciparum malaria: prime-boost immunization regimens incorporating human and simian adenoviral vectors and poxviral vectors expressing an optimized antigen based on merozoite surface protein 1. *Infect Immun*. 2010. **78**: 4601–4612.

165 **Draper, S. J., Biswas, S., Spencer, A. J., Remarque, E. J., Capone, S. *et al.,* Hill, A. V. S.**, Enhancing blood-stage malaria subunit vaccine immunogenicity in rhesus macaques by combining adenovirus, poxvirus, and protein-in-adjuvant vaccines. *J Immunol*. 2010. **185**: 7583–7595.

166 **Sheehy, S. H., Duncan, C. J. A., Elias, S. C., Collins, K. A., Ewer, K. J. *et al.,* Draper, S. J.**, Phase Ia clinical evaluation of the Plasmodium falciparum blood-stage antigen MSP1 in ChAd63 and MVA vaccine vectors. *Mol Ther*. 2011. **19**: 2269–2276.

167 **Sheehy, S. H., Duncan, C. J. A., Elias, S. C., Biswas, S., Collins, K. A. *et al.,* Draper, S. J.**, Phase Ia clinical evaluation of the safety and immunogenicity of the Plasmodium falciparum blood-stage antigen AMA1 in ChAd63 and MVA vaccine vectors. *PLoS One*. 2012. **7**: e31208.

168 **Biswas, S., Choudhary, P., Elias, S. C., Miura, K., Milne, K. H. *et al.,* Draper, S. J.**, Assessment of humoral immune responses to blood-stage malaria antigens

following ChAd63-MVA immunization, controlled human malaria infection and natural exposure. *PLoS One*. 2014. **9**: e107903.

169 **Elias, S. C., Choudhary, P., de Cassan, S. C., Biswas, S., Collins, K. A. *et al.,* Draper, S. J.**, Analysis of human B-cell responses following ChAd63-MVA MSP1 and AMA1 immunization and controlled malaria infection. *Immunology*. 2014. **141**: 628–644.

170 **Elias, S. C., Collins, K. A., Halstead, F. D., Choudhary, P., Bliss, C. M. *et al.,* Draper, S. J.**, Assessment of immune interference, antagonism, and diversion following human immunization with biallelic blood-stage malaria viral-vectored vaccines and controlled malaria infection. *J Immunol*. 2013. **190**: 1135–1147.

171 **Sheehy, S. H., Duncan, C. J. A., Elias, S. C., Choudhary, P., Biswas, S. *et al.,* Draper, S. J.**, ChAd63-MVA-vectored blood-stage malaria vaccines targeting MSP1 and AMA1: assessment of efficacy against mosquito bite challenge in humans. *Mol Ther*. 2012. **20**: 2355–2368.

172 **Crosnier, C., Bustamante, L. Y., Bartholdson, S. J., Bei, A. K., Theron, M. *et al.,* Wright, G. J.**, Basigin is a receptor essential for erythrocyte invasion by Plasmodium falciparum. *Nature*. 2011. **480**: 534–537.

173 **Baum, J., Chen, L., Healer, J., Lopaticki, S., Boyle, M. *et al.,* Cowman, A. F.**, Reticulocyte-binding protein homologue 5 - an essential adhesin involved in invasion of human erythrocytes by Plasmodium falciparum. *Int J Parasitol*. 2009. **39**: 371–380.

174 **Cowman, A. F. and Crabb, B. S.**, Invasion of red blood cells by malaria parasites. *Cell*. 2006. **124**: 755–766.

175 **Douglas, A. D., Williams, A. R., Illingworth, J. J., Kamuyu, G., Biswas, S. *et al.,* Draper, S. J.**, The blood-stage malaria antigen PfRH5 is susceptible to vaccine-inducible cross-strain neutralizing antibody. *Nat Commun*. 2011. **2**: 601.

176 **Douglas, A. D., Baldeviano, G. C., Lucas, C. M., Lugo-Roman, L. A., Crosnier, C. *et al.,* Draper, S. J.**, A PfRH5-Based Vaccine Is Efficacious against Heterologous Strain Blood-Stage Plasmodium falciparum Infection in Aotus Monkeys. *Cell Host Microbe*. 2015. **17**: 130–139.

177 The malERA Consultative Group on Vaccines, A research agenda for malaria eradication: vaccines. *PLoS Med*. 2011. **8**: e1000398.

178 **Kang, J.-M., Ju, H.-L., Moon, S.-U., Cho, P.-Y., Bahk, Y.-Y. *et al.,* Na, B.-K.**, Limited sequence polymorphisms of four transmission-blocking vaccine candidate antigens in Plasmodium vivax Korean isolates. *Malaria journal*. 2013. **12**: 144.

179 **Sinden, R. E., Carter, R., Drakeley, C. and Leroy, D.**, The biology of sexual development of Plasmodium: the design and implementation of transmission-blocking strategies. *Malar J*. 2012. **11**: 70.

180 **Kaslow, D. C., Quakyi, I. A., Syin, C., Raum, M. G., Keister, D. B. *et al.,* Miller, L. H.**, A vaccine candidate from the sexual stage of human malaria that contains EGF-like domains. *Nature*. 1988. **333**: 74–76.

181 **Ockenhouse, C. F., Sun, P. F., Lanar, D. E., Wellde, B. T., Hall, B. T. *et al.,* Ballou, W. R.**, Phase I/IIa safety, immunogenicity, and efficacy trial of NYVAC-Pf7, a pox-

vectored, multiantigen, multistage vaccine candidate for Plasmodium falciparum malaria. *J Infect Dis*. 1998. **177**: 1664–1673.

182 **Malkin, E. M., Durbin, A. P., Diemert, D. J., Sattabongkot, J., Wu, Y. *et al.,* Saul, A.**, Phase 1 vaccine trial of Pvs25H: a transmission blocking vaccine for Plasmodium vivax malaria. *Vaccine*. 2005. **23**: 3131–3138.

183 **Shimp, R. L. J., Rowe, C., Reiter, K., Chen, B., Nguyen, V. *et al.,* Narum, D. L.**, Development of a Pfs25-EPA malaria transmission blocking vaccine as a chemically conjugated nanoparticle. *Vaccine*. 2013. **31**: 2954–2962.

184 **Jones, R. M., Chichester, J. A., Mett, V., Jaje, J., Tottey, S. *et al.,* Yusibov, V.**, A plant-produced Pfs25 VLP malaria vaccine candidate induces persistent transmission blocking antibodies against Plasmodium falciparum in immunized mice. *PLoS One*. 2013. **8**: e79538.

185 **Goodman, A. L., Blagborough, A. M., Biswas, S., Wu, Y., Hill, A. V. S. *et al.,* Draper, S. J.**, A viral vectored prime-boost immunization regime targeting the malaria Pfs25 antigen induces transmission-blocking activity. *PLoS One*. 2011. **6**: e29428.

186 **Forbes, E. K., de Cassan, S. C., Llewellyn, D., Biswas, S., Goodman, A. L. *et al.,* Draper, S. J.**, T cell responses induced by adenoviral vectored vaccines can be adjuvanted by fusion of antigen to the oligomerization domain of C4b-binding protein. *PLoS One*. 2012. **7**: e44943.

187 **Nikolaeva, D., Draper, S. J. and Biswas, S.**, Toward the development of effective transmission-blocking vaccines for malaria. *Expert Rev Vaccines*. 2015: 1–28.

188 **Weiss, W. R., Sedegah, M., Beaudoin, R. L., Miller, L. H. and Good, M. F.**, CD8+ T cells (cytotoxic/suppressors) are required for protection in mice immunized with malaria sporozoites. *Proc Natl Acad Sci U S A*. 1988. **85**: 573–576.

189 **Ploemen, I. H. J., Prudêncio, M., Douradinha, B. G., Ramesar, J., Fonager, J. *et al.,* Franke-Fayard, B. M. D.**, Visualisation and quantitative analysis of the rodent malaria liver stage by real time imaging. *PloS one*. 2009. **4**: e7881.

190 **Burbelo, P. D., Ching, K. H., Klimavicz, C. M. and Iadarola, M. J.**, Antibody profiling by Luciferase Immunoprecipitation Systems (LIPS). *J Vis Exp*. 2009.

191 **Ogwang, C., Kimani, D., Edwards, N. J., Roberts, R., Mwacharo, J. *et al.,* Bejon, P.**, Prime-boost vaccination with chimpanzee adenovirus and modified vaccinia Ankara encoding TRAP provides partial protection against Plasmodium falciparum infection in Kenyan adults. *Science translational medicine*. 2015. **7**: 286.

192 **Forbes, E. K., Biswas, S., Collins, K. A., Gilbert, S. C., Hill, A. V. and Draper, S. J.**, Combining liver- and blood-stage malaria viral-vectored vaccines: investigating mechanisms of CD8+ T cell interference. *Journal of immunology (Baltimore, Md. 1950)*. 2011. **187**: 3738–3750.

193 **Pichyangkul, S., Tongtawe, P., Kum-Arb, U., Yongvanitchit, K., Gettayacamin, M. *et al.,* Miller, R. S.**, Evaluation of the safety and immunogenicity of Plasmodium falciparum apical membrane antigen 1, merozoite surface protein 1 or RTS,S vaccines with adjuvant system AS02A administered alone or concurrently in rhesus monkeys. *Vaccine*. 2009. **28**: 452–462.

194 **Grifantini, R., Finco, O., Bartolini, E., Draghi, M., Del, G. G. *et al.,* Grandi, G.**, Multi-plasmid DNA vaccination avoids antigenic competition and enhances immunogenicity of a poorly immunogenic plasmid. *European journal of immunology*. 1998. **28**: 1225–1232.

195 **Jiang, G., Charoenvit, Y., Moreno, A., Baraceros, M. F., Banania, G. *et al.,* Doolan, D. L.**, Induction of multi-antigen multi-stage immune responses against Plasmodium falciparum in rhesus monkeys, in the absence of antigen interference, with heterologous DNA prime/poxvirus boost immunization. *Malaria journal*. 2007. **6**: 135.

196 **Guerin-Marchand, C., Druilhe, P., Galey, B., Londono, A., Patarapotikul, J. *et al.,* Langsley, G.**, A liver-stage-specific antigen of Plasmodium falciparum characterized by gene cloning. *Nature*. 1987. **329**: 164–167.

197 **Fidock, D. A., Gras-Masse, H., Lepers, J. P., Brahimi, K., Benmohamed, L. *et al.,* Meis, J. F.**, Plasmodium falciparum liver stage antigen-1 is well conserved and contains potent B and T cell determinants. *Journal of immunology (Baltimore, Md. 1950)*. 1994. **153**: 190–204.

198 **Mikolajczak, S. A., Sacci, J. B., La Vega, P.** de, **Camargo, N., VanBuskirk, K. *et al.,* Kappe, S. H. I.**, Disruption of the Plasmodium falciparum liver-stage antigen-1 locus causes a differentiation defect in late liver-stage parasites. *Cellular microbiology*. 2011. **13**: 1250–1260.

199 **Krzych, U., Lyon, J. A., Jareed, T., Schneider, I., Hollingdale, M. R. *et al.,* Ballou, W. R.**, T lymphocytes from volunteers immunized with irradiated Plasmodium falciparum sporozoites recognize liver and blood stage malaria antigens. *Journal of immunology (Baltimore, Md. 1950)*. 1995. **155**: 4072–4077.

200 **Hill, A. V., Elvin, J., Willis, A. C., Aidoo, M., Allsopp, C. E. *et al.,* Townsend, A. R.**, Molecular analysis of the association of HLA-B53 and resistance to severe malaria. *Nature*. 1992. **360**: 434–439.

201 **Cummings, J. F., Spring, M. D., Schwenk, R. J., Ockenhouse, C. F., Kester, K. E. *et al.,* Heppner, D. G.**, Recombinant Liver Stage Antigen-1 (LSA-1) formulated with AS01 or AS02 is safe, elicits high titer antibody and induces IFN-gamma/IL-2 CD4+ T cells but does not protect against experimental Plasmodium falciparum infection. *Vaccine*. 2010. **28**: 5135–5144.

202 **Porter, D. W., Thompson, F. M., Berthoud, T. K., Hutchings, C. L., Andrews, L. *et al.,* Hill, A. V. S.**, A human Phase I/IIa malaria challenge trial of a polyprotein malaria vaccine. *Vaccine*. 2011. **29**: 7514–7522.

203 **Ny, T., Elgh, F. and Lund, B.**, The structure of the human tissue-type plasminogen activator gene: correlation of intron and exon structures to functional and structural domains. *Proceedings of the National Academy of Sciences of the United States of America*. 1984. **81**: 5355–5359.

204 **Luo, M., Tao, P., Li, J., Zhou, S., Guo, D. and Pan, Z.**, Immunization with plasmid DNA encoding influenza A virus nucleoprotein fused to a tissue plasminogen activator signal sequence elicits strong immune responses and protection against H5N1 challenge in mice. *Journal of virological methods*. 2008. **154**: 121–127.

205 **Becker, S. I., Wang, R., Hedstrom, R. C., Aguiar, J. C., Jones, T. R. *et al.*, Gardner, M. J.**, Protection of mice against Plasmodium yoelii sporozoite challenge with P. yoelii merozoite surface protein 1 DNA vaccines. *Infection and immunity*. 1998. **66**: 3457–3461.

206 **Li, Z., Howard, A., Kelley, C., Delogu, G., Collins, F. and Morris, S.**, Immunogenicity of DNA vaccines expressing tuberculosis proteins fused to tissue plasminogen activator signal sequences. *Infection and immunity*. 1999. **67**: 4780–4786.

207 **Siau, A., Silvie, O., Franetich, J.-F., Yalaoui, S., Marinach, C. *et al.*, Mazier, D.**, Temperature shift and host cell contact up-regulate sporozoite expression of Plasmodium falciparum genes involved in hepatocyte infection. *PLoS pathogens*. 2008. **4**: e1000121.

208 **Spielmann, T., Montagna, G. N., Hecht, L. and Matuschewski, K.**, Molecular make-up of the Plasmodium parasitophorous vacuolar membrane. *International journal of medical microbiology IJMM*. 2012. **302**: 179–186.

209 **Kaiser, K., Matuschewski, K., Camargo, N., Ross, J. and Kappe, S. H. I.**, Differential transcriptome profiling identifies Plasmodium genes encoding pre-erythrocytic stage-specific proteins. *Molecular microbiology*. 2004. **51**: 1221–1232.

210 **Matuschewski, K., Ross, J., Brown, S. M., Kaiser, K., Nussenzweig, V. and Kappe, S. H. I.**, Infectivity-associated changes in the transcriptional repertoire of the malaria parasite sporozoite stage. *The Journal of biological chemistry*. 2002. **277**: 41948–41953.

211 **Tarun, A. S., Dumpit, R. F., Camargo, N., Labaied, M., Liu, P. *et al.*, Kappe, S. H. I.**, Protracted sterile protection with Plasmodium yoelii pre-erythrocytic genetically attenuated parasite malaria vaccines is independent of significant liver-stage persistence and is mediated by CD8+ T cells. *The Journal of infectious diseases*. 2007. **196**: 608–616.

212 **Hoffman, B. U. and Chattopadhyay, R.**, Plasmodium falciparum: effect of radiation on levels of gene transcripts in sporozoites. *Exp Parasitol*. 2008. **118**: 247–252.

213 **Mikolajczak, S. A., Jacobs-Lorena, V., MacKellar, D. C., Camargo, N. and Kappe, S. H. I.**, L-FABP is a critical host factor for successful malaria liver stage development. *International journal for parasitology*. 2007. **37**: 483–489.

214 **Sharma, A., Yogavel, M., Akhouri, R. R., Gill, J. and Sharma, A.**, Crystal structure of soluble domain of malaria sporozoite protein UIS3 in complex with lipid. *The Journal of biological chemistry*. 2008. **283**: 24077–24088.

215 **Favretto, F., Assfalg, M., Molinari, H. and D'Onofrio, M.**, Evidence from NMR interaction studies challenges the hypothesis of direct lipid transfer from L-FABP to malaria sporozoite protein UIS3. *Protein science a publication of the Protein Society*. 2013. **22**: 133–138.

216 **Limbach, K., Aguiar, J. C., Gowda, K., Patterson, N., Abot, E. N. *et al.*, Richie, T.**, Identification of two new protective pre-erythrocytic malaria vaccine antigen candidates. *Malar J*. 2011. **10**: 65.

217 **Rennenberg, A., Lehmann, C., Heitmann, A., Witt, T., Hansen, G. *et al.,* Heussler, V. T.**, Exoerythrocytic Plasmodium parasites secrete a cysteine protease inhibitor involved in sporozoite invasion and capable of blocking cell death of host hepatocytes. *PLoS Pathog*. 2010. **6**: e1000825.

218 **Pandey, K. C., Singh, N., Arastu-Kapur, S., Bogyo, M. and Rosenthal, P. J.**, Falstatin, a cysteine protease inhibitor of Plasmodium falciparum, facilitates erythrocyte invasion. *PLoS pathogens*. 2006. **2**: e117.

219 **Boysen, K. E. and Matuschewski, K.**, Inhibitor of cysteine proteases is critical for motility and infectivity of Plasmodium sporozoites. *mBio*. 2013. **4**: 13.

220 **Doolan, D. L., Southwood, S., Freilich, D. A., Sidney, J., Graber, N. L. *et al.,* Sette, A.**, Identification of Plasmodium falciparum antigens by antigenic analysis of genomic and proteomic data. *Proceedings of the National Academy of Sciences of the United States of America*. 2003. **100**: 9952–9957.

221 **Gruner, A. C., Mauduit, M., Tewari, R., Romero, J. F., Depinay, N. *et al.,* Renia, L.**, Sterile protection against malaria is independent of immune responses to the circumsporozoite protein. *PloS one*. 2007. **2**: e1371.

222 **Kumar, K. A., Sano, G.-i., Boscardin, S., Nussenzweig, R. S., Nussenzweig, M. C. *et al.,* Nussenzweig, V.**, The circumsporozoite protein is an immunodominant protective antigen in irradiated sporozoites. *Nature*. 2006. **444**: 937–940.

223 **Mauduit, M., Tewari, R., Depinay, N., Kayibanda, M., Lallemand, E. *et al.,* Gruner, A. C.**, Minimal role for the circumsporozoite protein in the induction of sterile immunity by vaccination with live rodent malaria sporozoites. *Infection and immunity*. 2010. **78**: 2182–2188.

224 **Sedegah, M., Charoenvit, Y., Minh, L., Belmonte, M., Majam, V. F. *et al.,* Rogers, W. O.**, Reduced immunogenicity of DNA vaccine plasmids in mixtures. *Gene therapy*. 2004. **11**: 448–456.

225 **Reyes-Sandoval, A., Wyllie, D. H., Bauza, K., Milicic, A., Forbes, E. K. *et al.,* Hill, A. V. S.**, CD8+ T effector memory cells protect against liver-stage malaria. *J Immunol*. 2011. **187**: 1347–1357.

226 **Berenzon, D., Schwenk, R. J., Letellier, L., Guebre-Xabier, M., Williams, J. and Krzych, U.**, Protracted protection to Plasmodium berghei malaria is linked to functionally and phenotypically heterogeneous liver memory CD8+ T cells. *Journal of immunology (Baltimore, Md. 1950)*. 2003. **171**: 2024–2034.

227 **Krzych, U., Schwenk, R., Guebre-Xabier, M., Sun, P., Palmer, D. *et al.,* Chalom, I.**, The role of intrahepatic lymphocytes in mediating protective immunity induced by attenuated Plasmodium berghei sporozoites. *Immunological reviews*. 2000. **174**: 123–134.

228 **Nganou-Makamdop, K., van Gemert, G.-J., Arens, T., Hermsen, C. C. and Sauerwein, R. W.**, Long term protection after immunization with P. berghei sporozoites correlates with sustained IFNγ responses of hepatic CD8+ memory T cells. *PLoS One*. 2012. **7**: e36508.

229 **Hollingdale, M. R., Aikawa, M., Atkinson, C. T., Ballou, W. R., Chen, G. X. *et al.,* Zhu, J. D.**, Non-CS pre-erythrocytic protective antigens. *Immunology letters*. 1990. **25**: 71–76.

230 **Montagna, G. N., Beigier-Bompadre, M., Becker, M., Kroczek, R. A., Kaufmann, S. H. E. and Matuschewski, K.**, Antigen export during liver infection of the malaria parasite augments protective immunity. *mBio*. 2014. **5**: 14.

231 **Kedl, R. M., Rees, W. A., Hildeman, D. A., Schaefer, B., Mitchell, T. *et al.,* Marrack, P.**, T cells compete for access to antigen-bearing antigen-presenting cells. *The Journal of experimental medicine*. 2000. **192**: 1105–1113.

232 **Capone, S., Naddeo, M., D'Alise, A. M., Abbate, A., Grazioli, F. *et al.,* Folgori, A.**, Fusion of HCV Nonstructural Antigen to MHC Class II-associated Invariant Chain Enhances T-cell Responses Induced by Vectored Vaccines in Nonhuman Primates. *Mol Ther*. 2014.

233 **Genuardi, M. and Saunders, G. F.**, Localization of the HLA class II-associated invariant chain gene to human chromosome band 5q32. *Immunogenetics*. 1988. **28**: 53–56.

234 **Paul, W. E.**, *Fundamental Immunology*. Wolters Kluwer Health 2012.

235 **Broeke, T.** ten, **Wubbolts, R. and Stoorvogel, W.**, MHC Class II Antigen Presentation by Dendritic Cells Regulated through Endosomal Sorting. *Cold Spring Harb Perspect Biol*. 2013. **5**.

236 **Bakke, O. and Dobberstein, B.**, MHC class II-associated invariant chain contains a sorting signal for endosomal compartments. *Cell*. 1990. **63**: 707–716.

237 **Pieters, J., Bakke, O. and Dobberstein, B.**, The MHC class II-associated invariant chain contains two endosomal targeting signals within its cytoplasmic tail. *J Cell Sci*. 1993. **106 (Pt 3)**: 831–846.

238 **Bremnes, B., Madsen, T., Gedde-Dahl, M. and Bakke, O.**, An LI and ML motif in the cytoplasmic tail of the MHC-associated invariant chain mediate rapid internalization. *Journal of cell science*. 1994. **107 (Pt 7)**: 2021–2032.

239 **Cloutier, M., Gauthier, C., Fortin, J.-S. and Thibodeau, J.**, The invariant chain p35 isoform promotes formation of nonameric complexes with MHC II molecules. *Immunol Cell Biol*. 2014.

240 **Cresswell, P. and Roche, P. A.**, Invariant chain-MHC class II complexes: always odd and never invariant. *Immunol Cell Biol*. 2014.

241 **Bijlmakers, M. J., Benaroch, P. and Ploegh, H. L.**, Mapping functional regions in the lumenal domain of the class II-associated invariant chain. *The Journal of experimental medicine*. 1994. **180**: 623–629.

242 **Gedde-Dahl, M., Freisewinkel, I., Staschewski, M., Schenck, K., Koch, N. and Bakke, O.**, Exon 6 is essential for invariant chain trimerization and induction of large endosomal structures. *The Journal of biological chemistry*. 1997. **272**: 8281–8287.

243 **Malcherek, G., Gnau, V., Jung, G., Rammensee, H. G. and Melms, A.**, Supermotifs enable natural invariant chain-derived peptides to interact with many major

histocompatibility complex-class II molecules. *The Journal of experimental medicine*. 1995. **181**: 527–536.

244 **Sette, A., Southwood, S., Miller, J. and Appella, E.**, Binding of major histocompatibility complex class II to the invariant chain-derived peptide, CLIP, is regulated by allelic polymorphism in class II. *The Journal of experimental medicine*. 1995. **181**: 677–683.

245 **Stumptner, P. and Benaroch, P.**, Interaction of MHC class II molecules with the invariant chain: role of the invariant chain (81-90) region. *The EMBO journal*. 1997. **16**: 5807–5818.

246 **Neumann, J. and Koch, N.**, A novel domain on HLA-DRbeta chain regulates the chaperone role of the invariant chain. *Journal of cell science*. 2006. **119**: 4207–4214.

247 **Siebenkotten, I. M., Carstens, C. and Koch, N.**, Identification of a sequence that mediates promiscuous binding of invariant chain to MHC class II allotypes. *Journal of immunology (Baltimore, Md. 1950)*. 1998. **160**: 3355–3362.

248 **Thayer, W. P., Ignatowicz, L., Weber, D. A. and Jensen, P. E.**, Class II-associated invariant chain peptide-independent binding of invariant chain to class II MHC molecules. *Journal of immunology (Baltimore, Md. 1950)*. 1999. **162**: 1502–1509.

249 **Castellino, F., Han, R. and Germain, R. N.**, The transmembrane segment of invariant chain mediates binding to MHC class II molecules in a CLIP-independent manner. *European journal of immunology*. 2001. **31**: 841–850.

250 **Adams, S. and Humphreys, R. E.**, Invariant chain peptides enhancing or inhibiting the presentation of antigenic peptides by major histocompatibility complex class II molecules. *European journal of immunology*. 1995. **25**: 1693–1702.

251 **Chen, F., Meng, F., Pan, L., Xu, F., Liu, X. and Yu, W.**, Boosting immune response with the invariant chain segments via association with non-peptide binding region of major histocompatibility complex class II molecules. *BMC immunology*. 2012. **13**: 55.

252 **Perez, S. A., Peoples, G. E., Papamichail, M. and Baxevanis, C. N.**, Invariant chain-peptide fusion vaccine using HER-2/neu. *Methods Mol Biol*. 2014. **1139**: 321–336.

253 **Xu, M., Li, J., Gulfo, J. V., Hofe, E.** von and **Humphreys, R. E.**, MHC class II allosteric site drugs: new immunotherapeutics for malignant, infectious and autoimmune diseases. *Scandinavian journal of immunology*. 2001. **54**: 39–44.

254 **Ashman, J. B. and Miller, J.**, A role for the transmembrane domain in the trimerization of the MHC class II-associated invariant chain. *J Immunol*. 1999. **163**: 2704–2712.

255 **Kukol, A., Torres, J. and Arkin, I. T.**, A structure for the trimeric MHC class II-associated invariant chain transmembrane domain. *Journal of molecular biology*. 2002. **320**: 1109–1117.

256 **Landsverk, O. J. B., Bakke, O. and Gregers, T. F.**, MHC II and the endocytic pathway: regulation by invariant chain. *Scand J Immunol*. 2009. **70**: 184–193.

257 **Fortin, J.-S., Cloutier, M. and Thibodeau, J.**, Exposing the Specific Roles of the Invariant Chain Isoforms in Shaping the MHC Class II Peptidome. *Front Immunol.* 2013. **4**: 443.

258 **Roche, P. A., Marks, M. S. and Cresswell, P.**, Formation of a nine-subunit complex by HLA class II glycoproteins and the invariant chain. *Nature*. 1991. **354**: 392–394.

259 **Koch, N., McLellan, A. D. and Neumann, J.**, A revised model for invariant chain-mediated assembly of MHC class II peptide receptors. *Trends in biochemical sciences*. 2007. **32**: 532–537.

260 **Blum, J. S., Wearsch, P. A. and Cresswell, P.**, Pathways of antigen processing. *Annu Rev Immunol.* 2013. **31**: 443–473.

261 **Kvist, S., Wiman, K., Claesson, L., Peterson, P. A. and Dobberstein, B.**, Membrane insertion and oligomeric assembly of HLA-DR histocompatibility antigens. *Cell*. 1982. **29**: 61–69.

262 **Sekaly, R. P., Tonnelle, C., Strubin, M., Mach, B. and Long, E. O.**, Cell surface expression of class II histocompatibility antigens occurs in the absence of the invariant chain. *The Journal of experimental medicine*. 1986. **164**: 1490–1504.

263 **Marks, M. S., Blum, J. S. and Cresswell, P.**, Invariant chain trimers are sequestered in the rough endoplasmic reticulum in the absence of association with HLA class II antigens. *The Journal of cell biology*. 1990. **111**: 839–855.

264 **Cerundolo, V., Elliott, T., Elvin, J., Bastin, J. and Townsend, A.**, Association of the human invariant chain with H-2 Db class I molecules. *European journal of immunology*. 1992. **22**: 2243–2248.

265 **Sugita, M. and Brenner, M. B.**, Association of the invariant chain with major histocompatibility complex class I molecules directs trafficking to endocytic compartments. *The Journal of biological chemistry*. 1995. **270**: 1443–1448.

266 **Vigna, J. L., Smith, K. D. and Lutz, C. T.**, Invariant chain association with MHC class I: preference for HLA class I/beta 2-microglobulin heterodimers, specificity, and influence of the MHC peptide-binding groove. *Journal of immunology (Baltimore, Md. 1950)*. 1996. **157**: 4503–4510.

267 **Kleijmeer, M. J., Escola, J. M., UytdeHaag, F. G., Jakobson, E., Griffith, J. M. *et al.*, Geuze, H. J.**, Antigen loading of MHC class I molecules in the endocytic tract. *Traffic (Copenhagen, Denmark)*. 2001. **2**: 124–137.

268 **Reber, A. J., Turnquist, H. R., Thomas, H. J., Lutz, C. T. and Solheim, J. C.**, Expression of invariant chain can cause an allele-dependent increase in the surface expression of MHC class I molecules. *Immunogenetics*. 2002. **54**: 74–81.

269 **Basha, G., Omilusik, K., Chavez-Steenbock, A., Reinicke, A. T., Lack, N. *et al.*, Jefferies, W. A.**, A CD74-dependent MHC class I endolysosomal cross-presentation pathway. *Nat Immunol.* 2012. **13**: 237–245.

270 **Duan, F. and Srivastava, P. K.**, An invariant road to cross-presentation. *Nat Immunol.* 2012. **13**: 207–208.

271 **Walchli, S., Kumari, S., Fallang, L.-E.,** Sand, Kine M K, **Yang, W. *et al.*, Gregers, T. F.**, Invariant Chain as a vehicle to load antigenic peptides on human MHC class I for cytotoxic T-cell activation. *Eur J Immunol.* 2013.

272 **Ma, W. and** Van den Eynde, Benoit J, Endosomal compartment: Also a dock for MHC class I peptide loading. *Eur J Immunol*. 2014. **44**: 650–653.
273 **Sanderson, S., Frauwirth, K. and Shastri, N.**, Expression of endogenous peptide-major histocompatibility complex class II complexes derived from invariant chain-antigen fusion proteins. *Proc Natl Acad Sci U S A*. 1995. **92**: 7217–7221.
274 **Malcherek, G., Wirblich, C., Willcox, N., Rammensee, H. G., Trowsdale, J. and Melms, A.**, MHC class II-associated invariant chain peptide replacement by T cell epitopes: engineered invariant chain as a vehicle for directed and enhanced MHC class II antigen processing and presentation. *Eur J Immunol*. 1998. **28**: 1524–1533.
275 **Sponaas, A., Carstens, C. and Koch, N.**, C-terminal extension of the MHC class II-associated invariant chain by an antigenic sequence triggers activation of naive T cells. *Gene Ther*. 1999. **6**: 1826–1834.
276 **Diebold, S. S., Cotten, M., Koch, N. and Zenke, M.**, MHC class II presentation of endogenously expressed antigens by transfected dendritic cells. *Gene Ther*. 2001. **8**: 487–493.
277 **Rowe, H. M., Lopes, L., Ikeda, Y., Bailey, R., Barde, I. *et al.*, Collins, M. K.**, Immunization with a lentiviral vector stimulates both CD4 and CD8 T cell responses to an ovalbumin transgene. *Mol Ther*. 2006. **13**: 310–319.
278 **Holst, P. J., Sorensen, M. R., Mandrup Jensen, C. M., Orskov, C., Thomsen, A. R. and Christensen, J. P.**, MHC class II-associated invariant chain linkage of antigen dramatically improves cell-mediated immunity induced by adenovirus vaccines. *J Immunol*. 2008. **180**: 3339–3346.
279 **Grujic, M., Holst, P. J., Christensen, J. P. and Thomsen, A. R.**, Fusion of a viral antigen to invariant chain leads to augmented T-cell immunity and improved protection in gene-gun DNA-vaccinated mice. *J Gen Virol*. 2009. **90**: 414–422.
280 **Mikkelsen, M., Holst, P. J., Bukh, J., Thomsen, A. R. and Christensen, J. P.**, Enhanced and sustained CD8+ T cell responses with an adenoviral vector-based hepatitis C virus vaccine encoding NS3 linked to the MHC class II chaperone protein invariant chain. *J Immunol*. 2011. **186**: 2355–2364.
281 **Jensen, S., Steffensen, M. A., Jensen, B. A. H., Schluter, D., Christensen, J. P. and Thomsen, A. R.**, Adenovirus-based vaccine against Listeria monocytogenes: extending the concept of invariant chain linkage. *J Immunol*. 2013. **191**: 4152–4164.
282 **Holst, P. J., Christensen, J. P. and Thomsen, A. R.**, Vaccination against lymphocytic choriomeningitis virus infection in MHC class II-deficient mice. *J Immunol*. 2011. **186**: 3997–4007.
283 **Baraliakos, X., Baerlecken, N. T., Witte, T., Heldmann, F. and Braun, J.**, High prevalence of anti-CD74 antibodies specific for the HLA class II-associated invariant chain peptide (CLIP) in patients with axial spondyloarthritis. *Ann Rheum Dis*. 2013.
284 **Baerlecken, N. T., Nothdorft, S., Stummvoll, G. H., Sieper, J., Rudwaleit, M. *et al.*, Witte, T.**, Autoantibodies against CD74 in spondyloarthritis. *Ann Rheum Dis*. 2013.
285 **Duffy, P. E., Sahu, T., Akue, A., Milman, N. and Anderson, C.**, Pre-erythrocytic malaria vaccines: identifying the targets. *Expert Rev Vaccines*. 2012. **11**: 1261–1280.

286 **Larsen, K. C., Spencer, A. J., Goodman, A. L., Gilchrist, A., Furze, J. *et al.,* Wyllie, D. H.**, Expression of tak1 and tram induces synergistic pro-inflammatory signalling and adjuvants DNA vaccines. *Vaccine*. 2009. **27**: 5589–5598.

287 **Spencer, A. J., Furze, J., Honeycutt, J. D., Calvert, A., Saurya, S. *et al.,* Hill, A. V. S.**, 4-1BBL enhances CD8+ T cell responses induced by vectored vaccines in mice but fails to improve immunogenicity in rhesus macaques. *PLoS One*. 2014. **9**: e105520.

288 **Germain, R. N.**, Uncovering the Role of Invariant Chain in Controlling MHC Class II Antigen Capture. Accessed 2 July 2013.

289 **Sorensen, M. R., Holst, P. J., Pircher, H., Christensen, J. P. and Thomsen, A. R.**, Vaccination with an adenoviral vector encoding the tumor antigen directly linked to invariant chain induces potent CD4(+) T-cell-independent CD8(+) T-cell-mediated tumor control. *Eur J Immunol*. 2009. **39**: 2725–2736.

290 **Ogun, S. A., Dumon-Seignovert, L., Marchand, J.-B., Holder, A. A. and Hill, F.**, The Oligomerization Domain of C4-Binding Protein (C4bp) Acts as an Adjuvant, and the Fusion Protein Comprised of the 19-Kilodalton Merozoite Surface Protein 1 Fused with the Murine C4bp Domain Protects Mice against Malaria. *Infect Immun*. 2008. **76**: 3817–3823.

291 **van Braeckel-Budimir, N. and Harty, J. T.**, CD8 T-cell-mediated protection against liver-stage malaria: lessons from a mouse model. *Front Microbiol*. 2014. **5**: 272.

292 **Dicks, M. D. J., Spencer, A. J., Edwards, N. J., Wadell, G., Bojang, K. *et al.,* Cottingham, M. G.**, A novel chimpanzee adenovirus vector with low human seroprevalence: improved systems for vector derivation and comparative immunogenicity. *PloS one*. 2012. **7**: e40385.

293 **Antrobus, R. D., Coughlan, L., Berthoud, T. K., Dicks, M. D., Hill, A. V. *et al.,* Gilbert, S. C.**, Clinical assessment of a novel recombinant simian adenovirus ChAdOx1 as a vectored vaccine expressing conserved Influenza A antigens. *Molecular therapy the journal of the American Society of Gene Therapy*. 2014. **22**: 668–674.

294 **Cappuccini, F., Stribbling, S., Pollock, E., Hill, A. V. S. and Redchenko, I.**, Immunogenicity and efficacy of the novel cancer vaccine based on simian adenovirus and MVA vectors alone and in combination with PD-1 mAb in a mouse model of prostate cancer. *Cancer immunology, immunotherapy CII*. 2016. **65**: 701–713.

295 **Dicks, M. D. J., Guzman, E., Spencer, A. J., Gilbert, S. C., Charleston, B. *et al.,* Cottingham, M. G.**, The relative magnitude of transgene-specific adaptive immune responses induced by human and chimpanzee adenovirus vectors differs between laboratory animals and a target species. *Vaccine*. 2015. **33**: 1121–1128.

296 **Dulal, P., Wright, D., Ashfield, R., Hill, A. V. S., Charleston, B. and Warimwe, G. M.**, Potency of a thermostabilised chimpanzee adenovirus Rift Valley Fever vaccine in cattle. *Vaccine*. 2016. **34**: 2296–2298.

297 **Stylianou, E., Griffiths, K. L., Poyntz, H. C., Harrington-Kandt, R., Dicks, M. D. *et al.,* McShane, H.**, Improvement of BCG protective efficacy with a novel

chimpanzee adenovirus and a modified vaccinia Ankara virus both expressing Ag85A. *Vaccine*. 2015. **33**: 6800–6808.

298 **Warimwe, G. M., Gesharisha, J., Carr, B. V., Otieno, S., Otingah, K. *et al.,* Hill, A. V. S.**, Chimpanzee Adenovirus Vaccine Provides Multispecies Protection against Rift Valley Fever. *Scientific reports*. 2016. **6**: 20617.

299 **Schliehe, C., Bitzer, A., van den Broek, M. and Groettrup, M.**, Stable antigen is most effective for eliciting CD8+ T-cell responses after DNA vaccination and infection with recombinant vaccinia virus in vivo. *Journal of virology*. 2012. **86**: 9782–9793.

300 **Bins, A. D., Wolkers, M. C.,** van den Boom, Marly D, Haanen, John B A G and **Schumacher, T. N. M.**, In vivo antigen stability affects DNA vaccine immunogenicity. *Journal of immunology (Baltimore, Md. 1950)*. 2007. **179**: 2126–2133.

301 **Dixon, A. M., Stanley, B. J., Matthews, E. E., Dawson, J. P. and Engelman, D. M.**, Invariant chain transmembrane domain trimerization: a step in MHC class II assembly. *Biochemistry*. 2006. **45**: 5228–5234.

302 **Smith, E. C., Smith, S. E., Carter, J. R., Webb, S. R., Gibson, K. M. *et al.,* Dutch, R. E.**, Trimeric transmembrane domain interactions in paramyxovirus fusion proteins: roles in protein folding, stability, and function. *J Biol Chem*. 2013. **288**: 35726–35735.

303 **Leng, L., Metz, C. N., Fang, Y., Xu, J., Donnelly, S. *et al.,* Bucala, R.**, MIF signal transduction initiated by binding to CD74. *The Journal of experimental medicine*. 2003. **197**: 1467–1476.

304 **Naujokas, M. F., Morin, M., Anderson, M. S., Peterson, M. and Miller, J.**, The chondroitin sulfate form of invariant chain can enhance stimulation of T cell responses through interaction with CD44. *Cell*. 1993. **74**: 257–268.

305 **Matza, D., Wolstein, O., Dikstein, R. and Shachar, I.**, Invariant chain induces B cell maturation by activating a TAF(II)105-NF-kappaB-dependent transcription program. *The Journal of biological chemistry*. 2001. **276**: 27203–27206.

306 **Walline, C. C., Deffit, S. N., Wang, N., Guindon, L. M., Crotzer, V. L. *et al.,* Blum, J. S.**, Virus-encoded ectopic CD74 enhances poxvirus vaccine efficacy. *Immunology*. 2014. **141**: 531–539.

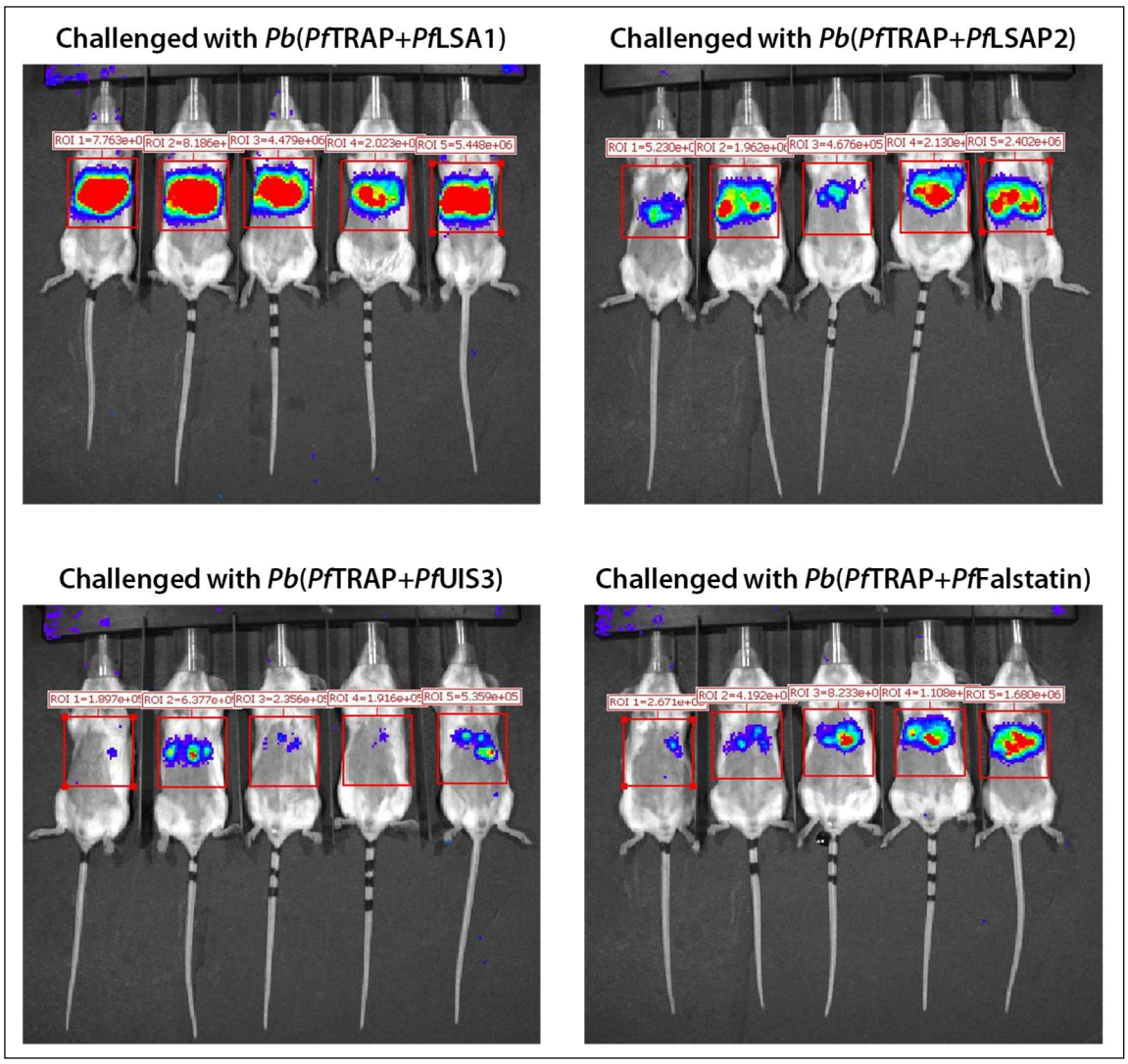
307 **Rampling, T., Ewer, K. J., Bowyer, G., Bliss, C. M., Edwards, N. J. *et al.,* Hill, A. V. S.**, Safety and High Level Efficacy of the Combination Malaria Vaccine Regimen of RTS,S/AS01B with ChAd-MVA Vectored Vaccines Expressing ME-TRAP. *The Journal of infectious diseases*. 2016.

308 **Georgieva, E. R., Borbat, P. P., Norman, H. D. and Freed, J. H.**, Mechanism of influenza A M2 transmembrane domain assembly in lipid membranes. *Scientific reports*. 2015. **5**: 11757.

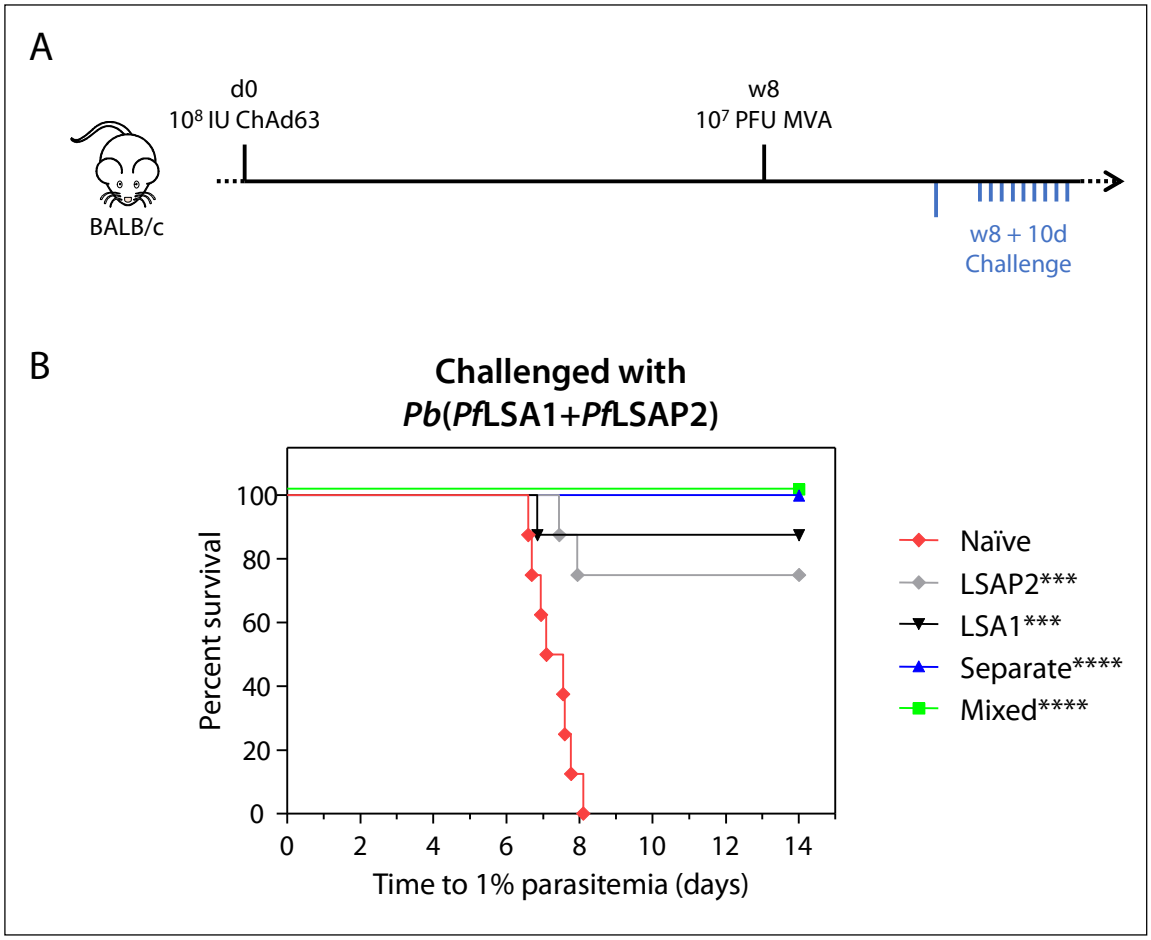
# Chapter I

# Appendix

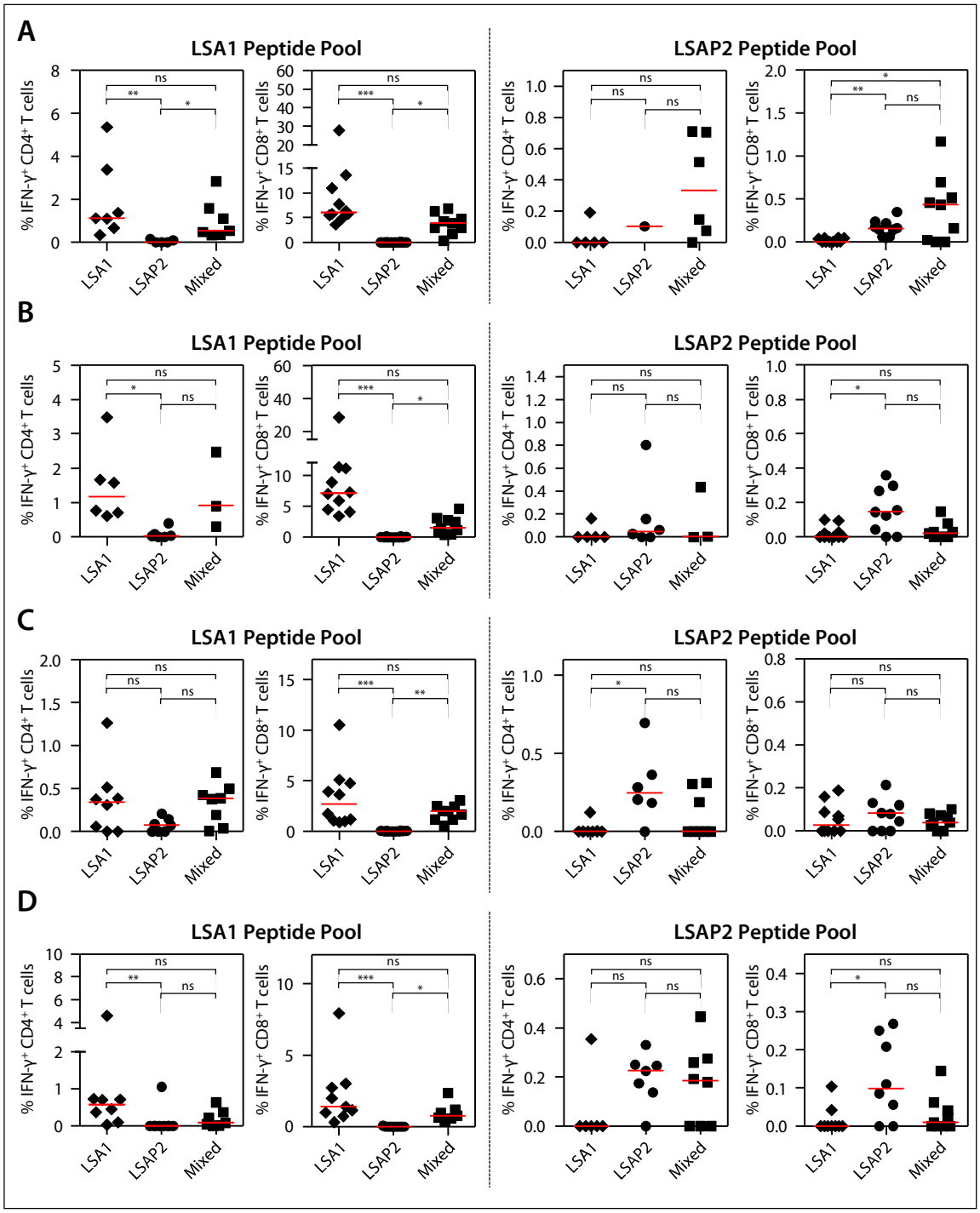
# I1 Supplemental Figures



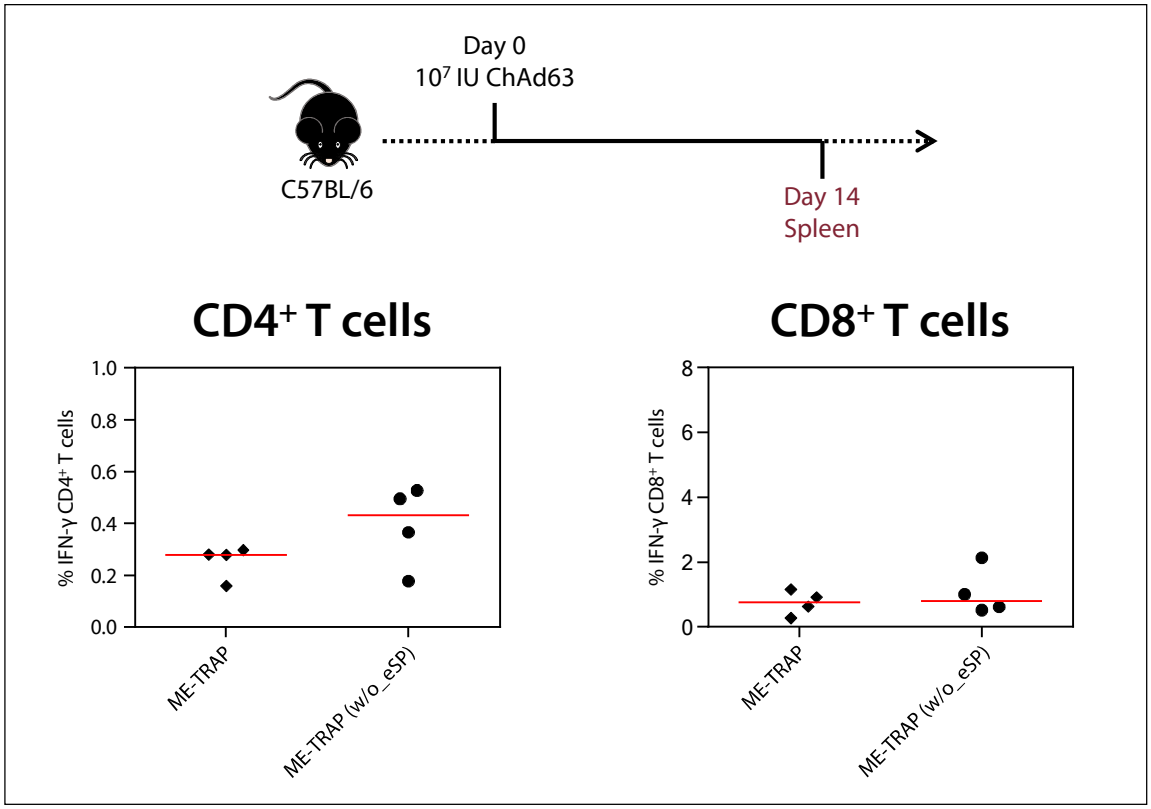

**Supplemental Figure I-1. In vivo imaging**. Naive BALB/c mice were challenged with transgenic chimeric sporozoites. Parasite liver loads were quantified by measuring luminescence levels 44 h after infection using an IVIS 200 system as described in B2.3.9 (p. 46) in collaboration with Dr Ahmed Salman.



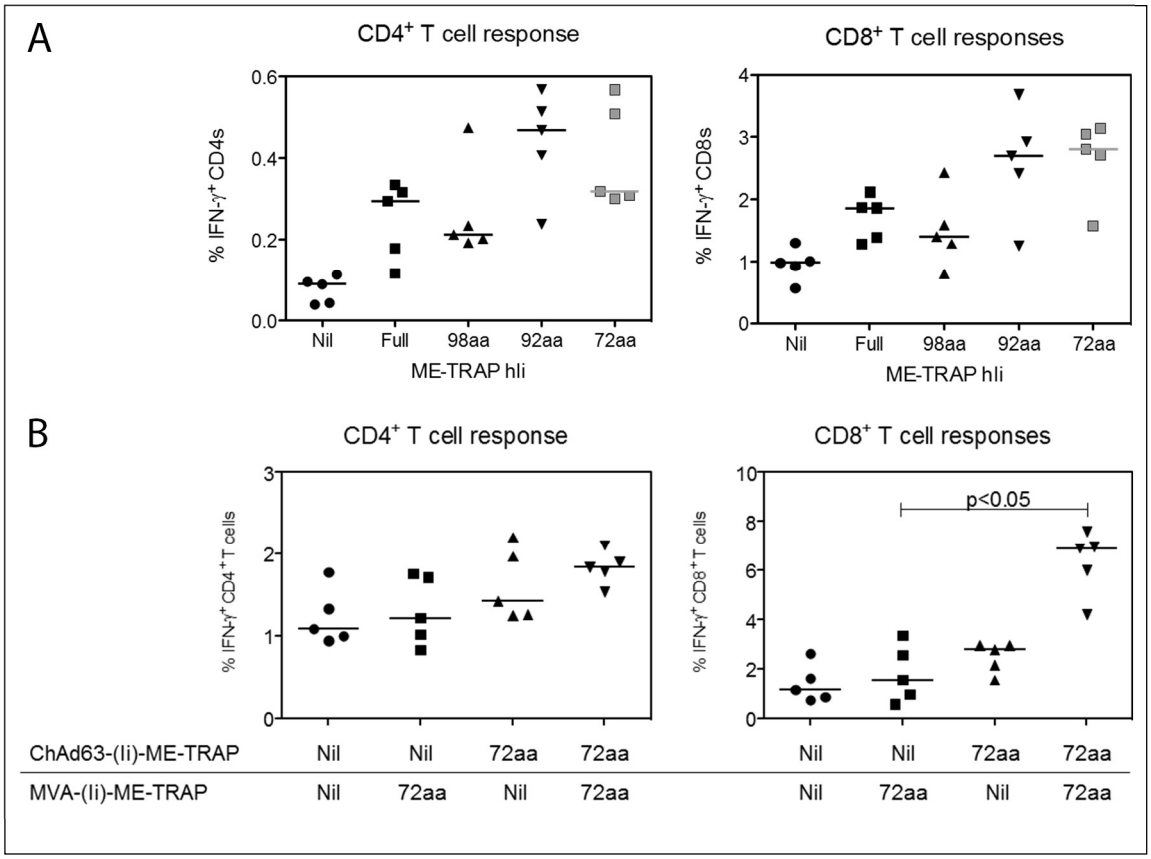

**Supplemental Figure I-2. Efficacy of a ChAd63-MVA prime-boost regimen encoding LSA1 and LSAP2.** This experiment was designed and conducted by Dr Ahmed Salman (The Jenner Institute, University of Oxford). (A) Outline of the experimental setup. Eight BALB/c mice per group were vaccinated with 108 IU ChAd63 and 107 PFU MVA encoding either LSA1, LSAP2 or both in combination. When two vaccines were given, mice were vaccinated with a full dose of each vaccine administered in separate legs ("Separate") or mixed prior to administration in both legs ("Mixed"). (B) Efficacy data. Mice were challenged with 1,000 chimeric *P. berghei* sporozoites expressing *P. falciparum* LSA1 and LSAP2 on day 10 post boost. Blood smears were taken daily from four days after sporozoite challenge and analysed by Giemsa staining and light microscopy to determine parasitaemia. Mice that were negative for blood-stage malaria until 15 days after sporozoite challenge were considered to be sterilely protected. Time to 1% parasitaemia is plotted on a Kaplan-Meier Survival Curve. Data was analysed with the log-rank (Mantel-Cox) test. Asterisks denote the level of statistical significance when compared to the naïve control group (***, $p<0.001$; ****, $p<0.0001$).



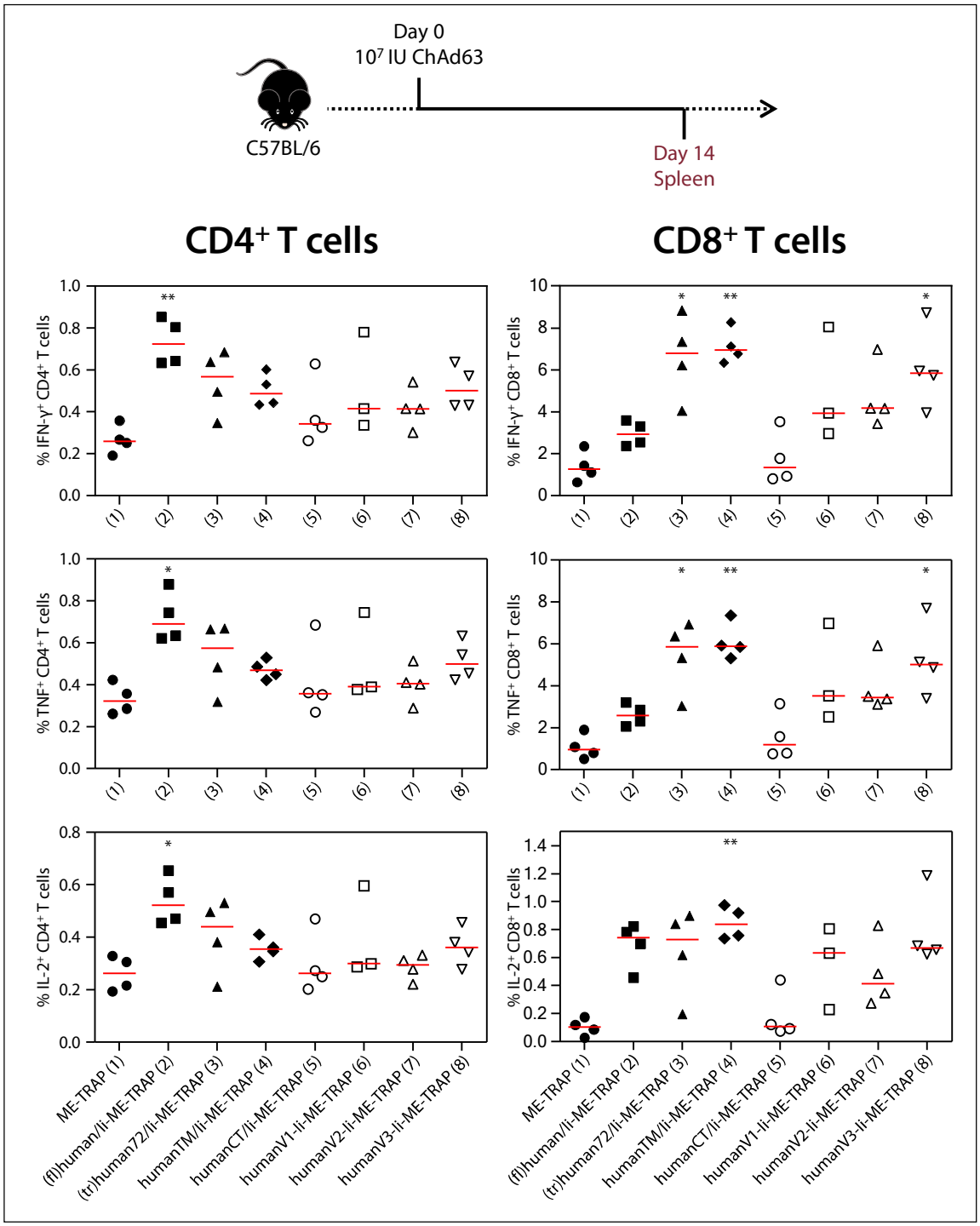

**Supplemental Figure I-3. Long-term post-boost immunogenicity.** A blood sample was taken in (A) month 3, (B) month 4, (C) month 5, and (D) month 6 of the experiment as described in Figure C-8 (p. 76) and analysed by ICS after stimulation with an LSA1 or LSAP2 peptide pool. Graphs represent the frequency of $CD4^+IFN\text{-}\gamma^+$ or $CD8^+IFN\text{-}\gamma^+$ T cells. Single points indicate T-cell responses of individual mice and red lines show the median response per group. Data was analysed with a one-way analysis of variance with Dunn's multiple comparison post-test. Asterisks denote the level of statistical significance when compared to each other (*, $p<0.05$; **, $p<0.01$; ***, $p<0.001$; ns, non-significant).



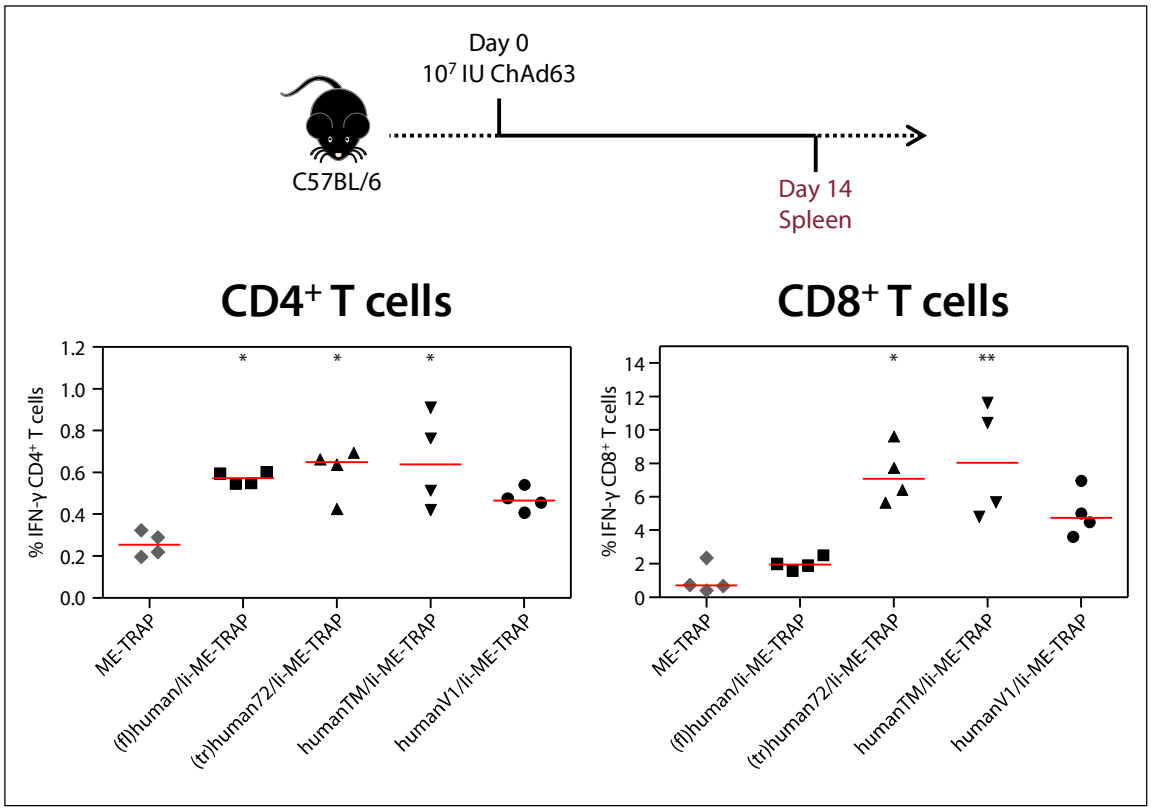

**Supplemental Figure I-4. Effect of endogenous signal peptide (eSP) removal from TRAP.** C57BL/6 mice were immunised with $10^8$ IU ChAd63 vectors encoding ME-TRAP with or without its endogenous signal peptide. Spleens were harvested two weeks later. $CD4^+$ and $CD8^+$ T-cell responses to a TRAP peptide pool are shown by measuring intracellular IFN-γ using flow cytometry. Single points represent T-cell responses of individual mice and red lines indicate the median response per group. Data was analysed with a one-way analysis of variance. No statistical difference was found between the groups.



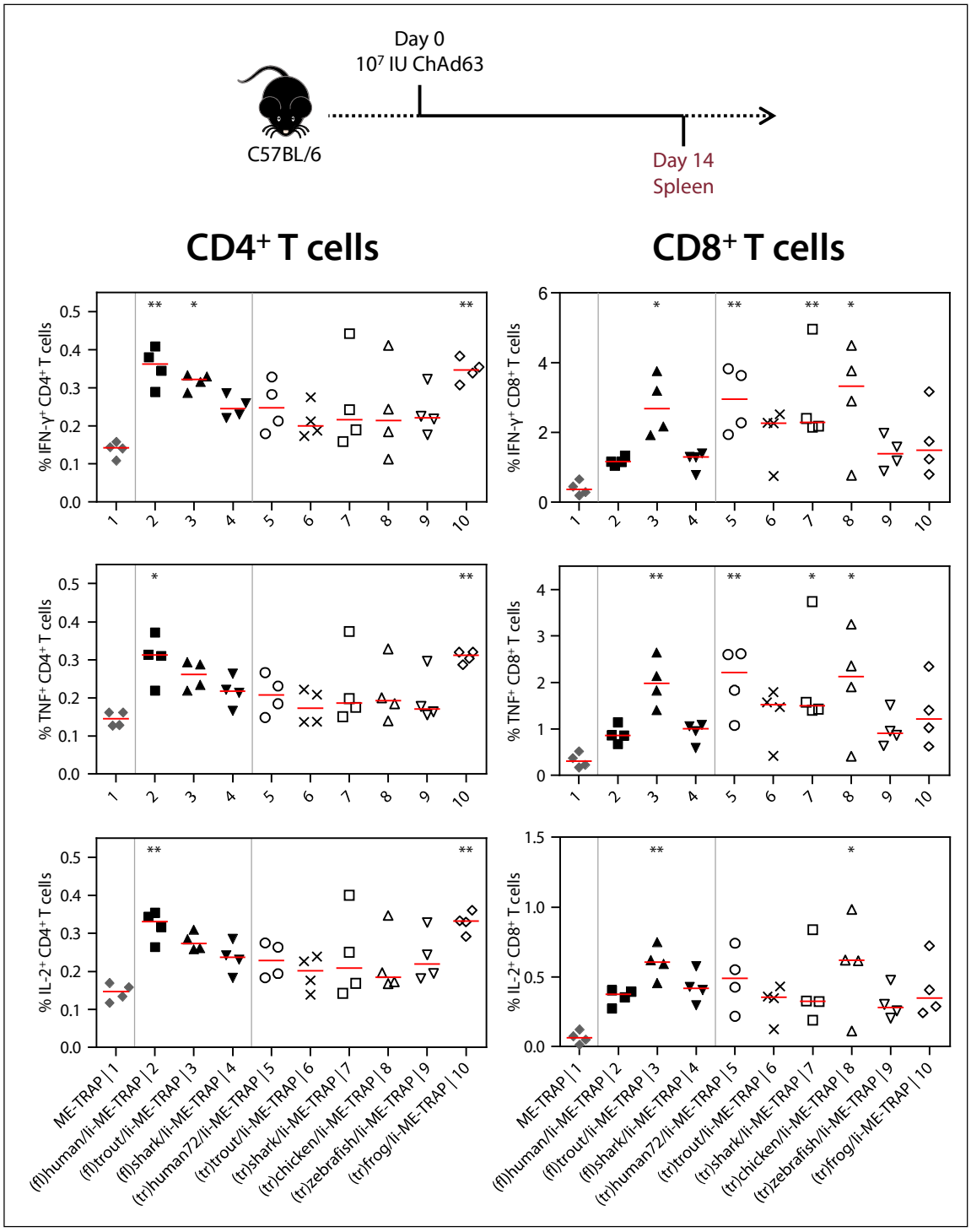

**Supplemental Figure I-5. Immune response to ME-TRAP fused to Ii truncations.** A) C57BL/6 mice were vaccinated IM with $10^7$ IU of ChAd63 vectors encoding unfused ME-TRAP (Nil) or ME-TRAP fused to (fl)human/Ii-ME-TRAP (Full), (tr)human98/Ii (98aa), (tr)human92/Ii (92aa), or (tr)human72/Ii (72aa). Spleens were harvested two weeks later and T-cell responses to TRAP were measured by ICS. Points represent individual mice after mice after subtraction of background responses and lines represent the median. B) C57BL/6 mice were immunised IM with $10^8$ IU of ChAd63 encoding unfused ME-TRAP (Nil) or (tr)human72/Ii-ME-TRAP (72aa) and 8 weeks later boosted with either 107 PFU MVA-ME-TRAP (Nil) or MVA-(tr)human72/Ii-ME-TRAP (72aa).



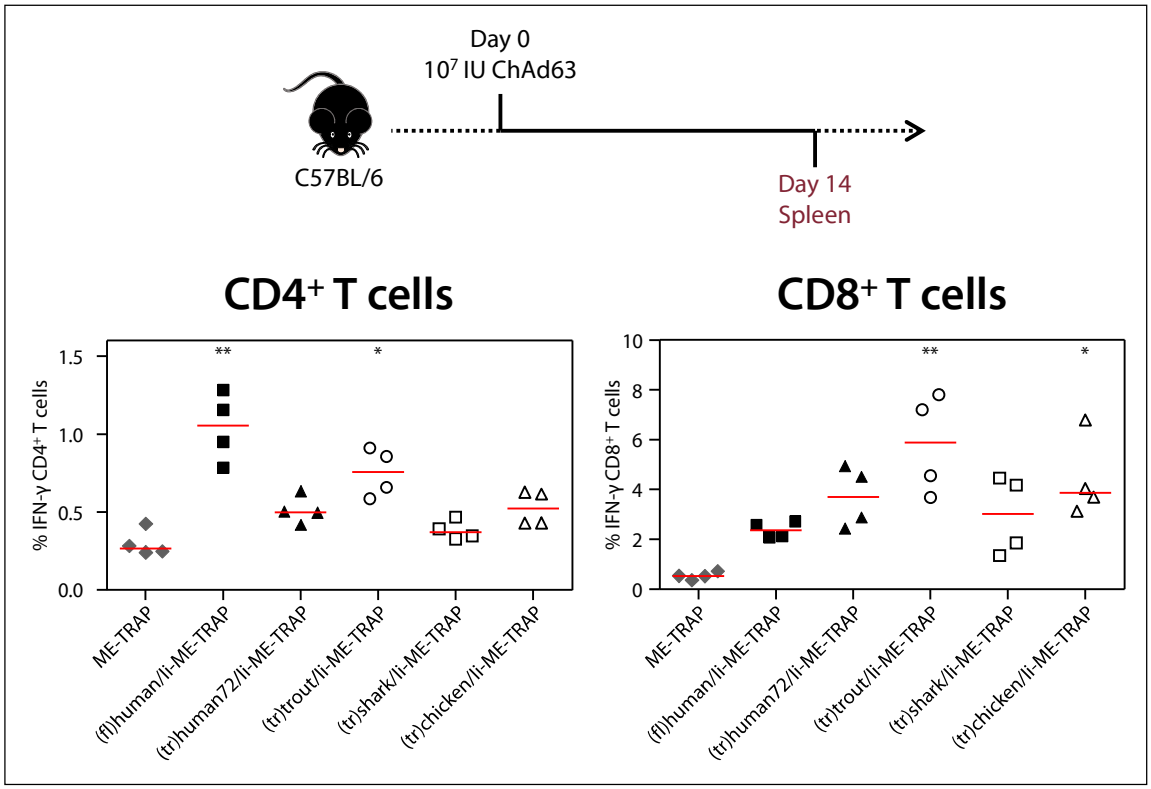

**Supplemental Figure I-6. Effect of fusion of ME-TRAP to (truncated) Ii in mice vaccinated with ChAd63 vectors.** C57BL/6 mice were immunised with $10^7$ IU ChAd63 vectors with spleens harvested two weeks post vaccination. T-cell responses to a TRAP peptide pool were analysed by ICS. The percentage of $CD4^+$ and $CD8^+$ T cells positive for IFN-γ, TNF, or IL-2 are shown. Single points indicate T-cell responses of individual mice and red lines denote the median response per group. Data was analysed with a one-way analysis of variance with Dunn's multiple comparison post-test. Asterisks denote the level of statistical significance when compared to the control ME-TRAP vaccinated group (*, $p<0.05$; **, $p<0.01$).



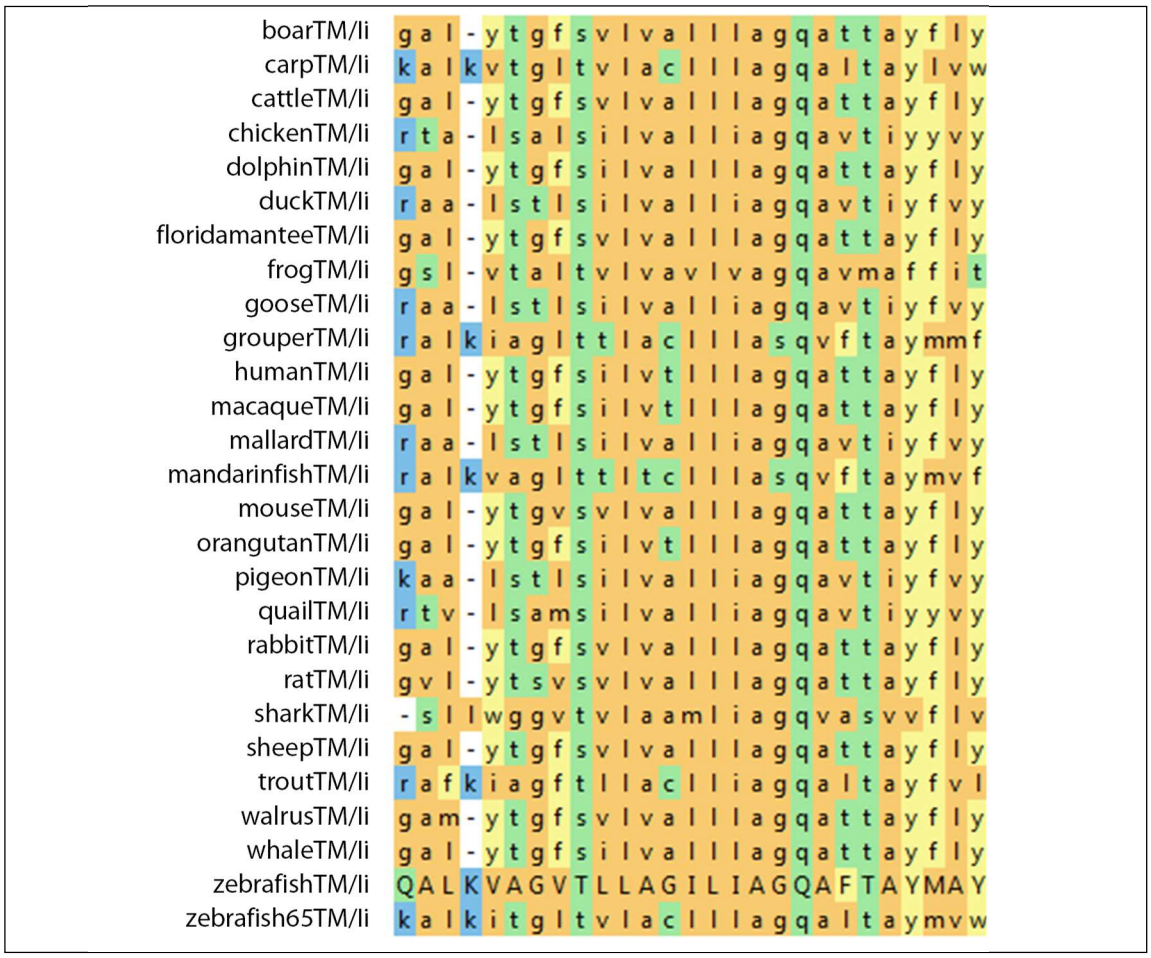

**Supplemental Figure I-7. Effect of truncated Ii sequences as adjuvant.** C57BL/6 mice were immunised with $10^7$ IU ChAd63 vectors and spleens were harvested two weeks later. T-cell responses to a TRAP peptide pool were analysed by ICS. The percentage of $CD4^+$ and $CD8^+$ T cells positive for IFN-γ are shown. Single points indicate T-cell responses of individual mice and red lines denote the median response per group. Data was analysed with a one-way analysis of variance with Dunn's multiple comparison post-test. Asterisks denote the level of statistical significance when compared to the control ME-TRAP vaccinated group (*, $p<0.05$; **, $p<0.01$).



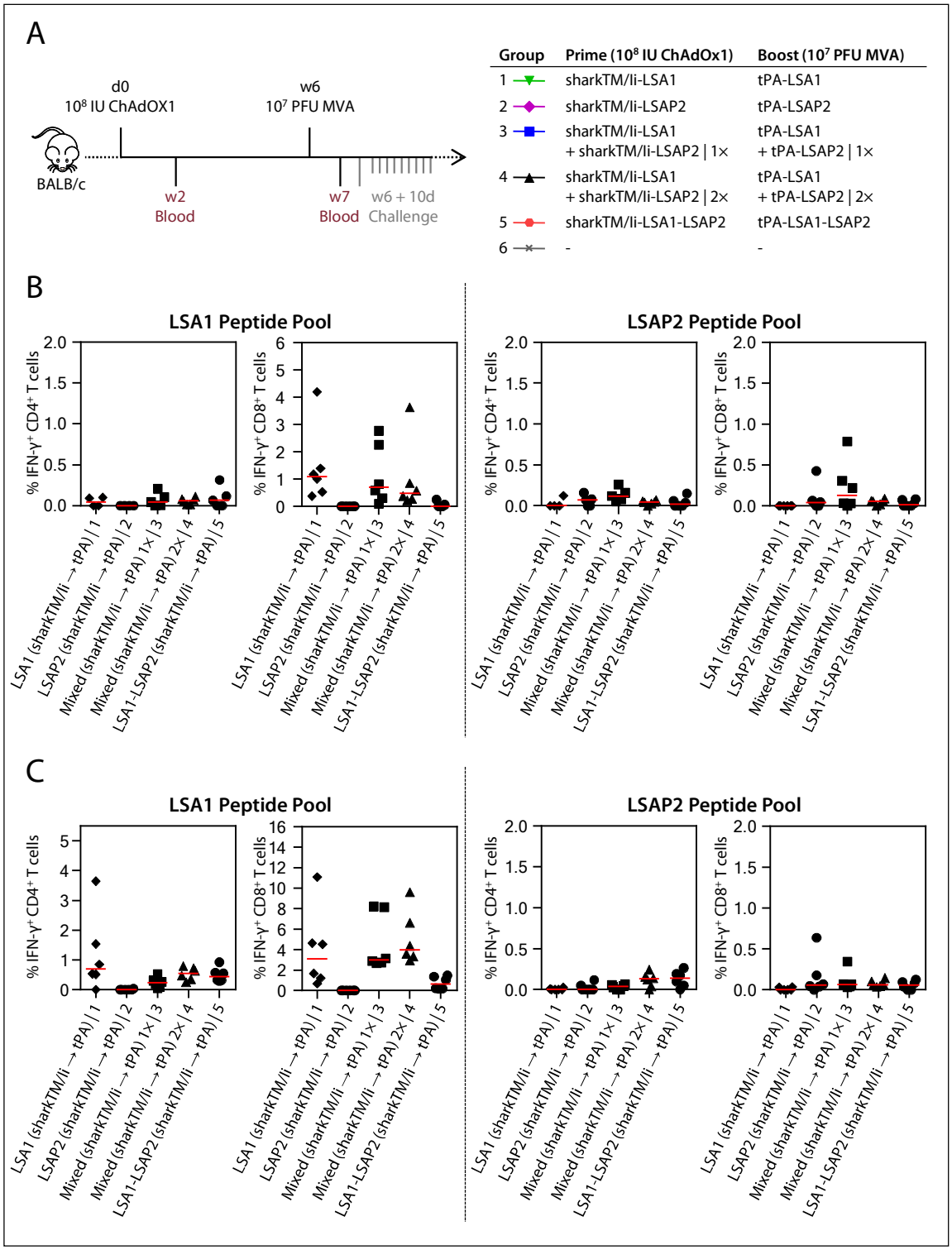

**Supplemental Figure I-8. Effect of fusion of ME-TRAP to xenogenised Ii in mice vaccinated with ChAd63 vectors**. C57BL/6 mice were immunised with $10^7$ IU ChAd63 vectors with spleens harvested two weeks post vaccination. T-cell responses to a TRAP peptide pool were analysed by ICS. The percentage of $CD4^+$ and $CD8^+$ T cells positive for IFN-γ, TNF, or IL-2 are shown. Single points indicate T-cell responses of individual mice and red lines denote the median response per group. Data was analysed with a one-way analysis of variance with Dunn's multiple comparison post-test. Asterisks denote the level of statistical significance when compared to the control ME-TRAP vaccinated group (*, $p<0.05$; **, $p<0.01$).



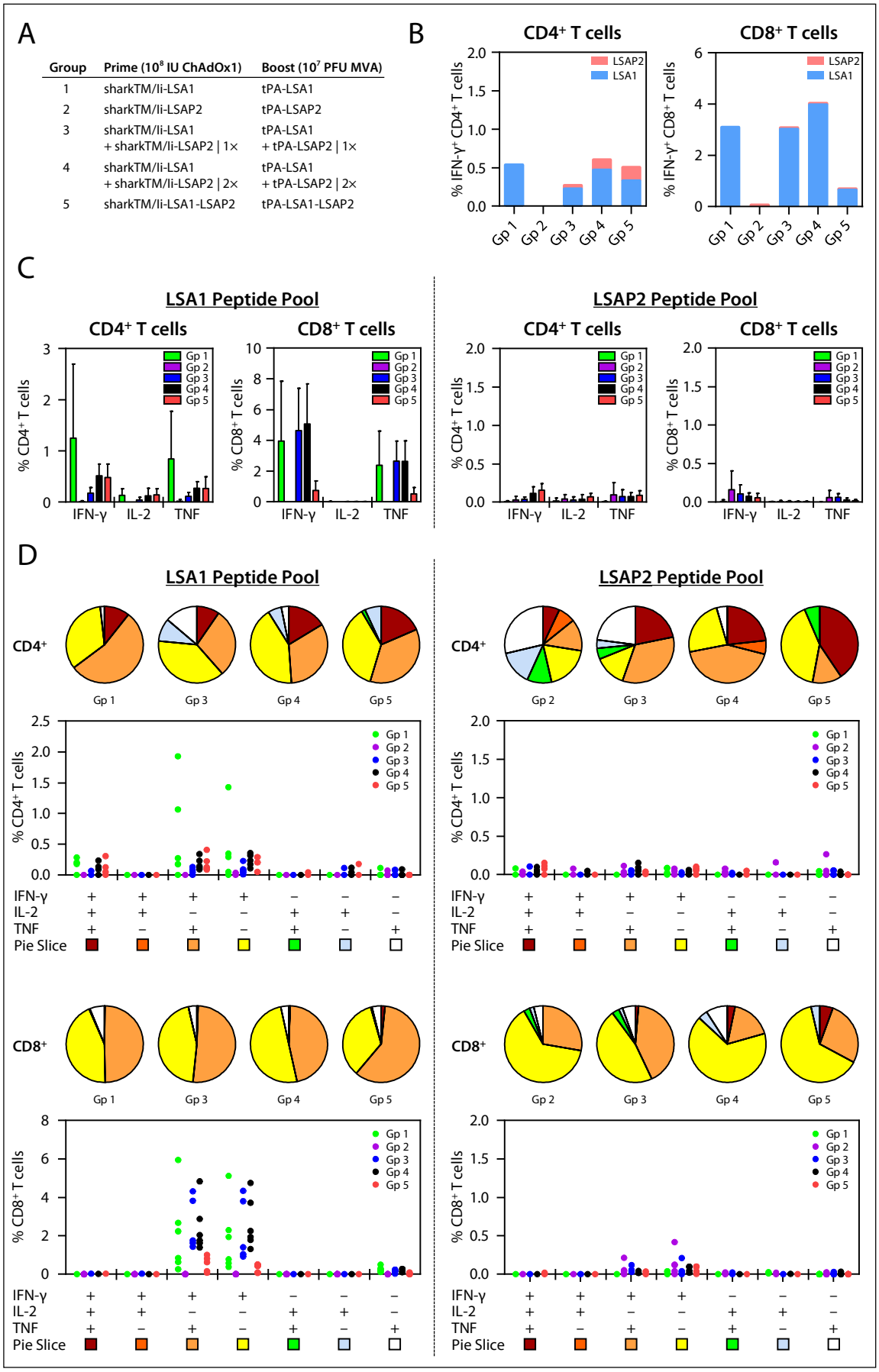

**Supplemental Figure I-9. Adjuvanticity of selected xenogenised Ii sequences.** C57BL/6 mice were immunised with $10^7$ IU ChAd63 vectors encoding ME-TRAP adjuvanted by xenogenised Ii or unfused ME-TRAP as control. Spleens were harvested two weeks later and T-cell responses to a TRAP peptide pool analysed by ICS. The percentage of $CD4^+$ and $CD8^+$ T cells positive for IFN-γ are shown. Single points indicate T-cell responses of individual mice and red lines denote the median response per group. Data was analysed with a one-way analysis of variance with Dunn's multiple comparison post-test. Asterisks denote the level of statistical significance when compared to the control ME-TRAP vaccinated group (*, $p<0.05$; **, $p<0.01$).




**Supplemental Figure I-10.** MUSCLE alignment of Ii transmembrane domains.

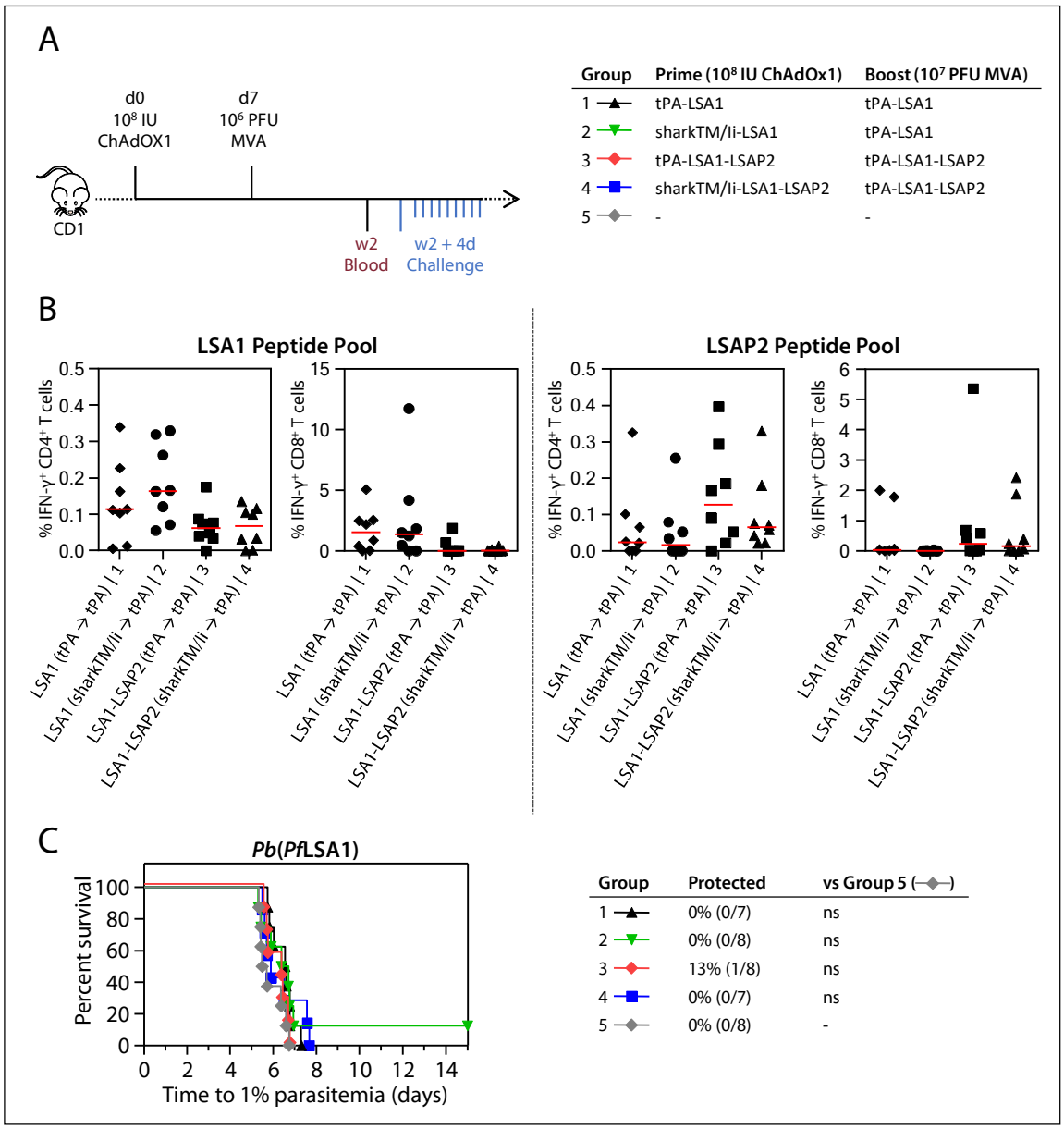



**Supplemental Figure I-11. Immunogenicity of a 6-week prime boost regimen with ChAdOX1 and MVA vectors in BALB/c mice.** (A) Experimental setup. After immunising six BALB/c mice per group with $10^8$ IU of ChAdOX1, the immune response was boosted with $10^6$ PFU MVA as indicated in the table. A blood sample was taken in week 7; three days later mice were challenged (results in Figure E-15). Immunogenicity data of week 2 (B) and week 7 (C). T-cell responses of blood PBMC to an LSA1 or LSAP2 peptide pool were analysed by ICS. The percentage of $CD4^+$ and $CD8^+$ T cells positive for IFN-γ are shown. Single points indicate T-cell responses of individual mice and red lines denote the median response per group.

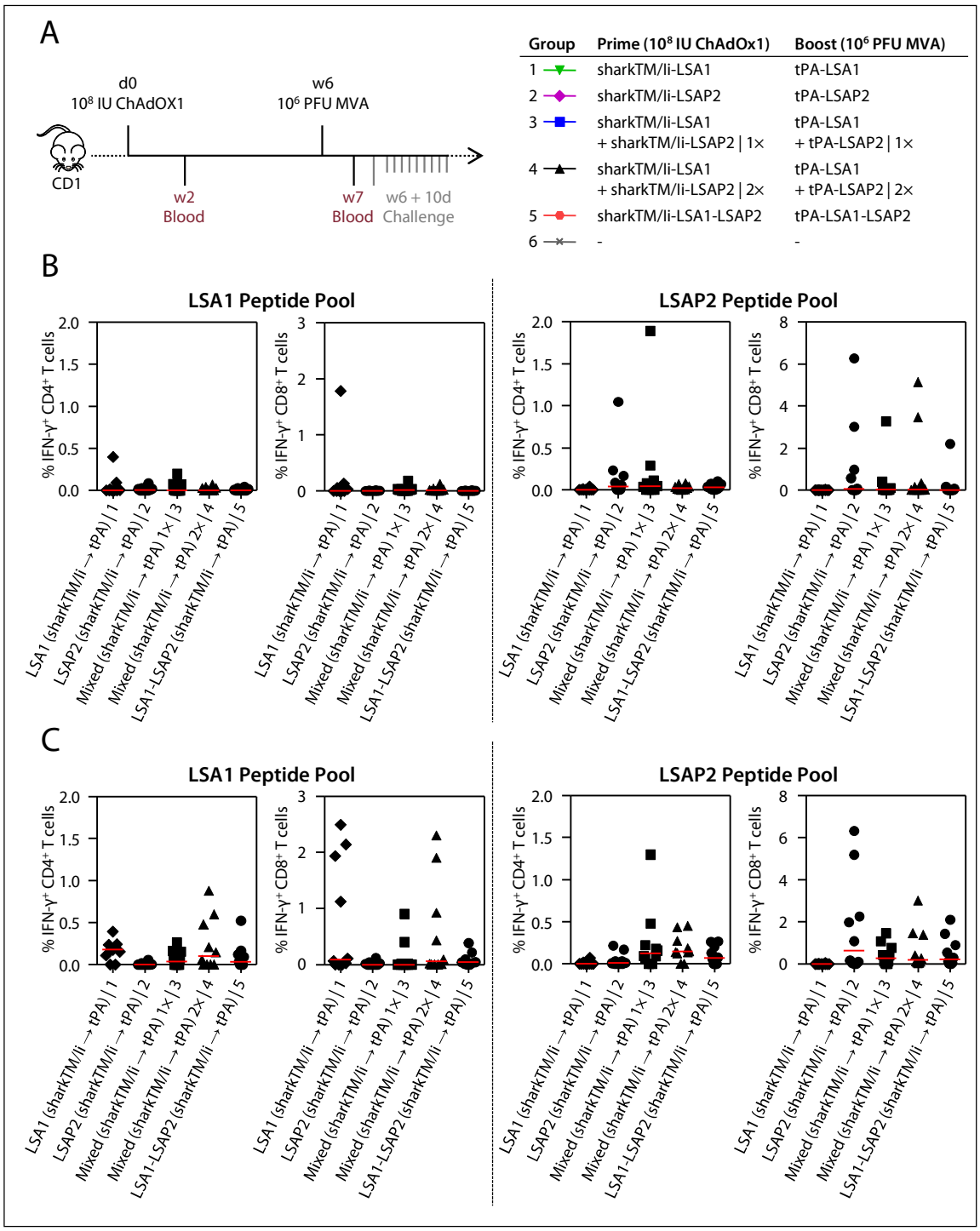



**Supplemental Figure I-12. Functionality of antigen-specific CD4⁺ and CD8⁺ T cells post boost.** (A) Study groups. 6 BALB/c mice per group were immunised with $10^8$ IU of ChAdOX1 and $10^7$ PFU MVA

vectors as outlined in the table. One week post boost, blood PBMC were analysed by ICS after stimulation with a LSA1 or LSAP2 peptide pool. (B) Columns represent the median frequency of LSA1- and LSAP2-specific $CD4^+IFN\text{-}\gamma^+$ or $CD8^+IFN\text{-}\gamma^+$ T cells as indicated in the figure legend. (C) Mean frequencies (with the standard error of the mean, SEM) of IFN-γ, IL-2, or TNF secreting $CD4^+$ and $CD8^+$ T cells are shown. (D) Pie charts summarise the fractions of $CD4^+$ or $CD8^+$ T-cells that are positive for one, two, or three cytokines. All possible combinations are shown in the bar chart stratified by vaccination groups, with the ordinate showing the percentage of $CD4^+$ or CD8 T cells. Single points indicate T-cell responses of individual mice.




**Supplemental Figure I-13. Efficacy of single and dual antigen expressing vectors against sporozoite challenge with *Pb*(*Pf*LSA1).** (A) Experimental setup. After immunising eight CD1 mice per group with $10^8$ IU of ChAdOX1 encoding sharkTM/Ii-LSA1, the immune response was boosted with $10^7$ PFU MVA as indicated in the table. A blood sample was taken on day 14; four days later mice were challenged. (B) Immunogenicity data. T-cell responses of blood PBMC to an LSA1 or LSAP2 peptide pool were analysed by ICS. The percentage of $CD4^+$ and $CD8^+$ T cells positive for IFN-γ are shown. Single points indicate T-cell responses of individual mice and red lines denote the median response per group. (C) Efficacy data. Mice were challenged with 1,000 chimeric P. berghei sporozoites expressing P. falciparum LSA1 only on day 18 post immunisation. Blood smears were taken daily from four days after sporozoite challenge and analysed by Giemsa staining and light microscopy to determine parasitaemia. Mice that were negative for blood-stage malaria until 14 days after sporozoite challenge were considered to be sterilely protected. Time to 1% parasitaemia is plotted on a Kaplan-Meier Survival Curve. Data was analysed with the log-rank (Mantel-Cox) test. Number of protected animals and levels of statistical significance when compared to the naïve control group are shown in the table.




**Supplemental Figure I-14. Immunogenicity of a 6-week prime boost regimen with ChAdOX1 and MVA vectors in CD1 mice.** (A) Experimental setup. After immunising eight CD1 mice per group with $10^8$ IU of ChAdOX1, the immune response was boosted with $10^6$ PFU MVA as indicated in the table. A blood sample was taken in week 7; three days later mice were challenged (results in Figure E-15). Immunogenicity data of week 2 (B) and week 7 (C). T-cell responses of blood PBMC to an LSA1 or LSAP2 peptide pool were analysed by ICS. The percentage of $CD4^+$ and $CD8^+$ T cells positive for IFN-γ are shown. Single points indicate T-cell responses of individual mice and red lines denote the median response per group.

# I2 Supplemental Tables

**Supplemental Table I-1.** Summary of cloned plasmid DNA and bacterial artificial chromosomes.

| Plasmid No | Plasmid Name | Cloning Strategy, Description |
|---|---|---|
| p1916 | pChAd63-DEST | Destination vector for ChAd63 virus production |
| p1990 | pENTR4/LPTOS | Empty entry vector with normal hCMV immediate-early promoter |
| P2022 | pENTR4/Mono | Empty entry vector with an intron-less, non-splicing version of the hCMV immediate-early promoter |
| p2084 | pENTR4/LP-ME-TRAP | Cloned by Dr Matthew Dicks; encodes ME-TRAP |
| p2563 | pBAC_ChAdOX1-DEST | Destination vector for ChAdOX1 virus production |
| p2718 | pENTR4/LPTOS-eGFP | Cloned by Dr Matthew Dicks; encodes eGFP |
| p2812 | pENTR4/Mono-LSAP2 | Cloned by Dr Rhea Longley; encodes the liver-stage antigen LSAP2 |
| p2813 | pENTR4/Mono-LSA1 | Cloned by Dr Rhea Longley; encodes the liver-stage antigen LSA1 |
| p2918 | pMVA/TD/GFP-LSA1 | Cloned by Dr Rhea Longley; MVA destination plasmid encoding LSA1 |
| p3072 | pENTR4/LPTOS-(fl)human/Ii-ME-TRAP | Cloned by Dr Sarah Sebastian; encodes ME-TRAP fused to the full-length human Ii |
| p3269 | pENTR4/LPTOS-(tr)human72/Ii-ME-TRAP | Cloned by Dr Sarah Sebastian; encodes ME-TRAP fused to the N-terminal 72 aa of the human Ii |
| p3270 | pENTR4/LPTOS-(tr)human92/Ii-ME-TRAP | Cloned by Dr Sarah Sebastian; encodes ME-TRAP fused to the N-terminal 92 aa of the human Ii |
| p3271 | pENTR4/LPTOS-(tr)human98/Ii-ME-TRAP | Cloned by Dr Sarah Sebastian; encodes ME-TRAP fused to the N-terminal 98 aa of the human Ii |
| p3426 | pENTR4/LPTOS-ME-TRAP | Cloned by Dr Sarah Sebastian; encodes unfused ME-TRAP |
| p3451 | pENTR4/LPTOS-tPA-OVA | Cloned by Daniel Alanine; encodes OVA fused to the N-terminal 33 aa of the human tissue-type plasminogen activator (t-PA) |
| p3651 | pENTR4/LPTOS-(tr)chicken/Ii-ME-TRAP | In-Fusion® cloning of GeneArt™ String in p3269; encodes ME-TRAP fused to the N-terminal 56 aa of chicken Ii (NP_001001613) |
| p3652 | pENTR4/LPTOS-(tr)trout/Ii-ME-TRAP | In-Fusion® cloning of GeneArt™ String in p3269; encodes ME-TRAP fused to the N-terminal 57 aa of trout Ii (NP_001117913) |
| p3654 | pENTR4/LPTOS-(tr)shark/Ii-ME-TRAP | In-Fusion® cloning of GeneArt™ String in p3269; encodes ME-TRAP fused to the N-terminal 65 aa of shark Ii (AEX34752) |
| p3655 | pENTR4/LPTOS-humanTM/Ii-ME-TRAP | In-Fusion® cloning of GeneArt™ String in p3269; encodes ME-TRAP fused to the TMD of the human Ii |
| p3656 | pENTR4/LPTOS-(tr)human(Q64A)/Ii-ME-TRAP | Cloned by Sarah Sebastian; encodes ME-TRAP fused to a version of the N-terminal 72 aa of the human Ii with a point mutation at position 64 |

| Plasmid No | Plasmid Name | Cloning Strategy, Description |
|---|---|---|
| p3778 | pChAd63/LPTOS-(tr)chicken/Ii-ME-TRAP | LR clonase reaction between p1916 and p3651; encodes insert of p3651 in the ChAd63 destination vector for virus production |
| p3779 | pChAd63/LPTOS-(tr)trout/Ii-ME-TRAP | LR clonase reaction between p1916 and p3652; encodes insert of p3652 in the ChAd63 destination vector for virus production |
| p3780 | pChAd63/LPTOS-(tr)shark/Ii-ME-TRAP | LR clonase reaction between p1916 and p3654; encodes insert of p3654 in the ChAd63 destination vector for virus production |
| p3781 | pChAd63/LPTOS-humanTM/Ii-ME-TRAP | LR clonase reaction between p1916 and p3655; encodes insert of p3655 in the ChAd63 destination vector for virus production |
| p3782 | pChAd63/LPTOS-(tr)human(Q64A)/Ii-ME-TRAP | LR clonase reaction between p1916 and p3656; encodes insert of p3656 in the ChAd63 destination vector for virus production |
| p3849 | pENTR4/LPTOS-humanCT/Ii-ME-TRAP | Site-directed deletion in p3269; encodes ME-TRAP fused to the cytoplasmic tail of the human Ii |
| p3850 | pENTR4/LPTOS-humanV1/Ii-ME-TRAP | Site-directed deletion in p3269; encodes ME-TRAP fused to parts of the cytoplasmic tail of the human Ii |
| p3851 | pENTR4/LPTOS-humanV2/Ii-ME-TRAP | Site-directed deletion in p3269; encodes ME-TRAP fused to parts of the cytoplasmic tail of the human Ii |
| p3852 | pENTR4/LPTOS-humanV3/Ii-ME-TRAP | Site-directed deletion in p3269; encodes ME-TRAP fused to parts of the cytoplasmic tail of the human Ii |
| p3853 | pENTR4/LPTOS-(tr)zebrafish/Ii-ME-TRAP | In-Fusion® cloning of GeneArt™ String in p3269; encodes ME-TRAP fused to the N-terminal 54 aa of zebra fish Ii (NP_571447) |
| p3854 | pENTR4/LPTOS-(tr)zebrafish65/Ii-ME-TRAP | In-Fusion® cloning of GeneArt™ String in p3269; encodes ME-TRAP fused to the N-terminal 58 aa of zebra fish Ii (NP_571665) |
| p3855 | pENTR4/LPTOS-(tr)frog/Ii-ME-TRAP | In-Fusion® cloning of GeneArt™ String in p3269; encodes ME-TRAP fused to the N-terminal 58 aa of frog Ii (NP_001184041) |
| p3856 | pENTR4/LPTOS-(tr)mandarinfish/Ii-ME-TRAP | In-Fusion® cloning of GeneArt™ String in p3269; encodes ME-TRAP fused to the N-terminal 61 aa of mandarin fish Ii (AAS77256) |
| p3857 | pENTR4/LPTOS-(tr)mallard/Ii-ME-TRAP | In-Fusion® cloning of GeneArt™ String in p3269; encodes ME-TRAP fused to the N-terminal 64 aa of mallard Ii (XP_005010602) |
| p3858 | pENTR4/LPTOS-(tr)grouper/Ii-ME-TRAP | In-Fusion® cloning of GeneArt™ String in p3269; encodes ME-TRAP fused to the N-terminal 61 aa of grouper Ii (AEA39679) |
| p3881 | pChAd63/LPTOS-humanCT/Ii-ME-TRAP | LR clonase reaction between p1916 and p3849; encodes insert of p3849 in the ChAd63 destination vector for virus production |
| p3882 | pChAd63/LPTOS-humanV1/Ii-ME-TRAP | LR clonase reaction between p1916 and p3850; encodes insert of p3850 in the ChAd63 destination vector for virus production |

| Plasmid No | Plasmid Name | Cloning Strategy, Description |
|---|---|---|
| p3883 | pChAd63/LPTOS-humanV2/Ii-ME-TRAP | LR clonase reaction between p1916 and p3851; encodes insert of p3851 in the ChAd63 destination vector for virus production |
| p3884 | pChAd63/LPTOS-humanV3/Ii-ME-TRAP | LR clonase reaction between p1916 and p3852; encodes insert of p3852 in the ChAd63 destination vector for virus production |
| p3885 | pChAd63/LPTOS-(tr)zebrafish/Ii-ME-TRAP | LR clonase reaction between p1916 and p3853; encodes insert of p3853 in the ChAd63 destination vector for virus production |
| p3886 | pChAd63/LPTOS-(tr)zebrafish65/Ii-ME-TRAP | LR clonase reaction between p1916 and p3854; encodes insert of p3854 in the ChAd63 destination vector for virus production |
| p3887 | pChAd63/LPTOS-(tr)frog/Ii-ME-TRAP | LR clonase reaction between p1916 and p3855; encodes insert of p3855 in the ChAd63 destination vector for virus production |
| p3888 | pChAd63/LPTOS-(tr)mandarinfish/Ii-ME-TRAP | LR clonase reaction between p1916 and p3856; encodes insert of p3856 in the ChAd63 destination vector for virus production |
| p3889 | pChAd63/LPTOS-(tr)mallard/Ii-ME-TRAP | LR clonase reaction between p1916 and p3857; encodes insert of p3857 in the ChAd63 destination vector for virus production |
| p3890 | pChAd63/LPTOS-(tr)grouper/Ii-ME-TRAP | LR clonase reaction between p1916 and p3858; encodes insert of p3858 in the ChAd63 destination vector for virus production |
| p4025 | pENTR4/LPTOS-(fl)trout/Ii-ME-TRAP | In-Fusion® cloning of GeneArt™ String in p3269; encodes ME-TRAP fused to the full-length trout Ii (NP_001117913) |
| p4026 | pENTR4/LPTOS-(fl)shark/Ii-ME-TRAP | In-Fusion® cloning of GeneArt™ String in p3269; encodes ME-TRAP fused to full-length shark Ii (AEX34752) |
| p4027 | pChAd63/LPTOS-(fl)trout/Ii-ME-TRAP | LR clonase reaction between p1916 and p4025; encodes insert of p4025 in the ChAd63 destination vector for virus production |
| p4028 | pChAd63/LPTOS-(fl)shark/Ii-ME-TRAP | LR clonase reaction between p1916 and p4026; encodes insert of p4026 in the ChAd63 destination vector for virus production |
| p4073 | pENTR4/LPTOS-(tr)mouse/Ii-ME-TRAP | In-Fusion® cloning of GeneArt™ String in p3269; encodes ME-TRAP fused to the N-terminal 55 aa of mouse Ii (NP_034675) |
| p4074 | pENTR4/LPTOS-(fl)mouse/Ii-ME-TRAP | In-Fusion® cloning of GeneArt™ String in p3269; encodes ME-TRAP fused to the full-length mouse Ii (NP_034675) |
| p4075 | pChAd63/LPTOS-(tr)mouse/Ii-ME-TRAP | LR clonase reaction between p1916 and p4073; encodes insert of p4073 in the ChAd63 destination vector for virus production |
| p4076 | pChAd63/LPTOS-(fl)mouse/Ii-ME-TRAP | LR clonase reaction between p1916 and p4074; encodes insert of p4074 in the ChAd63 destination vector for virus production |
| p4290 | pENTR4/Mono-tPA-LSA1 | In-Fusion® cloning of GeneArt™ String in p2813; encodes LSA1 fused to the N-terminal 33 aa of the human tissue-type plasminogen activator (t-PA) |

| Plasmid No | Plasmid Name | Cloning Strategy, Description |
|---|---|---|
| p4291 | pENTR4/Mono-(tr)trout/Ii-LSA1 | In-Fusion® cloning of PCR fragment from p3652 in p2813; encodes LSA1 fused to the N-terminal 57 aa of trout Ii (NP_001117913) |
| p4292 | pENTR4/Mono-(tr)shark/Ii-LSA1 | In-Fusion® cloning of PCR fragment from p3654 in p2813; encodes LSA1 fused to the N-terminal 65 aa of shark Ii (AEX34752) |
| p4293 | pENTR4/Mono-tPA-LSAP2 | In-Fusion® cloning of GeneArt™ String in p2812; encodes LSAP2 fused to the N-terminal 33 aa of the human tissue-type plasminogen activator (t-PA) |
| p4294 | pENTR4/Mono-(tr)trout/Ii-LSAP2 | In-Fusion® cloning of PCR fragment from p3652 in p2812; encodes LSAP2 fused to the N-terminal 57 aa of trout Ii (NP_001117913) |
| p4295 | pENTR4/Mono-(tr)shark/Ii-LSAP2 | In-Fusion® cloning of PCR fragment from p3654 in p2812; encodes LSAP2 fused to the N-terminal 65 aa of shark Ii (AEX34752) |
| p4296 | pBAC_ChAdOX1/Mono-tPA-LSA1 | LR clonase reaction between p4290 and p2563; encodes insert of p4290 in the ChAdOX1 destination vector for virus production |
| p4297 | pBAC_ChAdOX1/Mono-(tr)trout/Ii-LSA1 | LR clonase reaction between p4291 and p2563; encodes insert of p4291 in the ChAdOX1 destination vector for virus production |
| p4298 | pBAC_ChAdOX1/Mono-(tr)shark/Ii-LSA1 | LR clonase reaction between p4292 and p2563; encodes insert of p4292 in the ChAdOX1 destination vector for virus production |
| p4299 | pBAC_ChAdOX1/Mono-tPA-LSAP2 | LR clonase reaction between p4293 and p2563; encodes insert of p4293 in the ChAdOX1 destination vector for virus production |
| p4300 | pBAC_ChAdOX1/Mono-(tr)trout/Ii-LSAP2 | LR clonase reaction between p4294 and p2563; encodes insert of p4294 in the ChAdOX1 destination vector for virus production |
| p4301 | pBAC_ChAdOX1/Mono-(tr)shark/Ii-LSAP2 | LR clonase reaction between p4295 and p2563; encodes insert of p4295 in the ChAdOX1 destination vector for virus production |
| p4414 | pENTR4/Mono-troutTM/Ii-LSA1 | In-Fusion® cloning of GeneArt™ String in p2813; encodes LSA1 fused to the TMD of trout Ii (NP_001117913) |
| p4415 | pENTR4/Mono-sharkTM/Ii-LSA1 | In-Fusion® cloning of GeneArt™ String in p2813; encodes LSA1 fused to the TMD of shark Ii (AEX34752) |
| p4416 | pENTR4/Mono-troutTM/II-LSAP2 | In-Fusion® cloning of GeneArt™ String in p2812; encodes LSAP2 fused to the TMD of trout Ii (NP_001117913) |
| p4417 | pENTR4/Mono-sharkTM/Ii-LSAP2 | In-Fusion® cloning of GeneArt™ String in p2812; encodes LSAP2 fused to the TMD of shark Ii (AEX34752) |
| p4435 | pENTR4/Mono-tPA-LSA1-LSAP2 | Insert of p2812 replaced by insert of p4451 (RE digest & ligation); LSA1 and LSAP2 are linked with a GGGPGGG peptide linker and fused to the N-terminal 33 aa of the human tissue-type plasminogen activator (t-PA) |
| p4436 | pENTR4/Mono-(tr)trout/Ii-LSA1-LSAP2 | In-Fusion® cloning of GeneArt™ String in p4435; LSA1 and LSAP2 are linked with a GGGPGGG peptide linker and fused to the N-terminal 57 aa of trout Ii (NP_001117913) |

| Plasmid No | Plasmid Name | Cloning Strategy, Description |
|---|---|---|
| p4437 | pENTR4/Mono-(tr)shark/Ii-LSA1-LSAP2 | In-Fusion® cloning of GeneArt™ String in p4435; LSA1 and LSAP2 are linked with a GGGPGGG peptide linker and fused to the N-terminal 65 aa of shark Ii (AEX34752) |
| p4438 | pENTR4/Mono-troutTM/Ii-LSA1-LSAP2 | In-Fusion® cloning of GeneArt™ String in p4435; LSA1 and LSAP2 are linked with a GGGPGGG peptide linker and fused to the TMD of trout Ii (NP_001117913) |
| p4439 | pENTR4/Mono-sharkTM/Ii-LSA1-LSAP2 | In-Fusion® cloning of GeneArt™ String in p4435; LSA1 and LSAP2 are linked with a GGGPGGG peptide linker and fused to the TMD of shark Ii (AEX34752) |
| p4440 | pBAC_ChAdOX1/Mono-troutTM/Ii-LSA1 | LR clonase reaction between p4414 and p2563; encodes insert of p4414 in the ChAdOX1 destination vector for virus production |
| p4441 | pBAC_ChAdOX1/Mono-sharkTM/Ii-LSA1 | LR clonase reaction between p4415 and p2563; encodes insert of p4415 in the ChAdOX1 destination vector for virus production |
| p4442 | pBAC_ChAdOX1/Mono-troutTM/Ii-LSAP2 | LR clonase reaction between p4416 and p2563; encodes insert of p4416 in the ChAdOX1 destination vector for virus production |
| p4443 | pBAC_ChAdOX1/Mono-sharkTM/Ii-LSAP2 | LR clonase reaction between p4417 and p2563; encodes insert of p4417 in the ChAdOX1 destination vector for virus production |
| p4444 | pBAC_ChAdOX1/Mono-tPA-LSA1-LSAP2 | LR clonase reaction between p4435 and p2563; encodes insert of p4435 in the ChAdOX1 destination vector for virus production |
| p4445 | pBAC_ChAdOX1/Mono-(tr)trout/Ii-LSA1-LSAP2 | LR clonase reaction between p4436 and p2563; encodes insert of p4436 in the ChAdOX1 destination vector for virus production |
| p4446 | pBAC_ChAdOX1/Mono-(tr)shark/Ii-LSA1-LSAP2 | LR clonase reaction between p4437 and p2563; encodes insert of p4437 in the ChAdOX1 destination vector for virus production |
| p4447 | pBAC_ChAdOX1/Mono-troutTM/Ii-LSA1-LSAP2 | LR clonase reaction between p4438 and p2563; encodes insert of p4438 in the ChAdOX1 destination vector for virus production |
| p4448 | pBAC_ChAdOX1/Mono-sharkTM/Ii-LSA1-LSAP2 | LR clonase reaction between p4439 and p2563; encodes insert of p4439 in the ChAdOX1 destination vector for virus production |
| p4451 | pGeneartK12-tPA-LSA1-LSAP2 | Plasmid encoding the tPA-LSA1-LSAP2 gene purchased from Geneart; LSA1 and LSAP2 are linked with a GGGPGGG peptide linker and fused to the N-terminal 33 aa of the human tissue-type plasminogen activator (t-PA) |
| p4503 | pMVA/TD/GFP-tPA-LSA1-LSAP2 | Insert of p2918 replaced by insert of p4435 (RE digest & ligation); encodes insert of p4435 in the MVA destination vector for virus production |
| p4504 | pMVA/TD/GFP-(tr)trout/Ii-LSA1-LSAP2 | Insert of p2918 replaced by insert of p4436 (RE digest & ligation); encodes insert of p4436 in the MVA destination vector for virus production |

| Plasmid No | Plasmid Name | Cloning Strategy, Description |
|---|---|---|
| p4505 | pMVA/TD/GFP-(tr)shark/li-LSA1-LSAP2 | Insert of p2918 replaced by insert of p4437 (RE digest & ligation); encodes insert of p4437 in the MVA destination vector for virus production |
| p4506 | pMVA/TD/GFP-troutTM/li-LSA1-LSAP2 | Insert of p2918 replaced by insert of p4438 (RE digest & ligation); encodes insert of p4438 in the MVA destination vector for virus production |
| p4507 | pMVA/TD/GFP-sharkTM/li-LSA1-LSAP2 | Insert of p2918 replaced by insert of p4439 (RE digest & ligation); encodes insert of p4439 in the MVA destination vector for virus production |
| p4555 | pMVA/TD/GFP-tPA-LSA1 | Insert of p2919 replaced by insert of p4290 (RE digest & ligation); encodes insert of p4290 in the MVA destination vector for virus production |
| p4556 | pMVA/TD/GFP-tPA-LSAP2 | Insert of p2918 replaced by insert of p4293 (RE digest & ligation); encodes insert of p4293 in the MVA destination vector for virus production |
| p4557 | pMVA/TD/GFP-sharkTM/li-LSA1 | Insert of p2918 replaced by insert of p4415 (RE digest & ligation); encodes insert of p4415 in the MVA destination vector for virus production |
| p4558 | pMVA/TD/GFP-sharkTM/li-LSAP2 | Insert of p2918 replaced by insert of p4417 (RE digest & ligation); encodes insert of p4417 in the MVA destination vector for virus production |
| p4559 | pENTR4/LPTOS-ME-TRAP(w/o_eSP) | Fragment of p2084 replaced by fragment of p2962 (RE digest & ligation); encodes ME-TRAP without the endogenous signal peptide of TRAP |
| p4582 | pENTR4/LPTOS-humanTM(gal47aaa)/li-ME-TRAP | Site-directed mutagenesis of p3655 |
| p4583 | pENTR4/LPTOS-humanTM(ytg50aaa)/li-ME-TRAP | Site-directed mutagenesis of p3655 |
| p4584 | pENTR4/LPTOS-humanTM(fsi53aaa)/li-ME-TRAP | Site-directed mutagenesis of p3655 |
| p4585 | pENTR4/LPTOS-humanTM(lvt56aaa)/li-ME-TRAP | Site-directed mutagenesis of p3655 |
| p4586 | pENTR4/LPTOS-humanTM(lll59aaa)/li-ME-TRAP | Site-directed mutagenesis of p3655 |
| p4587 | pENTR4/LPTOS-humanTM(agq62aaa)/li-ME-TRAP | Site-directed mutagenesis of p3655 |
| p4588 | pENTR4/LPTOS-humanTM(att65aaa)/li-ME-TRAP | Site-directed mutagenesis of p3655 |
| p4589 | pENTR4/LPTOS-humanTM(ayf68aaa)/li-ME-TRAP | Site-directed mutagenesis of p3655 |

| Plasmid No | Plasmid Name | Cloning Strategy, Description |
|---|---|---|
| p4590 | pENTR4/LPTOS-humanTM(Iy71aa)/Ii-ME-TRAP | Site-directed mutagenesis of p3655 |
| p4591 | pENTR4/LPTOS-humanTM(Mut02)/Ii-ME-TRAP | Site-directed mutagenesis of p3655 |
| p4592 | pENTR4/LP-ME-TRAP-LSA1 | InFusion® cloning of PCR fragment from p4290 in p2084; encodes an ME-TRAP-LSA1 fusion construct without a linker between the antigens |
| p4593 | pENTR4/LP-ME-TRAP-L-LSA1 | InFusion® cloning of GeneArt™ String in p4592; introduces a peptide linker (GGGPGGG) between ME-TRAP and LSA1 |
| p4604 | pENTR4/Mono-sharkTM/Ii-L-LSA1 | InFusion® cloning of GeneArt™ String in p4415; introduces a peptide linker (3× GGGGS) between the TMD of the shark Ii and LSA1 |
| p4605 | pENTR4/LPTOS-NC/TMD-ME-TRAP | In-Fusion® cloning of GeneArt™ String in p3655; encodes ME-TRAP fused to the TMD of the fusion protein of the Newcastle disease virus (P12572.2) |
| p4606 | pENTR4/LPTOS-sharkTM/Ii-ME-TRAP | In-Fusion® cloning of GeneArt™ String in p3655; encodes ME-TRAP fused to the TMD of the shark Ii (AEX34752) |
| p4613 | pChAd63/LP-ME-TRAP(w/o_eSP) | LR clonase reaction between p4559 and p1916; encodes insert of p4559 in the ChAd63 destination vector for virus production |
| p4614 | pChAd63/LPTOS-humanTM(lll59aaa)/Ii-ME-TRAP | LR clonase reaction between p4586 and p1916; encodes insert of p4586 in the ChAd63 destination vector for virus production |
| p4615 | pChAd63/LPTOS-ME-TRAP-L-LSA1 | LR clonase reaction between p4593 and p1916; encodes insert of p4593 in the ChAd63 destination vector for virus production |
| p4616 | pChAd63/LPTOS-NC/TMD-ME-TRAP | LR clonase reaction between p4594 and p1916; encodes insert of p4594 in the ChAd63 destination vector for virus production |
| p4617 | pChAd63/LPTOS-sharkTM/Ii-ME-TRAP | LR clonase reaction between p4606 and p1916; encodes insert of p4606 in the ChAd63 destination vector for virus production |
| p4618 | pBAC_ChAdOX1/Mono-sharkTM/Ii-L-LSA1 | LR clonase reaction between p4604 and p2563; encodes insert of p4604 in the ChAdOX1 destination vector for virus production |
| p4822 | pENTR4/Mono-sharkTM/Ii-LSA1woTMD | In-Fusion® cloning of GeneArt™ String in p4415; encodes LSA1 without its predicted TMD fused to the TMD of shark Ii (AEX34752) |
| p4823 | pENTR4/Mono-tPA-LSA1woTMD | In-Fusion® cloning of GeneArt™ String in p4415; encodes LSA1 without its predicted TMD fused to human t-PA |
| p4824 | pENTR4/Mono-NC/TMD-LSA1 | In-Fusion® cloning of GeneArt™ String in p4415; encodes LSA1 fused the the fusion protein of the Newcastle disease virus (P12572.2) |

| Plasmid No | Plasmid Name | Cloning Strategy, Description |
|---|---|---|
| p4825 | pENTR4/Mono-NC/TMD-LSA1woTMD | In-Fusion® cloning of GeneArt™ String in p4415; encodes LSA1without its predicted TMD fused the fusion protein of the Newcastle disease virus (P12572.2) |
| p4826 | pENTR4/LPTOS-AM/TMD-ME-TRAP | In-Fusion® cloning of GeneArt™ String in p4415; encodes ME-TRAP fused to the TMD of the fusion protein of the avian metapneumovirus (Q2Y2M3) |
| p4827 | pENTR4/LPTOS-M2/TMD-ME-TRAP | In-Fusion® cloning of GeneArt™ String in p4415; encodes ME-TRAP fused to the TMD of the influenza M2 protein TMD (Q67211) |
| p4828 | pBAC_ChAdOX1/Mono-sharkTM/Ii-LSA1woTMD | LR clonase reaction between p4822 and p2563; encodes insert of p4822 in the ChAdOX1 destination vector for virus production |
| p4829 | pBAC_ChAdOX1/Mono-tPA-LSA1woTMD | LR clonase reaction between p4823 and p2563; encodes insert of p4823 in the ChAdOX1 destination vector for virus production |
| p4830 | pBAC_ChAdOX1/Mono-NC/TMD-LSA1 | LR clonase reaction between p4824 and p2563; encodes insert of p4824 in the ChAdOX1 destination vector for virus production |
| p4831 | pBAC_ChAdOX1/Mono-NC/TMD-LSA1woTMD | LR clonase reaction between p4825 and p2563; encodes insert of p4825 in the ChAdOX1 destination vector for virus production |
| p4832 | pChAd63/LPTOS-AM/TMD-ME-TRAP | LR clonase reaction between p4826 and p1916; encodes insert of p4826 in the ChAdOX1 destination vector for virus production |
| p4833 | pChAd63/LPTOS-M2/TMD-ME-TRAP | LR clonase reaction between p4827 and p1916; encodes insert of p4827 in the ChAdOX1 destination vector for virus production |

**Supplemental Table I-2.** Summary of viral vectors.

| Vector No | Vector Name | Concentration | Description |
|---|---|---|---|
| 879 | ChAd63/LPTOS-tPA-TRIP | 2.30E+10 IU/mL | ChAd63 encoding TRIP |
| 945 | MVA-TRIP | 4.42E+09 PFU/mL | MVA encoding TRIP |
| 1120 | ChAd63/Mono-tPA-LSAP2 | 1.00E+11 IU/mL | ChAd63 encoding LSAP2 fused to the N-terminal 33 aa of the human tissue-type plasminogen activator (t-PA) |
| 1193 | ChAd63/LPTOS-(fl)human/Ii-ME-TRAP | 2.90E+10 IU/mL | ChAd63 encoding ME-TRAP fused to the full-length human Ii |
| 1314 | ChAd63/LPTOS-(tr)human72-ME-TRAP | 3.90E+10 IU/mL | ChAd63 encoding ME-TRAP fused to the N-terminal 72 aa of the human Ii |
| 1300 | ChAd63/LPTOS-ME-TRAP | 8.20E+10 IU/mL | ChAd63 encoding ME-TRAP |
| 1500 | ChAd63/LPTOS-ME-TRAP | 1.10E+11 IU/mL | ChAd63 encoding ME-TRAP |
| 1530 | MVA-tPA-LSA1 | 7.90E+08 PFU/mL | MVA encoding LSA1 fused to the N-terminal 33 aa of the human tissue-type plasminogen activator (t-PA) |
| 1544 | ChAd63/Mono-tPA-LSA1 | 7.80E+10 IU/mL | ChAd63 encoding LSA1 fused to the N-terminal 33 aa of the human tissue-type plasminogen activator (t-PA) |
| 1604 | ChAd63/LPTOS-(tr)chicken/Ii-ME-TRAP | 6.60E+10 IU/mL | ChAd63 encoding ME-TRAP fused to the N-terminal 56 aa of chicken Ii (NP_001001613) |
| 1605 | ChAd63/LPTOS-(tr)trout/Ii-ME-TRAP | 4.70E+10 IU/mL | ChAd63 encoding ME-TRAP fused to the N-terminal 57 aa of trout Ii (NP_001117913) |
| 1606 | ChAd63/LPTOS-(tr)shark/Ii-ME-TRAP | 7.30E+10 IU/mL | ChAd63 encoding ME-TRAP fused to the N-terminal 65 aa of shark Ii (AEX34752) |
| 1607 | ChAd63/LPTOS-humanTM/Ii-ME-TRAP | 9.60E+10 IU/mL | ChAd63 encoding ME-TRAP fused to the TMD of human Ii |
| 1608 | ChAd63/LPTOS-(tr)human(Q64A)-Ii-ME-TRAP | 7.30E+10 IU/mL | ChAd63 encoding ME-TRAP fused to a version of the N-terminal 72 aa of the human Ii with a point mutation at position 64 |
| 1609 | ChAd63/LPTOS-(tr)zebrafish/Ii-ME-TRAP | 3.30E+10 IU/mL | ChAd63 encoding ME-TRAP fused to the N-terminal 54 aa of zebra fish Ii (NP_571447) |
| 1610 | ChAd63/LPTOS-(tr)frog/Ii-ME-TRAP | 5.70E+10 IU/mL | ChAd63 encoding ME-TRAP fused to the N-terminal 58 aa of frog Ii (NP_001184041) |
| 1611 | ChAd63/LPTOS-humanV1/Ii-ME-TRAP | 3.90E+10 IU/mL | ChAd63 encoding ME-TRAP fused to parts of the cytoplasmic tail of the human Ii |
| 1618 | MVA-ME-TRAP | 6.80E+08 PFU/mL | MVA encoding ME-TRAP |

| Vector No | Vector Name | Concentration | Description |
|---|---|---|---|
| 1651 | ChAd63/LPTOS-humanV3/Ii-ME-TRAP | 7.20E+10 IU/mL | ChAd63 encoding ME-TRAP fused to parts of the cytoplasmic tail of the human Ii |
| 1683 | ChAd63/LPTOS-(fl)trout/Ii-ME-TRAP | 3.10E+10 IU/mL | ChAd63 encoding ME-TRAP fused to the full-length trout Ii (NP_001117913) |
| 1684 | ChAd63/LPTOS-(fl)shark/Ii-ME-TRAP | 2.10E+10 IU/mL | ChAd63 encoding ME-TRAP fused to the full-length shark Ii (AEX34752) |
| 1743 | ChAd63/LPTOS-ME-TRAP | 4.50E+10 IU/mL | ChAd63 encoding ME-TRAP |
| 1754 | ChAd63/LPTOS-humanCT/Ii-ME-TRAP | 1.74E+11 IU/mL | ChAd63 encoding ME-TRAP fused to the cytoplasmic tail of the human Ii |
| 1755 | ChAd63/LPTOS-humanV2/Ii-ME-TRAP | 4.35E+10 IU/mL | ChAd63 encoding ME-TRAP fused to parts of the cytoplasmic tail of the human Ii |
| 1756 | ChAd63/LPTOS-(tr)mouse/Ii-ME-TRAP | 1.66E+11 IU/mL | ChAd63 encoding ME-TRAP fused to the N-terminal 55 aa of mouse Ii (NP_034675) |
| 1757 | ChAd63/LPTOS-(fl)mouse/Ii-ME-TRAP | 6.36E+10 IU/mL | ChAd63 encoding ME-TRAP fused to the full-length mouse Ii (NP_034675) |
| 1902 | ChAdOX1/Mono-tPA-LSA1 | 7.56E+09 IU/mL | ChAdOX1 encoding LSA1 fused to the N-terminal 33 aa of the human tissue-type plasminogen activator (t-PA) |
| 1903 | ChAdOX1/Mono-(tr)trout/Ii-LSA1 | 1.77E+10 IU/mL | ChAdOX1 encoding LSA1 fused to the N-terminal 57 aa of trout Ii (NP_001117913) |
| 1904 | ChAdOX1/Mono-(tr)shark/Ii-LSA1 | 2.54E+10 IU/mL | ChAdOX1 encoding LSA1 fused to the N-terminal 65 aa of shark Ii (AEX34752) |
| 1905 | ChAdOX1/Mono-tPA-LSAP2 | 1.95E+10 IU/mL | ChAdOX1 encoding LSAP2 fused to the N-terminal 33 aa of the human tissue-type plasminogen activator (t-PA) |
| 1906 | ChAdOX1/Mono-(tr)trout/Ii-LSAP2 | 2.35E+10 IU/mL | ChAdOX1 encoding LSAP2 fused to the N-terminal 57 aa of trout Ii (NP_001117913) |
| 1907 | ChAdOX1/Mono-(tr)shark/Ii-LSAP2 | 4.56E+10 IU/mL | ChAdOX1 encoding LSAP2 fused to the N-terminal 65 aa of shark Ii (AEX34752) |
| 1940 | ChAdOX1/Mono-tPA-LSA1-LSAP2 | 1.80E+10 IU/mL | ChAdOX1 encoding LSA1 and LSAP2, linked with a GGGPGGG peptide linker and fused to the N-terminal 33 aa of the human tissue-type plasminogen activator (t-PA) |
| 1941 | ChAdOX1/Mono-(tr)shark/Ii-LSA1-LSAP2 | 1.08E+10 IU/mL | ChAdOX1 encoding LSA1 and LSAP2, linked with a GGGPGGG peptide linker and fused to the N-terminal 65 aa of shark Ii (AEX34752) |
| 1942 | ChAdOX1/Mono-sharkTM/Ii-LSA1-LSAP2 | 1.49E+10 IU/mL | ChAdOX1 encoding LSA1 and LSAP2, linked with a GGGPGGG peptide linker and fused to the TMD of shark Ii (AEX34752) |

| Vector No | Vector Name | Concentration | Description |
|---|---|---|---|
| 1943 | ChAdOX1/Mono-sharkTM/Ii-LSA1 | 1.58E+10 IU/mL | ChAdOX1 encoding LSA1 fused to the TMD of shark Ii (AEX34752) |
| 1944 | ChAdOX1/Mono-sharkTM/Ii-LSAP2 | 1.03E+10 IU/mL | ChAdOX1 encoding LSAP2 fused to the TMD of shark Ii (AEX34752) |
| 1945 | ChAdOX1/Mono-(tr)trout/Ii-LSA1-LSAP2 | 7.29E+09 IU/mL | ChAdOX1 encoding LSA1 and LSAP2, linked with a GGGPGGG peptide linker and fused to the N-terminal 57 aa of trout Ii (NP_001117913) |
| 1946 | ChAdOX1/Mono-troutTM/Ii-LSA1-LSAP2 | 9.20E+09 IU/mL | ChAdOX1 encoding LSA1 and LSAP2, linked with a GGGPGGG peptide linker and fused to the TMD of trout Ii (NP_001117913) |
| 1947 | ChAdOX1/Mono-troutTM/Ii-LSA1 | 1.20E+10 IU/mL | ChAdOX1 encoding LSA1 fused to the TMD of trout Ii (NP_001117913) |
| 1948 | ChAdOX1/Mono-troutTM/Ii-LSAP2 | 1.30E+10 IU/mL | ChAdOX1 encoding LSAP2 fused to the TMD of trout Ii (NP_001117913) |
| 1670 | ChAd63-E1(ME-TRAP)-E3(CSN) | 3.20E+10 IU/mL | ChAd63 encoding ME-TRAP in its E1 locus and CSN in its E3 locus |
| 1677 | ChAd63-BiCMV-CSN-ME-TRAP | 3.90E+10 IU/mL | ChAd63 encoding ME-TRAP and CSN under a bidirectional promotor |
| 1720 | MVA-tPA-Falstatin | 1.10E+09 PFU/mL | MVA encoding Falstatin fused to the N-terminal 33 aa of the human tissue-type plasminogen activator (t-PA) |
| 1721 | MVA-tPA-LSA1 | 1.70E+09 PFU/mL | MVA encoding LSA1 fused to the N-terminal 33 aa of the human tissue-type plasminogen activator (t-PA) |
| 1722 | MVA-TRIP | 2.61E+09 PFU/mL | MVA encoding TRIP |
| 2019 | MVA/TD/GFP-tPA-LSA1-LSAP2 | 8.84E+08 PFU/mL | MVA encoding LSA1 and LSAP2, linked with a GGGPGGG peptide linker, and fused to the N-terminal 33 aa of the human tissue-type plasminogen activator (t-PA) |
| 2020 | MVA/TD/GFP-troutTM/Ii-LSA1-LSAP2 | 4.02E+08 PFU/mL | MVA encoding LSA1 and LSAP2, linked with a GGGPGGG peptide linker, and fused to the TMD of trout Ii (NP_001117913) |
| 2021 | MVA/TD/GFP-sharkTM/Ii-LSA1-LSAP2 | 4.74E+08 PFU/mL | MVA encoding LSA1 and LSAP2, linked with a GGGPGGG peptide linker, and fused to the TMD of shark Ii (AEX34752) |
| 2088 | MVA/TD/GFP -tPA-LSAP2 | 5.82E+08 PFU/mL | MVA encoding LSAP2 fused to the N-terminal 33 aa of the human tissue-type plasminogen activator (t-PA) |
| 2116 | MVA/TD/GFP-tPA-LSA1 | 1.07E+09 PFU/mL | MVA encoding LSA1 fused to the N-terminal 33 aa of the human tissue-type plasminogen activator (t-PA) |

| Vector No | Vector Name | Concentration | Description |
|---|---|---|---|
| 2117 | MVA/TD/GFP-tPA-LSAP2 | 1.30E+09 PFU/mL | MVA encoding LSAP2 fused to the N-terminal 33 aa of the human tissue-type plasminogen activator (t-PA) |
| 2118 | MVA/TD/GFP-sharkTM/Ii-LSA1 | 9.46E+08 PFU/mL | MVA encoding LSA1 fused to the TMD of shark Ii (AEX34752) |
| 2142 | ChAd63/Mono-tPA-LSA1 | 1.92E+10 IU/mL | ChAd63 encoding LSA1 fused to the N-terminal 33 aa of the human tissue-type plasminogen activator (t-PA) |
| 2172 | MVA-tPA-LSA1 | 1.75E+09 PFU/mL | MVA encoding LSA1 fused to the N-terminal 33 aa of the human tissue-type plasminogen activator (t-PA) |
| 2178 | ChAd63/LPTOS-ME-TRAP(w/o_eSP) | 5.69E+10 IU/mL | ChAd63 encoding ME-TRAP without the endogenous signal peptide of TRAP |
| 2179 | ChAd63/LPTOS-humanTM(lll59aaa)/Ii-ME-TRAP | 5.36E+10 IU/mL | ChAd63 encoding ME-TRAP fused to a mutated version of the human Ii TMD |
| 2180 | ChAd63/LPTOS-ME-TRAP-L-LSA1 | 2.70E+10 IU/mL | ChAd63 encoding ME-TRAP and LSA1 (separated by a GGGPGGG peptide linker |
| 2181 | ChAd63/LPTOS-NC/TMD-ME-TRAP | 2.76E+10 IU/mL | ChAd63 encoding ME-TRAP fused to the TMD of the fusion protein of the Newcastle disease virus (P12572.2) |
| 2188 | ChAd63/LPTOS-sharkTM/Ii-ME-TRAP | 3.78E+10 IU/mL | ChAd63 encoding ME-TRAP fused to the TMD of shark Ii (AEX34752) |
| 2189 | ChAdOX1/Mono-sharkTM/Ii-L-LSA1 | 2.10E+10 IU/mL | ChAdOX1 encoding LSA1 fused the TMD of shark Ii (separated by a peptide linker) |
| 2476 | ChAd63/LPTOS-AM/TMD-ME-TRAP | 3.32E+09 IU/mL | ChAd63 encoding ME-TRAP fused the TMD of the fusion protein of the avian metapneumovirus |
| 2477 | ChAd63/LPTOS-M2/TMD-ME-TRAP | 1.89E+09 IU/mL | ChAd63 encoding ME-TRAP fused the TMD of influenza A virus M2 protein |
| 2350 | ChAdOX1/Mono-sharkTM/Ii-LSA1woTMD | 1.23E+10 IU/mL | ChAdOX1 encoding LSA1 (without its N-terminal TMD) fused the TMD of shark Ii (separated by a peptide linker) |
| 2351 | ChAdOX1/Mono-tPA-LSA1woTMD | 1.69E+10 IU/mL | ChAdOX1 encoding LSA1 (without its N-terminal TMD) fused the N-terminal 33 aa of the human tissue-type plasminogen activator (t-PA) |
| 2520 | ChAdOX1/Mono-NC/TMD-LSA1 | Not yet defined | ChAdOX1 encoding fused to the TMD of the fusion protein of the Newcastle disease virus (P12572.2) |
| 2533 | ChAdOX1/Mono-NC/TMD-LSA1woTMD | Not yet defined | ChAdOX1 encoding LSA1 (without its N-terminal TMD) fused to the TMD of the fusion protein of the Newcastle disease virus (P12572.2) |

**Supplemental Table I-3. Homology Analysis of full-length Ii sequences.** Full-length Ii sequences of various species were compared for homology to the full-length human and mouse Ii sequences. Entitled name, GenBank identifier/NCBI Reference Sequence, and sequence homology with (fl)human/Ii or (fl)mouse/Ii sequence are listed. Homology was analysed using the ClustalW algorithm in DNAStar® Megalign. Constructs in red font were fused to the N-terminal end of ME-TRAP, cloned into pENTR™4-LPTOS plasmid, and also produced in ChAd63 vectors.

| Name | GenBank Identifier/ NCBI Reference Sequence | Homology with (fl)human/Ii | Homology with (fl)mouse/Ii |
|---|---|---|---|
| (fl)human/Ii | NP_004346 | 100% | 73.8% |
| (fl)orangutan/Ii | NP_001124630.1 | 98.7% | 32.2% |
| (fl)macaque/Ii | XP_002804624.1 | 86.8% | 39.1% |
| (fl)floridamantee/Ii | XP_004384950.1 | 78.3% | 29.1% |
| (fl)cat/Ii | XP_003981534.1 | 77.3% | 33.6% |
| (fl)walrus/Ii | XP_004402873.1 | 79.5% | 29.6% |
| (fl)mouse/Ii | NP_034675 | 73.8% | 100% |
| (fl)rat/Ii | NP_037201.1 | 74.9% | 86% |
| (fl)whale/Ii | XP_004280397.1 | 76.2% | 75.9% |
| (fl)dolphin/Ii | XP_004326859.1 | 77.1% | 75.5% |
| (fl)boar/Ii | NP_998939.1 | 77.6% | 77.4% |
| (fl)sheep/Ii | XP_004009025.1 | 78.4% | 78.7% |
| (fl)cattle/Ii | BAA12156.1 | 79.9% | 79.2% |
| (fl)rabbit/Ii | XP_002710211.1 | 73.6% | 76.2% |
| (fl)duck/Ii | AEB71788.1 | 45.5% | 42.9% |
| (fl)mallard/Ii | XP_005010602.1 | 42.9% | 40.2% |
| (fl)goose/Ii | ADK11994.1 | 44.6% | 43.3% |
| (fl)quail/Ii | ADG01642.1 | 41.1% | 38.8% |
| (fl)chicken/Ii | NP_001001613.1 | 40% | 37.2% |
| (fl)pigeon/Ii | AAX47311.1 | 46.5% | 44.9% |
| (fl)frog/Ii | NP_001184041.1 | 27.8% | 28.5% |
| (fl)grouper/Ii | AEA39679.1 | 23.7% | 22.6% |
| (fl)mandarinfish/Ii | AAS77256.1 | 22.5% | 22.5% |
| (fl)zebrafish65/Ii | NP_571665.1 | 20.1% | 20.7% |
| (fl)carp/Ii | AEZ67439.1 | 19.1% | 18.6% |
| (fl)zebrafish/Ii | NP_571447.1 | 16.4% | 16.9% |
| (fl)trout/Ii | NP_001117913.1 | 20% | 18.4% |
| (fl)shark/Ii | AEX34752.1 | 21.9% | 22.1% |

# I3 Peptides

**Supplemental Table I-4.** Peptide sequences of *P. falciparum 3D7* LSA1.

| Peptide ID | Peptide Sequence |
|---|---|
| LSA1-1 | MKHILYISFYFILVNLLIFH |
| LSA1-2 | FILVNLLIFHINGKIIKNSE |
| LSA1-3 | INGKIIKNSEKDEIIKSNLR |
| LSA1-4 | KDEIIKSNLRSGSSNSRNRI |
| LSA1-5 | SGSSNSRNRINEEKHEKKHV |
| LSA1-6 | NEEKHEKKHVLSHNSYEKTK |
| LSA1-7 | LSHNSYEKTKNNENNKFFDK |
| LSA1-8 | NNENNKFFDKDKELTMSNVK |
| LSA1-9 | DKELTMSNVKNVSQTNFKSL |
| LSA1-10 | NVSQTNFKSLLRNLGVSENI |
| LSA1-11 | LRNLGVSENIFLKENKLNKE |
| LSA1-12 | FLKENKLNKEGKLIEHIIND |
| LSA1-13 | GKLIEHIINDDDDKKKYIKG |
| LSA1-14 | DDDKKKYIKGQDENRQEDPQ |
| LSA1-15 | QDENRQEDPQRDLEQRKADT |
| LSA1-16 | RDLEQRKADTKKNLERKKEH |
| LSA1-17 | KKNLERKKEHGDVLAEDLYG |
| LSA1-18 | GDVLAEDLYGRLEIPAIELP |
| LSA1-19 | RLEIPAIELPSENERGYYIP |
| LSA1-20 | SENERGYYIPHQSSLPQDNR |
| LSA1-21 | HQSSLPQDNRGNSRDSKEIS |
| LSA1-22 | GNSRDSKEISIIEKTNRESI |
| LSA1-23 | IIEKTNRESITTNVEGRRDI |
| LSA1-24 | TTNVEGRRDIHKGHLEEKKD |
| LSA1-25 | HKGHLEEKKDGSIKPEQKED |
| LSA1-26 | GSIKPEQKEDKSADIQNHTL |
| LSA1-27 | KSADIQNHTLETVNISDVND |
| LSA1-28 | ETVNISDVNDFQISKYEDEI |
| LSA1-29 | FQISKYEDEISAEYDDSLID |
| LSA1-30 | SAEYDDSLIDEEEDDEDLDE |
| LSA1-31 | EEEDDEDLDEFKPIVQYDNF |
| LSA1-32 | FKPIVQYDNFQDEENIGIYK |
| LSA1-33 | QDEENIGIYKELEDLIEKNE |
| LSA1-34 | ELEDLIEKNENLDDLDEGIE |
| LSA1-35 | NLDDLDEGIEKSSEELSEEK |

| Peptide ID | Peptide Sequence |
|---|---|
| LSA1-36 | KSSEELSEEKIKKGKKYEKT |
| LSA1-37 | IKKGKKYEKTKDNNFKPNDK |
| LSA1-38 | KDNNFKPNDKSLYDEHIKKY |
| LSA1-39 | SLYDEHIKKYKNDKQVNKEK |
| LSA1-40 | KNDKQVNKEKEKFIKSLFHI |
| LSA1-41 | EKFIKSLFHIFDGDNEILQI |
| LSA1-42 | FDGDNEILQIVDELSEDITK |
| LSA1-43 | VDELSEDITKYFMKL |

**Supplemental Table I-5.** Peptide sequences of *P. falciparum 3D7* LSAP2.

| Peptide ID | Peptide Sequence |
|---|---|
| LSAP2-1 | MKRGLCCVLLLCGAVFVSPS |
| LSAP2-2 | LCGAVFVSPSQEIHARFRRG |
| LSAP2-3 | QEIHARFRRGMWLCKRGLSV |
| LSAP2-4 | MWLCKRGLSVNDTTKCDVPC |
| LSAP2-5 | NDTTKCDVPCKDFYMLFLSN |
| LSAP2-6 | KDFYMLFLSNKKEKIKCGTF |
| LSAP2-7 | KKEKIKCGTFFGYIFLSKFM |
| LSAP2-8 | FGYIFLSKFMKLSISLLLLA |
| LSAP2-9 | KLSISLLLLALIQNILLSNV |
| LSAP2-10 | LIQNILLSNVSLISGSHLYK |
| LSAP2-11 | SLISGSHLYKRNSRKFAEGY |
| LSAP2-12 | RNSRKFAEGYMKGSGSEKNV |
| LSAP2-13 | MKGSGSEKNVYLSNKNKEIN |
| LSAP2-14 | YLSNKNKEINMNQQSDNKMC |
| LSAP2-15 | MNQQSDNKMCDECDDMNQPG |
| LSAP2-16 | DECDDMNQPGDVNKNDKTSN |
| LSAP2-17 | DVNKNDKTSNDQANSSDSDC |
| LSAP2-18 | DQANSSDSDCEPLPFGLKPS |
| LSAP2-19 | EPLPFGLKPSDLNRKVTEED |
| LSAP2-20 | DLNRKVTEEDLERMIIELPG |
| LSAP2-21 | LERMIIELPGKLERKDMYLI |
| LSAP2-22 | KLERKDMYLIWHYSHSLLRD |
| LSAP2-23 | WHYSHSLLRDKFNKMKSSLW |
| LSAP2-24 | KFNKMKSSLWSICGKLAHEH |
| LSAP2-25 | SICGKLAHEHKLPFKIKMKK |

| Peptide ID | Peptide Sequence |
|---|---|
| LSAP2-26 | KLPFKIKMKKWWKCCGHVTD |
| LSAP2-27 | WWKCCGHVTDELLIKEHDDY |
| LSAP2-28 | ELLIKEHDDYNSIYNYINNE |
| LSAP2-29 | NSIYNYINNESSSREQFLIF |
| LSAP2-30 | SSSREQFLIFLNMIKHSWTT |
| LSAP2-31 | LNMIKHSWTTFTMETFIKCK |
| LSAP2-32 | FTMETFIKCKISLENNMRNV |
| LSAP2-33 | ISLENNMRNVTN |

**Supplemental Table I-6.** Peptide sequences of *P. falciparum 3D7* UIS3.

| Peptide ID | Peptide Sequence |
|---|---|
| UIS3-1 | MKVSKLVLFAHIFFIINILC |
| UIS3-2 | HIFFIINILCQYICLNASKV |
| UIS3-3 | QYICLNASKVNKKGKIAEEK |
| UIS3-4 | NKKGKIAEEKKRKNIKNIDK |
| UIS3-5 | KRKNIKNIDKAIEEHNKRKK |
| UIS3-6 | AIEEHNKRKKLIYYSLIASG |
| UIS3-7 | LIYYSLIASGAIASVAAILG |
| UIS3-8 | AIASVAAILGLGYYGYKKSR |
| UIS3-9 | LGYYGYKKSREDDLYYNKYL |
| UIS3-10 | EDDLYYNKYLEYRNGEYNIK |
| UIS3-11 | EYRNGEYNIKYQDGAIASTS |
| UIS3-12 | YQDGAIASTSEFYIEPEGIN |
| UIS3-13 | EFYIEPEGINKINLNKPIIE |
| UIS3-14 | KINLNKPIIENKNNVDVSIK |
| UIS3-15 | NKNNVDVSIKRYNNFVDIAR |
| UIS3-16 | RYNNFVDIARLSIQKHFEHL |
| UIS3-17 | LSIQKHFEHLSNDQKDSHVN |
| UIS3-18 | SNDQKDSHVNNMEYMQKFVQ |
| UIS3-19 | NMEYMQKFVQGLQENRNISL |
| UIS3-20 | GLQENRNISLSKYQENKAVM |
| UIS3-21 | SKYQENKAVMDLKYHLQKVY |
| UIS3-22 | DLKYHLQKVYANYLSQEEN |

**Supplemental Table I-7.** Peptide sequences of *P. falciparum* Falstatin.

| Peptide ID | Peptide Sequence |
|---|---|
| Falstatin-1 | MKRGLCCVLLLCGAVFVSPS |
| Falstatin-2 | LCGAVFVSPSQEIHARFRRG |
| Falstatin-3 | QEIHARFRRGMNLLVFFCFF |
| Falstatin-4 | MNLLVFFCFFLLSCIVHLSR |
| Falstatin-5 | LLSCIVHLSRCSDNNSYSFE |
| Falstatin-6 | CSDNNSYSFEIVNRSTWLNI |
| Falstatin-7 | IVNRSTWLNIAERIFKGNAP |
| Falstatin-8 | AERIFKGNAPFNFTIIPYNY |
| Falstatin-9 | FNFTIIPYNYVNNSTEENNN |
| Falstatin-10 | VNNSTEENNNKDSVLLISKN |
| Falstatin-11 | KDSVLLISKNLKNSSNPVDE |
| Falstatin-12 | LKNSSNPVDENNHIIDSTKK |
| Falstatin-13 | NNHIIDSTKKNTSNNNNNNS |
| Falstatin-14 | NTSNNNNNNSNIVGIYESQV |
| Falstatin-15 | NIVGIYESQVHEEKIKEDNT |
| Falstatin-16 | HEEKIKEDNTRQDNINKKEN |
| Falstatin-17 | RQDNINKKENEIINNNHQIP |
| Falstatin-18 | EIINNNHQIPVSNIFSENID |
| Falstatin-19 | VSNIFSENIDNNKNYIESNY |
| Falstatin-20 | NNKNYIESNYKSTYNNNPEL |
| Falstatin-21 | KSTYNNNPELIHSTDFIGSN |
| Falstatin-22 | IHSTDFIGSNNNHTFNFLSR |
| Falstatin-23 | NNHTFNFLSRYNNSVLNNMQ |
| Falstatin-24 | YNNSVLNNMQGNTKVPGNVP |
| Falstatin-25 | GNTKVPGNVPELKARIFSEE |
| Falstatin-26 | ELKARIFSEEENTEVESAEN |
| Falstatin-27 | ENTEVESAENNHTNSLNPNE |
| Falstatin-28 | NHTNSLNPNESCDQIIKLGD |
| Falstatin-29 | SCDQIIKLGDIINSVNEKII |
| Falstatin-30 | IINSVNEKIISINSTVNNVL |
| Falstatin-31 | SINSTVNNVLCINLDSVNGN |
| Falstatin-32 | CINLDSVNGNGFVWTLLGVH |
| Falstatin-33 | GFVWTLLGVHKKKPLIDPSN |
| Falstatin-34 | KKKPLIDPSNFPTKRVTQSY |
| Falstatin-35 | FPTKRVTQSYVSPDISVTNP |
| Falstatin-36 | VSPDISVTNPVPIPKNSNTN |
| Falstatin-37 | VPIPKNSNTNKDDSINNKQD |

| Peptide ID | Peptide Sequence |
|---|---|
| Falstatin-38 | KDDSINNKQDGSQNNTTTNH |
| Falstatin-39 | GSQNNTTTNHFPKPREQLVG |
| Falstatin-40 | FPKPREQLVGGSSMLISKIK |
| Falstatin-41 | GSSMLISKIKPHKPGKYFIV |
| Falstatin-42 | PHKPGKYFIVYSYYRPFDPT |
| Falstatin-43 | YSYYRPFDPTRDTNTRIVEL |
| Falstatin-44 | RDTNTRIVELNVQ |

**Supplemental Table I-8.** Peptide sequences of *P. falciparum 3D7* CSP.

| Peptide ID | Peptide Sequence |
|---|---|
| CSP-1 | MRKLAILSVSSFLFV |
| CSP-2 | ILSVSSFLFVEALFQ |
| CSP-3 | SFLFVEALFQEYQCY |
| CSP-4 | EALFQEYQCYGSSSN |
| CSP-5 | EYQCYGSSSNTRVLN |
| CSP-6 | GSSSNTRVLNELNYD |
| CSP-7 | TRVLNELNYDNAGTN |
| CSP-8 | ELNYDNAGTNLYNEL |
| CSP-9 | NAGTNLYNELEMNYY |
| CSP-10 | LYNELEMNYYGKQEN |
| CSP-11 | EMNYYGKQENWYSLK |
| CSP-12 | GKQENWYSLKKNSRS |
| CSP-13 | WYSLKKNSRSLGEND |
| CSP-14 | KNSRSLGENDDGNNE |
| CSP-15 | LGENDDGNNEDNEKL |
| CSP-16 | DGNNEDNEKLRKPKH |
| CSP-17 | DNEKLRKPKHKKLKQ |
| CSP-18 | RKPKHKKLKQPADGN |
| CSP-19 | KKLKQPADGNPDPNA |
| CSP-20 | PADGNPDPNANPNVD |
| CSP-21 | PDPNANPNVDPNANP |
| CSP-22 | NPNVDPNANPNVDPN |
| CSP-23 | PNANPNVDPNANPNV |
| CSP-24 | NVDPNANPNVDPNAN |
| CSP-25 | ANPNVDPNANPNANP |
| CSP-26 | DPNANPNANPNANPN |
| CSP-27 | PNANPNANPNANPNA |

| Peptide ID | Peptide Sequence |
|---|---|
| CSP-28 | NANPNANPNANPNAN |
| CSP-29 | ANPNANPNANPNANP |
| CSP-30 | NPNANPNANPNANPN |
| CSP-31 | PNANPNANPNANPNA |
| CSP-32 | NANPNANPNANPNKN |
| CSP-33 | ANPNANPNKNNQGNG |
| CSP-34 | NPNKNNQGNGQGHNM |
| CSP-35 | NQGNGQGHNMPNDPN |
| CSP-36 | QGHNMPNDPNRNVDE |
| CSP-37 | PNDPNRNVDENANAN |
| CSP-38 | RNVDENANANSAVKN |
| CSP-39 | NANANSAVKNNNNEE |
| CSP-40 | SAVKNNNNEEPSDKH |
| CSP-41 | NNNEEPSDKHIKEYL |
| CSP-42 | PSDKHIKEYLNKIQN |
| CSP-43 | IKEYLNKIQNSLSTE |
| CSP-44 | NKIQNSLSTEWSPCS |
| CSP-45 | SLSTEWSPCSVTCGN |
| CSP-46 | WSPCSVTCGNGIQVR |
| CSP-47 | VTCGNGIQVRIKPGS |
| CSP-48 | GIQVRIKPGSANKPK |
| CSP-49 | IKPGSANKPKDELDY |
| CSP-50 | ANKPKDELDYANDIE |
| CSP-51 | DELDYANDIEKKICK |
| CSP-52 | ANDIEKKICKMEKCS |
| CSP-53 | KKICKMEKCSSVFNV |
| CSP-54 | MEKCSSVFNVVNSSI |
| CSP-55 | SVFNVVNSSIG |

**Supplemental Table I-9.** Peptide sequences of *P. falciparum T996* TRAP and *P. falciparum 3D7* TRAP (= TRIP).

| Peptide ID | Peptide Sequence | Peptide ID | Peptide Sequence |
|---|---|---|---|
| TRAP-1 | MNHLGNVKYLVIVFLIFFDL | TRIP-1 | MNHLGNVKYLVIVFLIFFDL |
| TRAP-2 | VIVFLIFFDLFLVNGRDVQN | TRIP-2 | VIVFLIFFDLFLVNGRDVQN |
| TRAP-3 | FLVNGRDVQNNIVDEIKYSE | TRIP-3 | FLVNGRDVQNNIVDEIKYRE |
| TRAP-4 | NIVDEIKYSEEVCNDQVDLY | TRIP-4 | NIVDEIKYREEVCNDEVDLY |
| TRAP-5 | EVCNDQVDLYLLMDCSGSIR | TRIP-5 | EVCNDEVDLYLLMDCSGSIR |

| Peptide ID | Peptide Sequence | Peptide ID | Peptide Sequence |
|---|---|---|---|
| TRAP-6 | LLMDCSGSIRRHNWVNHAVP | TRIP-6 | LLMDCSGSIRRHNWVNHAVP |
| TRAP-7 | RHNWVNHAVPLAMKLIQQLN | TRIP-7 | RHNWVNHAVPLAMKLIQQLN |
| TRAP-8 | LAMKLIQQLNLNDNAIHLYV | TRIP-8 | LAMKLIQQLNLNDNAIHLYA |
| TRAP-9 | LNDNAIHLYVNVFSNNAKEI | TRIP-9 | LNDNAIHLYASVFSNNAREI |
| TRAP-10 | NVFSNNAKEIIRLHSDASKN | TRIP-10 | SVFSNNAREIIRLHSDASKN |
| TRAP-11 | IRLHSDASKNKEKALIIIRS | TRIP-11 | IRLHSDASKNKEKALIIIKS |
| TRAP-12 | KEKALIIIRSLLSTNLPYGR | TRIP-12 | KEKALIIIKSLLSTNLPYGK |
| TRAP-13 | LLSTNLPYGRTNLTDALLQV | TRIP-13 | LLSTNLPYGKTNLTDALLQV |
| TRAP-14 | TNLTDALLQVRKHLNDRINR | TRIP-14 | TNLTDALLQVRKHLNDRINR |
| TRAP-15 | RKHLNDRINRENANQLVVIL | TRIP-15 | RKHLNDRINRENANQLVVIL |
| TRAP-16 | ENANQLVVILTDGIPDSIQD | TRIP-16 | ENANQLVVILTDGIPDSIQD |
| TRAP-17 | TDGIPDSIQDSLKESRKLSD | TRIP-17 | TDGIPDSIQDSLKESRKLSD |
| TRAP-18 | SLKESRKLSDRGVKIAVFGI | TRIP-18 | SLKESRKLSDRGVKIAVFGI |
| TRAP-19 | RGVKIAVFGIGQGINVAFNR | TRIP-19 | RGVKIAVFGIGQGINVAFNR |
| TRAP-20 | GQGINVAFNRFLVGCHPSDG | TRIP-20 | GQGINVAFNRFLVGCHPSDG |
| TRAP-21 | FLVGCHPSDGKCNLYADSAW | TRIP-21 | FLVGCHPSDGKCNLYADSAW |
| TRAP-22 | KCNLYADSAWENVKNVIGPF | TRIP-22 | KCNLYADSAWENVKNVIGPF |
| TRAP-23 | ENVKNVIGPFMKAVCVEVEK | TRIP-23 | ENVKNVIGPFMKAVCVEVEK |
| TRAP-24 | MKAVCVEVEKTASCGVWDEW | TRIP-24 | MKAVCVEVEKTASCGVWDEW |
| TRAP-25 | TASCGVWDEWSPCSVTCGKG | TRIP-25 | TASCGVWDEWSPCSVTCGKG |
| TRAP-26 | SPCSVTCGKGTRSRKREILH | TRIP-26 | SPCSVTCGKGTRSRKREILH |
| TRAP-27 | TRSRKREILHEGCTSEIQEQ | TRIP-27 | TRSRKREILHEGCTSELQEQ |
| TRAP-28 | EGCTSEIQEQCEEERCPPKW | TRIP-28 | EGCTSELQEQCEEERCLPKR |
| TRAP-29 | CEEERCPPKWEPLDVPDEPE | TRIP-29 | CEEERCLPKREPLDVPDEPE |
| TRAP-30 | EPLDVPDEPEDDQPRPRGDN | TRIP-30 | EPLDVPDEPEDDQPRPRGDN |
| TRAP-31 | DDQPRPRGDNSSVQKPEENI | TRIP-31 | DDQPRPRGDNFAVEKPNENI |
| TRAP-32 | SSVQKPEENIIDNNPQEPSP | TRIP-32 | FAVEKPNENIIDNNPQEPSP |
| TRAP-33 | IDNNPQEPSPNPEEGKDENP | TRIP-33 | IDNNPQEPSPNPEEGKGENP |
| TRAP-34 | NPEEGKDENPNGFDLDENPE | TRIP-34 | NPEEGKGENPNGFDLDENPE |
| TRAP-35 | NGFDLDENPENPPNPDIPEQ | TRIP-35 | NGFDLDENPENPPNPDIPEQ |
| TRAP-36 | NPPNPDIPEQKPNIPEDSEK | TRIP-36 | NPPNPDIPEQEPNIPEDSEK |
| TRAP-37 | DIPEQKPNIPEDSEKEVPSD | TRIP-37 | DIPEQEPNIPEDSEKEVPSD |
| TRAP-38 | EDSEKEVPSDVPKNPEDDRE | TRIP-38 | EDSEKEVPSDVPKNPEDDRE |
| TRAP-39 | VPKNPEDDREENFDIPKKPE | TRIP-39 | VPKNPEDDREENFDIPKKPE |
| TRAP-40 | ENFDIPKKPENKHDNQNNLP | TRIP-40 | ENFDIPKKPENKHDNQNNLP |
| TRAP-41 | NKHDNQNNLPNDKSDRNIPY | TRIP-41 | NKHDNQNNLPNDKSDRYIPY |
| TRAP-42 | NDKSDRNIPYSPLPPKVLDN | TRIP-42 | NDKSDRYIPYSPLSPKVLDN |
| TRAP-43 | SPLPPKVLDNERKQSDPQSQ | TRIP-43 | SPLSPKVLDNERKQSDPQSQ |

| Peptide ID | Peptide Sequence | Peptide ID | Peptide Sequence |
|---|---|---|---|
| TRAP-44 | ERKQSDPQSQDNNGNRHVPN | TRIP-44 | ERKQSDPQSQDNNGNRHVPN |
| TRAP-45 | DNNGNRHVPNSEDRETRPHG | TRIP-45 | DNNGNRHVPNSEDRETRPHG |
| TRAP-46 | SEDRETRPHGRNNENRSYNR | TRIP-46 | SEDRETRPHGRNNENRSYNR |
| TRAP-47 | RNNENRSYNRKYNDTPKHPE | TRIP-47 | RNNENRSYNRKHNNTPKHPE |
| TRAP-48 | KYNDTPKHPEREEHEKPDNN | TRIP-48 | KHNNTPKHPEREEHEKPDNN |
| TRAP-49 | REEHEKPDNNKKKGESDNKY | TRIP-49 | REEHEKPDNNKKKAGSDNKY |
| TRAP-50 | KKKGESDNKYKIAGGIAGGL | TRIP-50 | KKKAGSDNKYK |
| TRAP-51 | KIAGGIAGGLALLACAGLAY | | |
| TRAP-52 | ALLACAGLAYKFVVPGAATP | | |
| TRAP-53 | KFVVPGAATPYAGEPAPFDE | | |
| TRAP-54 | YAGEPAPFDETLGEEDKDLD | | |
| TRAP-55 | TLGEEDKDLDEPEQFRLPEE | | |
| TRAP-56 | EPEQFRLPEENEWN | | |

**Supplemental Table I-10.** Peptide sequences of the human Ii.

| Peptide ID | Peptide Sequence |
|---|---|
| Ii-1 | MHRRRSRSCREDQKP |
| Ii-2 | RSRSCREDQKPVMDD |
| Ii-3 | CREDQKPVMDDQRDL |
| Ii-4 | QKPVMDDQRDLISNN |
| Ii-5 | MDDQRDLISNNEQLP |
| Ii-6 | RDLISNNEQLPMLGR |
| Ii-7 | SNNEQLPMLGRRPGA |
| Ii-8 | QLPMLGRRPGAPESK |
| Ii-9 | LGRRPGAPESKCSRG |
| Ii-10 | PGAPESKCSRGALYT |
| Ii-11 | ESKCSRGALYTGFSI |
| Ii-12 | SRGALYTGFSILVTL |
| Ii-13 | LYTGFSILVTLLLAG |
| Ii-14 | FSILVTLLLAGQATT |
| Ii-15 | VTLLLAGQATTAYFL |
| Ii-16 | LAGQATTAYFLYQQQ |
| Ii-17 | ATTAYFLYQQQGRLD |
| Ii-18 | YFLYQQQGRLDKLTV |
| Ii-19 | QQQGRLDKLTVTSQN |
| Ii-20 | RLDKLTVTSQNLQLE |
| Ii-21 | LTVTSQNLQLENLRM |

| Peptide ID | Peptide Sequence |
|---|---|
| Ii-22 | SQNLQLENLRMKLPK |
| Ii-23 | QLENLRMKLPKPPKP |
| Ii-24 | LRMKLPKPPKPVSKM |
| Ii-25 | LPKPPKPVSKMRMAT |
| Ii-26 | PKPVSKMRMATPLLM |
| Ii-27 | SKMRMATPLLMQALP |
| Ii-28 | MATPLLMQALPMGAL |
| Ii-29 | LLMQALPMGALPQGP |
| Ii-30 | ALPMGALPQGPMQNA |
| Ii-31 | GALPQGPMQNATKYG |
| Ii-32 | QGPMQNATKYGNMTE |
| Ii-33 | QNATKYGNMTEDHVM |
| Ii-34 | KYGNMTEDHVMHLLQ |
| Ii-35 | MTEDHVMHLLQNADP |
| Ii-36 | HVMHLLQNADPLKVY |
| Ii-37 | LLQNADPLKVYPPLK |
| Ii-38 | ADPLKVYPPLKGSFP |
| Ii-39 | KVYPPLKGSFPENLR |
| Ii-40 | PLKGSFPENLRHLKN |
| Ii-41 | SFPENLRHLKNTMET |
| Ii-42 | NLRHLKNTMETIDWK |
| Ii-43 | LKNTMETIDWKVFES |
| Ii-44 | METIDWKVFESWMHH |
| Ii-45 | DWKVFESWMHHWLLF |
| Ii-46 | FESWMHHWLLFEMSR |
| Ii-47 | MHHWLLFEMSRHSLE |
| Ii-48 | LLFEMSRHSLEQKPT |
| Ii-49 | MSRHSLEQKPTDAPP |
| Ii-50 | SLEQKPTDAPPKESL |
| Ii-51 | KPTDAPPKESLELED |
| Ii-52 | APPKESLELEDPSSG |
| Ii-53 | ESLELEDPSSGLGVT |
| Ii-54 | LEDPSSGLGVTKQDL |
| Ii-55 | SSGLGVTKQDLGPVP |
| Ii-56 | SGLGVTKQDLGPVPM |